Assessment and alleviation of soil pollution through agro-ecotechnological interventions: role of areca nut husk biochar and vetiver grass

A thesis submitted

by

NIHAL GUJRE

In partial fulfillment of the requirements for the award of the degree of

Doctor of Philosophy

School of Agro & Rural Technology
Indian Institute of Technology Guwahati
Guwahati-781039, Assam, India

September 2021

SCHOOL OF AGRO & RURAL TECHNOLOGY

INDIAN INSTITUTE OF TECHNOLOGY GUWAHATI

STATEMENT

I, undersigned hereby declare that the research embodied in this thesis entitled "**Assessment and alleviation of soil pollution through agro-ecotechnological interventions: role of areca nut husk biochar and vetiver grass**" is the result of experiments carried out in the School of Agro & Rural Technology, Indian Institute of Technology Guwahati, India, under the supervisions of Prof. Sudip Mitra and Prof. Latha Rangan.

In keeping with the general practice of reporting scientific observations, due acknowledgments have been made wherever the work described is based on the finding of other research.

01 September, 2021

Nihal Gujre
(Roll No. 166154104)
Research Scholar
School of Agro & Rural Technology
(S.A.R.T.), IIT Guwahati

SCHOOL OF AGRO & RURAL TECHNOLOGY

INDIAN INSTITUTE OF TECHNOLOGY GUWAHATI

CERTIFICATE

This is to certified that the work described in this thesis entitled **"Assessment and alleviation of soil pollution through agro-ecotechnological interventions: role of areca nut husk biochar and vetiver grass"** by Nihal Gujre (Roll No. 166154104) for the award of degree of Doctor of Philosophy is an authentic record of the result obtained from the research work carried out under our joint supervision in the School of Agro & Rural Technology, IITG. The work carried out in this thesis has not been submitted elsewhere for a degree.

01 September, 2021

Prof. Sudip Mitra
Thesis Supervisor
School of Agro & Rural Technology
Indian Institute of Technology Guwahati
Assam 781039, India

Prof. Latha Rangan
Co-supervisor
Department of Biosciences and Bioengineering
Indian Institute of Technology Guwahati
Assam 781039, India

Acknowledgements

Present work owes its existence to the cooperation, assistance and inspiration of several people. I express my sincere gratitude to the people in my life for their constant support and motivation in one way or other during this awesome journey.

First and foremost, I am extremely grateful to my Supervisor, Prof. Sudip Mitra, for keeping his belief in me and on my ability to do good research. I would like to thank him for his constant encouragement and support. His guidance, brainstorming sessions, especially during the initial year has helped me a lot. His motivation for achieving my professional goals has been priceless. He was very kind and always ready to help despite his other commitments. Thank you, Sir, for all your help and support.

I would also like to thank my co-supervisor Prof. Latha Rangan, for her guidance and support. I am very much thankful to Chairman of my Doctoral committee Prof. Sashindra K. Kakoty and other members Dr. Siddhartha Singha and Dr. Pankaj Kalita for their valuable insights and suggestions.

My sincere thank go to Prof. Sanjukta Patra, Head, School of Agro & Rural Technology, IITG for her encouragement and providing existing facilities of the school. I also thank RuTAG for providing necessary facilities and a conducive academic environment. My sincere thanks go to the Ministry of Human Resource Development, India for providing financial support. I am equally grateful to DBT-Twining, Department of Biotechnology, India (BT/PR16795/NER/95/292/2015). I am grateful for the timely support and cooperation extended by various Departments and Centres IITG (Bioscience and Bioengineering, Civil Engineering, Chemical Engineering, Centre for Environment, and Central Instrument facility).

I would also like to thank ICAR-IISR, Indore, North Eastern Regional Institute of Water and Land Management (NERIWALM), for their timely help in allowing me to use their instruments for carrying out various sample analyses.

I heartfelt thank to all the people who are responsible for creating a conducive environment in the Agro Ecotechnology lab (AEL) at SART. It was my pleasure in getting associated with the AEL

and work closely with Mrs. Sudha Sahu, Mr. Ankit Soni, Mr. Suranjit Basumatary, Mr. Manas P. Rajbonshi, Ms. Anamika Ghose, Ms. Ankita Datta, Mr. Debaditya Gupta and Ms. Ashmita Das. Thanks to other present and past AEL members viz. Mr. Sajid Ali, Mr. Stayam Raj and Mr. Gourishankar Bhattacharya.

I am very thankful to Prof. Mahaveer P. Sharma, Dr. Pallabi Borah, Dr. Richa Agnihotri, Ms. Suchetana Ghose and Mr. Ashutosh Kumar Mishra for their timely help during my research tenure.

I am indebted to my friends: Mr. Bhaskar Kalita, Ms. Shivani Gupta, Mr. Kushagra Agarwal, Ms. Jenasree Hazarika, Mr. Nilkamal Kalita and Ms. Deepa Sachan who have stood by me throughout, especially during the hard times of my PhD journey.

Most importantly, I thank to my parents, Shri. Dhanraj Gujre and Smt. Anita Gujre. I deeply thank both of them for their unconditional blessings, love and support.

Last but not the least; I thank almighty lord Mahakal and Maa Kamakhya for showering their blessings and providing me opportunity to carry this work in IIT Guwahati amidst such beautiful people and nature.

Abbreviations

AAS= Atomic absorption spectrophotometer
ABS=Absorption factor
AC=Ash content
ADD=Average daily dose
AET=Agro ecotechnology
AH=Areca nut husk
AHB= Areca nut husk biochar
AMF= Arbuscular mycorrhizal fungi
As=Aresnic
Av K=Available potassium
Av N=Available nitrogen
Av Na=Available sodium
Av P=Available phosphorus
BC=Biochar
BCF=Bio-concentration factor
BD=Bulk density
BDL=Below detectable limit
BET= Brunauer-Emmett-Teller
BI=Brick industry
BJH =Barrett-Joyner-Halender
BK1=Brick kiln sampling location
BMI= Body mass index
BSA =Bovine serum albumin
BW=Body weight
CBK= Contemporary brick kiln
Cd= Cadmium
CEC=Cation exchange capacity
Chla=Chlorophyll a
Chlb=Chlorophyll b
CR=Carcinogenic risk
Cr=Chromium
CRD=Complete randomize design
Cu=Copper
D1= Dumping site sampling location
DLS= Dynamic light scattering
DSC= Differential scanning calorimetry
DTPA= Diethyl triamine pentaacetic acid
ED=Exposure duration
EDX= Energy dispersive X-ray spectroscopy
EF =Enrichment factor
FC=Fixed carbon
FCBTK =Fixed chimney bulls trench kiln

FESEM= Field emission scanning electron microscopy
FTIR= Fourier transform infrared
GCF =Global contamination factor.
GPS =Global positioning system
HI=Hazard index
HM=Heavy metals
HQ=Hazard quotient
ICF=Individual contamination factor
I_{geo} =Geo-accumulation index
LOI=Loss of ignition
LT=life time
MBC=Microbial biomass carbon
MC=Moisture content
MF-%=Mobility factor
Mha =million hectares
Mn=Manganese
MT=Meteric tones
Ni=Nickel
OC=Organic carbon
OM=Organic matter
ORP =Oxidative–reductive potential
PAHs=Poly aromatic hydrocarbon
Pb=Lead
PCA= Principal component analysis
PCB=Printed circuit boards
PD=Particle density
PEF=Particle emission factor
PERI =Potential ecological risk index
PLI=Pollution load index
POR=Porosity
RBC= Red blood cell
RDW=Root dry weight
RSM= Response surface method
RWC=Relative water content
SAF=Skin adherence factor
SDH=Soil dehydrogenase
SDW=Shoot dry weight
SEA=Soil enzyme activities
SF= Slope factor
SMC=Soil moisture content
SOM=Stable organic matter
SOMYI=Stable organic matter yield index
SRM=Standard reference materials
SSA=Specific surface area
TBK= Traditional brick kilns
TF=Translocation factor

TGA =Thermo gravimetric analysis

UR=Urease
VM=Volatile matter
WL=Weight loss

XRD= X-Ray diffraction

Zn=Zinc

Units

° C= Degree centigrade
µg g^{-1}=Microgram per gram
µg= Microgram
cm= Centimeter
cm^{-1}= Wavenumber
cmol kg^{-1}= Centimole of charge per 1 kilogram
d $year^{-1}$= Days per year
g cm^{-1}= Gram per centimeter cube
g kg^{-1}= Gram per kilogram
g= Gram
h= Hours
K min^{-1}=Kelvin per minute
kg ha^{-1}=Kilogram per hectare
m= Meter
M=Molar
mL=Mili liter
m^2 g^{-1}=meter square per gram
m^3 kg^{-1}= Meter cube per kilogram
mg cm^{-2} h^{-1}= Miligram per centimeter per hour
mg d^{-1}=Miligram per day
mg gm^{-1}=Miligram per gram
mg kg^{-1}= Miligram per kilogram
mg L^{-1}=Milligram per liter
mg= Miligram
min=Minutes
mM= Milimolar
mS cm=Micro Siemens
nm=Nanometer
ppm= Parts per million
t ha^{-1}= Tonnes per hectare
v/v=Volume/ Volume
w/v= Weight/ Volume
wt= Weight

List of Tables

List of Figures

Abstract

Ever increasing population, generation of unmanageable amount of wastes, increasing demands for food, and decrease in arable land; besides, encroaching of agricultural lands and ecologically vulnerable sites by unscientific dumping are some of the grave menaces of the developing world. Extensive industrialization, urbanization, and consumerism have disarrayed well established modes of solid waste management (SWM). The unsegregated metal wastes from batteries, household lighting equipment, computers, and emissions from brick kiln have become predominant stationary pollution sources, with protracted effects. Several anthropogenic activities have become the preeminent sources of contamination by heavy metals (HMs), and the resultant deterioration in soil quality. Thus, the present study attempts to address the issues of soil quality degradation and its management in an environmentally compatible manner. Further, it explores agro-ecotechnological measures to improve the soil quality utilizing locally available resources. In the present study, two contaminated areas were selected in Assam to assess soil quality impact on human health and identify suitable management options. Boragaon dumping site at Guwahati (Site-1) is contaminated with municipal solid wastes (MSW) and shares a common boundary with the ecologically sensitive area, Deepor Beel (Ramsar site No. 1207); is a part of the lower Brahmaputra valley. The second site is in the vicinity of a brick kiln industry (Site-2) located in the rural area of Napaam, Tezpur, which comes under the north bank plain agro-climatic zone of the state. To comprehend soil quality, different physico-chemical parameters, and estimation of HMs contamination were carried out using standard protocols. Results revealed that the soil quality in both areas was degraded by increasing HM concentrations and decreased levels of nutrients. Cadmium (Cd), and chromium (Cr) are the two crucial HMs which posed severe ecological and health risk to the surrounding areas.

Consequently, there is an urgent need to address these issues. In the quest for indigenous solutions, the present study has attempted to prepare and characterize biochar (BC) from locally available crop refuse, i.e., areca nut husk (AH). Year-round availability of feedstock and waste valorization were the cardinal reasons for selecting AH as feedstock for biochar preparation. Areca nut husk biochar (AHB) prepared at a lower temperature (250° C), has intermediate stability in soil and higher soil agronomic properties, rendering it ideal for mass production as a soil amendment. The present study also explored the potential of AHB to remediate HMs contaminated

soils in conjunction with vetiver grass (*Chrysopogon zizanioides* L.), which is well known for its various environment friendly characteristics. Results showed that AHB, along with the vetiver, has an additive effect, which includes remediation of Cd and Cr, enhanced mycorrhizal growth, and glomalin production, along with nutrient enrichment. The results demonstrated that AHB at a dose of 15 t ha^{-1} was most suitable for soil rejuvenation, improving soil physico-chemical, and biochemical properties.

Keywords: Areca nut husk biochar, Brick kiln bottom ash, Heavy metals, Municipal solid waste, Vetiver.

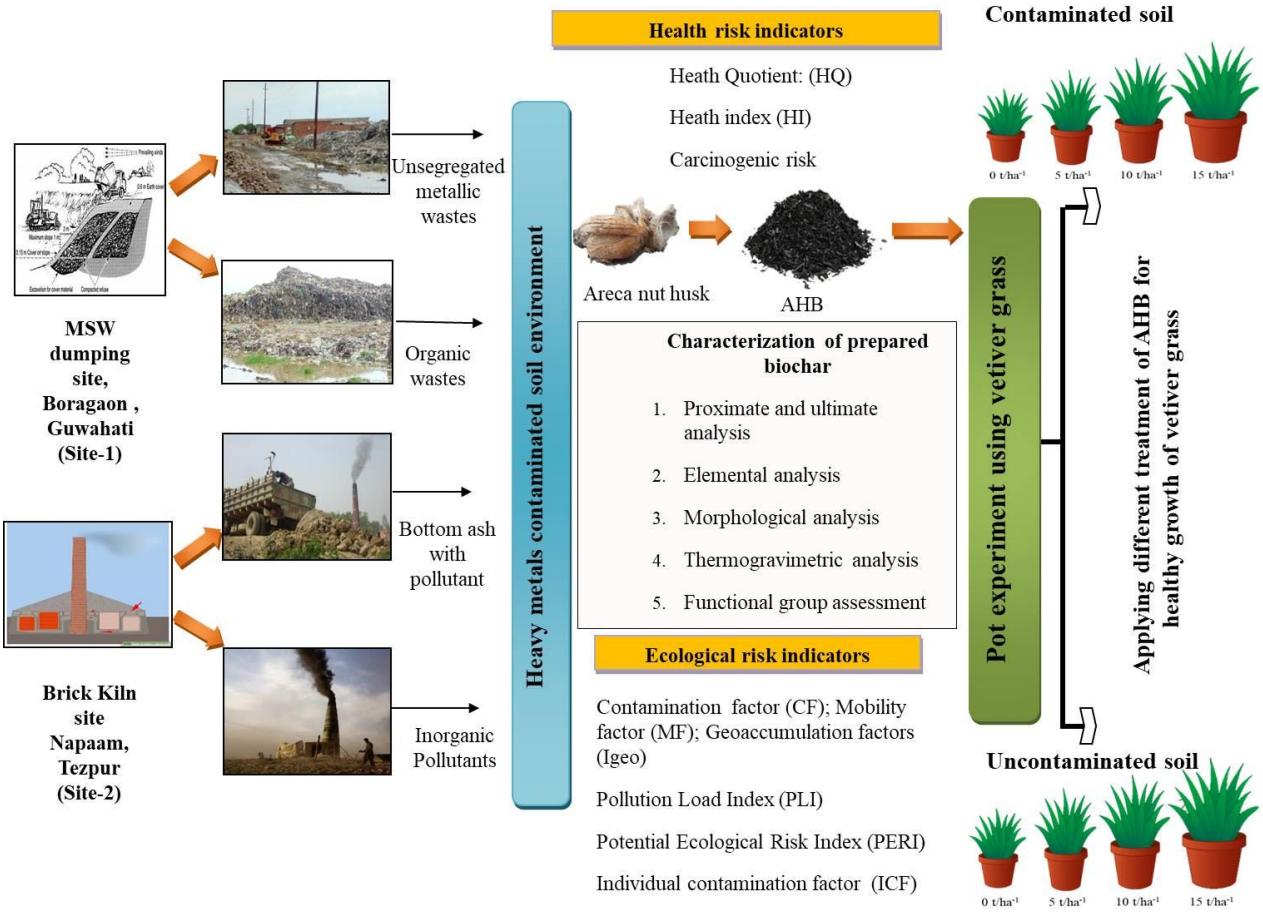

CHAPTER 1

Introduction

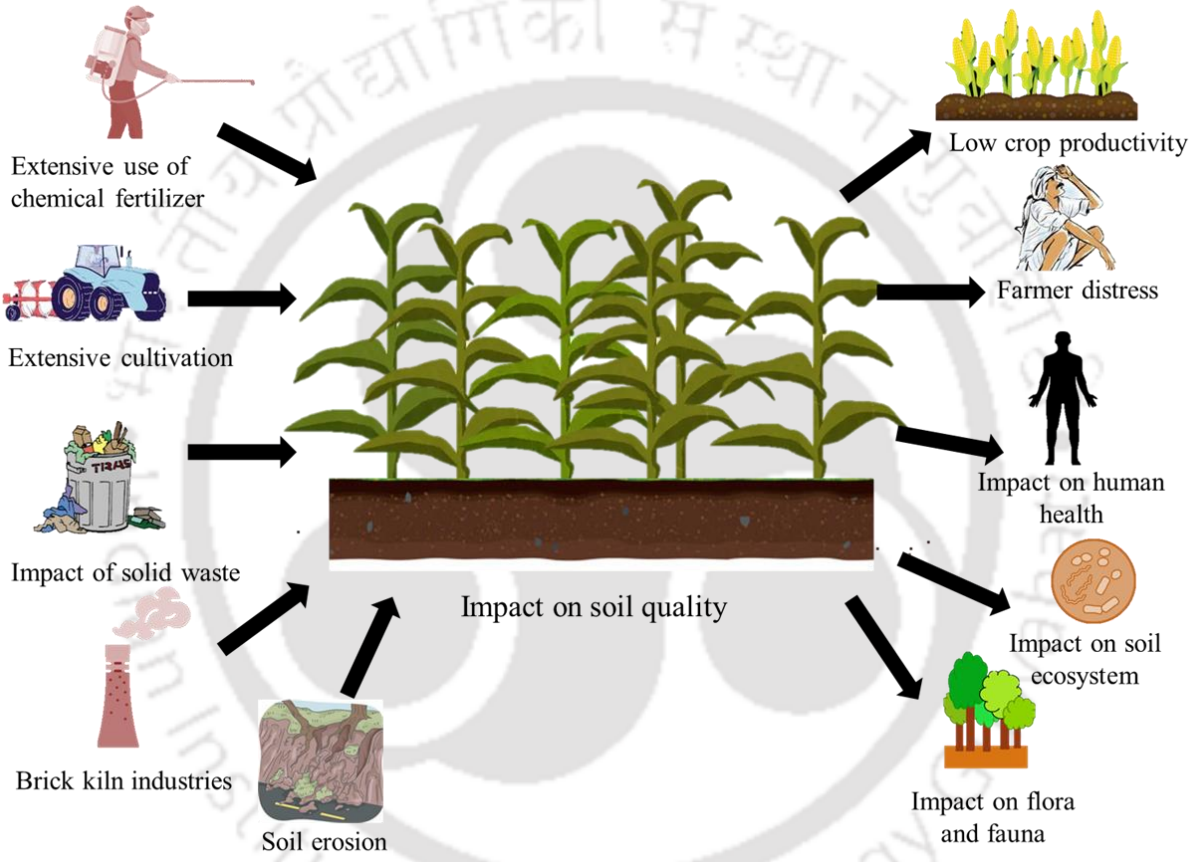

"This chapter introduces soil quality management, the different factors which affect soil quality, and its cascading effects on the surrounding environment and human health. It also contains the specific objectives and structure of the thesis."

1. Introduction

1.1. Background

Among the developing nations, India is one of the largest producers of municipal solid waste (MSW), with an average daily output of 0.5 MT (Das et al., 2019). Approximately, 62 million tons of MSW is generated on an annual basis in India; and an escalation to 165 million tons is projected by 2030 (Joshi and Ahmed, 2016). Though, India and other developing countries, employ landfills as cost effective and convenient options for MSW disposal, their utility is overturned by the ensuing soil contamination and water pollution (surface and groundwater) (Alam et al., 2020). The concomitant toxicity of soil heavy metals (HMs) to plants, animals, and human beings is reinforced by bio-magnification, emanating from prolonged residence of HMs in the soil. The extended exposure negatively affects the human respiratory, gastric, and central nervous systems (Khanam et al., 2019; Tseng et al., 2019). As a natural corollary, HMs absorbed by different aquatic organisms; exacerbate the ecological risks, particularly when amplified by the food web (Dash et al., 2019). Consequently, comprehensive assessment studies on HMs in soils and the potential human health risks are the need of the hour; unfortunately, in depth and holistic assessments are conspicuous by their absence. Therefore, the investigation of soil HM pollution was undertaken at the MSW dumping site in Boragaon, at Guwahati, in Assam, India. The site has the dual advantage of close proximity to Guwahati (a densely populated city) and Deepor Beel (a globally important Ramsar site), facilitating assessment of both human health and ecological risks. Thus, Boragaon dumping Site was selected to examine the soil contamination, ecological, and human health risks associated with six important HMs; Chromium (Cr), Zinc (Zn), Manganese (Mn), Cadmium (Cd), Copper (Cu) and Nickel (Ni).

The concerted global effort to contain detrimental effects of the brick industry (BI); is not matched by developing countries like India, Pakistan and Bangladesh. Ignoring BI as a burgeoning

source of gaseous and HM pollution is catastrophic, as HMs deposited on the soil surface, redoubles soil pollution over time (Kamal et al., 2014). India is the second largest brick producer in the south Asia, manufacturing about 240-260 billion bricks annually (Kamyotra et al., 2015). In addition, the emission from the brick kilns is considered harmful to communities living in their vicinity. There are about 1.4 lakhs BIs located in the India and the majority of them are located in rural areas. Thus, the sheer volume of brick production in India, and in particular, the location of BIs in the middle of agricultural fields in Assam, markedly heightens the pollution liability and demands comprehensive audit of the environmental and human health fallout. The brick kilns are of mainly two types: 1) Traditional brick kilns (TBK), which include mainly fixed chimney bulls trench kiln (FCBTK), and 2), contemporary brick kilns (CBK), that are technically modified at various stages of development (Khan et al., 2019). However, in developing countries like India the FCBTK are widely used for brick manufacturing, marking them as potential emitter of pollutants.

The issues pertaining to the persistent degradation of the soil quality, initiated the hypothesis that thermo-chemical valorization of waste areca nut husk (AH) to biochar (BC) could improve soil fertility. Three factors ensure the sustained availability of raw material (AH) for BC development; India's position as global leader in areca nut production, Assam being the 3rd largest areca production hub in the country, and the significant loss of AH as solid waste, without monetary incentive for its utility. The process of pyrolysis offers multifaceted applications enabling conversion of heterogeneous biomass into useful forms like BC, which can be tailored to user needs. Pyrolysis induces structural transformation of biomass into higher aromatic and hydrophobic fractions; which retain high aromaticity, stability, and resistance to degradation (Huang et al., 2019). Areca nut husk biochar (AHB), as a biomass pyrolyzed product or BC, is handicapped by lack of viable research on its soil applications, and effect on non-cropping plants.

Therefore, selecting suitable BCs in accordance with the site-specific conditions, and utilization of locally available biomass, has attained mandatory status, for integrated soil quality management. Based on the aforesaid deliberations, the specific objectives of the present research work have been derived and detailed.

1.2. Objectives of the study

1. To assess the physico-chemical properties of the soils contaminated by municipal solid waste and brick kiln bottom ash.
2. To study the heavy metals concentration profile in the soils contaminated by municipal solid waste and brick kiln bottom ash.
3. To prepare and characterize biochar from locally available areca nut husks.
4. To study the heavy metal remediation potential of biochar.
5. To assess the nutrient dynamics in plant and soil.

1.3. Overview of thesis organization

The thesis is organised into eight different chapters (Fig. 1.1). The first chapter of the thesis consists of a brief discussion on the problems and challenges for sustainable soil quality management, targeted at the two major sources of soil pollution in Assam; the MSW dumping site and brick manufacturing industries. Subsequently, the scope of BC prepared from locally available AH for soil amendment, in keeping with the specific objectives of the present study is delineated. The second chapter covers the detailed review of literature on soil quality status across the world and in India. It also deals with the previous studies, background information, and existing research gaps. The third chapter focuses on the first objective and details the assessment of the physico-

chemical properties of the soil contaminated with MSW wastes and brick kiln bottom ash. Chapter four deals with profiling HMs from the respective sites using six geochemical fractions. Environmental and human health risks are delineated using various indices, factors and risks. In fifth chapter, preparation and characterization of AHB are explained along with their agronomic properties. The selection of low temperature pyrolysis for BC preparation along with physical, chemical, morphological and thermochemical assessment of BC, form part of this chapter. In the sixth chapter HMs remediation potential of AHB is assessed using vetiver as test plant. The remediation potential as translocation factor (TF) and bio-concentration factor (BCF) are computed using application-based pot experiments. In the seventh chapter nutrient dynamics of the AHB doses are assessed by changes in the soil nutrient, plant morphological parameters, and associated arbuscular mycorrhizal fungi (AMF) parameters. The important parameters with the it's dynamics of plant and soil were studied using principal component analysis (PCA). Finally, the eighth chapter deals with the summary derived from the objectives and suggestions for future research.

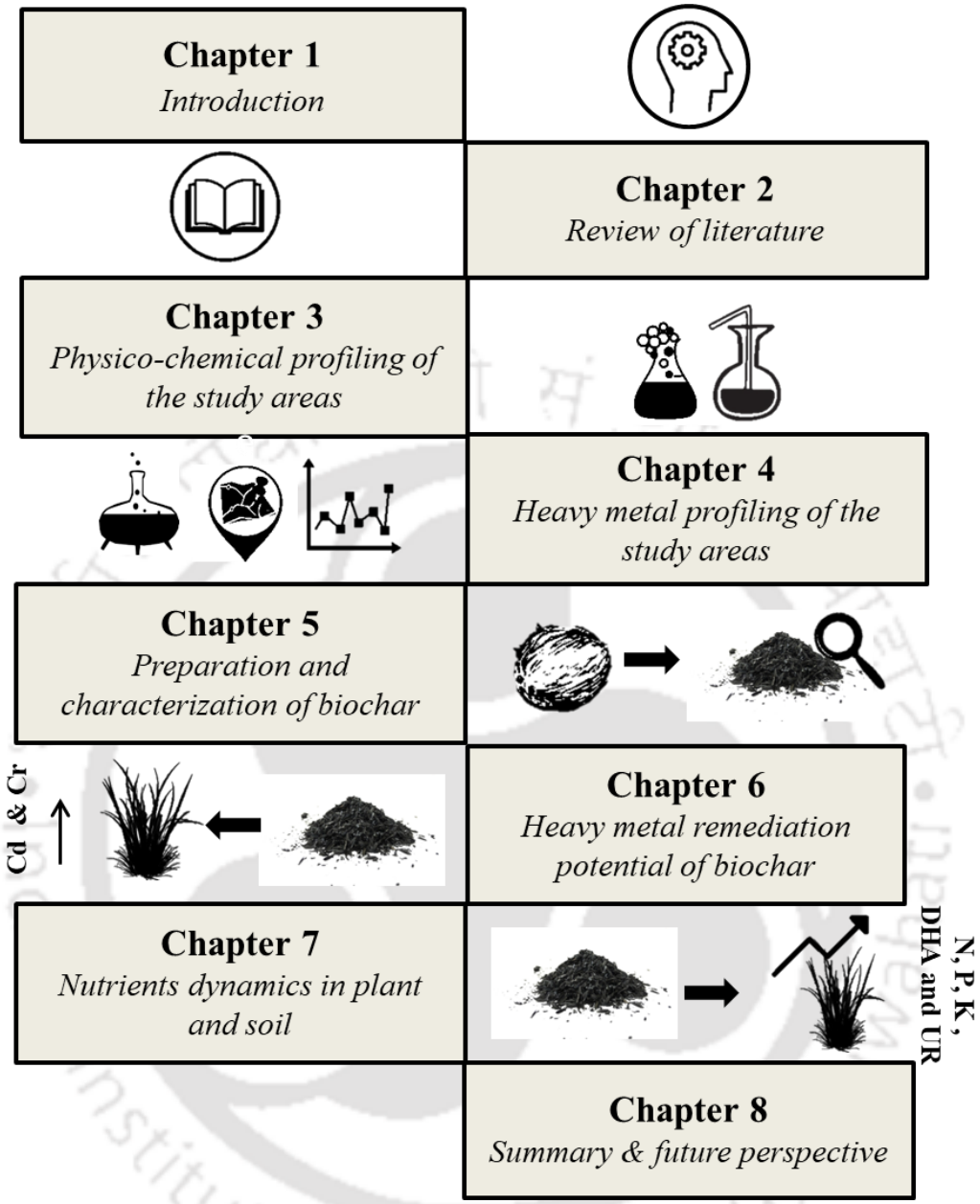

Fig. 1.2. Overview of thesis chapters.

References

Alam, P., Sharholy, M., Ahmad, K., 2020. A study on the landfill leachate and its impact on groundwater quality of Ghazipur area, New Delhi, India, in: Recent Developments in Waste Management. Springer, Singapore, pp. 345-358.

Das, S., Lee, S.H., Kumar, P., Kim, K.H., Lee, S.S., Bhattacharya, S.S., 2019. Solid waste management: Scope and the challenge of sustainability. J. Clean. Prod. 228, 658-678.

Dash, S., Borah, S.S., Kalamdhad, A., 2019. A modified indexing approach for assessment of heavy metal contamination in Deepor Beel, India. Ecol. Indic. 106, 105444.

Huang, M., Li, Z., Luo, N., Yang, R., Wen, J., Huang, B., Zeng, G., 2019. Application potential of biochar in environment: Insight from degradation of biochar-derived DOM and complexation of DOM with heavy metals. Sci. Total Environ. 646, 220–228.

Joshi, R., Ahmed, S., 2016. Status and challenges of municipal solid waste management in India: A review. Cogent Environ. Sci. 2, 1139434.

Kamal, A., Malik, R.N., Martellini, T., Cincinelli, A., 2014. Cancer risk evaluation of brick kiln workers exposed to dust bound PAHs in Punjab province (Pakistan). Sci. Total Environ. 493, 562–570.

Kamyotra, J. S., 2015. Brick Kiln in India. Anil Agarwal Dialogue, March 11, 2015. https://cdn.cseindia.org/docs/aad2015/11.03.2015%20Brick%20Presentation.pdf (accessed 23 December 2019).

Khanam, R., Kumar, A., Nayak, A., Shahid, M., Tripathi, R., Vijayakumar, S., Bhaduri, D., Kumar, U., Mohanty, S., Panneerselvam, P., Chatterjee, D., 2019. Metal(loid)s (As, Hg, Se, Pb and Cd) in paddy soil: bioavailability and potential risk to human health. Sci. Total Environ. 699, 134330.

Tseng, C.H., Lee, I.H., Chen, Y.C., 2019. Evaluation of hexavalent chromium concentration in water and its health risk with a system dynamics model. Sci. Total Environ. 669, 103-111.

CHAPTER 2

Review of Literature

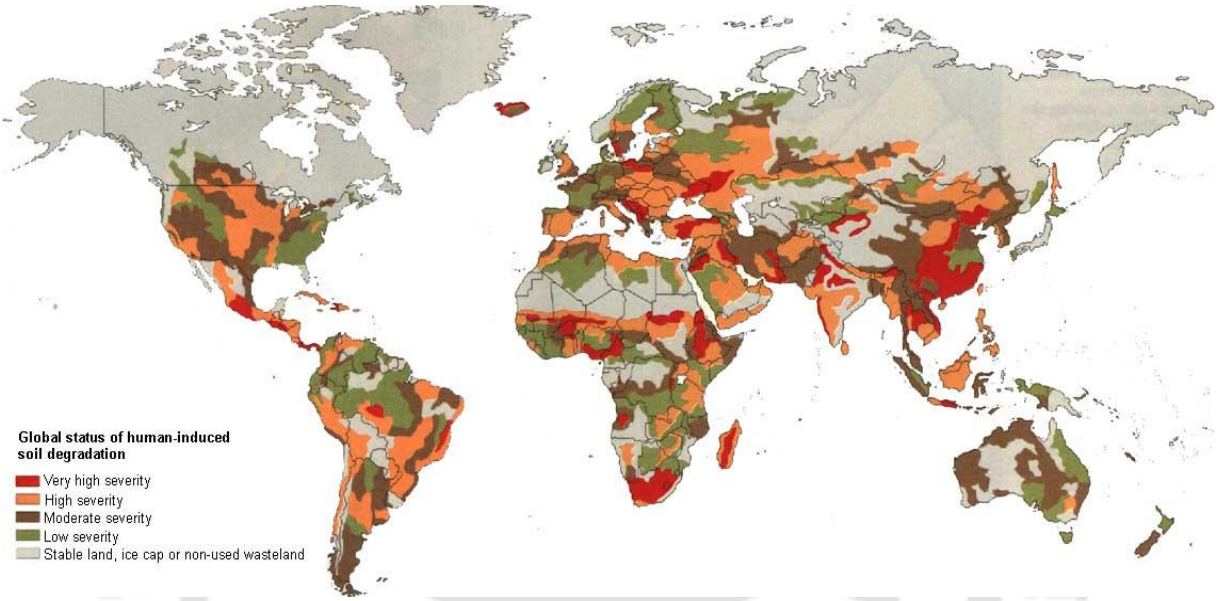

Global status of human induced soil degradation **(**Sources: SET, 2021**)**

"*This chapter includes a comprehensive and in-depth review of literature on the current status of the soil quality across the world and India. It further elaborates the challenges of the soil contaminated with MSW waste and brick kiln bottom ash. This chapter also focuses on biochar and its physico-chemical and biological properties."*

2. Review of literature

2.1. Need for soil quality management

The world population continues to rise. Today's population of around 7 billion is expected to increase by about 9.7 billion by 2050 (FAO, 2018). By this time, another one billion tons of cereals and 200 million extra tones of livestock products will need to be produced every year. For nutrition to improve and for food security and undernourishment to recede, future agriculture production will rise faster than population growth. Improvement will thus have to come from sustainable intensification that makes effective use of land resources. But rapid population growth and economic development in the country are degrading the soil environment through the uncontrolled growth of urbanization and industrialization, expansion and intensification of agriculture, and the destruction of natural habitats.

2.2. Soil quality degradation

Soil degradation refers to a decline in the soil's productivity through adverse changes in nutrient status, soil organic matter, structural attributes, and toxic chemicals. It is a process that lowers the soil's current and future capacity to produce goods or services. Soils are a non-renewable and dynamic source of a living system. With time, soil quality degradation has become evident due to increased pressure on land resources associated with the expansion and intensification of anthropogenic activities (Stefanowicz et al., 2020). Globally, soil degradation has been defined as a "worldwide contagion" (de Long et al., 2015). Soil degradation includes loss of soil cover, soil erosion, increase in salinity, acidification and contamination through HMs. Contamination through HMs in soil has become a severe problem in many parts of the world (Duan et al., 2016). Deterioration in the soil quality will ultimately menace the sustainability of agricultural production

and pose permanent harm to ecology and human health (Khorshid and Thiele-Bruhn, 2016; Pender, 2009). HMs is cytotoxic, concealed, persistent, and biological accumulator in nature (Zhang et al., 2017). Generally speaking, soil quality depends upon different biological and non-biological factors, which can be severely affected by HMs (Gujre et al., 2021a). Therefore, it is necessary to assess the HMs sources and contamination levels and suggest mitigation measures.

2.3. Soil quality status in India

In India, humungous pressure is brought to bear on 2.4% of land area occupied by 18% and 15% of the global human and livestock population, respectively (Gujre et al., 2021c). Due to soil degradation, the average size of land holdings in agriculture declined from 2.30 to 1.16 ha during 1970–2010. In India, about 60% of the land is rainfed and low in productivity, leading to high inter-annual fluctuations in agricultural output. About 200 million rural poor depend on these rainfed areas for their livelihood (Mythili and Goedecke, 2016). The land resources in India face severe degradation in terms of both availability and fertility. The increase in extreme climatic events, conversion of productive agricultural lands to non-agricultural uses, unscientific disposal of wastes from cities and industries have further exacerbated the magnitude of soil quality degradation. As a result, 147.75 million hectares (Mha) of land in India got degraded (NBSSLUP, 2004). Assam, a northeastern state of India, is affected by various kind of soil degradation issues. In Assam, 0.7 Mha land is affected by soil erosion, while 0.6 and 0.9 Mha is due to acidic soil and complex problem. The total degraded area in the Assam state is 2.2 Mha (Bhattacharyya et al., 2015). The consequent economic and social ramifications result in slower economic growth, heightened food insecurity, increased poverty, and livelihood vulnerability, disrupting sustained

agricultural production in the developing regions, especially in the tropical regimes (Gujre et al., 2021c).

2.4. Existing challenges to the soil quality

In a predominantly rural area with very little scientific and management intervention, such rapidly decreasing soil fertility threatens the people's livelihood. In Assam, the soil remains the center point of rural and urban environments, and in both places, soil quality management is critical. In Assam, one of the significant reasons for deteriorating soil quality is the unscientific management of MSW. The waste consists of synthetic products that contaminate the agricultural soils with carcinogenic HMs (Asgher, 2004). In developing countries such as India, unscientific disposal of MSW is of significant environmental and health concern. In addition to a lack of scientific inputs, there is a lack of administrative will, financial capacity, and poor handling of the complex multidimensional system of solid waste management in developing countries (Tsai et al., 2020). Pollutants releasing from the waste have a higher potential risk toward ecology and human health (Borah et al., 2020; Gujre et al., 2021a; Gujre et al., 2021b). HMs in soil are toxic to plants, animals and humans; furthermore, more prolonged exposure leads to bio-magnification (Gao et al., 2019). MSW generally comprises toxic and carcinogenic HMs in different forms, which could be leached into the soil and water bodies. Cd, Cr and Ni are classified as group 1 carcinogens by the International Agency for Research on Cancer, which are also toxic (IARC, 2018). Furthermore, HMs enrichment can cause severe ecological risks by getting absorbed by different aquatic organisms, thereby entering a complex food chain (Dash et al., 2019). It also directly impacts the functioning of soil enzymes (Singh et al., 2020) and microbial biomass (Zhang et al., 2016).

Across the world, many studies have cited the role of different indices in evaluating soil pollution (Borah et al., 2017, 2018, 2020; Gujre et al., 2021a; Gujre et al., 2021b; Nkinahamira et al., 2019). The indices-based approach is most widely accepted and facilitates identification and quantification of the pollution levels. For evaluating the soil quality, different indices and factors were applied as a comprehensive tool. This tool enables us to assess the severity of the contamination in the area and its surrounding. The waste disposal problem and its segregation are pronounced in developing nations due to a lack of technological interventions and infrastructure. In the Middle East and Africa, many studies have reported and analyzed the soil HMs pollution severity around MSW dumping site stating the area is severely contaminated with lead (Pb), Cd, Ni and mercury (Hg) (Ali et al., 2019; Essien et al., 2019; Ihedioha et al., 2017; Sheijany et al., 2020). Likewise, numerous researchers in Asia have employed environmental and health indices to analyze the risk associated with HMs, such as Thongyuan et al. (2020), who investigated 14 HMs in the areas near the landfill site Chiang Rak Noi town of Phra Nakhon Si Ayutthaya province, Thailand. Ma et al. (2018) assessed the contamination of the HMs including Cr, Pb, Cu, Ni, Zn, Cd, Hg, and arsenic (As) at MSW incinerator in North China using the PLI and reported higher contamination due to the As and Cd. In India, Borah et al. (2020) investigated the contamination of the Cu, Mn and Zn in the Ramsar site of the Guwahati. They observed lower ecological risk due to studied HMs using PERI indices. Recently, Gujre et al. (2021a) used six different indices and factors to investigate Cr, Mn and Zn in the soil adjacent to the MSW dumping site at Boragaon, Guwahati India. Considering the challenging situation in developing nations, especially in waste management, most local bodies have been looking for opportunities to improve their waste collection and segregation system.

Apart from MSW, the unscientific operation of the coal-fired brick industry in rural areas of Assam steadily creating an agro-ecological imbalance. The disturbance generated by the brick-manufacturing adversely affects human health (Bhanarkar et al., 2002). Brick kiln emits a wide range of pollutants like SO_X, NO_X, polychlorinated dibenzo-p-dioxins and dibenzofurans, several of which are the most toxic, HMs generated by operation facilities, raising serious risks (Ying et al., 2020). In addition, excessive HMs accumulation in soil leads to the introduction of toxic elements in the vegetation and influences crop productivity in the nearby area (Jha et al., 2008). On a global scale, India accounts for over 10% of brick production, lies second after China; this leads to the consumption of around 35 million tons of coal per year (Lalchandani and Maithel, 2013). There are about 1.4 lakh brick manufacturing industries in India that produce about 240-260 billion bricks annually (Kamyotra, 2015). In Assam, about 731 brick manufacturing industries are under operation, and most are located in rural areas (Sentinel, 2012).

Across the globe, different studies have carried out to evaluate and assess the harmful effect of BIs (David et al., 2020; Jahan et al., 2016; Khan et al., 2019; Proshad et al., 2017; Ying et al., 2020). For example, a recent study suggested that TBK, in which rubber is used as fuel, possess severe impacts on human health compared to CBK (Khan et al., 2019). The brick kiln is the familiar sources of SO_2, CO, CO_2, NOx, PM, fluoride compounds, and carcinogenic dioxins. Similarly, Kamal et al. (2014) employed the cancer risk model (CR-Model 1) and the incremental lifetime cancer risk model (ILCR-Model 2) to predict the harmful impact of polyaromatic hydrocarbons (PAHs) emanating from the BI in the Punjab province of Pakistan. In India, a study carried out in Assam, and West Bengal India suggested that the brick kiln bottom ash is one of the critical sources of HMs polluting the nearby environment and possess severe human health risks

(Mondal et al., 2017). A similar indices-based study was also carried out in the Tangail district, Bangladesh, which reflected the higher ecological risks from As and Cd (Proshad et al., 2017).

A study deciphering the reproductive and biochemical status of the human revealed higher oxidative stress in the adult male blood of the BI workers and the decreased rate of BMI, RBC count and haematocrit. This might be attributed to the Ni, Cd, Zn and Cr concentrations (Jahan et al., 2016). A questionnaire-based survey was also carried in Nepal, which suggested the higher respiratory disorder like chronic cough (14.3%), phlegm (16.6%) and bronchitis (19.0%) (Sanjel et al., 2017). Apart from human health, some studies have focused on the effect of BI in plants and animals. For example, a survey conducted by Rajbongshi and Das, (2018) suggested an alteration in the plankton community nearby aquatic bodies of the BI. Under these crucial circumstances, utilization of environmentally sound, economically viable and socially acceptable technologies is the need of the hour.

2.5. About biochar

BC is a carbon-based by-product of biomass that has drawn government, academic and scientific attention. Several studies have indicated that BC on land could effectively sequester carbon in soils and thus reduce global warming. When BC is added to the soil, it can also give other possible benefits, including improved fertility and crop productivity. Over millennia, BC in ancient terra preta soil has improved soil health (Gaunt and Lehmann, 2008; Lehmann and Rondon, 2006; Ogawa et al., 2006; Woolf et al., 2010). The origin of this BC can be traced back to volcanic eruptions and forest fires, which burnt the biomass that later accumulated over centuries in the soil. BC enhances the quality of soil and mitigates the greenhouse gaseous (carbon dioxide and methane) directly by sequestering carbon. In addition, BC cum fertilizer application can improve

soil quality, plant growth, and nutrition (Li et al., 2019; Palansooriya et al., 2020). With its innate heterogeneity of pores and surface structure, BC increases available surface area inside the soil, facilitating water and gaseous exchange, nutrient recycling, and carbon storage (Mitra et al., 2016; Ruan et al., 2019; Zheng et al., 2018). The structure of BC also augments the habitat for microbiota within the soil matrix, thus actively aiding soil rejuvenation (Mia et al., 2014; Yu et al., 2019).

2.6. Biochar and its physical properties

A wide range of biomass yield biochar after pyrolysis in an oxygen-depleted environment; for example, wood chips, crop residues, nutshells, seed mill screenings, and algal biomass constitutes the conventional feedstock. BC's physical and chemical characteristics are dictated by feedstock and pyrolysis parameters (Tomczyk et al., 2020; Wan et al., 2020). Wood-based BC has a comparatively higher pH than BC from crop residue and manure (Brewer and Brown, 2012; Shaheen et al., 2019). BC with high pH induces liming effect in the soil (Fig. 2.1). A study indicated an increase of 0.59–1.05 in soil pH after the application of BC from different feedstock (Yuan and Xu, 2010).

Temperatures of 300–700 °C with long residence time are characteristics of slow pyrolysis, whereas fast pyrolysis proceeds at the high heating rate (>700 °C) with a short residence time of less than 10 s. Pore size, a prime component of BC surface morphology, is also dependent on residence time. BC obtained from slow pyrolysis has increased porosity, higher pH (≥7), and a greater surface area of 100–800 m^2 g^{-1} (Weber and Quicker, 2018). When residence time is increased to 120 min at 500–900 °C, the pore size increases, but beyond 120 min, it displays an apparent reduction in size. Micrograph assessment revealed pores with honeycomb-like structures

in certain BC, possibly induced by entwined biopolymers connected by biomolecule structural bonds in feedstock cells (Wu et al., 2016).

Biomass degradation occurs in three stages; the first at less than 150 °C allows evaporation of moisture, light volatile compounds and hemicellulose breakdown. The second ranges from 150 to 400 °C causing cellulose to break down, and in the third stage, decomposition of lignin and combustion of the residual char are triggered by temperatures >400 °C (Narzari et al., 2017). The application of BC is predominantly dictated by its surface morphology (Ho et al., 2017; Mitra et al., 2016; Premarathna et al., 2019). BC with broader surface area and pores offer potential sites for soil microbiota, creating diverse microbial community structures inside the soil (Lehmann et al., 2011; Jaafar et al., 2014). In addition, the porous structure offers rich carbon, nutrient, and water sources for microbial growth and reproduction (Yu et al., 2019). The enlarged pore surface is thus helpful for soil nutrition retention, enhanced nutrient transfer to plants, and concomitant prevention of nutrient loss from soil (Pradhan et al., 2018).

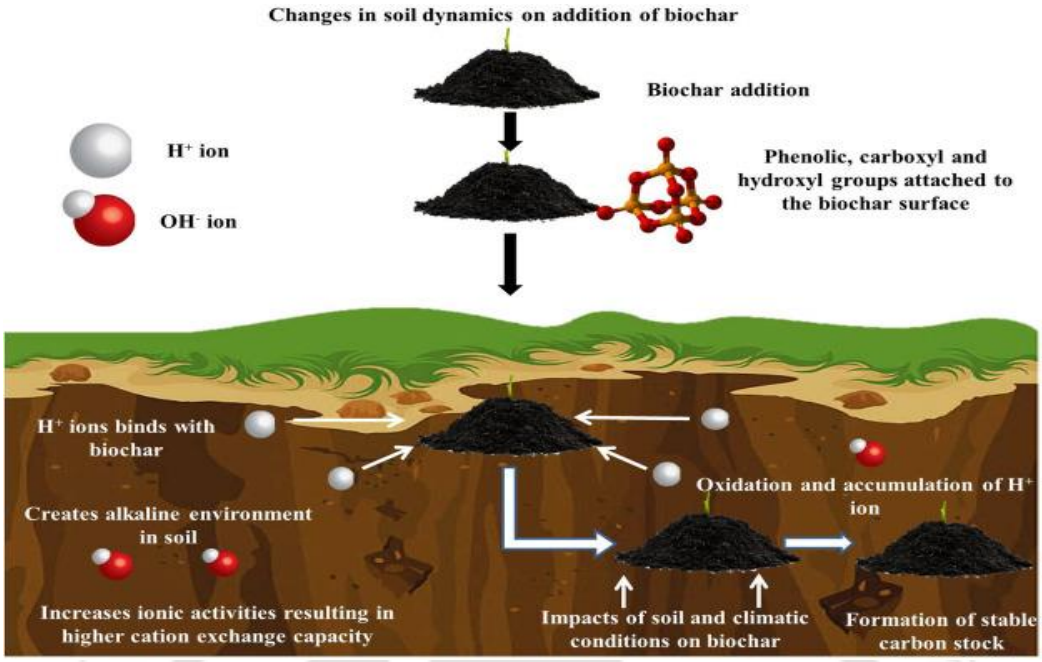

Fig. 2.1. Impact of biochar amendment on soil dynamics (Source: Gujre et al., 2021c).

2.7. Biochar and its chemical properties

The chemical properties of biochar are pH-dependent, which ultimately increases CEC (Cation exchange capacity) (Ahmad et al., 2014). The elemental analysis of BC reveals that it mainly consists of carbon (C), hydrogen (H), oxygen (O), ash, and trace amounts of nitrogen (N) and sulphur (S). In most of the BC, H, N and O contents decreased with an increase in temperature, ascribed to loss of volatile components and dehydration of organic compounds (Weber and Quicker, 2018). Similarly, H:C and O:C ratios also decreased with the increase in temperature, suggesting that the BC surfaces were more aromatic and less hydrophobic (Weber and Quicker, 2018). O:C ratio is an indicative tool used to assess the stability of BC (Fig. 2.2). If O:C is less than 0.2, it indicates a stable BC with a half-life of more than 1000 years. However, if the ratio is 0.2–0.6, it shows an intermediate half-life period (100–1000 years) (Spokas, 2013).

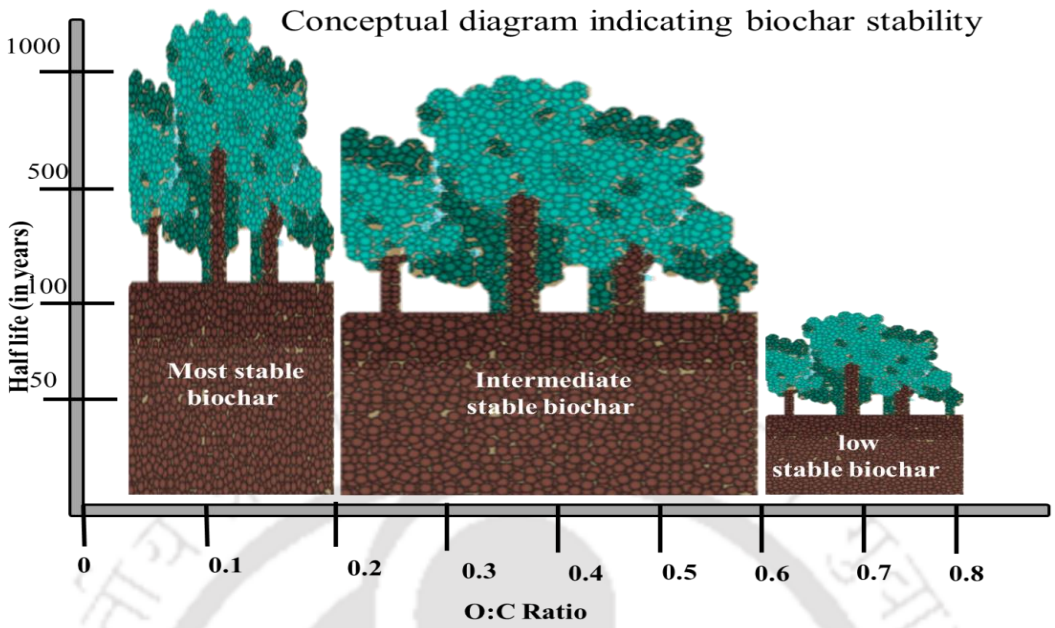

Fig. 2.2. Conceptual diagram indicating BC stability using O:C ratio.

Higher surface area and alkaline BC supports higher metal absorption capacities and faster uptake kinetics (Shen et al., 2019). BC is helpful in the remediation of other toxic elements such as dioxins (Chai et al., 2012), PAHs (Kong et al., 2018; Xiong et al., 2017), and pesticides (Mandal et al., 2017; Niazi et al., 2018; Tabassum et al., 2019).

2.8. Biochar and its effect on soil biology

BC is virtually persistent because it interacts with various biotic and abiotic components in addition to the soil. In general, BC addition to the soil results in an overall increase in crop productivity, crop yield, soil microbial biomass, and rhizobia nodulation (He et al., 2016; Kim et al., 2016; Lehmann and Joseph, 2015; Sun et al., 2019; Yu et al., 2019). The productivity prevails with BC induced the increase in various macro and micronutrients contents in soil. BC orifices benefit microbial communities with increased air supply, humidity, nutrient content and residence

time, thereby increasing the physical and chemical conditions for plant and biota growth (O'Neill et al., 2009; Yu et al., 2019; Jaafar et al., 2014). Consequently, the addition of BC expands the incidence and diversity of bacterial population in anthrosol soil up to a depth of 1 m (O'Neill et al., 2009). Some theories also suggest that BC ultimately alters microbial community structure and soil enzyme activities, as microbes living within its pores are shielded from microarthropods (Fig. 2.3).

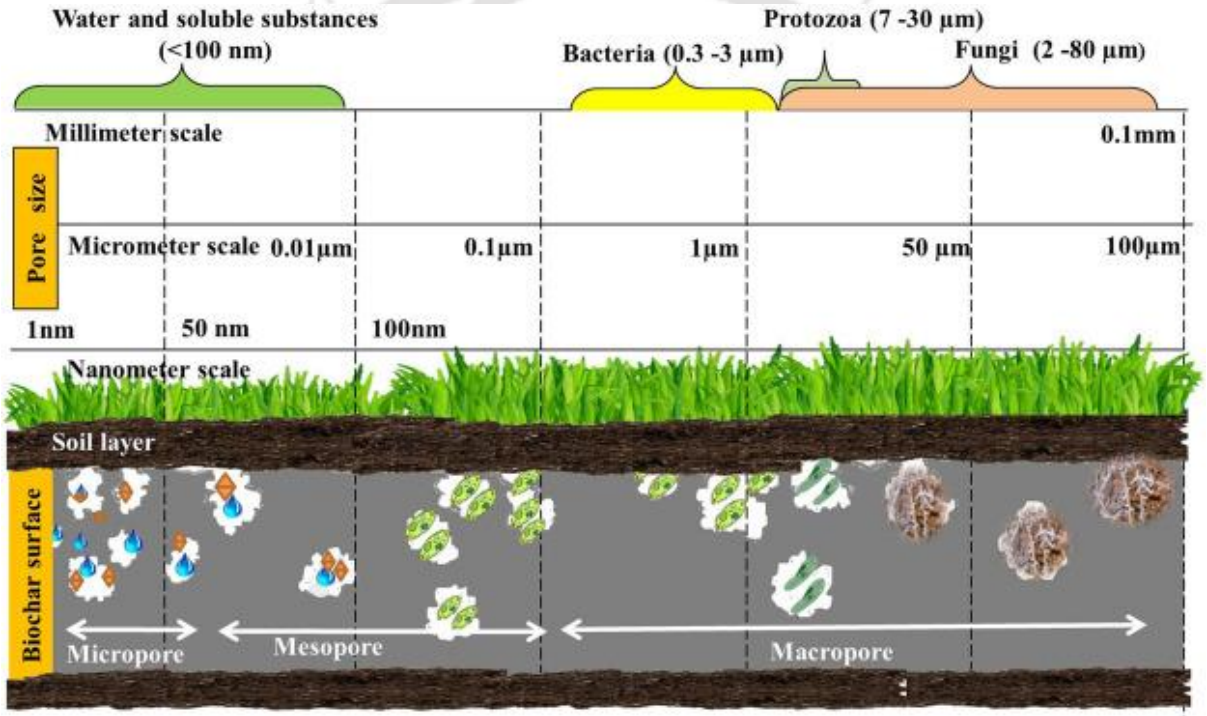

Fig. 2.3. Biochar and its interaction with different microbes inside the soil (Source: Gujre et al., 2021c).

In soil, the application of BC provides the microorganisms with an artificial habitat. Bacteria present in the soil accumulate in the pore with 0.3-3 µm pore size, i.e., *Pseudomonas* sp., *Azotobacter* sp., *Rhizobium* sp. and *Azospirilium* sp. (Awasthi et al., 2020). The pore size of the 7-

30 µm is suitable for protozoa habitation. Protozoa play a crucial role in mineralizing nutrients, making them available for plants and other microbiota. The majority of protozoa consume bacteria, but the vampyrellids group of amoebae, eat fungi. Another essential microorganism in the soil is fungi, which found in between 2-80 µm pore size, protecting them from fungivores rodents. In soil biota, three different fungi are dominants, i.e. decomposers, mutualists, pathogens, or parasitic fungi. Water molecules in the soil have a deep relation with the decomposition of BC, and it plays a significant role in processes such as dissolution, hydrolysis, carbonation and de-carbonation, hydration, and redox reactions. Thus, water and dissolved substances would fill in the pore size between 1 nm to 50 nm or < 100 nm and provide balanced water resources to microbes. Even though practice of BC application for soil quality is prevalent in India, the modern and scientific approach to integrated soil quality management is new and has not been critically evaluated in the present context. The extent of this BC effect, as well as the impact of increased frequency of application and plant response to biochar application rate, needs to be further determined or explored.

To date, limited research has been performed to examine the effects of AHB incorporation on soil properties. Therefore, the present study was conducted to evaluate the hypothesis that AHB applications would enhance soil productivity, but the degree of benefit depends on their quality and quantity of applications. Therefore, AHB applications for integrated soil quality management were considered a vital characteristic and studied in present research in great detail.

References

Ahmad, M., Rajapaksha, A.U., Lim, J.E., Zhang, M., Bolan, N., Mohan, D., 2014. Biochar as a sorbent for contaminant management in soil and water: a review. Chemosphere 99, 19-33.

Alam, P., Sharholy, M., Ahmad, K., 2020. A study on the landfill leachate and its impact on groundwater quality of Ghazipur area, New Delhi, India, in: Recent Developments in Waste Management. Springer, Singapore, pp. 345-358.

Ali, I.H., Siddeeg, S.M., Idris, A.M., Brima, E.I., Ibrahim, K.A., Ebraheem, S.A., Arshad, M., 2019. Contamination and human health risk assessment of heavy metals in soil of a municipal solid waste dumpsite in Khamees-Mushait, Saudi Arabia. Toxin Rev. 40 , 102-115.

Asgher, Md. S., 2004. Land Degradation and Environmental Pollution: Impact of Brick Kilns, B. R. Publishing Corporation, Delhi.

Awasthi, M.K., Duan, Y., Liu, T., Awasthi, S.K., Zhang, Z., 2020. Relevance of biochar to influence the bacterial succession during pig manure composting. Bioresour. Technol. 122962.

Bhanarkar, A. D., Gajghate, D. G., Hasan, M. Z., 2002. Assessment of air pollution from small scale industry. Environ. Monit. Assess. 2002, 80, 125–133.

Bhattacharyya, R., Ghosh, B. N., Mishra, P. K., Mandal, B., Rao, C. S., Sarkar, D., Das, K., Anil K. S., Lalitha, M., Hati K., Joseph A.F., 2015. Soil Degradation in India: Challenges and Potential Solutions. Sustainability, 7, 3528-3570.

Borah, P., Paul, A., Bora, P., Bhattacharyya, P., Karak, T., Mitra, S., 2017. Assessment of heavy metal pollution in soils around a paper mill using metal fractionation and multivariate analysis. Int. J. Environ. Sci. Technol. 14, 1-14.

Borah, P., Singh, P., Rangan, L., Karak, T., Mitra, S., 2018. Mobility, bioavailability and ecological risk assessment of cadmium and chromium in soils contaminated by paper mill wastes. Groundwater Sust. Dev. 6, 189-199.

Borah, P., Gujre, N., Rene, E.R., Rangan, L., Paul, R.K., Karak, T., Mitra, S., 2020. Assessment of mobility and environmental risks associated with copper, manganese and zinc in soils of a dumping site around a Ramsar site. Chemosphere 254, 126852.

Brewer, C.E., Brown, R.C., 2012. Biochar. In: Sayigh, A. (Ed.), Comprehensive Renewable Energy. Elsevier, Oxford, pp. 357-384.

Chai, Y.Z., Currie, R.J., Davis, J.W., Wilken, M., Martin, G.D., Fishman, V.N., Ghosh, U., 2012. Effectiveness of activated carbon and biochar in reducing the availability of polychlorinated dibenzo-p-dioxins/dibenzofurans in soils. Environ. Sci.Technol. 46, 1035-1043.

Dash, S., Borah, S.S., Kalamdhad, A., 2019. A modified indexing approach for assessment of heavy metal contamination in Deepor Beel, India. Ecol. Indic. 106, 105444.

David, M., Turi, N., Ain, Q. ul, Rahman, H., Jahan, S., 2020. Evaluation of environmental effects of heavy metals on biochemical profile and oxidative stress among children at brick kiln sites. Arch. Environ. Occup. Heal. https://doi.org/10.1080/19338244.2020.1854645

De Long, C., Cruse, R., Wieneret, J., 2015. The Soil Degradation Paradox: Compromising Our Resources When We Need Them the Most. Sustainability 7, 866–879.

Duan, H., Hu, J., Tan, Q., Liu, L., Wang, Y., Li, J., 2016. Systematic characterization of generation and management of e-waste in China. Environ. Sci. Pollut. Res. Int. 23, 1929–1943.

Essien, J.P., Inam, E.D., Ikpe, D.I., Udofia, G.E., Benson, N.U., 2019. Ecotoxicological status and risk assessment of heavy metals in municipal solid wastes dumpsite impacted soil in Nigeria. Environ. Nanotechnol. Monit. Manag. 11, 100215.

FAO. 2018. The future of food and agriculture – Alternative pathways to 2050. Summary version. Rome. 60 pp

Gao, M., Lin, Y., Shi, G.Z., Li, H.H., Yang, Z.B., Xu, X.X., Xian, J.R., Yang, Y.X., Cheng, Z., 2019. Bioaccumulation and health risk assessments of trace elements in housefly (*Musca domestica* L.) larvae fed with food wastes. Sci. Total Environ. 682, 485-493.

Gaunt, J.L., Lehmann, J., 2008. Energy balance and Emissions associated with biochar sequestration and pyrolysis bioenergy production. Environ. Sci. Technol. 42, 4152-4158.

Gujre, N., Mitra, S., Soni, A., Agnihotri, R., Rangan, L., Rene, E.R., Sharma, M.P., 2021a. Speciation, contamination, ecological, and human health risks assessment of heavy metals in soils dumped with municipal solid wastes. Chemosphere, 262, 128013.

Gujre, N., Rangan, L., Mitra, S., 2021b. Occurrence, geochemical fraction, ecological and health risk assessment of cadmium, copper and nickel in soils contaminated with municipal solid wastes. Chemosphere, 271, 129573.

Gujre, N., Soni, A., Rangan, L., Tsang, D.C. and Mitra, S., 2021c. Sustainable improvement of soil health utilizing biochar and arbuscular mycorrhizal fungi: A review. Environ. Pollut. 115549.

He, L., Liu, Y., Zhao, J., Bi, Y., Zhao, X., Wang, S., Xing, G., 2016. Comparison of strawbiochar-mediated changes in nitrification and ammonia oxidizers in agricultural oxisols and cambosols. Biol. Fertil. Soils 52, 137-149.

Ho, S.H., Chen, Y.D., Yang, Z.K., Nagarajan, D., Chang, J.S., Ren, N.Q., 2017. High-efficiency removal of lead from wastewater by biochar derived from anaerobic digestion sludge. Bioresour. Technol. 246, 142-149.

IARC, 2018. Chromium (IV) compounds. IARC monograph 100C. https://monographs.iarc.fr/wp-content/uploads/2018/06/mono100C-9.pdf (accessed 24 January 2020).

Ihedioha, J.N., Ukoha, P.O., Ekere, N.R., 2017. Ecological and human health risk assessment of heavy metal contamination in soil of a municipal solid waste dump in Uyo, Nigeria. Environ. Geochem. Health 39, 497-515.

Jaafar, N.M., Clode, P.L., Abbott, L.K., 2014. Microscopy observations of habitable space in biochar for colonisation by fungal hyphae from soil. J. Integr. Agr. 13, 483-490.

Jahan, S., Falah, S., Ullah, H., Ullah, A., Rauf, N., 2016. Antioxidant enzymes status and reproductive health of adult male workers exposed to brick kiln pollutants in Pakistan. Environ. Sci. Pollut. Res. 23, 12932–12940.

Jha, S. K., Nayak, A. K., Sharma, Y. K., Mishra, V. K., Sharma, D. K., 2008. Fluoride accumulation in soil and vegetation in the vicinity of brick fields. Bull. Environ. Contam. Toxicol. 80, 369–373.

Kamal, A., Malik, R.N., Martellini, T., Cincinelli, A., 2014. Cancer risk evaluation of brick kiln workers exposed to dust bound PAHs in Punjab province (Pakistan). Sci. Total Environ. 493, 562–570.

Kamyotra, J. S., 2015. Brick Kiln in India. Anil Agarwal Dialogue, March 11, 2015. https://cdn.cseindia.org/docs/aad2015/11.03.2015%20Brick%20Presentation.pdf (accessed 23 December 2019).

Khan, M.W., Ali, Y., De Felice, F., Salman, A., Petrillo, A., 2019. Impact of brick kilns industry on environment and human health in Pakistan. Sci. Total Environ. 678, 383–389.

Khorshid, M.S.H., Thiele-Bruhn, S., 2016. Contamination status and assessment of urban and non-urban soils in the region of Sulaimani City, Kurdistan, Iraq. Environ. Earth Sci. 75, 1171.

Kim, H.-S., Kim, K.-R., Yang, J.E., Ok, Y.S., Owens, G., Nehls, T., Wessolek, G., Kim, K.- H., 2016. Effect of biochar on reclaimed tidal land soil properties and maize (*Zea mays* L.) response. Chemosphere 142, 153-159.

Kong, L., Gao, Y., Zhou, Q., Zhao, X., Sun, Z., 2018. Biochar accelerates PAHs biodegradation in petroleum-polluted soil by biostimulation strategy. J. Hazard Mater. 343, 276-284.

Lalchandani, D., Maithel S., 2013. Towards Cleaner Brick Kilns in India: A win–win approach based on Zigzag firing technology. New Delhi: Greentech Knowledge Solutions Pvt. Ltd.

Lehmann, J., Rillig, M.C., Thies, J., Masiello, C.A., Hockaday, W.C., Crowley, D., 2011. Biochar effects on soil biota e a review. Soil Biol. Biochem. 43, 1812-1836.

Lehmann, J., Rondon, M., 2006. Bio-char soil management on highly weathered soils in the humid tropics. In: Uphoff, N., Ball, A.S., Fernandes, E., Herren, H., Husson, O., Laing, M., Palm, C., Pretty, J., Sanchez, P., Sanginga, N., Thies, J. (Eds.), Biological Approaches to Sustainable Soil Systems. Taylor and Francis Group, Boca Raton, pp. 517-530.

Li, Q., Zhang, H., Guo, S., Fu, K., Liao, L., Xu, Y., Cheng, S., 2019. Groundwater pollution source apportionment using principal component analysis in a multiple landuse area in southwestern China. Environ. Sci. Pollut. Res. 27, 9000-9011.

Ma, W., Tai, L., Qiao, Z., Zhong, L., Wang, Z., Fu, K., Chen, G., 2018. Contamination source apportionment and health risk assessment of heavy metals in soil around municipal solid waste incinerator: a case study in North China. Sci. Total Environ. 631, 348-357.

Mandal, A., Singh, N., Purakayastha, T.J., 2017. Characterization of pesticide sorption behaviour of slow pyrolysis biochars as low-cost adsorbent for atrazine and imidacloprid removal. Sci. Total Environ. 577, 376-385.

Mia, S., Van Groenigen, J., Van de Voorde, T., Oram, N., Bezemer, T., Mommer, L., Jeffery, S., 2014. Biochar application rate affects biological nitrogen fixation in red clover conditional on potassium availability. Agric. Ecosyst. Environ. 191, 83-91.

Mitra, S., Singh, P., Manzoor, S., Bhattacharyya, P., Bera, T., Kumar Patra, A., Rangan, L., Borah, P., 2016. Can rice and wheat biochar amendment protect the carbon loss from tropical soils-An experimental study. Environ. Prog. Sustain. Energy 35, 183-188.

Mondal, A., Das, S., Sah, R.K., Bhattacharyya, P., Bhattacharya, S.S., 2017. Environmental footprints of brick kiln bottom ashes: Geostatistical approach for assessment of metal toxicity. Sci. Total Environ. 609, 215-224.

Mythili, G., Goedecke, J., 2016. Economics of land degradation in India. In: Economics of land degradation and improvement–a global assessment for sustainable development. Springer, Cham. pp. 431-469.

Narzari, R., Bordoloi, N., Sarma, B., Gogoi, L., Gogoi, N., Borkotoki, B., Kataki, R., 2017. Fabrication of biochars obtained fromvalorization of biowaste and evaluation of its physicochemical properties. Bioresour. Technol. 242, 324-328.

NBSSLUP (National Bureau of Soil Survey & Land Use Planning), 2004. Soil Map (1:1 Million Scales); NBSS&LUP: Nagpur, India.

Niazi, N.K., Bibi, I., Shahid, M., Ok, Y.S., Burton, E.D., Wang, H., Shaheen, S.M., Rinklebe, J., Lüttge, A., 2018. Arsenic removal by perilla leaf biochar in aqueous solutions and groundwater: an integrated spectroscopic and microscopic examination. Environ. Pollut. 232, 31-41.

Nkinahamira, F., Suanon, F., Chi, Q., Li, Y., Feng, M., Huang, X., Yu, C.P., Sun, Q., 2019. Occurrence, geochemical fractionation, and environmental risk assessment of major and trace elements in sewage sludge. J. Environ. Manag. 249, 109427.

O'Neill, B., Grossman, J., Tsai, M.T., Gomes, J.E., Lehmann, J., Peterson, J., Neves, E., Thies, J.E., 2009. Bacterial community composition in Brazilian Anthrosols and adjacent soils characterized using culturing and molecular identification. Microb. Ecol. 58, 23-35.

Ogawa, M., Okimori, Y., Takahashi, F., 2006. Carbon sequestration by carbonization of biomass and forestation: three case studies. Mitig. Adapt. Strategies Glob.Change 11, 429-444.

Palansooriya, K.N., Shaheen, S.M., Chen, S.S., Tsang, D.C., Hashimoto, Y., Hou, D., Bolan, N.S., Rinklebe, J., Ok, Y.S., 2020. Soil amendments for immobilization of potentially toxic elements in contaminated soils: a critical review. Environ. Int. 134, 105046.

Pender, J., 2009. The world food crisis, land degradation, and sustainable land manage- ment: linkages, opportunities, and constraints. IFPRI, New York, USA.

Pradhan, A., Chan, C., Roul, P.K., Halbrendt, J., Sipes, B., 2018. Potential of conservation agriculture (CA) for climate change adaptation and food security under rainfed uplands of India: a transdisciplinary approach. Agric. Syst. 163, 27-35.

Premarathna, K.S.D., Rajapaksha, A.U., Sarkar, B., Kwon, E.E., Bhatnagar, A., Ok, Y.S., Vithanage, M., 2019. Biochar-based engineered composites for sorptive decontamination of water: a review. Chem. Eng. J. 372, 536-550.

Proshad, R., Ahmed, S., Rahman, M., Kumar, T., 2017. Apportionment of Hazardous Elements in Agricultural Soils Around the Vicinity of Brick Kiln in Bangladesh. J. Environ. Anal. Toxicol. 07. https://doi.org/10.4172/2161-0525.1000439

Rajbongshi, P., Das, T., 2018. Effect of Brick Kiln Industries on the Community Composition of Plankton in the Lentic Systems of Cachar District in Assam, Northeast India. Int. J. Res. Appl. Sci. Eng. Tech. 6, 2473-2480.

Ruan, X., Sun, Y., Du, W., Tang, Y., Liu, Q., Zhang, Z., Doherty, W., Frost, R.L., Qian, G., Tsang, D.C.W., 2019. Formation, characteristics, and applications of environmentally persistent free radicals in biochars: a review. Bioresour. Technol. 281, 457-468.

Sanjel, S., Khanal, S.N., Thygerson, S.M., Carter, W.S., Johnston, J.D., Joshi, S.K., 2017. Respiratory symptoms and illnesses related to the concentration of airborne particulate matter among brick kiln workers in Kathmandu valley, Nepal. Ann. Occup. Environ. Med. 29, 1–12.

Sentinel, 2013. 193 illegal brick kilns in Assam. India Environment Portal http://www.indiaenvironmentportal.org.in/content/374053/193-illegal-brick-kilns-in-assam/ (assessed 24 January 2019).

SET (Swiss Environmental Technology AG), 2021. Land degradation and pollution. http://www.asente.ch/environmental-issues/land-degradation (assessed 24 April 2021).

Shaheen, S.M., Niazi, N.K., Hassan, N.E., Bibi, I., Wang, H., Tsang, D.C., Ok, Y.S., Bolan, N., Rinklebe, J., 2019. Wood-based biochar for the removal of potentially toxic elements inwater and wastewater: a critical review. Int. Mater. Rev. 64, 216-247.

Sheijany, M.S.P., Shariati, F., Mahabadi, N.Y., Karimzadegan, H., 2020. Evaluation of heavy metal contamination and ecological risk of soil adjacent to Saravan municipal solid waste disposal site, Rasht, Iran. Environ. Monit. Assess. 192,1-19.

Shen, Z., Hou, D., Jin, F., Shi, J., Fan, X., Tsang, D.C., Alessi, D.S., 2019. Effect of production temperature on lead removal mechanisms by rice straw biochars. Sci. Total Environ. 655, 751-758.

Spokas, K.A., 2013. Impact of biochar field aging on laboratory greenhouse gas production potentials. Glob. Change Biol. Bioenergy 5, 165-176.

Stefanowicz, A.M., Kapusta, P., Zubek, S., Stanek, M., Woch, M.W., 2020. Soil organic matter prevails over heavy metal pollution and vegetation as a factor shaping soil microbial communities at historical Zn–Pb mining sites. Chemosphere, 240, 124-922.

Sun, H., Dan, A., Feng, Y., Vithanage, M., Mandal, S., Shaheen, S.M., Rinklebe, J., Shi, W., Wang, H., 2019. Floating duckweed mitigated ammonia volatilization and increased grain yield and nitrogen use efficiency of rice in biochar amended paddy soils. Chemosphere 237, 124532.

Tabassum, R.A., Shahid, M., Niazi, N.K., Dumat, C., Zhang, Y., Imran, M., Bakhat, H.F., Hussain, I., Khalid, S., 2019. Arsenic removal from aqueous solutions and groundwater using agricultural biowastes-derived biosorbents and biochar: a column-scale investigation. Int. J. Phytoremediation 21, 509-518.

Thongyuan, S., Khantamoon, T., Aendo, P., Binot, A., Tulayakul, P., 2020. Ecological and health risk assessment, carcinogenic and non-carcinogenic effects of heavy metals contamination in the soil from municipal solid waste landfill in Central, Thailand. Hum. Ecol. Risk Assess. 27, 876-897.

Tomczyk, A., Sokołowska, Z., Boguta, P., 2020. Biochar physicochemical properties: pyrolysis temperature and feedstock kind effects. Rev. Environ. Sci. Biotechnol. 19, 191-215.

Tsai, F.M., Bui, T.D., Tseng, M.L., Wu, K.J., 2020. A causal municipal solid waste management model for sustainable cities in Vietnam under uncertainty: A comparison. Resour. Conserve. Recy. 154, 104599.

Wan, Z., Sun, Y., Tsang, D.C.W., Hou, D., Cao, X., Zhang, S., Gao, B., Ok, Y.S., 2020. Electroactive biochars for green and sustainable environmental remediation: mechanisms and outlook. Green Chem. 22, 2688-2711.

Weber, K., Quicker, P., 2018. Properties of biochar. Fuel 217, 240-261.

Woolf, D., Amonette, J.E., Street-Perrot, F.A., Lehmann, J., Joseph, S., 2010. Sustainable biochar to mitigate global climate change. Nat. Commun. 1, 1-9.

Wu, A., Yan, J., Xu, W., Li, X., 2016. Fabrication of waste biomass derived carbon by pyrolysis. Mater. Lett. 173, 60-63.

Xiong, B., Zhang, Y., Hou, Y., Arp, H.P.H., Reid, B.J., Cai, C., 2017. Enhanced biodegradation of PAHs in historically contaminated soil by M. gilvum inoculated biochar. Chemosphere 182, 316-324.

Ying, Y., Ma, Y., Li, X., Lin, X., 2020. Emission and migration of PCDD/Fs and major air pollutants from co-processing of sewage sludge in brick kiln. Chemosphere 129120.

Yu, H., Zou, W., Chen, J., Chen, H., Yu, Z., Huang, J., Tang, H., Wei, X., Gao, B., 2019. Biochar amendment improves crop production in problem soils: a review. J. Environ. Manag. 232, 8-21.

Yuan, J.H., Xu, R.K., 2010. The amelioration effects of low temperature biochar generated from nine crop residues on an acidic Ultisol. Soil Use Manag. 27, 110-115.

Zhang, C., Nie, S., Liang, J., Zeng, G., Wu, H., Hua, S., Liu, J., Yuan, Y., Xiao, H., Deng, L., Xiang, H., 2016. Effects of heavy metals and soil physicochemical properties on wetland soil microbial biomass and bacterial community structure. Sci. Total Environ. 557, 785-790.

Zhang, J., Hua, P., Krebs, P., 2017. Influences of land use and antecedent dry-weather period on pollution level and ecological risk of heavy metals in road-deposited sediment. Environ. Pollut. 228, 158–168

Zheng, H., Wang, X., Chen, L., Wang, Z., Xia, Y., Zhang, Y., Wang, H., Luo, X., Xing, B., 2018. Enhanced growth of halophyte plants in biochar-amended coastal soil: roles of nutrient availability and rhizosphere microbial modulation. Plant Cell Environ. 41, 517-532

CHAPTER 3

Assessment of the physico-chemical properties of the soils as contaminated by municipal solid waste and brick kiln bottom ash

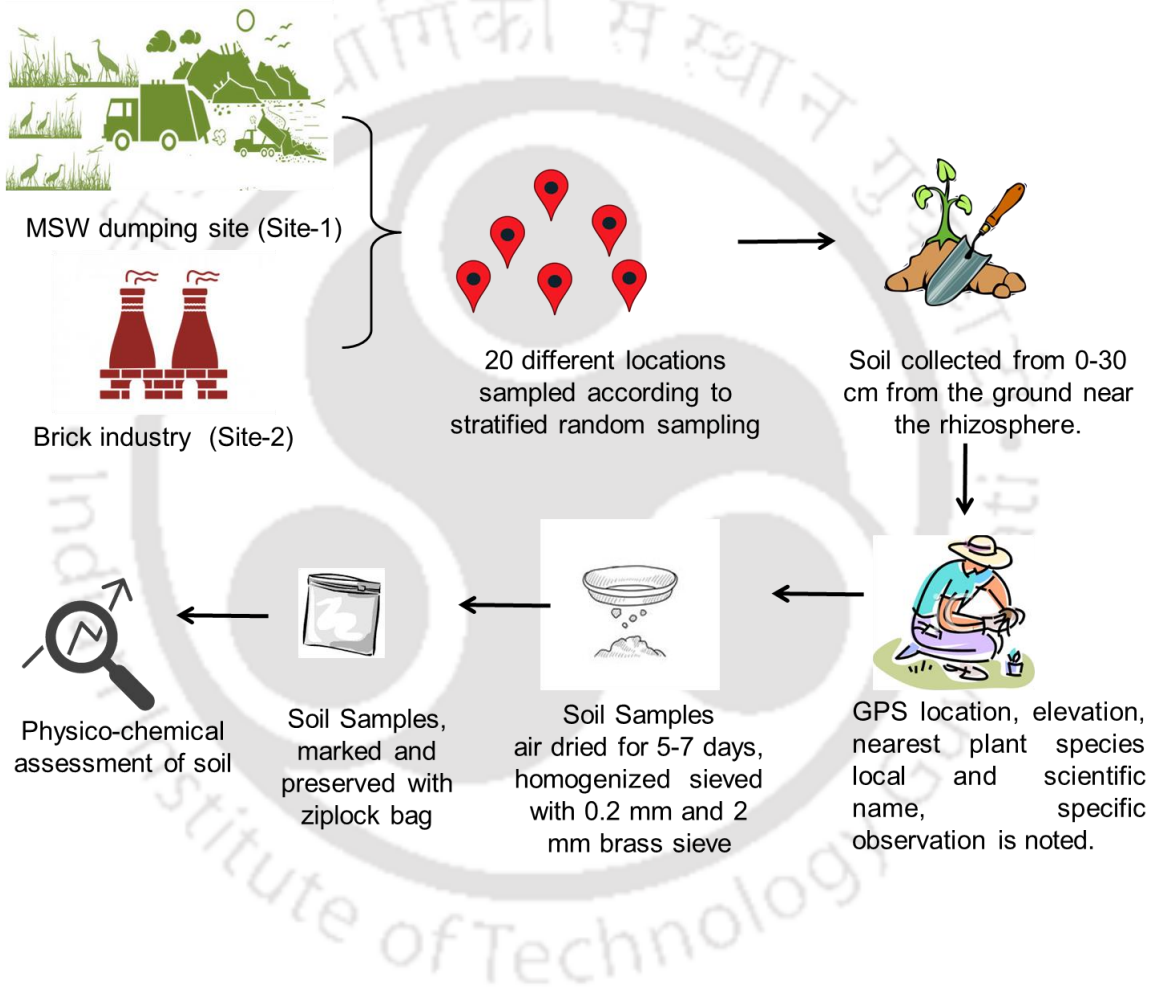

"*This chapter deals with the physico-chemical assessment of the two contaminated sites, i.e., MSW dumping site at Boragaon, Guwahati, Assam (Site-1) and Brick industry at Borghat, Tezpur, Assam (Site-2).*"

3. Assessment of the physico-chemical properties of the soils contaminated by municipal solid waste and brick kiln bottom ash

3.1. Introduction

Soil is a natural medium for growth, derived from the unconsolidated mineral matter of the Earth's outer crust. Soil is forged by a multitude of factors broadly categorized into edaphic, genetic, and environmental; or more specifically, parent material, climate, surface contamination, organisms, and topography. Therefore, soil profile analysis is a crucial step in defining surface characteristics, which in turn, directly impact the immediate environment and human health (ICAR, 2011). In the present study, the two sites under investigation, were subject to detailed soil profiling, followed by investigation of the physical and chemical properties. pH, electrical conductivity (EC), cation exchange capacity (CEC), soil texture, density, soil moisture content (SMC), and color constituted the physical parameters. Concurrently, organic carbon (OC), organic matter (OM), available nitrogen (Av N), sodium (Av Na), phosphorus (Av P), potassium (Av K), and microbial biomass carbon (MBC) constituted the chemical parameters.

Soil pH is a fundamental but very critical parameter, as it influences the bioavailability of nutrients and HMs. The EC evaluates the ionic transport in a solution, which in turn elucidates the soluble mineral salt content of the soil. Pure water with no mineral content is very poor conductor of electric current, whereas water with dissolved salts in soil conducts current, and thereby enhances its conductivity. The CEC is the total number of exchangeable cations that any given soil can hold; it is an important physical property, dictated by the clay and organic matter content. Physical and chemical properties of the soil share a direct relationship with the surface area of the particles, therefore, the soil texture or particle size distribution exert a significant influence. The

soil texture comprises mainly of three parts; sand (0.2 – 0.02 mm diameter), silt (0.002-0.02 mm diameter), and clay (<0.002 mm diameter).

Among chemical parameters, OM, OC, AvN, AvK, and AvP are critical factors. OM is derived from tissue of dead organisms, organic material < 2 mm size, and other microorganisms at various stages of decomposition. OM plays a significant role in the stabilization of the soil, water retention, and nutrient recycling; and is thus crucial for the agricultural productivity and environmental resilience (FAO, 2017). OC is the prime source of energy for soil microorganisms, though its availability is dependent on the state of transformation or decomposition (Datta et al., 2021). The soil OC/OM is attributed to play multifaceted roles in providing various ecosystem functions and services. Av N in the soil occurs predominantly in the organic form (97-99%) and is directly associated with the activity of microorganisms which enable decomposition of organic matter (NH_4-N and NO_3-N). However, denitrification increases rate of release of Av N from the soil organic matter. Av P is helpful in growth of legumes, as it enhances the activity of nitrogen fixing bacteria. In addition, it aids formation of seeds, fruits, and stimulates root growth and development. Av K helps in formation and synthesis of the amino acids and protein from ammonium ions which are absorbed from the soil and important for photosynthetic activities of leaves.

The aforementioned macronutrients of the soil are significantly affected by the MSW and brick kiln bottom ash. In India, extensive urbanization and consumerism have disarrayed well established modes of solid waste management. The unsegregated metal wastes from batteries, household lighting equipment, computers and other electronic waste have become predominant stationary pollution sources, with long-lasting impact (Dash et al., 2019; Gujre et al., 2021). In a similar manner, unregulated establishment of BIs have detrimental effects on the surrounding soil

micro-environment. The continuous deposition of the ash emanating from the kiln degrades the soil quality status and intensifies harmful human health issues (David et al., 2020).

3.2. Materials and methods

3.2.1. Study area and climate

Site-1:

The MSW dumping site is primarily located in Boragaon, Guwahati Assam, India (26° 06. 915' N latitude and 91° 40. 669' E longitude) (Fig. 3.1). The site comes under a moderate subtropical climate with three distinct seasons. The annual average temperature, precipitation and humidity are 24.22 (± 4.30) °C, 1720 (± 127) mm and 76.6 (± 8.6) %, respectively (Weather atlas, 2020). The 1.8 km^2 site is bound on the southwest by Boragaon and on the east by Deepor Beel. Boragaon is the sub urban part of the Guwahati city. Deepor beel is a Ramsar site (No. 1207), which lies in the eastern part of the dumping site. It is an important riverine wetland located about 10 km southwest of Guwahati city which covering an area of 9.27 km^2. The wetland receives the monsoon precipitation and inflows from Kalmani and Bharalu rivers. The two main soil types of the study area are laterite with silty and silty loam type texture. In the past few decades, the Guwahati city has experienced a significant escalation in industrialization, urbanization, and consumerism; the humungous waste generated is aggravated by lack of segregation at the multiple collection points. The dumping site thus contains unsegregated heaps of waste, composting plant, metal segregation unit and slums. City wastes are mostly organic, along with other elements like plastics, glasses, metallic cans, trash from the fuel residues, paint, ceramics, and other manufactured products, which are non-biodegradable and act as potential sources of HMs (Fig. 3.2a-d).

Site-2:

The study site is located at Borghat, in Tezpur, Assam, India (N 26º 42.934' and E 92º 50.055') (Fig. 3.1.). The BI site, covering an area of 1.1 km^2, is typically surrounded by the agriculture land, a feature inherent to BI locations in Assam. Therefore, rice fields are present in the south and the eastern part of the site, with some human habitation in the western side. The BIs located at Borghat use locally available sand and clay for brickmaking, and fuel the kilns with coal and rubber tires. Unregulated emission of the fly ash, inefficient combustion, and substantial loss of the thermal energy, were evident during the operation of the brick kilns. Consequently, the substantial emission of suspended particulate matter and generation of toxic bottom ash, have contaminated the topsoil of the adjacent and neighbouring agriculture lands. In addition, their proximity to the residential areas (0.5 km from Kiln) posed serious threats to human health and ecosystem of the rural areas (Fig. 3.2 e and f).

Control site:

The selected control Site was an agricultural near Pamohi, Guwahati (N 26º 06. 304 'and E 91º 41. 634'). The Site was planted with rice (*Oryza sativa*) during sampling. The physico-chemical characteristic of the control site are pH 5.26 (±0.53) ; EC 0.09 (±0.00) mS cm^{-1}; CEC 17.98 (±1.98) cmol kg^{-1}; BD 1.07 (±0.06) g cm^{-3}; PD 2.05 (±0.14) g cm^{-3}; POR 47.91 (±2.40) %; MC 60.57 (±4.24) % ; OC 85.19 (±5.54) g kg^{-1}; Av Na 89.60 (±7.97) kg ha^{-1}; Av K 90.25 (±4.15) kg ha^{-1}; Av P 55.62 (±1.60) kg ha^{-1}; Av N 1.68 (±0.08) g $kg^{-1}$and MBC 38.33(±2.51) µg g^{-1}.

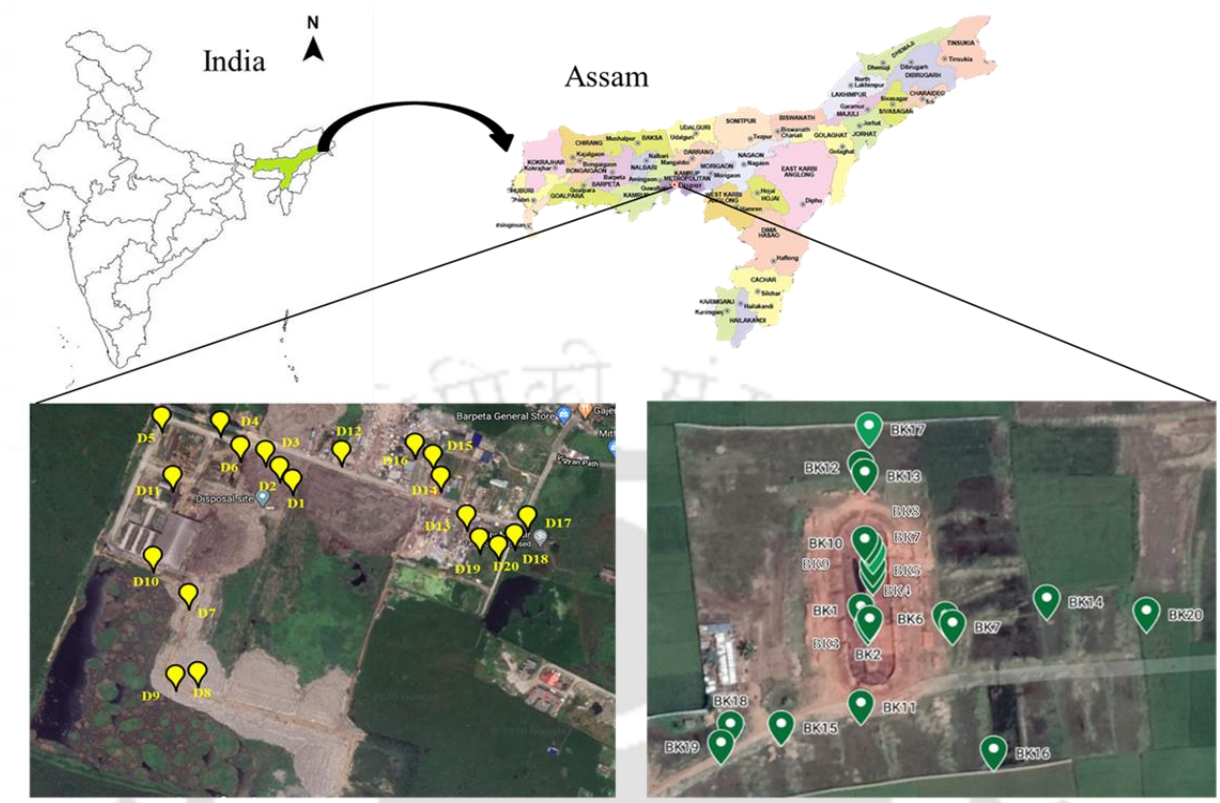

Site 1: MSW dumping site, Boragaon, Guwahati

Site 2: Brick kiln site, Borghat, Naapam, Tezpur

Fig. 3.1. Map showing study area, Site-1: MSW dumping site, Boragaon, Guwahati, Assam and; Site-2: Brick kiln site, Borghat, Naapam, Tezpur, Assam.

3.2.2. Sample collection and prepartion

A total of 20 soil samples (D1 to D20; BK1 TO BK20) were collected from sites 1 & 2 to a depth of 15 cm using stratified random sampling. Samples were collected in zip lock bags, marked with date of sampling, and location ID. Further details pertaining to global positioning system (GPS) location, elevation, approximate distance from point source, direction, nearest plant species, name (local and scientific), and any other specific observations were recorded. Sampling locations were tagged using GPS Gramin e-Trex 10. Samples were collected during the dry season (December, 2017), then air-dried for 4–8 days and large impurities were removed manually, followed by

sieving with 0.2 mm and 2 mm brass sieves. For further analysis, soil samples were stored in acid-washed containers.

3.2.3. Physico-chemical analysis

The soil pH and EC were measured at a ratio of 1:2.5 (*w/v*), using digital pH and EC meter (HI 98129, Hanna Instruments, USA) (Biswas and Mukherjee 2008). The CEC in soil samples was determined using the sodium saturation method (Bower et al., 1952). The particle density (PD), bulk density (BD), and porosity (POR) were determined using the pycnometer method (Blake and Hartge, 1986). Soil texture was assessed using the hydrometer method (Gee and Bauder, 1979). SMC was measured by the gravimetric method; the soil sample was placed in an oven at 105^0 C and dried to a constant weight. OC was determined by the potassium dichromate ($K_2Cr_2O_7$) method (Walkley and Black 1934) and OM was determined by factorial multiplication. It was assumed that OM contains about 58% of the OC (100/58=1.724) (Soil Survey Staff, 2011). The Kjeldahl method was employed for the Av N estimation (Subbiah and Asija, 1956) using an automatic digester cum distillation unit of Velp Scientifica UDK 129. Av Na and Av K were estimated using flame photometer; Systronics Model 126 following (Knudsen et al., 1982). Av P was estimated using Olsen method for alkaline soil (Olsen et al., 1954) and Bray's method (Bray and Kurtz, 1945) for acidic soil; the spectrophotometric analysis was carried out using Genesys 10S UV-Vis Spectrophotometer. MBC was estimated using new chloroform fumigation extraction method (Vance, 1987).

(a) MSW dumping site, Boragaon, Guwahati (Site-1)

(b) Greater adjutant (*Leptoptilos dubius*) on heap of MSW, Boragaon, Guwahati

(c) Western side of MSW dumping site

(d) Dumping vehicle of Guwahati Municipal Corporation (GMC)

(e) Brick Kiln industry at Napaam, Tezpur

(f) Brick Kiln industry surrounded by agriculture land at Napaam, Tezpur

Fig. 3.2. MSW dumping site, Boragaon, Guwahati (a,b,c,d) and brick industry (BI), Napaam, Tezpur, Assam, India (e and f).

3.3. Results and discussion

3.3.1. Physico-chemical parameters for MSW dumping site, Boragaon, Guwahati (Site-1)

Soil color, is one of the most common and clearly identifiable characters of soil, and it is based on 3 components: hue (a specific color value), value (darkness and lightness), and chroma (color intensity). Dusky brown (5YR 2/2), grayish red (Grayish red), brownish black (5YR 2/2) hues were observed in the studied area. Soil texture is the relative portion of sand, silt and clay. The textural class of the study area was mainly silt, while only 3 sampling locations i.e., D5, D11, D15 belonged to the silt loamy class (Table 3.1). Soils with these textures are reported to demonstrate HMs stabilization under higher oxidative–reductive potential (ORP) (Zhang et al., 2014). Soil pH is a vital parameter that determines the nature of soil. The soil pH exhibited was moderately to slight acidic, where 77% samples belonged to moderately acidic 5.6 (±0.45) - 6.9 (±0.55) with least significant difference (LSD) =0.76 following Duncan multiple range test (DMRT) at P=0.0.5, and the rest (23%) were slightly acidic in nature (3.3a). Neutral to slightly acidic pH is known to favor diffusion of HMs in soil (Qiao et al., 2020). EC indicates the ionic conductivity or the level of dissolved salts in the contaminated soil; they ranged from 0.06 (±0.00) - 1.24 (±0.14) mS cm^{-1} (LSD=0.04) (3.3b). Among all other sampling locations, comparatively higher salinity was observed in samples collected near the central heap of the dumping sites (D1 to D10). Although, overall salt concentration in the MSW soil was reported less than 0.15%, depicting the no effect of salinity on the soil. The CEC is an indication of the capacity of the soil to hold exchangeable cations on its surface. The CEC of MSW dumping site displayed values from 3.34 (±0.43) -33.53 (±2.51) cmol kg^{-1} (LSD=4.60) (Fig. 3.3c). While, D1 to D4 displayed a medium CEC (10-25 cmol kg^{-1}), a comparatively higher CEC was observed in D19. The latter might be attributed to the dense vegetation of banana trees, contributing higher organic matter to the soil and thereby enhancing CEC. Soil normally contains a finite amount of water, held on the surface of the colloids and pores

of other particles, which can be expressed as the SMC. SMC in the soil of MSW dumping site ranged from 6.58 (±0.47) - 37.50 (±2.57) % (LSD=2.64) (Fig. 3.3d). The highest SMC was observed at D17 (37.50%) adjacent to agriculture land, enriched by moisture in the inter-aggregate pore spaces, and intra-aggregate pore spaces. Overall, SMC helps in identifying the type of wastes (dry waste, wet waste, and leachate) that contaminate the soil from the MSW dumping site.

Table 3.1

Sampling locations and texture class of the soil at MSW dumping site (Site-1), Boragaon, Guwahati, Assam.

Sampling locations	Latitude (N)	Longitude (E)	Elevation (m amsl)	Clay (%)	Silt (%)	Sand (%)	USDA [a]texture class
D1	26º 06. 915 '	91º 40. 669'	44	1.36 (±0.02)	93.28 (±0.02)	05.36 (±0.01)	Si
D2	26º 06. 917 '	91º 40. 663'	33	1.36 (±0.01)	92.28 (±0.01)	06.36 (±0.01)	Si
D3	26º 06. 922 '	91º 40. 654'	45	1.36 (±0.01)	97.28 (±0.02)	01.36 (±0.02)	Si
D4	26º 06. 932 '	91º 40. 648'	45	1.36 (±0.01)	97.28 (±0.01)	01.36 (±0.02)	Si
D5	26º 06. 967 '	91º 40. 590'	37	7.36 (±0.01)	75.00 (±0.01)	17.64 (±0.01)	SiL
D6	26º 06. 949 '	91º 40. 630'	45	1.35 (±0.01)	97.28 (±0.01)	01.36 (±0.03)	Si
D7	26º 06. 77 9'	91º 40. 618'	46	1.36 (±0.02)	94.00 (±0.01)	04.64 (±0.02)	Si
D8	26º 06. 728 '	91º 40. 639'	49	2.36 (±0.02)	95.00 (±0.01)	02.64 (±0.02)	Si
D9	26º 06. 728 '	91º 40. 625'	49	3.36 (±0.02)	88.00 (±0.02)	08.64 (±0.02)	Si
D10	26º 06. 824 '	91º 40. 601'	60	4.36 (±0.01)	82.28 (±0.02)	13.36 (±0.03)	Si
D11	26º 06. 898 '	91º 40. 608'	48	7.36 (±0.02)	76.28 (±0.02)	16.36 (±0.02)	SiL
D12	26º 06. 921 '	91º 40. 731'	45	3.36 (±0.01)	80.28 (±0.02)	16.36 (±0.02)	Si
D13	26º 06. 854 '	91º 40. 860'	48	3.36 (±0.01)	87.28 (±0.01)	09.36 (±0.01)	Si
D14	26º 06. 889 '	91º 40. 857'	46	2.36 (±0.01)	89.28 (±0.01)	08.36 (±0.02)	Si
D15	26º 06. 913 '	91º 40. 844'	46	1.36 (±0.03)	78.28 (±0.02)	20.36 (±0.02)	SiL
D16	26º 06. 921 '	91º 40. 839'	41	1.35 (±0.02)	96.28 (±0.02)	02.36 (±0.01)	Si
D17	26º 06. 858 '	91º 40. 902'	41	1.36 (±0.02)	93.28 (±0.02)	05.36 (±0.02)	Si
D18	26º 06. 842 '	91º 40. 899'	47	1.35 (±0.01)	97.28 (±0.02)	01.35 (±0.02)	Si
D19	26º 06. 853 '	91º 40. 885'	42	1.36 (±0.01)	97.00 (±0.01)	01.64 (±0.01)	Si
D20	26º 06. 848 '	91º 40. 882'	45	3.36 (±0.02)	91.28 (±0.01)	05.36 (±0.02)	Si

Note: Si =Silt; SiL =Silt-loam

[a]USDA, 1993

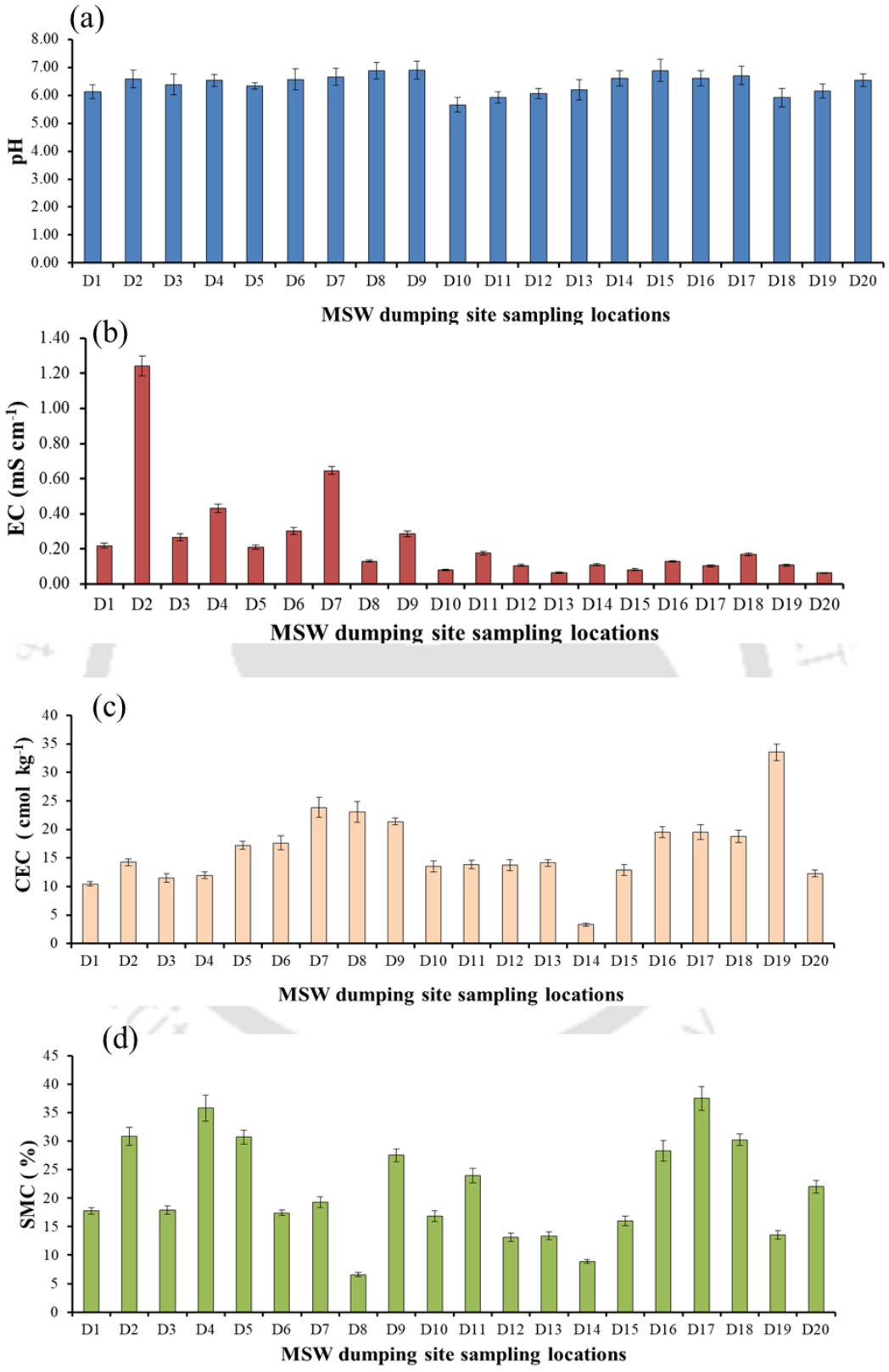

Fig. 3.3. Physico-chemical parameters at Site-1 (a) pH; (b) EC; (c) CEC; (d) SMC.

Soil BD is defined as the ratio of the mass of the oven dry soil to its bulk volume. While increased porosity means more space for roots to grow, conversely, lower porosity obstructs the rhizosphere growth of the plants. It is generally desirable to have soil with a low BD (<1.5 g cm^{-3}) (Hunt and Gilkes, 1992). Entire range of BD, i.e., 0.86 (±0.01) -1.36 (±0.10) (LSD=0.14) in the MSW dumping site are within 1.5 g cm^{-3},indicating optimum movement of air and water through the soil. Soil PD was determined from individual particles minus the void in between the pores. It ranged from 1.52 (±0.13) -2.58 (±0.18) g cm^{-3} (LSD=0.28) (Fig. 3.4). Generally, POR is an index of the porosity of the soil, along with information on the size, shape, arrangement of particles and voids inside soil matrix. In the samples under investigation, the POR ranged from 29.22 (±2.34) - 59.81 (±4.78) % (LSD=6.90) (Fig. 3.4). Comparatively higher POR was reported from D2 and D17 sampling locations as compared to the other sampling locations.

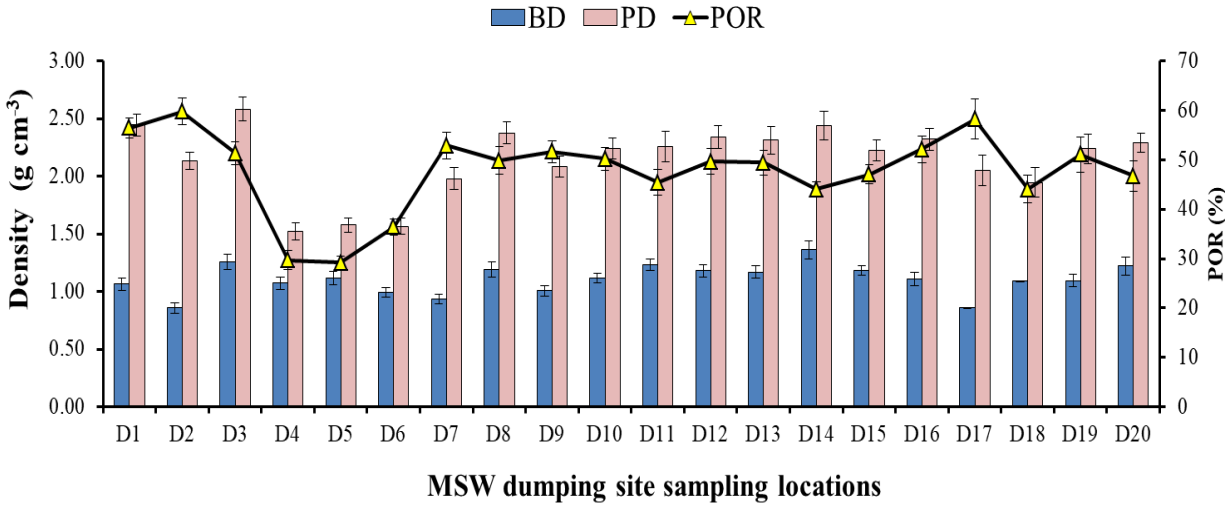

Fig. 3.4. BD, PD and POR of the sampling locations at Site-1.

Av N is the one of the fundamental plant macro nutrients is the organically bound nitrogen, or minerisable nitrogen, or Av N. Av N content in the soil ranged from 0.03 (±0.00) -1.46 (±0.11)

(LSD= 0.07) g kg^{-1}. The higher nitrogen content exhibited at location D8 was attributed to the abundance of Castor plants (*Ricinus communis*) at the sampling location (Fig. 3.5a). The Castor oil plant, and in particular the castor meal, has contains a high nitrogenous content 7.54% (Rosiane et al. 2011). Av Na has both exchangeable and water soluble parts; the former is dependant on the surrounding environment, and the latter is derived from the salinity of water. At the MSW dumping site, it ranged from 18.70 (±1.45) -187.77 (±10.02) (LSD= 13.30) kg ha^{-1}. D19 located near the washing area of the local inhabitants, exhibited the highest value (Fig. 3.5b). Av K is another essential macronutrient required for photosynthesis, protein synthesis, starch formation, and translocation of sugars. In general, a very low (< 120 kg ha^{-1}) Av K was reported over the entire study area; and ranged from 7.28 (±0.39) -77.28 (±4.37) (LSD= 4.58) kg ha^{-1}. The highest concentration obtained from D2 site (77.28 kg ha^{-1}), which was contaminated by unburned hospital waste materials (Fig. 3.5b). Inside soil matrix Av P is converted into unavailable forms both in acidic and alkaline soils, as Al/Fe phosphate or $Ca_3(PO_4)_2$ respectively. However, the extremely low Av P concentrations at Site-1 (5.03 (±0.32) -14.08 (±0.60) kg ha^{-1}) (LSD= 0.83), were incompatible with the optimal range of phosphorus for fertile soils (72-137 kg ha^{-1}); and suggested a near absence of phosphorus in the site (ICAR, 2011). The proximity of D18 to agricultural fields, seemed to stimulate a higher threshold value Av P (14.08 kg ha^{-1}), (Fig. 3.5b).

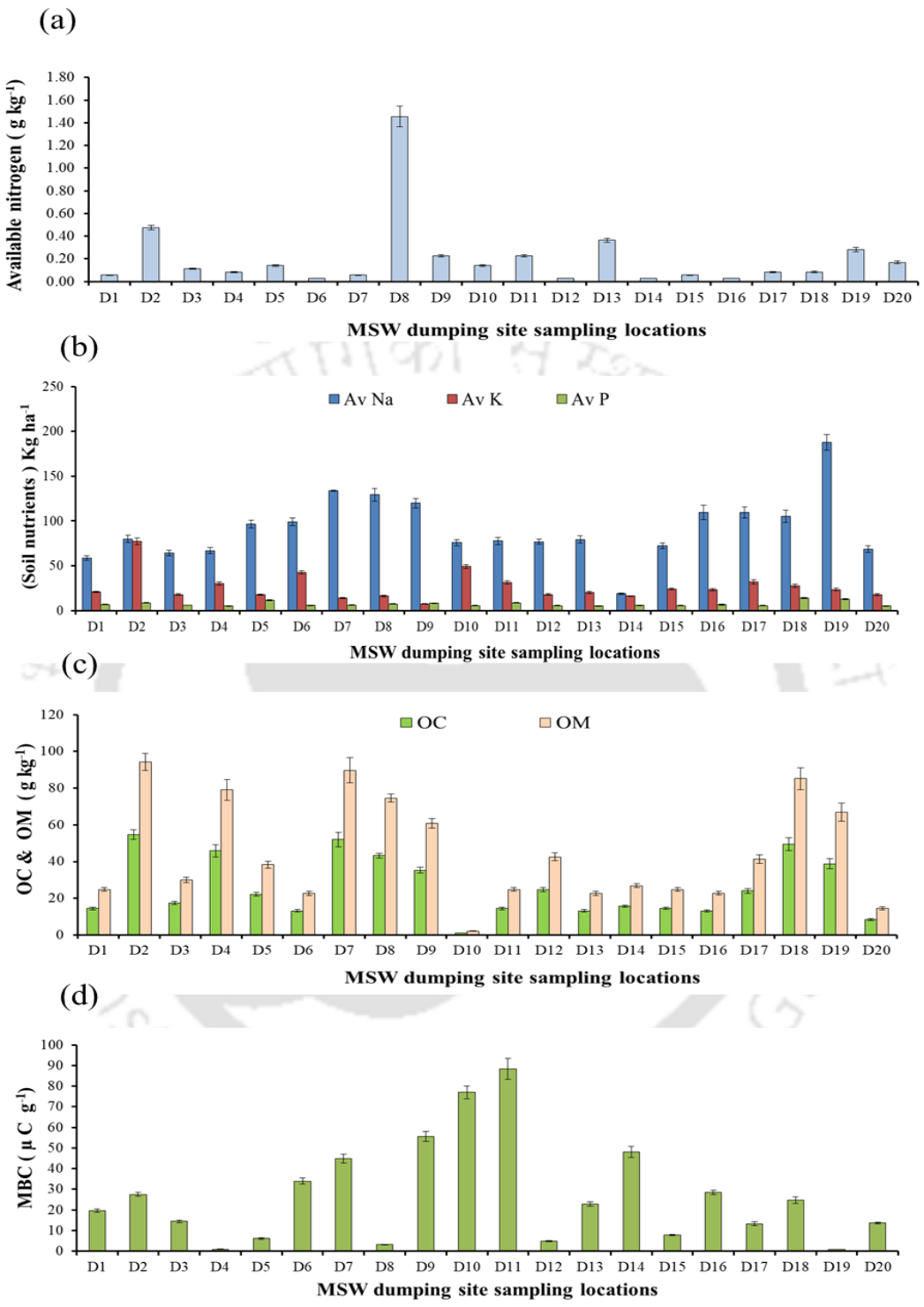

Fig. 3.5. Physico-chemical parameters at Site-1 (a) Av N; (b) Av Na, P, K; (c) OC & OM; (d) MBC.

OC generally consists of living organisms, besides, plant and dead animal residues, acting as reservoir for essential elements. It is the most chemically active portion of the soil. In the MSW site, OC content in soil ranged from 1.20 (±0.10) to 54.71 (±4.65) (LSD= 0.42) g kg^{-1}; whereas OM observed values ranged from 2.07 (±0.17) -94.31 (±8.02) g kg^{-1} (LSD= 9.05) (Fig. 3.5c). Higher OC was reported at Site-1 which might be due to theorganic decomposition of plant and animal residues, root exudates, living and dead microorganisms, and soil biota. MBC is comprised mainly of bacteria and fungi, which assisted in decomposition of crop residues and organic matter in soil (Fig. 3.5d). MBC content in soil ranged from 0.87 (±0.06) to 88.47 (±6.26) µg g^{-1} (LSD= 5.24). Higher MBC was reported in D9 and D11 locations, where the soil was collected from the root zone of diverse plant species, creating a niche for bacteria and fungi.

3.3.2. Physico-chemical parameters for brick kiln industry at Napaam, Tezpur (Site-2)

Soil color is an indicator of the mineral content of the area, and local aerobic and anaerobic conditions. Red is the predominant color near the brick kiln area. Different colors like very dusky red (10 R2/2), and grayish red (5R 4/2) were observed near the brick kiln, indicating presence of hematite (Fe_2O_3) in the topsoil, while sampling locations further away from the kiln displayed brownish gray hues (5YR 4/1). Soil texture of the site 2 was mostly silt. The entire soil pH was slightly alkaline and ranged from 5.06 (±0.51) -8.00(±0.78) (LSD=1.02), which might be due to silica SiO_2 and iron oxides Fe_2O_3 present in the bricks (Fig. 3.6a) (Khan et al., 2019). EC is an indication of the total ionized constituents of soil which ranged from 0.21 (±0.02) - 0.80 (±0.08) mS cm^{-1} (LSD=0.04) (Fig. 3.6b). Effect of salinity was negligible in Site-2 with a total salt concentration of less than 0.15%. Although, comparatively higher salinity was observed at BK1 and BK2 thus, it was observed that salinity decreased with distance from kiln.

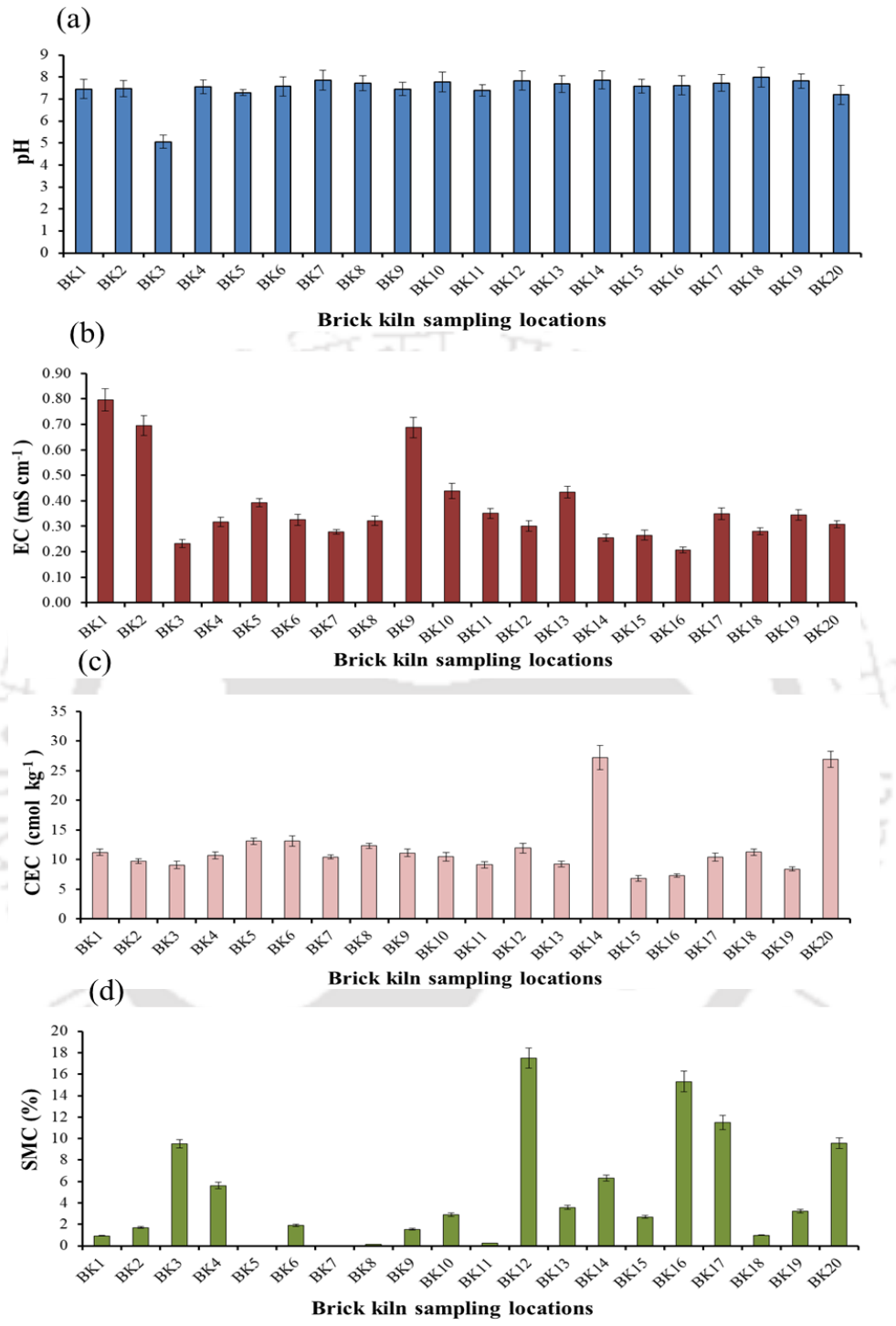

Fig. 3.6. Physico-chemical parameters at Site-2 (a) pH; (b) EC; (c) CEC; (d) SMC.

The CEC depends on the amount and kind of clay and organic matter present. In Site-2 the CEC ranged from 6.79 (±0.85) - 27.24 (±3.54) (LSD=1.795) cmol kg^{-1}, indicating low concentration of clay in soil matrix, with a concomitant reduction in surface for cation adsorption (Fig. 3.6c). BK14 reported higher CEC as compared to other sampling locations, which is near areas under agricultural soil. SMC of the Site-2 ranged from 0.01 (±0.51) - 17.48 (±0.51) %, (LSD=1.81) showing lack of soil moisture in the topsoil, due to operation of the brick industry (Fig. 3.6d). Soil BD and porosity reflects the size, shape and arrangement of particles and voids. BD was observed within 1.5 g cm^{-3}, i.e, 0.98 (±0.09) - 1.21 (±0.12) (LSD=0.160). PD was comparatively higher in BK-3, BK-15, BK-16, which might be attributed to large size of the particles, and particularly in BK-3, PD ranged from 1.38 (±0.12)- 4.21 (±0.29) (LSD=0.34). POR in soil ranged from 19.97 (±1.80) - 74.57 (±5.22) % (LSD=7.46) (Fig. 3.7). Higher porosity was investigated in the sampling locations, adjacent to rice and areca nut plants; while POR in BK-3 is due to the porous nature of the burnt ash from the kiln.

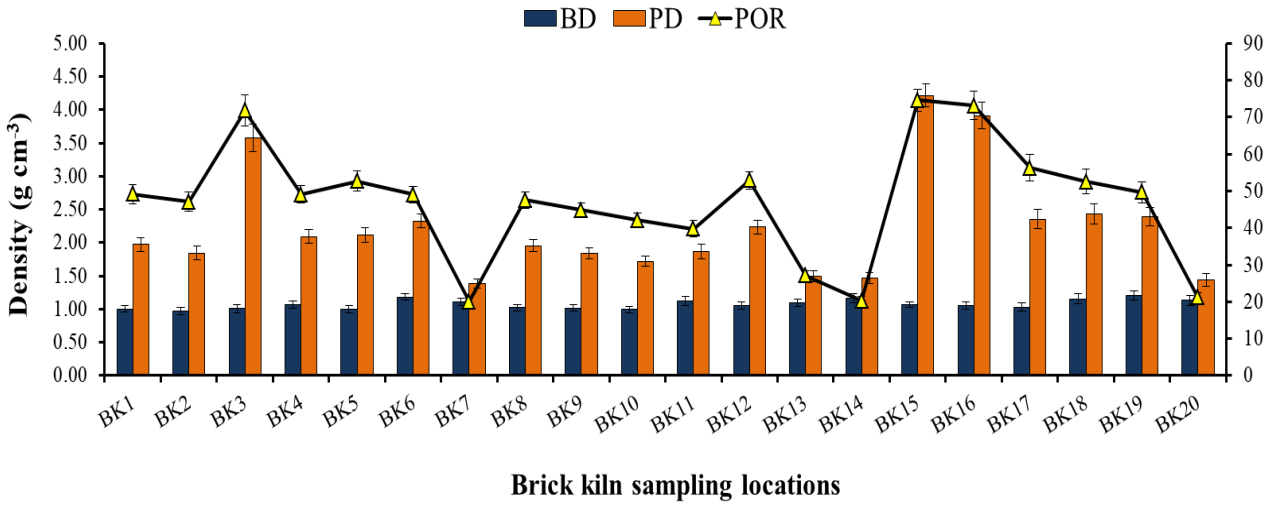

Fig. 3.7. BD, PD and POR of the sampling locations at Site-2.

Table 3.2

Sampling locations and textural classes of the soil at brick kiln industry (Site-2), Napaam, Tezpur, Assam.

Sampling locations	Latitude (N)	Longitude (E)	Elevation (m amsl)	Clay (%)	Silt (%)	Sand (%)	USDA texture class
BK1	26º 42. 934 '	92º 50. 055'	64	1.36 (±0.01)	95.28 (±0.02)	3.36 (±0.01)	Si
BK2	26º 42. 931 '	92º 50. 057'	65	1.36 (±0.02)	95.28 (±0.01)	3.36 (±0.01)	Si
BK3	26º 42' 55.85 '	92º 50' 3.56'	48	1.36 (±0.01)	91.28 (±0.02)	7.36 (±0.02)	Si
BK4	26º 42. 943 '	92º 50. 058'	62	4.86 (±0.01)	81.78 (±0.01)	13.36 (±0.02)	Si
BK5	26º 42. 944 '	92º 50. 058'	62	4.36 (±0.01)	83.28 (±0.01)	12.36 (±0.01)	Si
BK6	26º 42. 932 '	92º 50. 076'	62	4.86 (±0.01)	81.78 (±0.01)	13.36 (±0.03)	Si
BK7	26º 42. 932 '	92º 50. 078'	60	4.36 (±0.01)	82.28 (±0.01)	13.64 (±0.02)	Si
BK8	26º 42. 947 '	92º 50. 057'	61	3.36 (±0.02)	86.28 (±0.01)	10.36 (±0.02)	Si
BK9	26º 42. 949 '	92º 50. 057'	66	3.36 (±0.02)	85.28 (±0.02)	11.36 (±0.02)	Si
BK10	26º 42. 950 '	92º 50. 056'	62	4.86 (±0.01)	86.78 (±0.02)	8.36 (±0.03)	Si
BK11	26º 42. 911 '	92º 50. 055'	64	5.36 (±0.02)	71.28 (±0.02)	23.36 (±0.02)	SiL
BK12	26º 42. 968 '	92º 50. 055'	63	5.36 (±0.01)	74 (±0.02)	20.64 (±0.02)	SiL
BK13	26º 42. 966 '	92º 50. 056'	63	5.36 (±0.01)	85.28 (±0.01)	09.36 (±0.01)	Si
BK14	26º 42. 933 '	92º 50. 101'	60	3.86 (±0.01)	78.78 (±0.01)	17.36 (±0.02)	SiL
BK15	26º 42' 54.5 '	92º 50' 2.1'	63	3 (±0.03)	71.64 (±0.02)	25.36 (±0.02)	SiL
BK16	26º 42' 54.15'	92º 50' 5.45'	62	8.36 (±0.01)	61.28 (±0.02)	30.36 (±0.01)	SiL
BK17	26º 42. 977 '	92º 50. 057'	63	5.36 (±0.02)	81 (±0.02)	13.64 (±0.02)	Si
BK18	26º 42' 54.4'	92º 50' 1.34'	63	4.86 (±0.01)	81.78 (±0.02)	13.36 (±0.02)	Si
BK19	26º 42' 54.4 '	92º 50' 1.28'	60	2.36 (±0.01)	89.28 (±0.01)	8.36 (±0.01)	Si
BK20	26º 42. 933 '	92º 50. 0126'	62	3.36 (±0.02)	80.28 (±0.01)	16.36 (±0.02)	Si

Note: Si =Silt; SiL =Silt-loam

[a]USDA, 1993

Av N in soil ranged from 0.28 (±0.02) -2.24 (±0.03) g kg $^{-1}$ (LSD=0.81) (Fig. 3.8a). Location BK-19, was the only sampling locations that displayed 46% of nitrogen content due to presence of rice plants and availability of nitrogen from urea. The below detectable limits (BDL) of Av N form BK1 to BK5, reflected the high macro nutrient stress faced by locations near to the kiln (Bisht and Neupane, 2015). Overall, very low nitrogen content was observed from BK1 to BK10 (< 0.625 g kg $^{-1}$); while a medium range was visible till BK-17, with a clear reduction thereafter. Av Na values in soil ranged from 14.00 (±0.91) - 35.50 (±3.91) (LSD=3.92) kg ha^{-1}; with the maximal value reported from BK19 sampling location (35.50 kg ha^{-1}) (Fig. 3.8b). Likewise, Av K ranged from 0.67 (±0.05) -24.08 (±1.88) (LSD=2.56) kg ha^{-1}, however very low potassium (< 120 kg ha^{-1}) was observed in the Site-2 (Fig. 3.8b). Av P concentration in soil ranged from 0.06-11.81 (LSD=0.78)

kg ha^{-1}, and the entire study area lacked phosphorus (Suwal, 2018) (Fig. 3.8b). OC content in the soil varied from 1.40 (±0.09) -28.20 (±1.97) (LSD=1.80) g kg^{-1}. Medium range of OC occurred at BK1 and BK2, while comparatively higher OC was reported in BK3. Beyond sampling location BK-10, slight increase in OC was observed which correlates with more organic decomposition of plant and animal residues, root exudates, living and dead microorganisms, and soil biota (Bisht and Neupane, 2015). Following a similar trend, OM occurred in the range of 2.41 (±0.17) - 48.62 (±0.51) g kg^{-1} (LSD=3.11) (Fig. 3.8c). MBC content in soil ranged from 2.13 (±0.18) -27.27 (±2.04) (LSD=2.05) µg g^{-1}. Higher range occurred in BK-3 which offered higher pore surfaces that acted as niches for microbial community such as fungi etc (Fig. 3.8d).

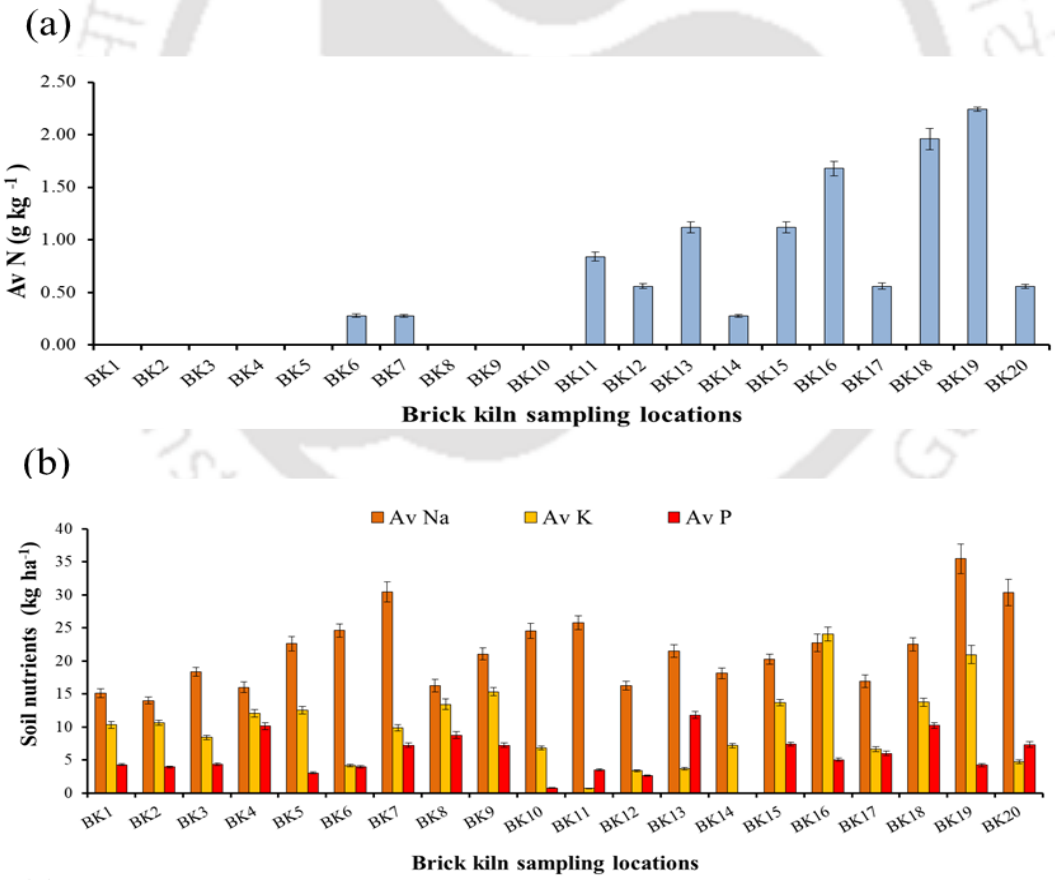

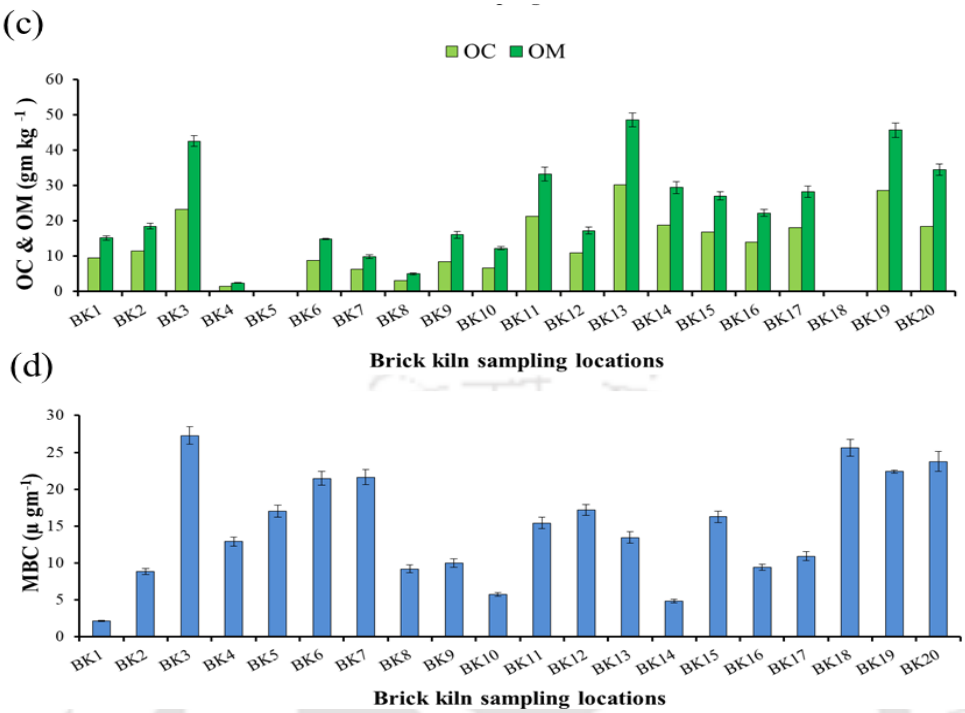

Fig. 3.8. Physico-chemical parameters at Site-2 (a) Av N; (b) Av Na, P, K; (c) OC & OM; (d) MBC.

3.4. Conclusion

A slightly acidic pH was observed in Site-1, whereas a slightly alkaline pH was observed in Site-2; this might be due to the nature of pollutants. Results revealed that EC was comparatively higher near the pollution sources. BD in both the sites were optimum; CEC, PD and POR varied according to the specific sampling locations. SMC of the soil was dependent upon the nature of waste, which was comparatively higher in Site-1 than Site-2. Further, OC and OM were higher at Site-1 due to household wastes and residues from plants and animals. In contrast, they were comparatively lower in Site -2, contaminated by an inorganic waste (bottom ash). In both sites, lower macronutrients content (Av N, Av P, Av K and Av Na) were observed, thus making both sites as degraded and highly stressed. MBC in both sites were dependent on the specific plant diversity present at the individual sampling locations.

References

Bray, R.H., Kurtz, L.T., 1945. Determination of total, organic and available forms of phosphorus in soils. Soil Sci. 59, 30-45.

Bisht, G., Neupane, S., 2015. Impact of Brick Kilns' emission on soil quality of agriculture fields in the vicinity of selected Bhaktapur Area of Nepal. Appl. Environ. Soil Sci. 409401, 8.

Biswas, T.D., Mukherjee, S.K., 2008. Textbook of Soil Science, second ed. Tata McGraw Hill publishing company, New Delhi.

Blake, G.R., Hartge, K.H., 1986. Bulk density, in: Klute, A. (Ed.), Methods of Soil Analysis, Part 1-Physical and Mineralogical Methods, second ed. American Society of Agronomy-Soil Science Society of America, Madison, USA, pp. 363-382.

Bower, C.A., Reitemeie, R.F., Fireman, M., 1952. Exchangeable cation analysis of saline and alkali soils. Soil Sci. 73, 251–262.

Dash, S., Borah, S.S., Kalamdhad, A., 2019. A modified indexing approach for assessment of heavy metal contamination in Deepor Beel, India. Ecol. Indic. 106, 105444.

David, M., Turi, N., Ain, Q. ul, Rahman, H., Jahan, S., 2020. Evaluation of environmental effects of heavy metals on biochemical profile and oxidative stress among children at brick kiln sites. Arch. Environ. Occup. Heal. 0, 1–9.

Datta, A., Gujre, N., Gupta, D., Agnihotri, R., Mitra, S., 2021. Application of enzymes as a diagnostic tool for soils as affected by municipal solid wastes. J. Environ. Manage. 286, 112169.

FAO 2017. Soil Organic Carbon: the hidden potential. Food and Agriculture Organization of the United Nations Rome, Italy.

Gee, G.W., Bauder, J.W., 1979. Particle size analysis by hydrometer: a simplified method for routine textural analysis and a sensitivity test of measurement parameters. Soil Sci. Soc. Am. J. 43, 1004-1007.

Gujre, N., Mitra, S., Soni, A., Agnihotri, R., Rangan, L., Rene, E.R., Sharma, M.P., 2021. Speciation, contamination, ecological, and human health risks assessment of heavy metals in soils dumped with municipal solid wastes. Chemosphere, 262, 128013.

Hunt N., Gilkes, B. 1992. Farm Monitoring Handbook. Published by University of Western Australia, Land Management Society, and National Dryland Salinity Program.

ICAR, 2011. Methods Manual Soil Testing in India. Department of Agriculture & Cooperation, Ministry of Agriculture, Government of India. https://agriculture.uk.gov.in/files/Soil_Testing_Method_by_Govt_of_India.pdf (Accessed on 24 March 2021).

Khan, M.W., Ali, Y., De Felice, F., Salman, A. and Petrillo, A., 2019. Impact of brick kilns industry on environment and human health in Pakistan. Sci. Total Environ. 678, 383-389.

Knudsen, D., Peterson, G.A., 1982. Lithium, sodium, and potassium. In: Page, A.L. (Ed.), Methods of Soil Analysis. Agronomy Monogram No. 9. American Society of Agronomy, Inc. Soil Sci. Soc. Of America Inc. Publisher Madison WB Consin, USA.

Olsen, S.R., Cole Watanable, F.S., Dean, L.A., 1954. Estimation of available phosphorus in soils by extraction with sodium bicarbonate. Circ. U.S. Dep. Agric. 939.

Qiao, D., Wang, G., Li, X., Wang, S., Zhao, Y., 2020. Pollution, sources and environmental risk assessment of heavy metals in the surface AMD water, sediments and surface soils around unexploited Rona Cu deposit, Tibet, China. Chemosphere, 248, 125988.

Rosiane L.S. Lima, Liv S. Severino, Ligia R. Sampaio, Valdinei Sofiatti, Jucélia A. Gomes, Napoleão E.M. Beltrão 2011. Blends of castor meal and castor husks for optimized use as organic fertilizer. Ind Crops Prod, 33, 364-368

Soil Survey Staff, 2011. In: Burt, R. (Ed.), Soil Survey Laboratory Information Manual. Soil Survey Investigations Report No. 45, Version 2.0. U.S. Department of Agriculture, Natural Resources Conservation Service.

Subbiah, B.V., Asija, G.L., 1956. A rapid procedure for the determination of available nitrogen in soils. Curr. Sci. 25, 259–260.

Suwal, G.B., 2018. Impact of brick kilns' emission on soil quality of agriculture fields in the vicinity of selected Bhaktapur area. J. Sci. Eng. 5, 34-42.

USDA (United States Department of Agriculture), 1993. Soil Survey Manual. USDA, SCS, Agric. Handb. 18. U.S. Gov. Print. Office, Washington, DC.

Vance, E.D., Brookes, P.C., Jenkinson, D.S., 1987. An extraction method for measuring soil microbial biomass C. Soil Boil. Biochem. 19, 703-707.

Walkley, A.J., Black, I.A., 1934. Estimation of soil organic carbon by the chromic acid titration method. Soil Sci. 37, 29–38.

Weather, Atlas 2020. monthly weather forecast and climate, Guwahati, Assam. https://www.weather-atlas.com/en/india/guwahati-climate. (Accessed 31 December 2020).

Zhang, C., Yu, Z.G., Zeng, G.M., Jiang, M., Yang, Z.Z., Cui, F., Zhu, M.Y., Shen, L.Q., Hu, L., 2014. Effects of sediment geochemical properties on heavy metal bioavailability. Environ. Int. 73, 270-281.

CHAPTER 4

Heavy metals concentration profile in the soil as contaminated by municipal solid waste and brick kiln bottom ash

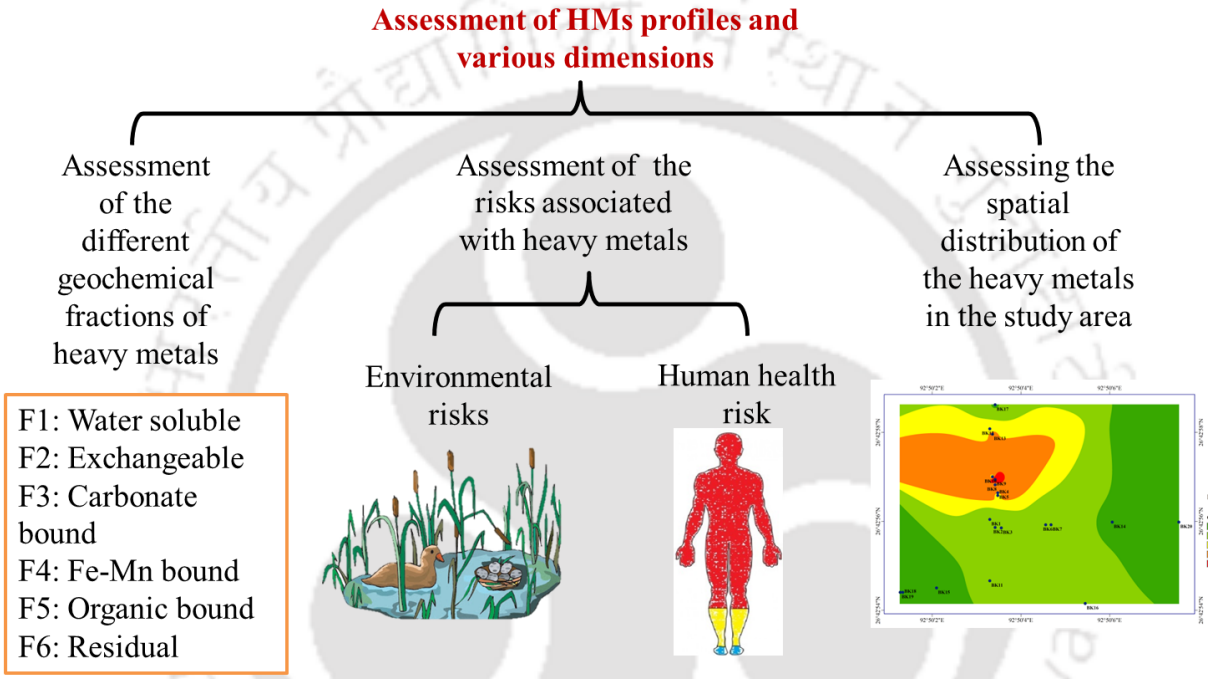

"*This chapter comprehensively portrays the heavy metals profiles of the study sites utilizing different tools such as geochemical fractions, environmental and human health risk indices and spatial assessment".*

4. Heavy metals concentration profile of the soil as contaminated by municipal solid waste and brick kiln bottom ash

4.1. Introduction

Intense urbanization and industrialization have created immense stress on the surrounding ecosystem, particularly through HM contamination associated with bioaccumulation and biotoxicity (Ancic et al., 2020; Thakur et al., 2020). Anthropogenic disposal of waste through open dumping and manual segregation has led to leaching of HMs, which severely impact wetland ecosystems (Karak et al., 2015; Dash et al., 2019; Singh et al., 2020). Also, the pollutants emanating from the BI industry disturb the surrounding environment such as plants, animals, air, water and soil. Conventional and alternative fuels used during firing operations produces toxic gaseous like CO, CO_2, NO, NOx and SO_2, smoke, particulate matter and hazardous organic compounds (Kamal et al., 2014). Technically, HMs are intrinsically marked by their protracted half-life, sustained persistence, and deep enrichment, easily permeates the food chain when absorbed by various living organisms, and stimulate precarious health hazards (Thakur et al., 2020). Therefore, in-depth assessment of HMs, their mobility and toxicity would significantly assist in mitigating severe threats to the ecosystem and human health. In soil system HM mobility and distribution is easily defined by their speciation in different geochemical fractions, ranging from the most bioavailable to non-bioavailable forms (Borah et al., 2020; Tessier et al., 1979). More specifically, they are characterized as water-soluble (F1), exchangeable (F2), carbonate bound (F3), Fe-Mn bound fraction (F4), and organic bound (F5); along with a residual fraction (F6) (Liu et al., 2020). The F1 to F3 fractions are generally mobile and readily absorbed by the aquatic organisms (Zhang et al., 2017a). Though, geochemical fractions do testify to a broad spectrum of physical and chemical profiles of HMs, but they do not endorse any specific impact of HMs on the surrounding environment and human health. Therefore, to assess the degree of risks,

we employed an indices-based approach which is most widely accepted and easy interpretation-based approach.

In present study we studied six HMs, among them, Cd is considered the most carcinogenic and toxic (Kubier et al., 2019); with the dubious distinction of being designated, 'carcinogenic to humans', by the WHO and the International Agency for Research on Cancer (IARC, 1993). In soil, Cd occurred in the different forms namely cadmium oxide (CdO), cadmium chloride ($CdCl_2$), cadmium sulfate ($CdSO_4$), and cadmium sulfide (CdS), (ATSDR, 2011). Electroplating, paint pigments, alloy preparations, batteries, industrial tools, besides Cd coated household wastes like home appliances and hand tools are the primary sources of Cd in soil (Gujre et al., 2021a). Cu is not a potentially toxic element; yet its elevated level can cause respiratory problems, dizziness, nausea, and diarrhea in human beings. The major anthropogenic sources of Cu in MSW are discarded printed circuit boards (PCB) (Xu et al., 2016). Ni is omnipresent in the different ecosystems and emanates in various forms; originating from both anthropogenic and natural sources. In an aquatic environment, the divalent state of nickel (Ni^{2+}) is the most prominent source of contamination (Forstner and Wittmann, 2012). Acute exposure of Ni can cause kidney, liver and brain damage, while chronic exposure leads to tissue damage, besides lung and nasal cancer.

Furthermore, Cr is one of the toxic and carcinogenic metals found in the soil (Tardif et al., 2019). Normally, Cr exists in two different states, hexavalent chromate [Cr (VI)] and trivalent chromite [Cr (III)]. Chromite is comparatively less soluble and less toxic whereas chromate occurs in the form of CrO_4^{2-}, $HCrO_4^-$, and $Cr_2O_7^{2-}$ which are more bioavailable and possess higher oxidation state (Yang et al., 2019). Higher Cr level in plant tissues results in reduction in plant growth, denaturation of the cell membrane, formation of reactive oxygen species (ROS) and alter the enzymatic activities (Gill et al., 2015). Some anthropogenic sources of Cr are chrome plating,

metals ceramics, colored glass, material for coating steel, dyes and paints, synthetic rubies and the tanning of leather (Poznanovic Spahic et al., 2019).

The other elements like Mn and Zn are micronutrients required for the plant to perform its biological function. Mn is not potentially toxic as the other HMs. Nevertheless, it has the ability to adsorb HMs and to act as an oxidant, affect the soil quality. In pedosphere, Mn occurs in three forms, which includes water soluble, exchangeable and insoluble oxides (Li et al., 2019). In soil matrix Mn sorption, oxidation and reduction are governed by the pH and its nodular form acts as sink for HMs (Alloway, 2012). Zn, the next metal in the current study is one of the important constituents of paints used for automobiles (Ma et al., 2018). However, Zn is comparatively nontoxic in nature, but its high exposure with other compounds e.g. zinc chloride ($ZnCl_2$), zinc oxide (ZnO) leads to dermal irritation and respiratory infection (Plum et al., 2010). High concentration of Zn in water increases its acidity and toxicity. Aquatic fauna (largely fishes) could accumulate Zn in their body and can transfer to the higher trophic level (Ouattara et al., 2020).

In developing countries like India, non-engineered landfills are considered to be a cost effective and convenient option to dispose MSW. However, this convenient option causes soil contamination, surface and groundwater pollution (Alam et al., 2020). Likewise, India is the second largest producer of bricks in the world and unregulated and unscientific establishment of the BI leads to the contamination of soil and surrounding biota. Therefore, it is urgently needed to conduct a comprehensive study on the HM pollution in soils around these sites, to get clearer picture of present status. In this study, Boragoan, Guwahati dumping site and brick kiln industry at Napaam were chosen to examine the soil contamination, ecological and human health risks associated with the six HMs namely Cu, Cd, Cr, Mn, Zn and Ni.

4.2. Materials and methods

4.2.1. Heavy metals assessment

Fractionation of soil samples were carried out using a six-step sequential extraction procedure (Borah et al., 2017; Tessier et al., 1979). Briefly, the F1 fraction was extracted with distilled water; the F2 fraction was extracted with 1.0 M magnesium chloride, and F3 and F4 fractions with 1.0 M sodium acetate (pH 5.0) and 0.04 hydroxyl ammonium chloride (acidified with 25 mL of 2 M HNO_3/HCL in 1L solution). The residues after extraction were digested with 0.02 M HNO_3 (for fraction 4), 30% hydrogen peroxide (for F5 fraction), and HCl-HNO_3-HF-$HClO_4$ (for F6 fraction). Metal concentration in the digested solution was measured using atomic absorption spectrophotometer (AAS Model: AA240, Agilent, Malaysia) (Fig. 4.1). Further using the total of six fractions spatial distributions of different metals were plotted using ArcGIS 10.1.

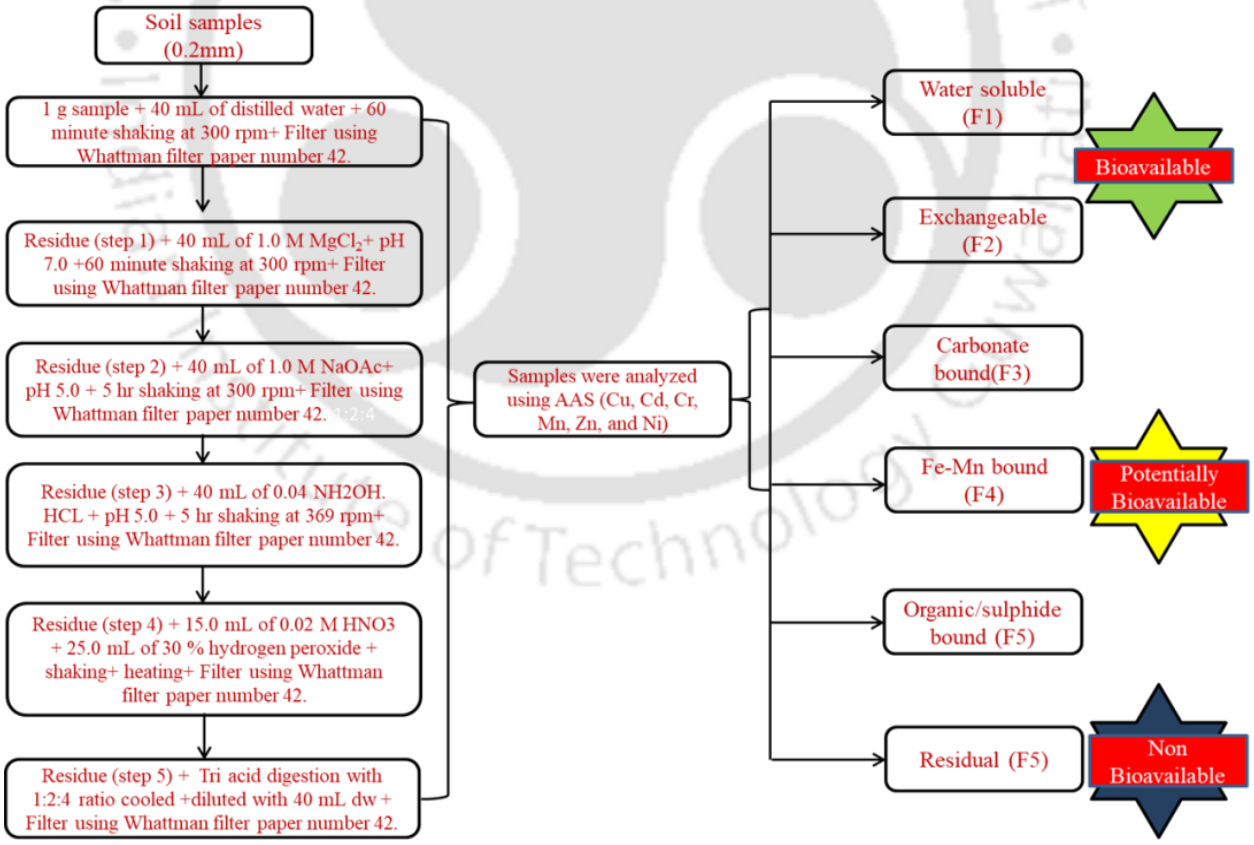

Fig. 4.1 Flowchart, showing the sequential extarction procedure of HMs (Tessier et al., 1979).

4.2.2. Quality control and quality assurance

During the analytical procedure, standard operating protocols, standard reference material (SRM), reagent blanks, and analysis of replicates were implemented to check the consistency of the results. Accuracy, precision, and reproducibility for HMs analysis were validated using SRM, i.e., SRM 2706 and SRM-1515 procured from National Institute of Standards and Technology, Madison, USA. The values obtained for Cr, Cd, Ni, Cu, Mn and Zn were 61.84 ± 0.56 (certified value 60.1 mg kg^{-1}), 0.31 ± 0.00 (certified value 0.31 mg kg^{-1}), 21.97 ± 0.55 (certified value 22.80 mg kg^{-1}), 89.11 ± 2.19 (certified value 88.1 mg kg^{-1}), 245.24 ± 11.28 (certified value 244 mg kg^{-1}) and 134.7 ± 0.62 (certified value 135.4 mg kg^{-1}) mg kg^{-1} respectively when SRM-2706 was analysed. When SRM-1515 was analysed, the values obtained for Cr, Cd, Ni, Cu, Mn, and Zn were 0.327 ± 0.02 (certified value 0.3 mg kg^{-1}), 0.0133 ± 0.00 (certified value 0.0132 mg kg^{-1}), 0.933 ± 0.01 (certified value 0.936 mg kg^{-1}), 5.71 ± 0.01 (certified value 5.69 mg kg^{-1}), 54.29 ± 3.25 (certified value 54.1 mg kg^{-1}) and 12.39 ± 1.01 (certified value 12.45 mg kg^{-1}), respectively. Analytical grade chemicals were used for the analysis (Sigma-Aldrich). All the analyses were carried out in triplicates. During all the experimental procedures, the glassware, plasticware and teflons tubes used were washed with labolene, soaked in the mild acid and rinsed thoroughly with the deionized water.

4.2.3. Environmental indices and factors

Geo-accumulation index

Geo-accumulation Index (I_{geo}) was originally defined by Müller in 1969 for metal concentrations in the 2-micron fraction and was developed as global standard shale values. I_{geo} tells about current

HMs pollution based on the comparison with the background concentration in soil. Mathematically I_{geo} can be computed using equation 1:

$$I_{geo} = Log_2\left(\frac{C_n}{1.5 \times B_n}\right) \quad (1)$$

Where, C_n is the concentration of given element in the topsoil while B_n is the concentration of the particular element in the upper continental crust or geochemical background (Taylor, 1964). 1.5 is the factor used for the correction of regional background differences. I_{geo} has been classified in the following classes: <0 practically none, 0-1 unpolluted, 1-2 moderately polluted to unpolluted, 2-3 moderately polluted, 3-4 moderately to highly polluted, 4-5 highly polluted, >5 very highly polluted.

Pollution load index (PLI)

PLI directly reflects the soil pollution and indicate the most contaminated elements. Single factor pollution load index (P_i) and integrated pollution load index (I_{Pi}) were employed to assess the overall level of heavy metals pollution in the soil samples of studied area. The pollution load index was determined using the following equation (Memoli et al., 2019).

$$P_i = \frac{C_i}{S_i} \quad (2)$$

Where, P_i is the pollution load index for the examined heavy metals, C_i is the concentration of heavy metal in a soil sample (mg kg^{-1}) and S_i is the permitted standard of the same metal (mg kg^{-1}) (CCME, 2007).

$$IP_i = \sqrt{\left(P^2_{imax} + P^2_{iave}\right)/2} \quad (3)$$

P_{imax} is the maximum value of P_i, and P_{iave} is the average value of the sum of all P_i i.e. the six heavy metals from the 20 sampling sites. If the P_i value is greater than unity, it suggests the existence of pollution or the presence of pollutants, while no pollution loads are inferred if the value is lower than or equal to unity. IP_i are classified as follows: low level of pollution when $IP_i \leq 1$; moderate level of pollution when the value is $1 < IP_i \leq 2$; high levels of pollution when $2 < IP_i \leq 5$, and finally a value of $IP_i > 5$ is considered as extremely high pollution levels.

Potential ecological risk index (PERI)

The potential ecological risk index (*PERI*) was introduced by Hakanson (1980) which is based on the elemental abundance and release capacity in environment. It is helpful in identifying the degree of pollution and ecological risk arising due to HMs contamination. This index can be calculated using following equations:

$$C_r^i = \frac{C_n^i}{C_b^i} \quad (4)$$

$$E_r^i = T_r^i \times C_r^i \quad (5)$$

$$RI = \sum_{i=1}^{n} \mathrm{E}_r^i \quad (6)$$

Where E^i_r is the potential ecological risk factor of a single element. C^i_r is the pollution factor for individual element. C^i_n is the concentration of metal *i* in soil sample and C^i_b is the background concentration or maximum permissible limit for *i* metal. T^i_r is the toxic response coefficient for

element i e.g. T^i_r is 2 for Cr, 30 for Cd, 5 for Cu, 6 for Ni and 1 for Zn and Mn, respectively (Hakanson, 1980). Risk index (*RI*) is the summation of the individual *PERI* for studied metals in the soil contaminated by municipal solid waste. On the basis of its severity *PERI* can be classified into 5 grades as low risk ($E^i_r \leq 40$), moderate risk ($40 < E^i_r \leq 80$), high risk ($80 < E^i_r \leq 160$), very high risk ($160 < E^i_r \leq 320$), or extremely high risk ($E^i_r > 320$). Similarly, *RI* is classified into 4 grades low risk ($RI \leq 150$), moderate risk ($150 < RI \leq 300$), high risk ($300 < RI \leq 600$), or very high risk ($RI > 600$), respectively.

Enrichment Factor (EF)

Enrichment factor (*EF*) can be calculated using the equation given by Leharne et al., 1992 and Zoller et al., 1974. It is used for the assessment of anthropogenic influence in the soil. It is simply calculated as normalization of the metal concentration against reference metal concentration which is taken as average shale or earth crust. Reference metals can be used in calculating *EF* is Al, Fe, Mn. In present study Fe was used as a reference metal for calculating *EF* (Turner and Simmonds, 2006):

$$EF = \left(\frac{C_m}{C_{fe}}\right)_{Sample} \Big/ \left(\frac{C_m}{C_{fe}}\right)_{background} \quad (7)$$

Where, C_m is the concentration of metal in sample and its average crustal abundance. C_{Fe} is the concentration of iron in sample and background. The average crustal abundance of Cr, Mn, Zn, Cd, Cu, Ni and Fe are 100, 950, 70, 0.2, 55, 75 and 56,300 mg kg^{-1} respectively (Taylor, 1964). The *EF* value between 0.5 to 1.5 indicates that the metallic origin is from crustal abundance or natural process, while value greater than 1.5 indicates metal source is from anthropogenic

influences (Zhang and Liu 2002). According to Chen et al., 2007, *EF*<1 indicates no enrichment, *EF*<3 is minor enrichment, *EF*= 3 to 5 is moderate enrichment, *EF*= 5 to 10 is moderately severe enrichment, *EF*=10 to 25 is severe enrichment, *EF*= 25 to 50 is a very severe enrichment, and *EF*>50 is extremely severe enrichment.

Mobility factor (MF)

Mobility factor (*MF%*) is a crucial factor which indicates the proportional mobility of metals inside the soil matrix. Factors which govern the mobility are soil pH, EC, CEC and OC (Borah et al., 2017). Mobility also tells about the leachability and the bioavailability of metals in soil. It is calculated by using the following equation (Narwal and Singh, 1998):

$$MF = \frac{F1 + F2 + F3}{F_{TOTAL}} \times 100 \qquad (8)$$

Here F1, F2 and F3 are the concentration of elements in water soluble, exchangeable and carbonates fractions respectively. F_{Total} is the summation of all fractions from F1 to F6. If *MF* values are higher, it indicates lower stability of HMs in the soil and tends to be more available to the biological systems (Olajire et al., 2003).

Individual contamination factor (ICF) and global contamination factor (GCF)

The *ICF* and *GCF* indicate the degree of contamination risk with respect to the retention time. A high contamination factor indicates low retention time or vice versa. It was calculated by dividing the sum of the non-residual fractions F1 (water-soluble) + F2 (exchangeable) + F3 (carbonate bound) + F4 (Fe-Mn bound) + F5 (organically bound) by the residual fraction F6 of each sample. While *GCF* for each site was calculated by summing the *ICF* of Cr, Mn, Zn, Cd, Cu and Ni

obtained from the contaminated soil samples (Ikem et al., 2003). Equation (9) and (10) were used to compute *ICF* and *GCF* which are as follows:

$$ICF_m = \sum_{i=A}^{D} \frac{C_{Fi}}{C_{FE}} \qquad (9)$$

$$GCF = \sum_{m=1}^{n} ICF_m \qquad (10)$$

Where, ICF_m is the contamination factor of the individual metal, C_{Fi} is the concentration of each non-residual fraction (mg kg^{-1}) and C_{FE} is the concentration of the residual fraction (mg kg^{-1}). Contamination factors $ICF < 0$ and $GCF < 6$ indicate low contamination, $1 < ICF < 3$ and $6 < GCF < 12$ moderate contamination, $3 < ICF < 6$ and $12 < GCF < 24$ considerable and $ICF > 6$ and $GCF > 24$ as high contamination.

4.2.4. Human health risk indices and factors

For assessing the human health risk various health risk indices can be used. It is mainly divided into two types, carcinogenic and non-carcinogenic risk which is further classified into three major pathways for contamination i.e., ingestion, inhalation and dermal. Elevated level of HMs, in soil poses risks mainly through ingestion and dermal adsorption (Cao et al., 2014). Very few studies indicate that dermal exposure is the main pathway for Cd and Cu contamination in human bodies (Li et al., 2014). In the present study, the average daily doses (ADDs) (mg $kg^{-1}d^{-1}$) of potentially toxic metals, via three different pathways were calculated (Luo et al., 2012); by taking into consideration the most bioavailable fractions (Water-soluble, exchangeable, carbonate and Fe-Mn oxides bound), using equation (11), (12) and (13) which are as follows:

$$ADD_{ing} = \frac{C \times IngR \times EF \times ED}{BW \times AT} \times 10^{-6} \qquad (11)$$

$$ADD_{inh} = \frac{C \times InhR \times EF \times ED}{PEF \times BW \times AT} \quad (12)$$

$$ADD_{der} = \frac{C \times SA \times SAF \times ABS_{dermal} \times EF \times ED}{BW \times AT} \times 10^{-6} \quad (13)$$

Where, *C* is the HM concentration of bioavailable fractions (mg kg^{-1}) (F1-F4), *IngR* = Ingestion rate (mg d^{-1}) 100 for adults and 200 for children (US EPA, 2001). *EF* is the exposure frequency (d $year^{-1}$), which is 60 for adults and 15 for children (US EPA, 1989; USDoE, 2011). *ED* is the duration of exposure expressed in years; 24 years for adults and 6 years for children (US EPA, 2001). *BW* is the body weight expressed in kg, 60 kg for adults and 15 kg for children, respectively. *AT* is the average time for non-carcinogenic risk i.e., *ED* × 365 years and for carcinogenic risk average time is calculated as *LT* (*life time*) × 365 years. In India, carcinogenic *LT* = is considered as 65 years (MoHFW, 2010). For ADD_{inh} calculation, particle emission factor (*PEF*) = 1.36×10^9 $m^3\,kg^{-1}$ is considered (US EPA, 2001). For $ADD_{der,}$ *SA* i.e., the skin surface area available for daily contact for adults is 5700 cm^2 and 2800 cm^2 for children (US EPA, 2001). *SAF* termed as skin adherence factor for soil = 0.07 mg cm^{-2} h^{-1} for adults and 0.2 mg cm^{-2} h^{-1} for children, *ABS* dermal is the dermal absorption factor which is 0.001 (Miguel et al., 2007; Shi et al., 2011; Zheng et al., 2010).

The human health risk is based on the physiology and behavioural pattern of an individual, and hence it is divided into two groups adults and children (Khairy et al., 2011). Overall Hazard index (*HI*) was calculated as the summation of hazard quotient (*HQ*) under three different pathways. Though, HQ_{ing}, HQ_{inh} and HQ_{der} were calculated using the standard equations (14), (15), (16) and (17) as follows:

$$HQ_{ing} = \frac{ADD_{ing}}{Rf\,D_{ing}} \quad (14)$$

$$HQ_{inh} = \frac{ADD_{inh}}{Rf\,D_{inh}} \quad (15)$$

$$HQ_{der} = \frac{ADD_{der}}{Rf\,D_{der}} \quad (16)$$

$$HI_{exp}\,P = \sum HQ_{exp}p \quad (17)$$

Where, RfD_{ing}, reference dosage for ingestion, Cr=0.003, Zn= 0.03, Mn=0.046, Cd= 0.001, Cu= 0.04, Ni= 0.02 (Miguel et al., 2007). RfD_{inh} reference dosage for inhalation Cr= 0.0000286, Zn=0.30, Mn=0.00005, Cd=0.001, Cu=0.04, Ni=0.0206 (Adimalla and Li, 2019). RfD_{der} = Reference dosage for dermal, Cr= 0.00006, Zn= 0.06, Mn= 0.00184, Cd=0.00001, Cu=0.012, Ni=0.0054 (Miguel et al., 2007).

HI value greater than 1 indicates the occurrence of significance non-carcinogenic risks, whereas *HI* lower than 1 showed no significant risk (US EPA, 2001). Following Dehghani et al. (2017) carcinogenic risk (*CR*) for the current study was calculated using equation (18) and (19):

$$CR_i = ADD_i \times SF_0 \quad (18)$$

$$CR = \sum CR_i \quad (19)$$

Where, SF_0 = Slope factor (Cr=0.42; Cd= 0.63; Ni= 0.84) (Chabukdhara and Nema, 2013). If *CR* value is higher than 1×10^{-4} it poses significant carcinogenic risk, while values lower than 1×10^{-6} indicate no significant health hazard (Tume et al., 2018).

4.3. Results and discussion (Site-1)

4.3.1. Assessment of geochemical fractions

Percentage distribution of metals in six geochemical fractions of the sequential extraction of Cu, Cd, Cr, Mn, Zn and Ni were investigated and discussed. The different geochemical fractions were investigated as F1 – Water Soluble; F2 – exchangeable fraction; F3 – carbonate bound, F4 – Fe-Mn bound fraction, F5 – Organic/sulphide bound elements, and F6 – residual fraction. F1 commonly the most bioavailable fraction of the metals, acquired by using water as a reagent. While in F2, the exchangeable fraction metal ion bound to the solid surface by a weak electrostatic force. In a soil environment, it is most bioavailable and can be replaced by salts. Positively charged ions can displace the metals weakly bound electrostatically organic or inorganic sites. The changes in pH govern F3 or carbonate bound fraction. It led to the metals leaching, specifically sorbed and organic or inorganic substrate. The F4 or Fe-Mn oxide bound fraction acting as a sink of the HMs. The fraction composed of precipitation, adsorption, surface complex formation and ion exchange. In organically bound fraction (F5 fraction), the metal remains in the soil matric for a longer duration and only immobilized by the decomposition procedure and under oxidizing process. In contrast, the last fraction or the residual fraction (F6) hold the metal within their crystalline lattice and release only when there are changes in environmental conditions.

Chromium (Cr) fractions

Cr from all sampling locations of Site-1 was primarily associated with Fe-Mn fraction (F4), which accounts for 44.23% (Fig. 4.2). The possible reason behind the association of Cr with F4 fraction inside soil matrix is the manganese oxide, which offers high surface area and acts as a strong scavenger for Cr (Stepniewska et al., 2004). Overall, Cr content in the soil follows a trend of F4 (44.23%) > F5 (41.12%) > F1 (11.73%) > F3 (1.82%) > F2 (1.10%) which showed a close agreement with recent study indicating higher association of Cr in F4 fraction (Nkinahamira et al.,

2019). Many studies across the world indicated that chromate is more mobile than its trivalent state, i.e. chromic, thus increased leaching would contaminate soil and groundwater (Gan et al., 2019).

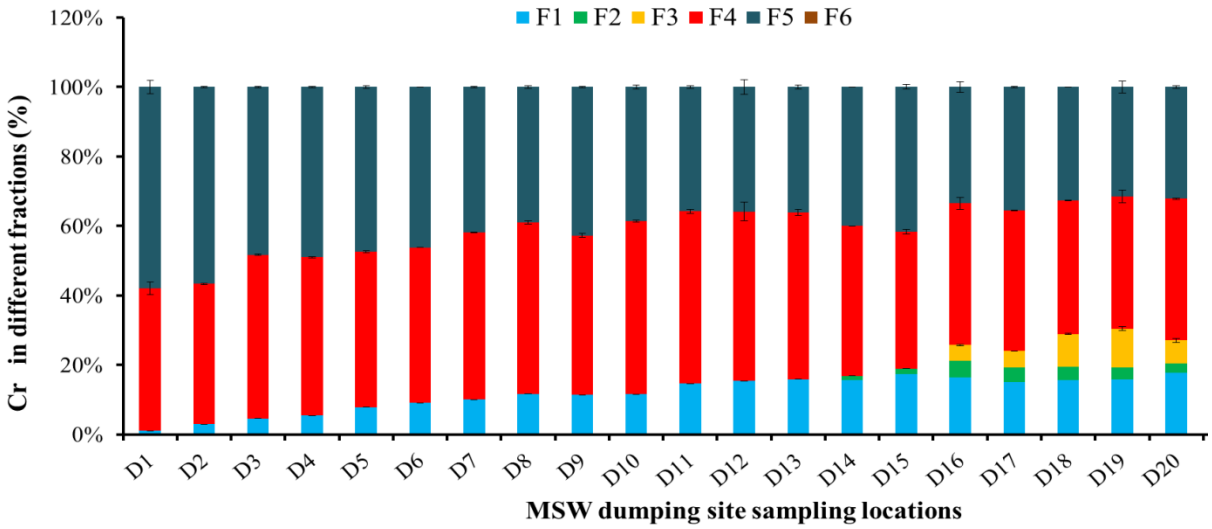

Fig. 4.2. Chromium in different fractions at MSW dumping sites in Guwahati, Assam.

Manganese (Mn) fractions

From geochemical fraction analysis of Mn following trend was obtained F2 (52.55%) > F4 (24.66%) > F3 (16.59%) > F6 (4.30%) > F5 (1.48%) > F1 (0.42%). Almost half of the Mn belonged to the exchangeable fraction (F2), creating the Mn more bioavailable (Zhang et al., 2018; Fig. 4.3). Site D17 lies close to agricultural land and experienced predominant Mn in the exchangeable fraction, which may be due to the chemical fertilizer (Sandra et al., 2012). Mn is an important constituent of the chemical fertilizer and added to the soil to increase plant growth. Geologically it occurs in the earth crust in manganese oxides (MnO) with a different affinity towards other metal ions (Negra et al., 2005). In the F4 fraction, the highest concentration was observed at the sampling location of D20, which is far from the MSW dumping site and near an agriculture site. This indicates that Mn has a different source of origin, and it is primarily not from the common pool of

waste. The lowest concentration of Mn was observed at the D9 sampling location near the wetland area. F1 to F4 fractions constitute a bioavailable and potentially bioavailable fraction of Zn, accounting for about 84.5% of the total Zn (Fig. 4.4).

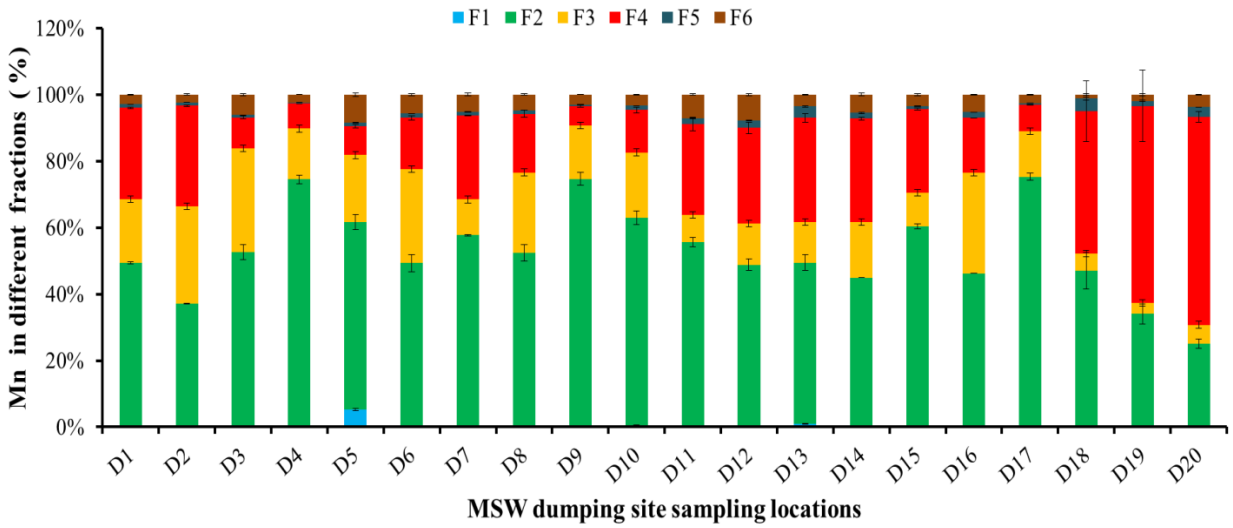

Fig. 4.3. Manganese in different fractions at MSW dumping sites in Guwahati, Assam.

Zinc (Zn) fractions

F1 to F4 fractions constitute a bioavailable and potentially bioavailable fraction of Zn, accounting for about 84.5% of Zn's total (Fig. 4.4). Overall, different fractions of Zn followed the order: F4 (39.68%) > F3 (27.49%) > F2 (16.83%) > F6 (11.84%) > F5 (3.65%) > F1 (0.50%). Overall, Zn was primarily associated with the Fe-Mn bound fraction (39.68%), and its highest concentration was observed at D16, near the metal waste segregation unit. It was observed that dry cell batteries, paints, rubber, ceramics, and old tires are the major contributor of Zn to the environment (Lane et al., 2020), and at this dumping site, most of these materials are disposed of indiscriminately. Carbonate bound fraction (F3) of Zn accounted for 27.49% of the total fractions. Water-soluble fraction (F1) accounted for only 0.50% among all different fractions investigated. D-16 site had the highest amount of F2 fraction, having 16.83% of the total fraction.

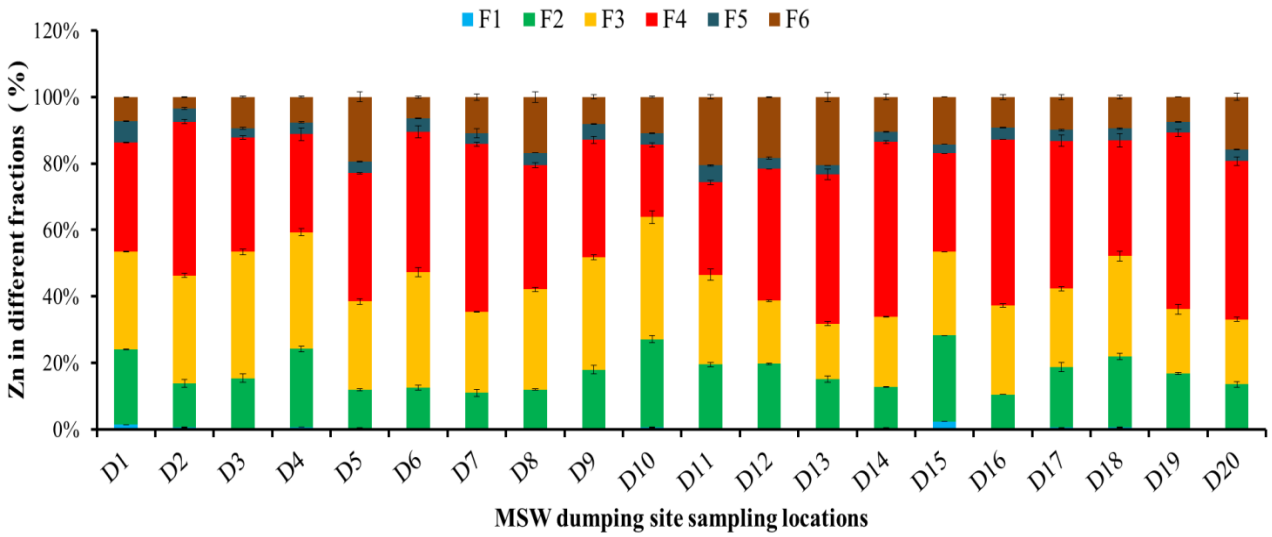

Fig. 4.4. Zinc in different fractions at MSW dumping sites in Guwahati, Assam.

Cadmium (Cd) fractions

In the study site, Cd was mainly concentrated in the carbonate bound phase, i.e. F3 (54.59%), and showed secondary association with the exchangeable phase (F2) (27.15%) (Fig. 4.5). Thus, the higher affinity of Cd in the acid-soluble phase (81.74%) may be due to the formation of Cd carbonate complexes, which is in close agreement with the previous studies (Xia et al., 2016; Zhang et al., 2017a). However, a recent study conducted by Kubier et al. (2019) suggested that the most stable Cd complexes are formed with carbonate, chloride, sulfate, and bisulfide anions as ligands. Also, in the F3 fraction, HMs can readily become more bioavailable as the pH changes, rendering them more toxic than any other fraction of HMs (Qiao et al., 2020).

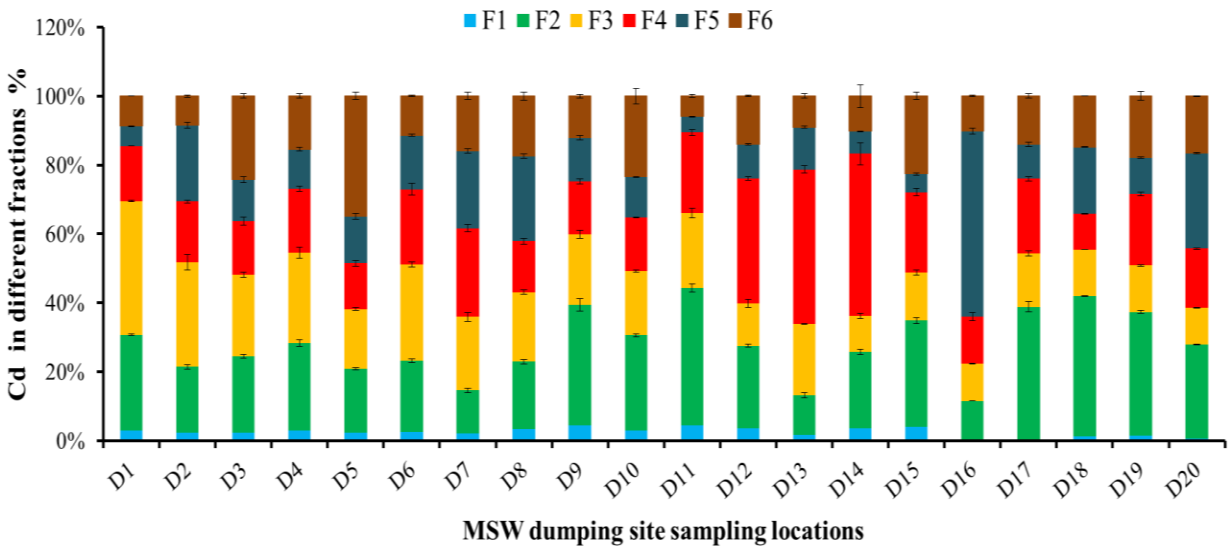

Fig. 4.5. Cadmium in different fractions at MSW dumping sites in Guwahati, Assam.

Copper (Cu) fractions

Cu primarily exists in the exchangeable fraction (F2), which accounts for 25.53%, and it is one of the labile forms. Labile fractions generally comprise of water-soluble (F1), exchangeable (F2), and the carbonate bound (F3) fractions that could be released to the surrounding environment under favorable environmental conditions created by the change in pH and Eh levels (Prartono et al., 2016; Ji et al., 2018). In the case of Cu, 47.36% belongs to the labile fraction, which constitutes 2.44% of F1, 25.53% of F2, and 19.39% of F3 fractions, respectively (Fig. 4.6). HM under these fractions was retained on the surface by a weak electrostatic force and released by the ion-exchange process. In addition, in the MSW, Cu might be derived from printed circuit boards (PCBs), which account for 65 -70% of copper (II) oxide (Wu et al., 2018). Overall, Cu in its different fraction follows the order of F2 > F4 > F3 > F5 > F6 > F1.

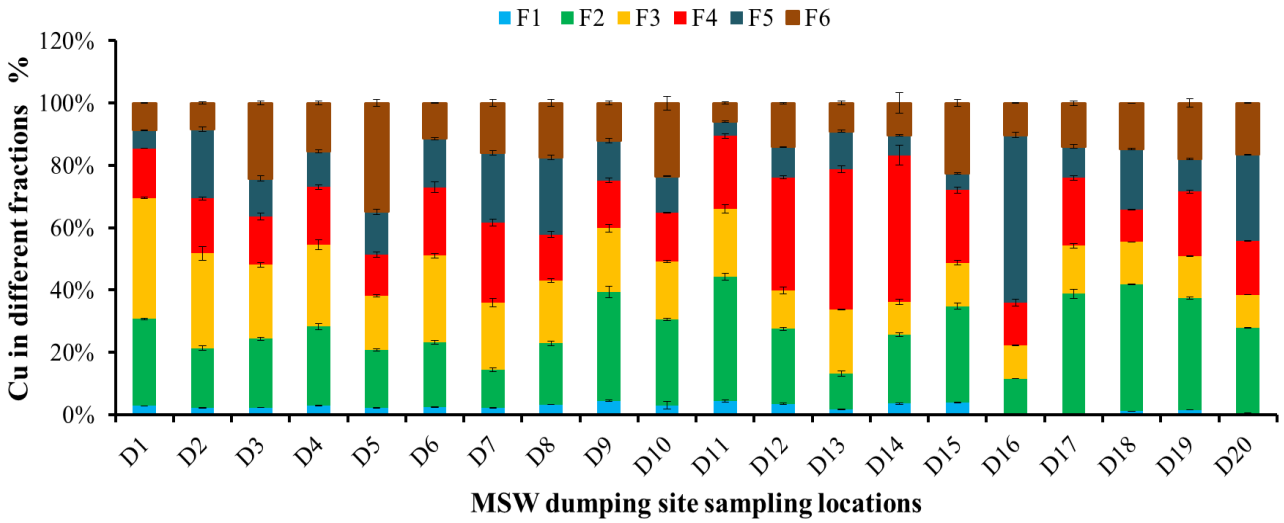

Fig. 4.6. Copper in different fractions at MSW dumping sites in Guwahati, Assam.

Nickel (Ni) fractions

At Site-1, Ni was strongly associated with the exchangeable phase F2 (40.60%) followed by the carbonate bound phase, i.e. F3 (29.48%) and the Fe-Mn bound phase F4 (17.76%) (Fig. 4.7). About 70% of the Ni is present in its bioavailable form possessing a higher risk to the soil environment. F2 fraction, which accounts for the highest contribution of weakly adsorbed Ni, gets easily dissociated in the soil under acidic pH (Al-Mur et al., 2020). Moreover, in its labile form, Ni is widely known for being extremely hazardous to human health and terrestrial and aquatic organisms. Inside the aquatic ecosystem, bioavailability of the Ni depends upon the water chemistry, chemical speciation and bioavailability of aquatic biota (Blewett and Leonard, 2017). Overall, the Ni in the different fractions is ordered as: F2 (40.60%)> F3 (29.48%) > F4 (17.76%) > F6 (12.16%). Generally, higher Ni concentration in the soils of dumping sites can be attributed to the use of Ni in electroplating industries, nickel-cadmium batteries, coins, and polishing industries.

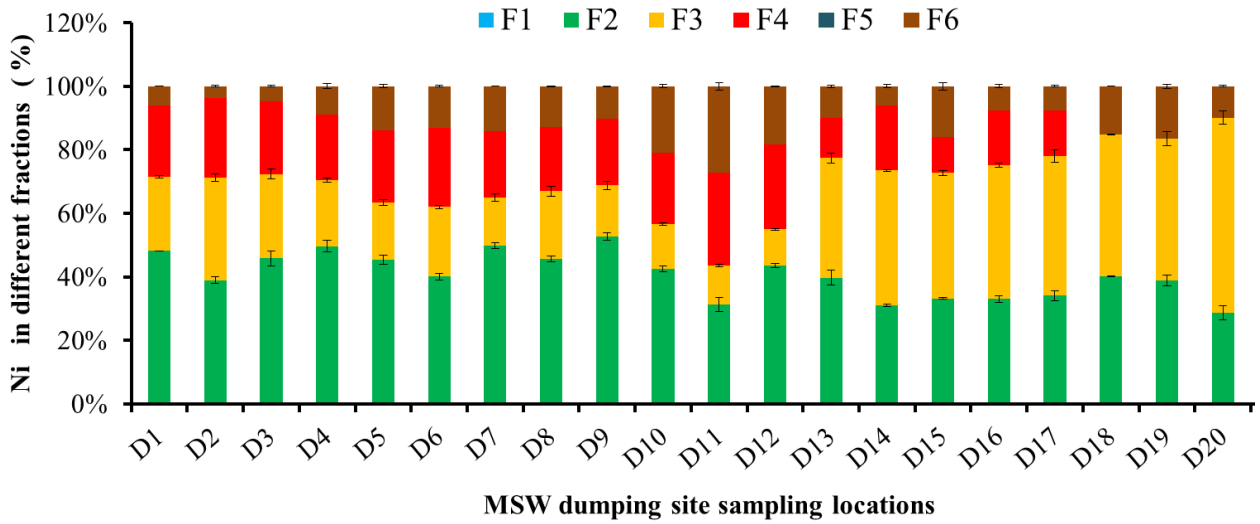

Fig. 4.7. Nickel in different fractions at MSW dumping sites in Guwahati, Assam.

4.3.2. Spatial distribution of the different metals

The spatial distribution maps show a high concentration of Cr in the soils of Site-1. Cr and Mn showed similar spatial patterns for the areas near the glass and metal segregation units. Ordinary analysis of kriging revealed that Cr and Mn contaminated the eastern and northern parts of the dumping site. But, their concentrations gradually decreased from the eastern part of the dumping site to the western side. However, Zn distribution showed an erratic pattern and largely concentrated in the northern and south western part of the dumping site (Fig. 4.8). Spatial analysis in sync with field observation revealed that many HMs originated from anthropogenic sources like manual glass and metal segregation units located in the eastern part of the dumping site. A similar pattern of increased concentration of Cr and Mn were observed in the proximity of the MSW dumping site, depicting a high level of contamination at the eastern end (Dash et al., 2019). Furthermore, from the literature, a higher concentration of HMs at nearby areas of anthropogenic sources was observed by many researchers (Wang et al., 2020; El Azhari et al., 2017). However,

the spatial distribution of HMs is attributed to several factors, which includes elevation, water channels, soil parent materials, built-up structures, and the orientation of sources (Jin et al., 2019).

Likewise, the spatial analysis revealed that Cd was more concentrated in the areas close to the dumping heap (D1, D2 and D3); consequently, their concentration decreased with the distance. The spatial profile also indicated a higher concentration towards Deepor Beel in the southwestern direction. An elevated level of Cd was also observed at location D7, which shares an embankment with the Deepor Beel, correlating the higher risk of Cd contamination with the slightly acidic pH of the sampling site (Karak et al., 2015). Conversely, the overall spread of the Ni contamination was mainly on the northeastern part of the MSW heap, where the electronics wastes were manually segregated. Ni is a strategic element, as an essential constituent of metallurgical electroplating and batteries. Apart from Ni and Cd, Cu showed an erratic pattern, mainly concentrated in the eastern part of the dumping site, rendering it hard to predict the potential source of Cu contamination.

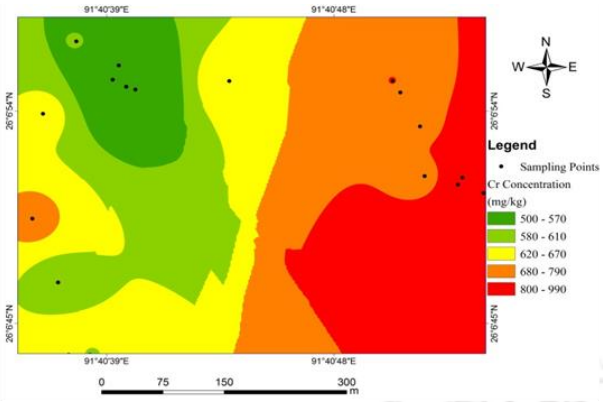

(a) Cd concentration at MSW dumping site

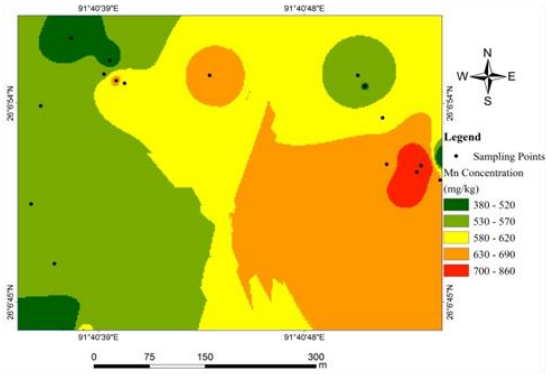

(b) Mn concentration at MSW dumping site

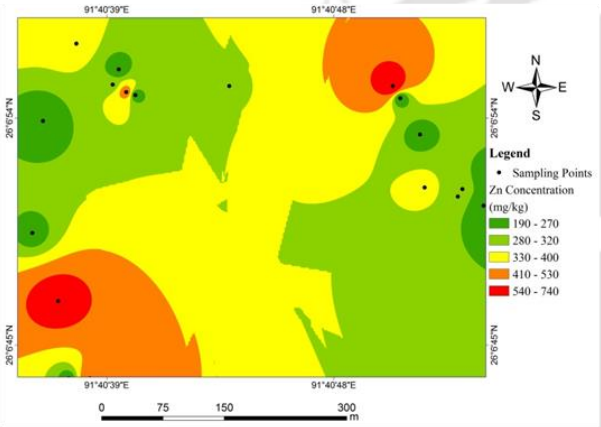

(c) Zn concentration at MSW dumping site

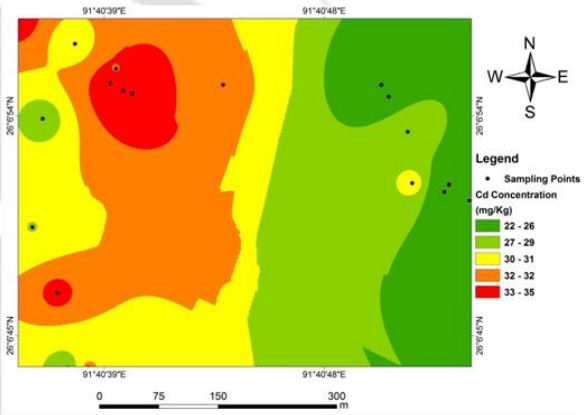

(d) Cd concentration at MSW dumping site

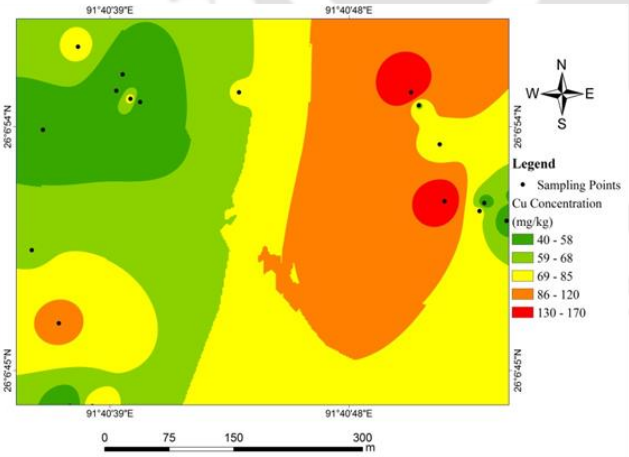

(e) Cu concentration at MSW dumping site

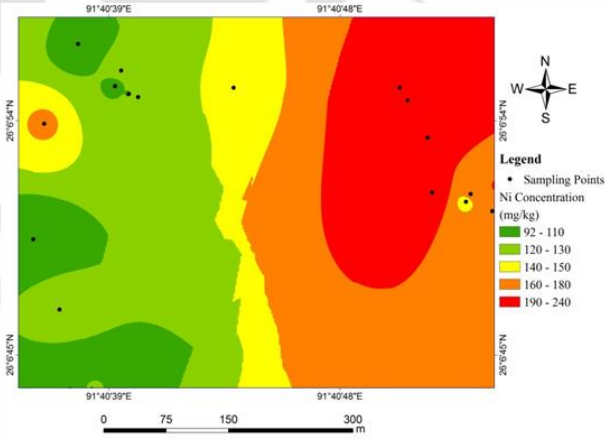

(f) Ni concentration at MSW dumping site

Fig. 4.8. Spatial distribution of the HMs at MSW dumping sites in Guwahati, Assam.

4.3.3. Environmental indices for ecological risk assessment

Geo-accumualtion index (I_{geo})

I_{geo} is a quantitative measure for the soil pollution level assessment (Fig. 4.9). For Cr, 80% of the sampling sites (D1-D16) fell under the heavily polluted category ($3 < I_{geo} \leq 4$), while the remaining 20% of the sampling locations which is nearby the metal segregation unit belonged strongly to extremely polluted category ($4 < I_{geo} \leq 5$). Pollution through the Mn is negligible in the study area and falls under the unpolluted category ($I_{geo} < 0$). However, the level of contamination varied for Zn and also its indices of geo-accumulation. About 55% of the sampling sites belong to the moderate pollution category ($1 < I_{geo} \leq 2$). Moderate to heavy pollution of Zn was observed at D2, D7, D8 and D16 sites ($2 < I_{geo} \leq 3$). Site D16, located near the metal and glass segregation unit, exhibited a strong level of contamination. Zn is an integral constituent of metallurgy (Ellis and Revitt, 2008). More than half of the soil samples belonged to the moderately to unpolluted (80%) category whereas remaining 10% each associated with moderately polluted and moderate to strongly polluted (10%) category. The Ni pollution in soil samples reached moderately polluted, moderately to heavily polluted, accounting for 65% and 35% of all samples, respectively. In the present study, among HMs, Cu showed the lowest pollution levels. Notably, Cd pollution in the present MSW contaminated soil reached levels of extremely polluted ($I_{geo} > 5$) condition for all samples; and these are most likely associated with the presence of nickel-cadmium batteries in MSW waste (Khan et al., 2017). Cd is also an essential constituent of pigments, metallic coatings and plating, and alloys (ATSDR, 2011). However, the polymetallic contamination due to Cd and Ni was most evident in the D16, which lies closer to the metal segregation unit.

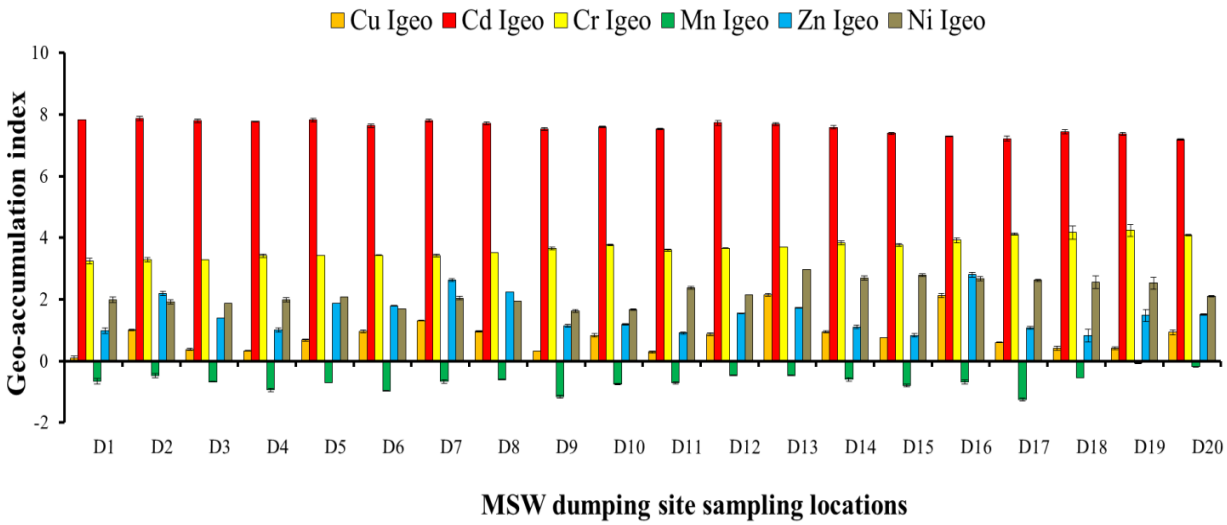

Fig. 4.9. I_{geo} index at MSW dumping sites in Guwahati, Assam.

Pollution load index (PLI)

PLI showed that Site-1 is seriously polluted with Cr metal contamination ($PLI > 5$), whereas the site is not much contaminated with the Mn ($PLI < 0$) (Fig. 4.10). Moderate to low level of pollution exhibited by Zn ($1 < PLI \leq 2$) in all sites except D16 and D17, where the level of Zn pollution is higher ($3 < PLI \leq 5$). The higher load index of Cr may be due to the e-waste, which typically contains about 9900 mg kg^{-1} of Cr (Xiong et al., 2019). As Cr exhibit a higher level of contamination, the reason could be related to the increased level of concentration in soil than a threshold value. In general, when the metal concentration exceeds a specific threshold value, it would negatively affect the environment and human health (Borah et al., 2017). The average value of Cd in all sampling locations exhibited a very heavy pollution load ($PLI \geq 5$), besides a heavy pollution load ($5 \leq PLI \geq 3$) of Ni in about 40% of the sampling locations. Additionally, moderate pollution load ($3 \leq PLI \geq 2$) of Ni was also observed in the 45% sampling locations adjacent to the significant heap of the dumping site. In contrast, the sampling site like D6 exhibited a very low

pollution load adjacent to the wetland areas. It implies that the Ni contamination was mainly concentrated in the northern and eastern part of the dumping site, whereas the western part remains moderately contaminated or uncontaminated. However, in the case of Cu, 90% of the sampling locations exhibited very low or no pollution load, except locations D13 and D16, which demonstrated moderate pollution ~~and~~ load. Regarding combined pollution effects from studied HMs, *PLI* indicates a very high pollution load due to contamination by Cd followed by Cd and Ni. Similar results indicating higher pollution load was also reported by Tian et al. (2017) and Ahmad et al. (2020).

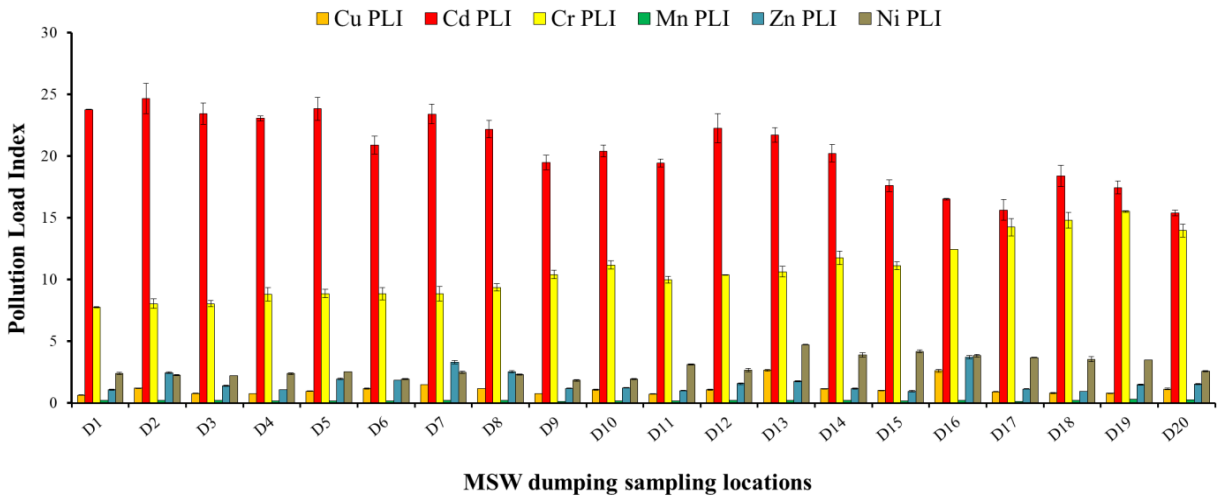

Fig. 4.10. Pollution load index (*PLI*) at MSW dumping sites in Guwahati, Assam.

Potential ecological risk index (PERI)

The potential ecological risk index (E^i_r) tells about the risk associated with HMs in an area. The E^i_r values for all the HMs except Cd of the sampling site were below 40 ($E^i_r < 40$), indicating that these elements pose a low potential ecological risk to the aquatic organism (Mondal et al., 2020). Overall ecological risks associated with Cr, Mn, Zn, Ni and Cu were under the low and very low-risk category ($E^i_r < 40$) (Fig.4.11). Notably, the above analysis showed a close agreement with the

recent research indicating lower ecological risk from Cr and Zn, respectively (Qiao et al., 2020). The E^i_r values for Cd in the MSW soil samples were higher than 320, with a maximum value of 739.71, indicating severe ecological risk across all the sampling locations (Fig. 4.11). The higher ecological risk extends from the heap of the dumping site near locations D1 and D2, suggesting that contamination would eventually travel from the heap to the surrounding areas. A decreasing trend of the ecological risk was observed as one moved away from the heap of the dumping site. The higher ecological risk from Cd would compound the risk of contamination in the soil and water bodies (Christophoridis et al., 2020). Deepor Beel, which lies close to the dumping site, is a habitat for various rare, endangered and threatened (RET) species, increasing potential widespread bio-magnification possibilities (Mozumder and Tripathi, 2014). The large MSW dumping heaps are consequently emerging as the epicentre of pollution and posing a distinct threat to the surrounding ecosystem.

The combined ecological risk index (*RI*) revealed a very high ecological risk. In 70% of the sampling locations, Cd exhibited high risk ($RI \geq 600$), whereas the remaining 30% of the sampling sites demonstrated considerable risk ($600 \leq PLI \geq 300$). Predominantly, the soil in the MSW dumping site demonstrated severe contamination and validated the higher ecological risk; the same has been manifestly correlated with increased concentration of Cd (Soledad Morales-García et al., 2020).

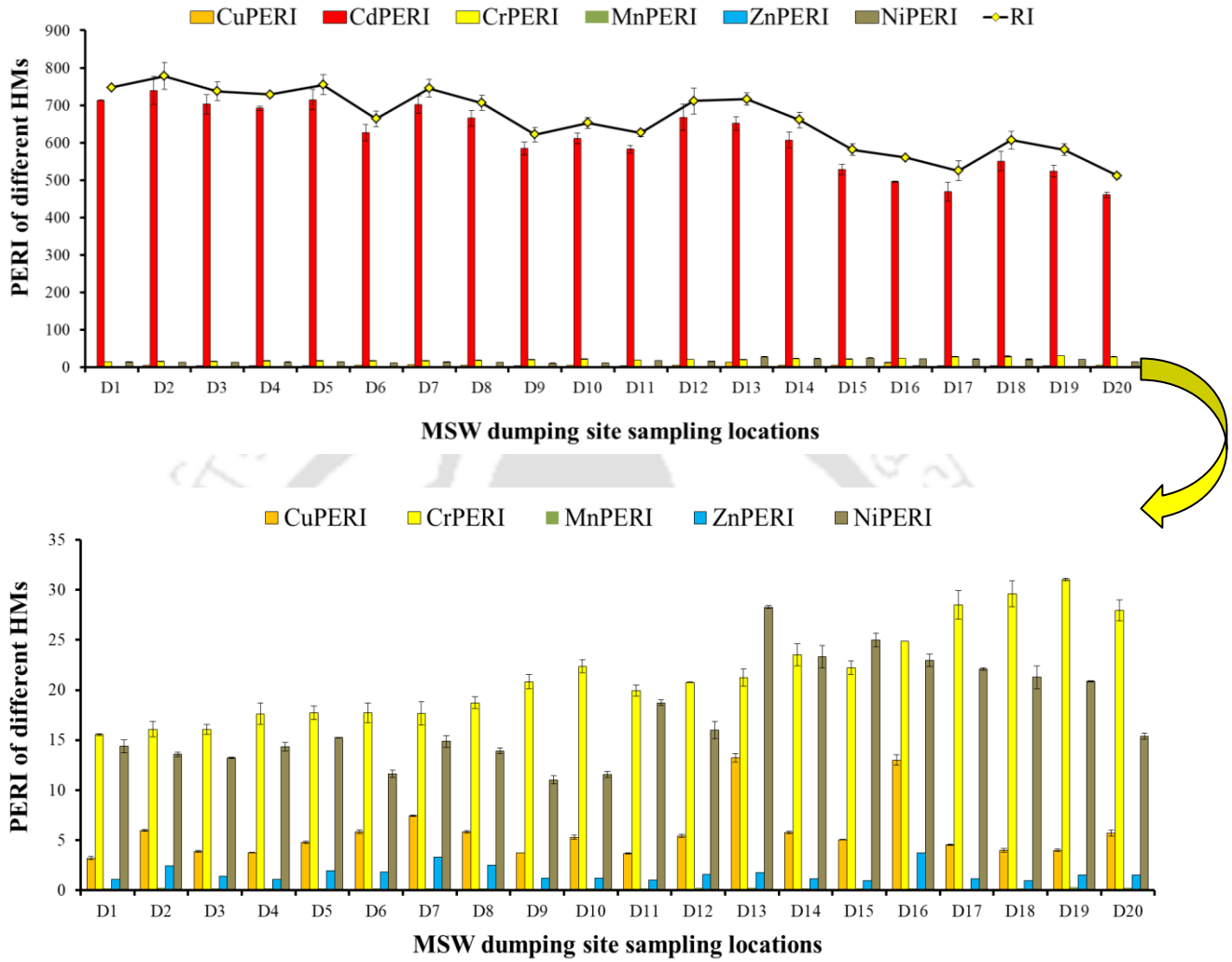

Fig. 4.11. Potential ecological risk index (*PERI*) at MSW dumping site in Guwahati, Assam.

Enrichment factor (EF)

Enrichment factor (*EF*) helps understand the influence of anthropogenic activities on the soil. Site D1 and D9 exhibited extremely high enrichment ($EF > 40$) of Cr, which are closer to the MSW dumping site (Fig. 4.12). A similar result was observed for D15 and D16, while about half of the sampling locations had only significant Cr enrichment ($5 < EF \leq 20$). Moreover, very high enrichment ($20 < EF \leq 40$) of Cr was observed at sampling locations D6, D15, D16, and D19,

respectively. Higher enrichment of the Cr indicates its origin from anthropogenic sources and is of prime concern due to its higher toxicity to the wetland ecosystem (Wang et al., 2020b). Minimal to moderate enrichment was observed for Mn. Only site D1, D9 and D20 had significant enrichment ($5 < EF \leq 20$) due to Mn. Extremely high enrichment of Zn was observed at D9, D16 and D20 ($EF > 40$), which could be due to the presence of battery, wastes tires and tubes (Lane et al., 2020). At the same time, significant enrichment ($5 < EF \leq 20$) and very high enrichment ($EF > 40$) of Zn were observed at other sampling locations.

Irrespective of the particular sampling location, all the sampling locations showed extremely high enrichment ($EF > 40$) of Cd; concurrent results were also obtained by some researchers investigating the HMs in the soil contaminated by MSW (Borah et al., 2018; Halwani et al., 2020). For most MSW dumping sites, the primary source of Cd is electronic waste (Panwar and Ahmed, 2018). Significant enrichment of Cu ($5 < EF \leq 20$) was observed in about 35% of the sampling locations. The sampling locations at D6, D7, D17 and D20 witnessed significant enrichment, which may be attributed to the runoff of chemical fertilizers and pesticides from the nearby agricultural fields. Besides, about 60% and 5% sampling locations were moderately ($2 < EF \leq 5$) and minimally enriched (≤ 2) with Cu, suggesting a lower level of anthropogenic influence concerning Cu. Significant enrichment of Ni was observed in about 85% of sampling locations at MSW dumping site, credited to anthropogenic sources of metals and scrap wastes, whereas only 15% of the sampling locations fell under the category of moderate enrichment ($2 < EF \leq 5$).

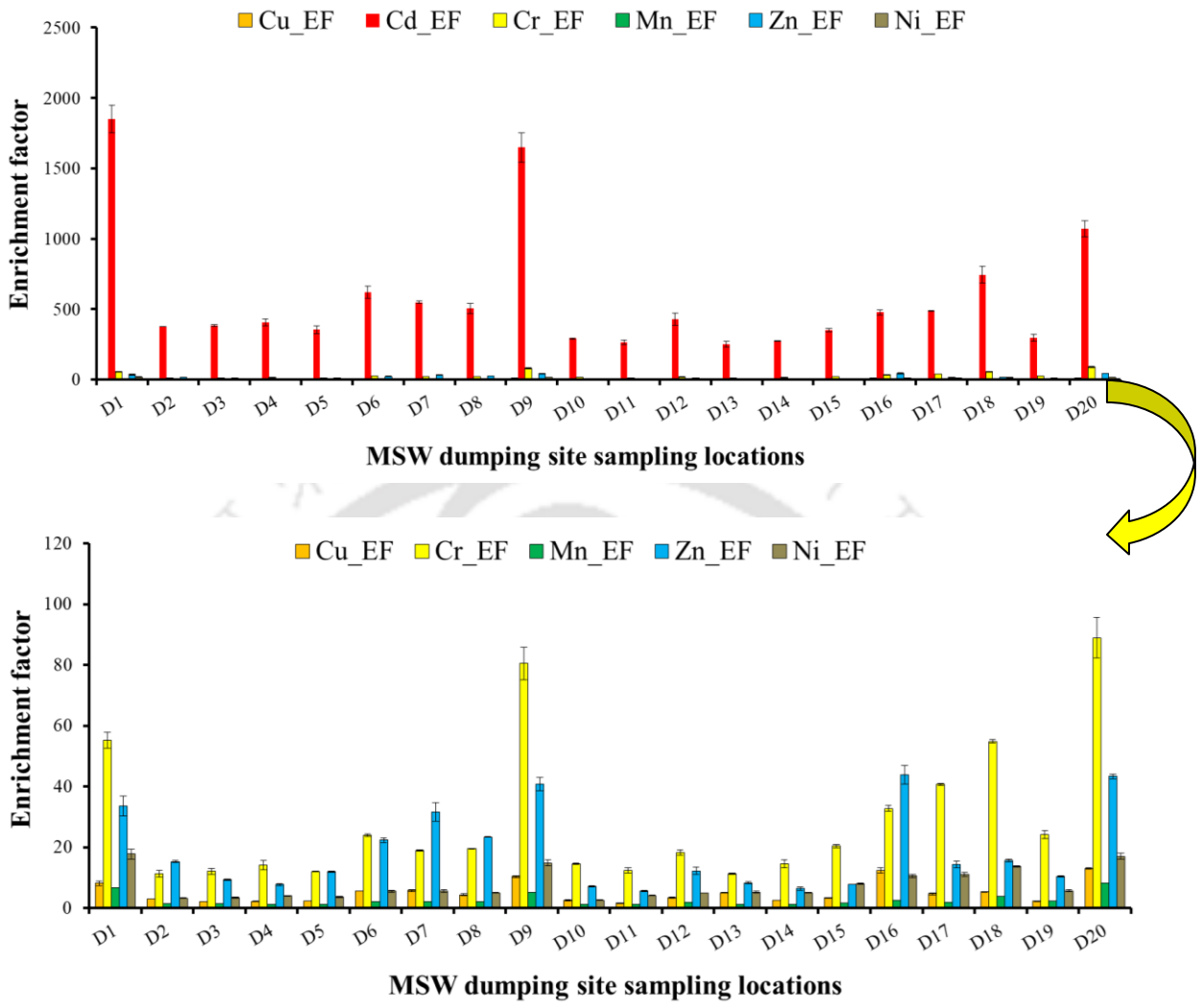

Fig. 4.12. Enrichment factor (*EF*) at MSW dumping site in Guwahati, Assam.

Mobility factor (MF)

Mobility of all studied HMs has been illustrated in Fig. 4.13. MF indicates the bioavailability of the metals in the soil matrix. Very low mobility of Cr, particularly from site D1 to D15, made it less bioavailable (0.98 - 18.89%). From sites D16 to D20, the mobility of Cr was comparatively higher (23.97 - 30.44%) due to the functioning of metallic and glass waste segregation operations. Some studies revealed that HMs from the e-waste is not reduced; rather, they get accumulated, transported, and diffused into the soil (Xiong et al., 2019). *MF* for Mn varied from 90.69 to

30.76%, which indicates that a considerable amount of Mn could be in the mobile phase and thus more bioavailable. Manganese is an essential element in plant mineral nutrient, playing an important role (Luo et al., 2020). For Zn, mobility was moderate to low, only the D10 site exhibited higher mobility, and this site lies close to the wetland embankment situated in the southwest direction and comparatively less polluted by dumped wastes. The average mobility factor (*MF*) for HMs in the MSW dumping site were in the following order of Cd (81.74%) > Ni (77.07%) > Cu (47.36%) > Mn (69.55%) > Zn (44.83%) > Cr (14.64%). It implies that Cd contamination is more bioavailable and toxic and might present a more serious threat to human health. In the present study, mobility of Cr was found comparatively lower than other HMS (Fig. 4.13). *MF* also provided considerable detail in evaluating the potential bioavailability and toxicity of the HMs. The higher the mobility, the greater is the bioavailability of HMs or vice versa.

Cd's very high mobility was observed, particularly from the locations D1 to D11, making Cd more bioavailable. Higher mobility was found in those sampling sites closer to the MSW heap, with MSW wastes and phosphate fertilizers used in the neighbouring agricultural fields as significant contributors. Higher OC, moderate pH, and higher redox potential are the drivers that enhance the soil's Cd mobility (Kubier et al., 2019). High mobility of Cu was observed in sampling location D1 as compared to the other sampling locations. Overall high and moderate mobility of Cu was detected in 55% and 35% of sampling locations of MSW dumping site, respectively. In addition, very high mobility of Ni was observed in sampling locations of D16 to D20, placed in between the glass and metal segregation units, whereas high mobility observed in 70% of the sampling sites.

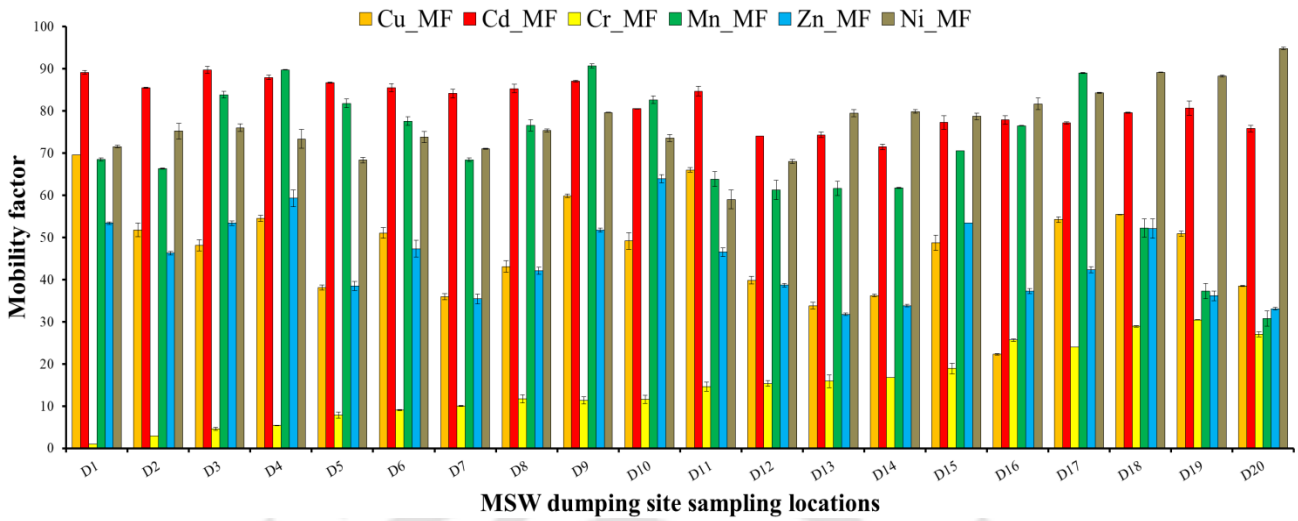

Fig. 4.13. Mobility factor (*MF*) at MSW dumping site in Guwahati, Assam.

Individual contamination factor (ICF) and global contamination factor (GCF)

ICF and *GCF* provide considerable data to evaluate the degree of contamination of HMs. *ICF* factor indicates the degree of potential ecological risk to the aquatic environment with respect to retention time. *ICF* of the Cr is not calculated since no residual concentration was found. However, *ICF* of Mn fell under the high-risk category with a higher potential to flow in the aquatic environment. Some recent studies agree that Mn under robust acidic environment and lower Eh flow inside the groundwater and contaminate it (McMahon et al., 2019). Recent studies indicate that elevated Mn level in groundwater can cause risks to human health (Rahman et al., 2017). For Zn, 65% of the sampling sites fell under the high-risk category. The D6 site is close to the aquatic body and hence could pollute this ecologically sensitive aquatic environment. Overall, 35% of the sites come under the considerable pollution category.

Based on *ICF*, the Cd possessed a higher contamination level (ICF > 6) (Fig. 4.14). This high contamination prevails in the entire study area irrespective of the sampling locations. Cu posed a

high and considerable ecological risk in approximately 50% and 45% sampling locations, respectively. High ecological risks occur in the sampling sites adjacent to the dumping heap and metal segregation units, i.e. D1, D2, D16 and D17. Ni in the soil posed high and considerable contamination risk in approximately 70% and 25% of sampling locations. The higher contamination value of *ICF* showed an apparent corresponding relationship with the higher mobility factor, suggesting a greater risk of contamination to the surrounding ecosystem over time. *GCF* showed a significant increase in contamination levels with a higher risk as posed by all sampling locations. Notably, the Cd was in the higher risk category, while Ni ranged from high risk to moderate risk. This might be attributed to the high amount of e-waste and unsegregated waste dumped at the dumping site, posing a severe ecological risk to aquatic biota of the wetland.

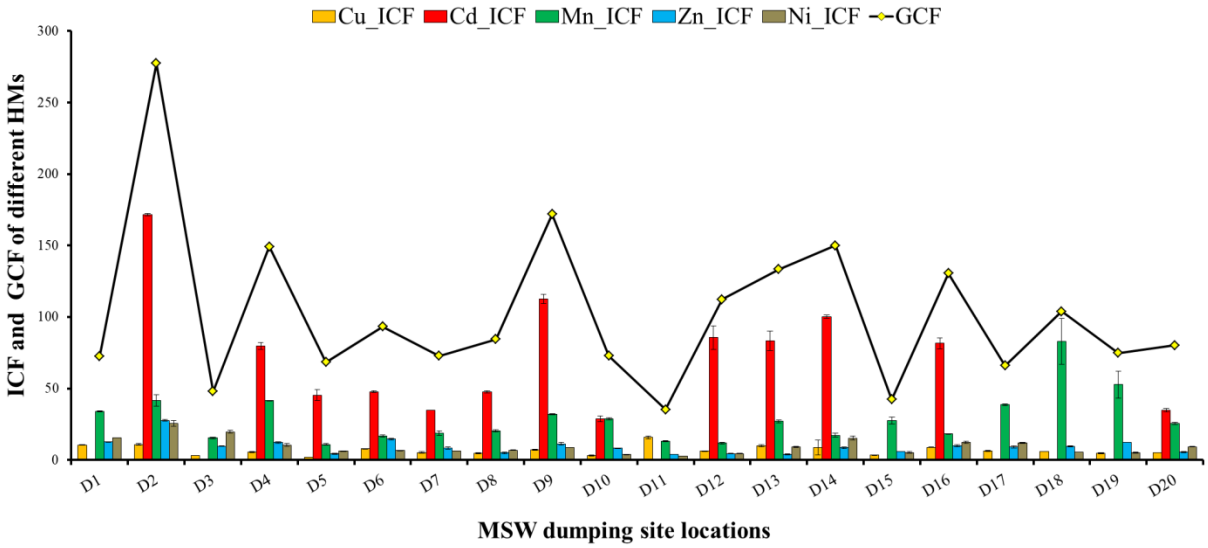

Fig. 4.14. *ICF* and *GCF* at MSW dumping sites in Guwahati, Assam.

4.3.4. Human health risk assessment

Non carcinogenic risk

Health risk assessment provides information about possible pathways of pollutant entry in the body and risks associated with it. Exposure assessment provides information about the rate of exposure and metal possess and the risk associated with it. Average daily doses (mg $kg^{-1}day^{-1}$) was reported higher for Mn > Cr > Zn > Ni > Cu > Cd (Fig. 4.15). Children are more prone to the risk as compared to the adults.

Non-carcinogenic risks posed by the HMs present in the soil of MSW dumping site for adults and children were evaluated through different exposure pathways (ingestion, inhalation and dermal) and expressed in term of hazard quotient (*HQ*). Non-carcinogenic and carcinogenic risks due to the metals in soil contaminated with MSW are presented in Table 4.1. In this study non-carcinogenic risks (*HQ*) associated with Cr followed the order as ingestion (0.22) > dermal (0.04) > inhalation (0.003) in adult and ingestion (1.76) > dermal (0.247) > inhalation (0.005) in children. Similar pattern of non-carcinogenic risk was found in Zn with ingestion (0.001) > dermal (3×10^{-5}) > inhalation (2×10^{-7}) in adult and ingestion (0.06) > dermal (1.7×10^{-4}) > inhalation (3.4×10^{-9}) in children. Health risk associated with Mn followed the order of ingestion (0.019)> inhalation (0.003) > dermal (0.001) in adult and ingestion (0.15) > inhalation (0.004) > dermal (0.001). Health risk in adult due to Mn is mainly due to ingestion (77%), followed by inhalation (13%) and then dermal (8%). While in case of child 97% of risks are associated with ingestion path only. For, Cd the order of average *HQ* (Hazard Quotient) value were ingestion (0.045) > dermal (0.018) > inhalation (7×10^{-6}) in adult and ingestion (0.3624) > dermal (0.101) > inhalation (1×10^{-5}). In Cu the *HQ* were in order of ingestion (0.002) > dermal (2.5×10^{-5}) > inhalation (2.8×10^{-7}) in adult and ingestion (0.0015) > dermal (1×10^{-4}) > inhalation (4×10^{-7}). Similarly, in Ni, the trend of the

HQ were ingestion (0.01) > dermal (2×10^{-4}) > inhalation (1.5×10^{-6}) in adult and ingestion (0.081) > dermal (8×10^{-4}) > inhalation (2×10^{-6}).

A hazard quotient (*HQ*) less than the threshold value of 1 indicate that there is no significant risk associated with the non-carcinogenic effect, whereas *HQ* higher than > 1 indicates significant non-carcinogenic risk (USEPA, 2001). In the present study, the non-carcinogenic risks associated with the studied HMs were non-significant (*HI* < 1) except Cr. Hence, it could be stated that non-carcinogenic risk in the MSW dumping area is low for all HMs except Cr (Fig. 4.16). Although, it was found that HQ_{ing} associated with Cr in children (1.76) was eight times higher than adults. These results indicated that children are more prone to risks associated with Cr present in the soil and the primary path of contamination risks is through ingestion. A recent study by Caparros-Gonzalez et al. (2019) indicated that Cr has a severe impact on children's neuropsychological development. Children are often involved in the segregations and collections of wastes at the study site, and they are exposed to more significant health risks. In this study, Cr exhibited seven times higher hazard index (*HI*) for children (2.017) than adult (0.268). Ingestion is considered one of the major pathways to the overall health risk, and similar observations were reported by the other researchers (Singh et al., 2019; Chabukdhara and Nema, 2013). While there is non-significant risk associated with Cd and Ni, but still for Cd, the contribution of *HQ* (hazard quotient) via ingestion to the *HI* (total risk for non-carcinogenic effects) was the highest, with values as high as 71% for adult and 78% for children, respectively. According to Ni, health risk in an adult is mainly through ingestion (98%), followed by the dermal route (2%). While in the case of children, 99% of risks are associated with the ingestion path only. Additionally, the non-carcinogenic risk from Cu in adults and children was 99% through ingestion and 1% through dermal contact.

Carcinogenic risk

Generally, Cu, Zn and Mn are considered non-carcinogenic according to the international agency for research on cancer (IARC, 2018); therefore, carcinogenic risk (*CR*) for only Cr, Cd and Ni were calculated and represented in Table 4.1. The *CR* values in soil for Cr in the adult were 0.028 (Cr_{ing}), 4.2×10-6 (Cr_{inh}), 1.1×10-4 (Cr_{der}) and 0.226 (Cr_{ing}), 6.3×10-6 (Cr_{inh}) and 0.001 (Cr_{der}) for children. In Cr, *CR* value through ingestion and dermal contact in children was ten times higher than that for adults. Overall, the mean values of the *CR* in the soils contaminated with MSW were 0.028 for adult and 0.227 for children. From the Cr value, it could be inferred that carcinogenic risk mainly occurs through the ingestion pathway followed by dermal contact. Ingestion of metals results in mild to severe liver abnormalities and gastrointestinal mucosal tissue damages (Pobi et al., 2020), whereas dermal contact would result in irritant dermatitis and severe allergic responses (ATSDR, 2004). The *CR* value was higher than 10^{-4}, indicating that carcinogenic risk from Cr in contaminated soil is very high and poses a severe threat to human health (Singh et al., 2019; Tume et al., 2019; Pobi et al., 2020). The calculated health risks indicated a higher risk for the children. A study site rag-picking of wastes was taken up by the children belonging to the age group of 5-16 years. Thus, children are exposed to severe health risk in terms of physical and mental well-being.

Carcinogenic risk (*CR*) for Cd in adults followed exposure pathway: ingestion (2.9×10^{-5}) > dermal (1.1×10^{-7}) > inhalation (4.2×10^{-9}). For children, *CR* values followed the similar trend as ingestion (2×10^{-4}) > dermal (6.4×10^{-7}) > inhalation (6.38×10^{-9}). Overall, the average *CR* values for Cd were 2.9×10^{-5} for adults and 2×10^{-4} for children, respectively. Especially in children, the *CR* value was higher than 10^{-4}, indicating that the carcinogenic risk from Cd in contaminated soil is very high, and it poses a serious threat to human health. In case of Ni, the *CR* for adult followed a similar trend; ingestion (0.00017) > dermal (6.8×10^{-7}) > inhalation (2.51×10^{-8}). Similar trend

was also observed in case of children; ingestion (0.001) > dermal (2.85×10^{-5}) > inhalation (3.8×10^{-8}).

Overall, the carcinogenic result revealed a vital fact that the significant risk to the children is mainly associated with Cr, Cd and Ni. Cd can occur in a soluble form and therefore is more bioavailable and potentially more toxic to humans and is readily absorbed by the kidney and affects the bones, even at a very low concentration (Zhang et al., 2017b). Likewise, results also suggested that ingestion was the most critical exposure pathway in the MSW dumping area, accounting for approximately 90% of the total Cd exposure. MSW dumping site receives a good amount of glass and ceramics waste that contain Cd as an essential constituent of pigments used in coloring and during manufacturing (ATSDR, 2011).

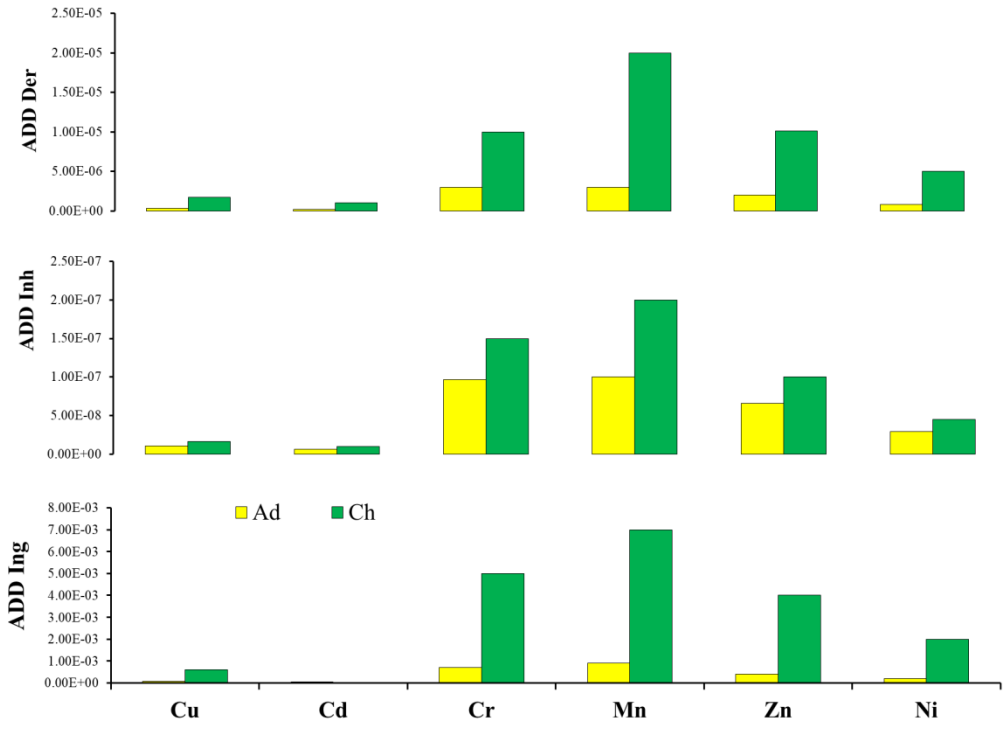

Fig. 4.15. Average daily doses (ADDs) of the HM exposure to the human health.

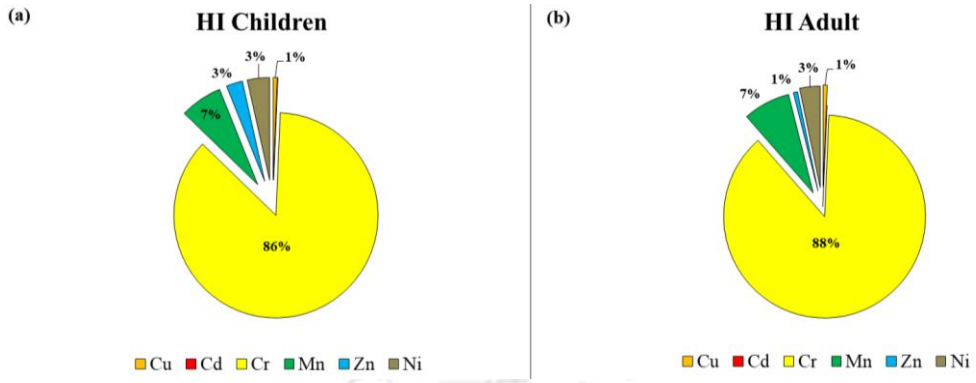

Fig. 4.16. Percentage contribution of HMs to the HI in both children and adult.

Table 4.1. Human health risk assessment for carcinogenic and non-carcinogenic risks at Site-1.

		Non-carcinogenic risks											
		Chromium		Manganese		Zinc		Cadmium		Nickel		Copper	
		Adult	Children	Adult	Children	Adult	Children	Adult	Children	Adult	Children	Adult	Children
HQ $_{ing}$	Min	0.1	0.83	0.012	0.1	8.00E-04	0.03	0.032	0.2537	0.006	0.047	0.001	0.01
	Max	0.38	3.04	0.029	0.23	0.004	0.15	0.06	0.4771	0.017	0.136	0.006	0.045
	Mean	0.22	1.76	0.019	0.15	0.001	0.06	0.045	0.3624	0.01	0.081	0.002	0.015
HQ $_{inh}$	Min	0.002	0.002	0.002	0.003	1.1E-07	1.7E-09	5E-06	7.1E-06	8.4E-07	1E-06	1.8E-07	3E-07
	Max	0.006	0.009	0.004	0.006	5.5E-07	8.4E-09	9E-06	1.3E-05	2.4E-06	4E-06	8.2E-07	1E-06
	Mean	0.003	0.005	0.003	0.004	2.2E-07	3.4E-09	7E-06	1E-05	1.5E-06	2E-06	2.8E-07	4E-07
HQ $_{der}$	Min	0.021	0.116	0.001	7.00E-04	1.5E-05	8.5E-05	0.013	0.071	9E-05	5E-04	1.6E-05	9E-05
	Max	0.076	0.426	0.003	0.002	7.5E-05	4.2E-04	0.024	0.134	3E-04	0.001	7.4E-05	4E-04
	Mean	0.044	0.247	0.002	0.001	3.0E-05	1.7E-04	0.018	0.101	2E-04	8E-04	2.5E-05	1E-04
HI	Min	0.126	0.949	0.015	0.101	0.001	0.030	3E-05	3E-04	0.006	0.047	0.001	0.01
	Max	0.462	3.479	0.036	0.243	0.004	0.150	6E-05	5E-04	0.017	0.137	0.006	0.045
	Mean	0.268	**2.017** *	0.023	0.156	0.002	0.060	5E-05	4E-04	0.01	0.082	0.002	0.015
		Carcinogenic risks											
CR $_{ing}$	Min	0.013	0.105	-	-	-	-	2E-05	2E-04	9.9E-05	8E-04	-	-
	Max	0.048	0.383	-	-	-	-	3.8E-05	3E-04	0.00028	0.002	-	-
	Mean	0.028	0.226	-	-	-	-	2.9E-05	2E-04	0.00017	0.001	-	-
CR $_{inh}$	Min	1.9E-06	2.9E-06	-	-	-	-	2.9E-09	4.47E-09	1.45E-08	2.2E-08	-	-
	Max	7.0E-06	1.1E-05	-	-	-	-	5.5E-09	8.4E-09	4.19E-08	6.4E-08	-	-

	Mean	4.2E-06	6.3E-06	-	-	-	-	4.2E-09	6.38E-09	2.51E-08	3.8E-08	-	-
CR $_{der}$	Min	5.2E-05	0.000	-	-	-	-	8E-08	4.5E-07	3.9E-07	2E-05	-	-
	Max	1.9E-04	0.001	-	-	-	-	1.5E-07	8.4E-07	1.1E-06	3.76E-05	-	-
	Mean	1.1E-04	0.001	-	-	-	-	1.1E-07	6.4E-07	6.8E-07	2.85E-05	-	-
CR	Min	0.013	0.105	-	-	-	-	2E-05	2E-04	1E-04	0.0008	-	-
	Max	0.048	0.385	-	-	-	-	3.8E-05	3E-04	0.0003	0.0023	-	-
	Mean	**0.028** **	**0.227 ** **	-	-	-	-	2.9E-05	**2E-04****	**0.0002****	**0.0014****	-	-

HQing=Hazard Quotient ingestion; HQinh=Hazard Quotient inhalation; HQdermal= Hazard Quotient dermal; HI=Hazard index; CRing=Carcinogenic risk ingestion; CRinh=Carcinogenic risk inhalation; CRder=Carcinogenic risk dermal.

** CR>10-4 indicate higher carcinogenic risk.

* HQ>1 indicate higher non-carcinogenic risk

4.4. Results and discussion (Site-2).

4.4.1. Geochemical fractions assessment

Chromium (Cr) fractions

The sequential extraction procedure revealed that Cr was absent in water-soluble (F1), exchangeable and residual fraction (F6) (Fig. 4.17). The organic bound phase (F5) was the dominant fraction accounting for about 48.43%, whereas the Fe-Mn bound accounted for 28.15%. A higher concentration of the F5 fraction reported in the BK5 locations, which corresponds to the deposition of the Cr during kiln operation. Cr in kiln leads to the formation of highly reactive oxygen species, which later converted into more lethal carcinogenic and mutagenic malonaldehyde (Jahan et al., 2016). Under natural condition, the Cr turns into highly soluble substances of chromate (Verbinnen et al., 2013). Cr generally exists in the form of chromate (CrO_4^{2-}), hydrogen chromate ($HCrO_4^-$) and dichromate ($Cr_2O_7^{2-}$), which is highly soluble and oxyanions (Yang et al., 2019). Furthermore, from metal speciation, the average values of Cr from all locations were mostly associated with the F5 fraction. The higher content of the Cr in the BI was in close agreement with the study conducted by Mondal et al., (2017) at Assam. It reported that coal ashes are the prime sources of the HMs which are converted from aerosol to volatilization during the heating process and further to condensation and deposition when the temperature comes down. Moreover, a small amount of Cr is also associated with the Fe- Mn bound fraction (28.15%), which is more readily released in the surrounding environment and increases the risk of bioaccumulation. Overall, Cr content in the soil follows a trend of F5 (48.45%) > F4 (28.15%) > F3 (23.41%). A very small Cr was present in its F3 fraction, suggesting its low potential to form carbonate compounds inside the soil matrix.

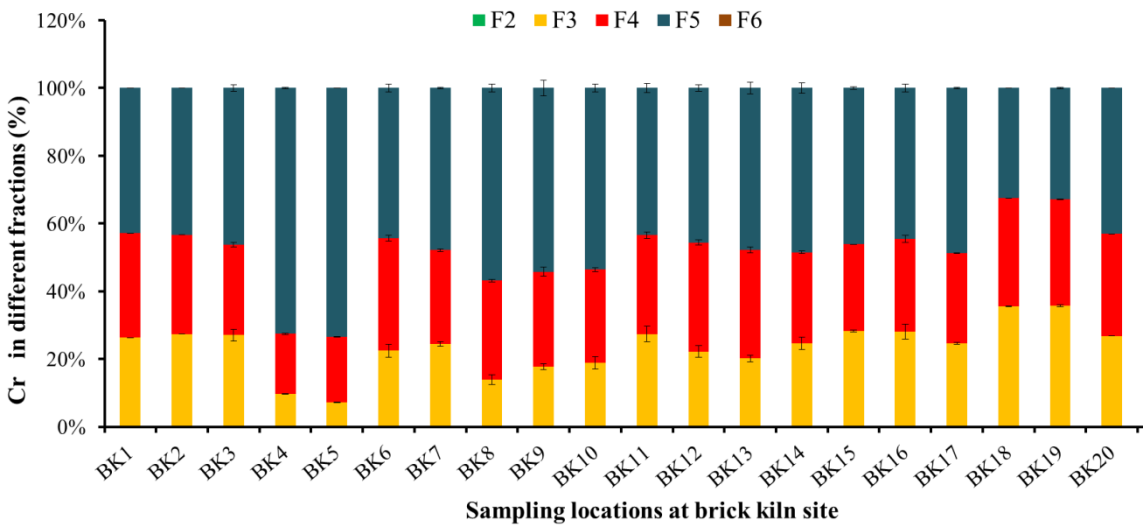

Fig. 4.17. Chromium in different fractions present in soils around brick kiln industry, Napaam, Tezpur.

Manganese (Mn) fractions

From speciation analysis of Mn following trend was obtained F2 (49.47%) > F4 (19.85%) > F6 (12.49%) > F3 (11.54%) > F5 (3.49%) > F1 (1.70%). Almost half of the Mn belonged to the exchangeable fraction creating the Mn more bioavailable (Zhang et al., 2018; Fig. 4.18). Sampling location BK8 lies close to a variety of plant green taro (*Colocasia esculenta*) and experienced predominant association of Mn in the exchangeable fraction, which may be due to the greater affinity of the plant to absorb the micronutrient as Mn. The first two sampling locations, i.e., BK1 and BK2, contribute some water-soluble fractions in Mn, which might be attributed to uptake of plant species belonging to the family Rhamnaceae, as Mn is a micronutrient under stress condition. BK-3 showed higher values of water-soluble Mn which might be ascribed due to the higher bottom ash percentage in soil which retains the Mn on its surface. Generally, Mn is a major constituent of the inorganic fertilizer and added to the soil to increase plant growth (Ye et al., 2020). In the F4 fraction, the highest concentration was observed at the sampling location of BK18, which is far

from the brick kiln and near an agriculture site. This indicates that Mn has a different source of origin, and it is primarily not from the kiln of the BI.

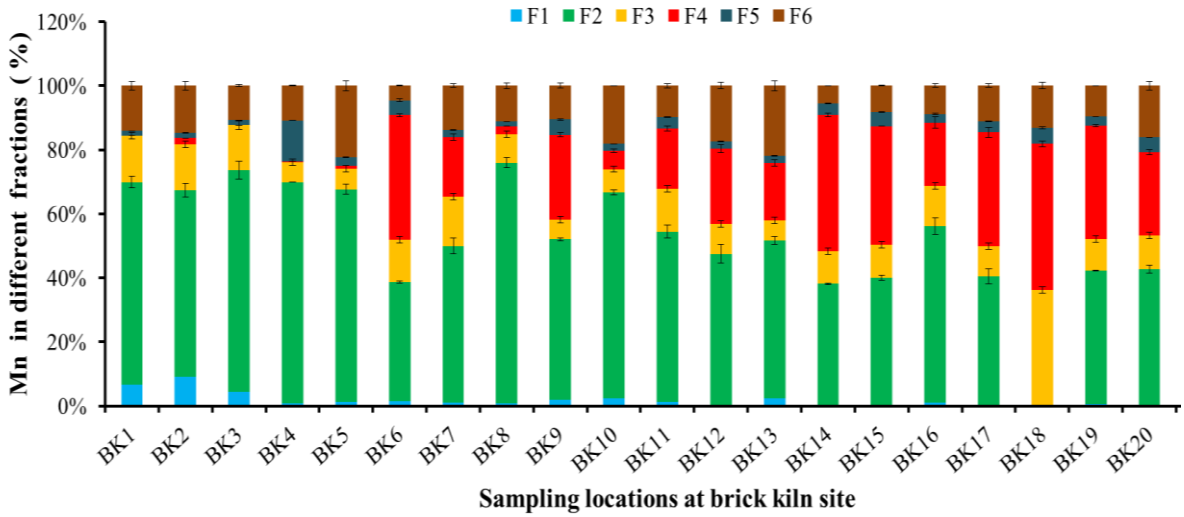

Fig. 4.18. Manganese in different fractions present in soils around brick kiln industry, Napaam, Tezpur.

Zinc (Zn) fractions

F1 to F3 fractions constitute a bioavailable fraction of Zn, accounting for about 39.98% of the total Zn, thus contributing to lesser contamination (Fig. 4.19). Further, it also indicates Zn is lesser mobile, and the water-soluble fraction is present only in the sampling locations of BK-1, BK-2 and BK-3, where the ash comparatively contaminates the soil more. Overall, different fractions of Zn followed the order: F6 (32.54%) > F3 (24.95%) > F4 (15.40%) > F2 (13.80%) > F5 (12.18%) > F1 (1.13%). The present investigation revealed that Zn was mostly present in the residual fraction suggesting the strongly bounded nature of the Zn in the soil matrix and not potentially bioavailable. Despite this fact, a recent study reported higher Zn content in the blood of the exposed group of worker (David et al., 2020). In BI, the ash emanating from the brick kilns are the important sources of Zn (Sharma et al., 2007).

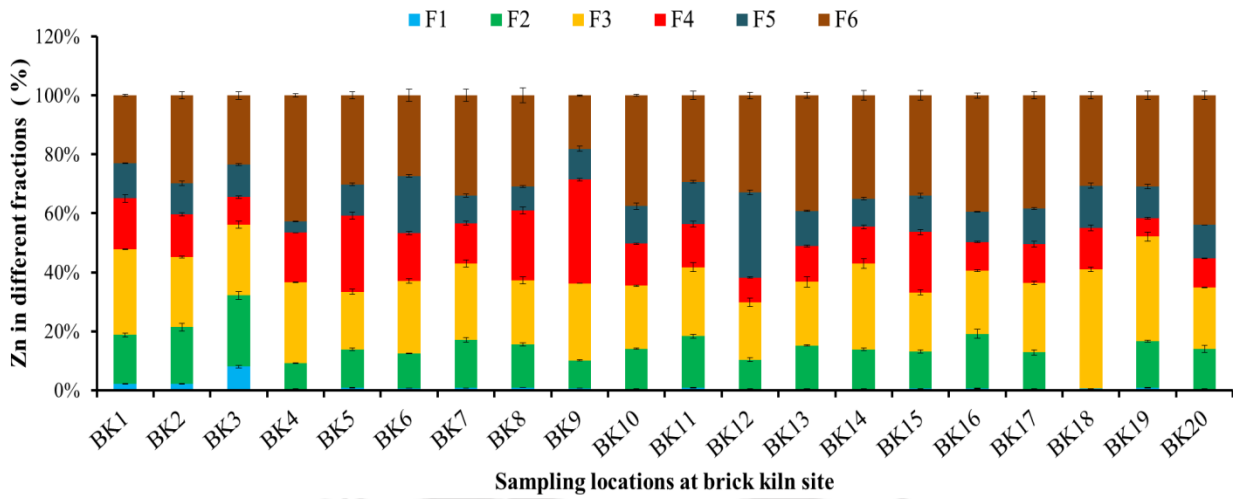

Fig. 4.19. Zinc in different fractions present in soils around brick kiln industry, Napaam, Tezpur.

Cadmium (Cd) fractions

The percentage of various chemical fractions of Cd in the soil contaminated with BI are presented in Fig. 4.20. In the study site, Cd was mainly concentrated in the carbonate bound phase, i.e., F3 (55.78%), and showed secondary association with the exchangeable phase (F2) (35.01%). The higher affinity of Cd in the acid-soluble phase (91.59%) may be due to the formation of Cd carbonate complexes. Concurrently, higher concentrations of Cd around BI were reported by many studies (Ismail et al., 2012; Proshad et al., 2017). Also, Cd gets easily associated with carbonate, chloride, sulfate, and bisulfide anions as ligands (Kubier et al., 2019). The F3 fraction of HMs can quickly become more bioavailable as the pH changes, rendering it more toxic than any other fraction of HMs (Qiao et al., 2020). The high concentration of HMs like Cd in the soil of BI might be attributed to the firing operation of coal and low-quality fuel like tires, rubbers and other waste in nonscientific ways (Achakzai et al., 2015). In areas surrounding BI, Cd exists in the divalent cation state, which complexes with other elements and forms, e.g., $CdCl_2$, $CdCaO_3$. A significant part of Cd is also associated with Fe-Mn bound residual fraction (F6), which accounts for 6.69%,

respectively. As shown in Fig. 4.20, the total proportion of the Cd in F1 + F2 + F3 was 90.79%, evoking higher mobility and bioavailability, thus clearly increasing human health and ecological risks. Overall, the average Cd fraction followed the order as F3 (55.78%) > F2 (35.01%) > F4 (6.69%) > F6 (2.48%) > F5 (0.04%).

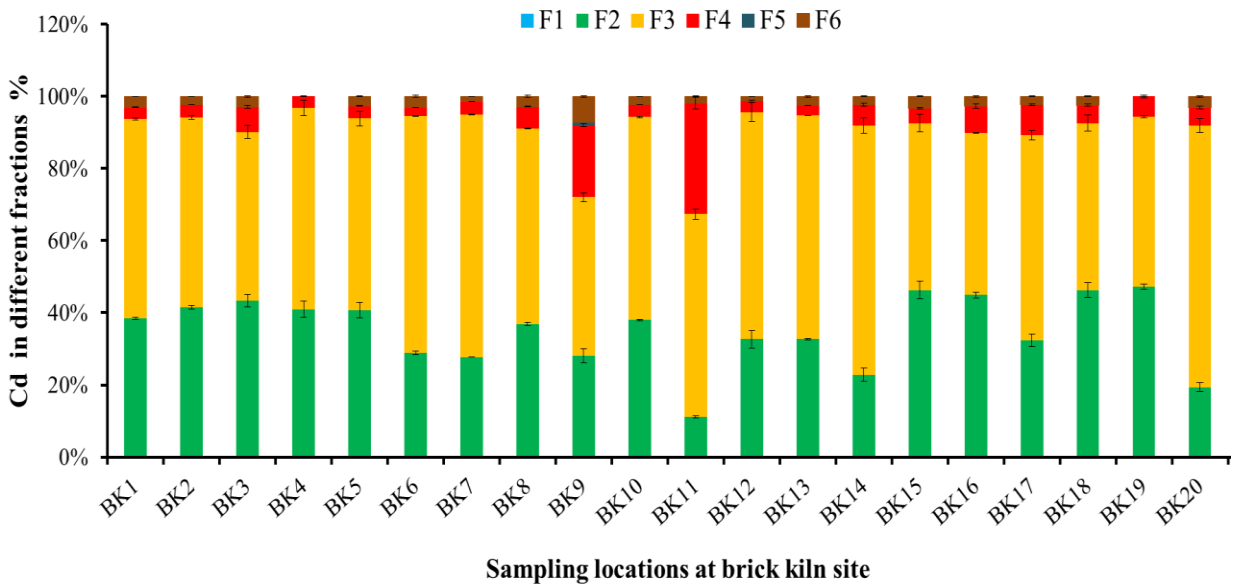

Fig. 4.20. Cadmium in different fractions present in soils around brick kiln industry, Napaam, Tezpur.

Copper (Cu) fractions

Cu primarily exists in the carbonate fraction (F3), which accounts for 32.80%, and is in labile form. Labile fractions generally comprise of water-soluble (F1), exchangeable (F2), and the carbonate bound (F3) fractions that could be released to the surrounding environment under favorable environmental conditions created by change in pH and Eh levels (Prartono et al., 2016; Ji et al., 2018). In the case of Cu, 46.41% belongs to the labile fraction, which constitutes 1.94% of F1, 11.51% of F2, and 32.96% of F3 fractions, respectively (Fig. 4.21). Cu under the above fractions retained on the surface by a weak electrostatic force and could be released by the ion-

exchange process. In addition, in the brick kiln industry, Cu might be derived from ash and firing operations inside the kiln. The other sources of Cu in the environment are the pesticide and fungicides. The other fraction which shares a significant contribution is the residual fraction, i.e. F6 fraction. Cu in this fraction may be bound to the soil matrix (Mondal et al., 2017). The Fe-Mn bound fraction (F4) contributes about 11.43%, attributed to various minerals available in the soil. Notably, Cu is the highest in the F3 fraction and at site BK18. This may be due to Cu present in the fungicide and insecticides applied in the field during rice cultivation, resulting in the dominance of Cu in the F3 fraction. Cu bound to the carbonate fractions since it was more available, which means that Cu in the contaminated soil can be easily exchanged. In the soil matrix, the availability of the Cu is governed by the pH; higher pH leads to the formation of $Cu(OH)_2$ and $CuCO_3$ (Sekine et al., 2017). Cu has been found to associate strongly with $CuCO_3$, CuO, and Cu_2O. Overall, Cu in its different fraction follows the order of F3 (32.96%) > F6 (31.83%) > F2 (11.51%) >F4 (11.43%) > F5 (10.33%).

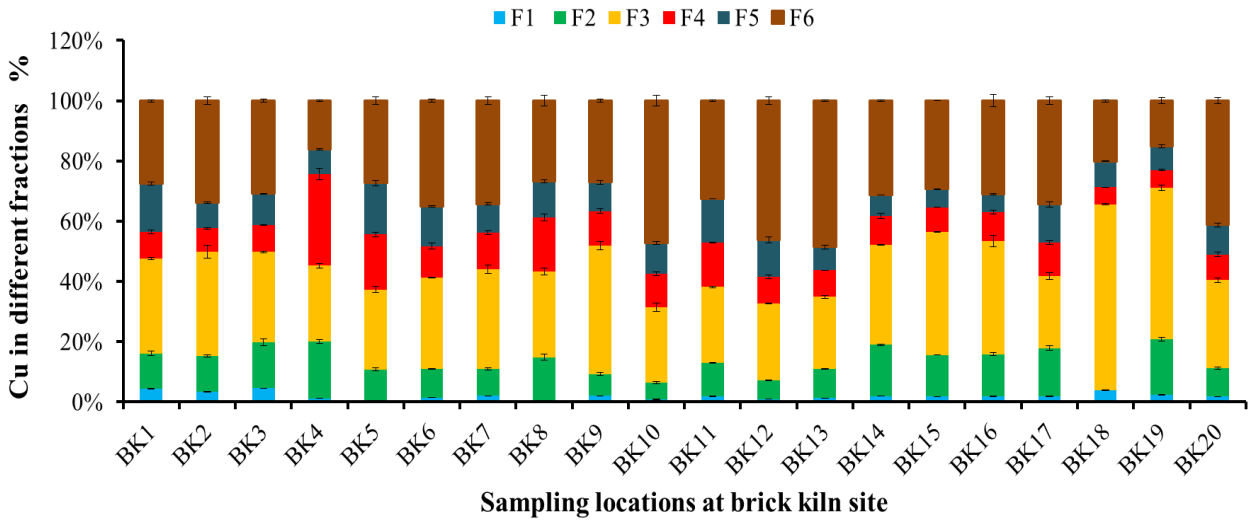

Fig. 4.21. Copper in different fractions present in soils around brick kiln industry, Napaam, Tezpur.

Nickel (Ni) fractions

Nickel was strongly associated with the Fe-Mn phase F4 (51.32%) followed by the residual phase, i.e. F6 (31.19%) and the exchangeable phase F2 (9.97%) (Fig. 4.22). More than 50% of the Ni present in its potentially bioavailable form possesses a higher risk to the soil environment and human health. Some research suggested that Ni causes homeostatic imbalances, particularly in male working in the brick kiln (David et al., 2020). Apart from the F4 fraction, a smaller portion (9.98%) was also associated with the exchangeable phase (F2). Under the F2 fraction, the weakly adsorbed Ni gets readily dissociated in the soil under changing pH conditions (Al-Mur et al., 2020). Ni generally occurs in the various oxidative states in the soil system, ranging from -1 to +4. Among which +2 oxidation states is highly reactive and poses a more significant threat to the living system.

Ni in its F4 fraction was reported the highest in the BK5, which laid in the northern part of the kiln. Whereas the carbonate bound fraction (F3) and organic bound (F5) account for 7.44% and 0.07%, respectively, this is quite low compared to the other fractions of Ni. Overall, the Ni in the different fractions ordered as: F4 > F6 > F2 > F3 > F5. Generally, higher Ni concentration in the soils of BI might be attributed to fly ash deposition during the firing operation. A similar and detrimental effect of Ni was reported by researchers in the areas near BI industries (David et al., 2020; Dey and Dey, 2017; Proshad et al., 2017).

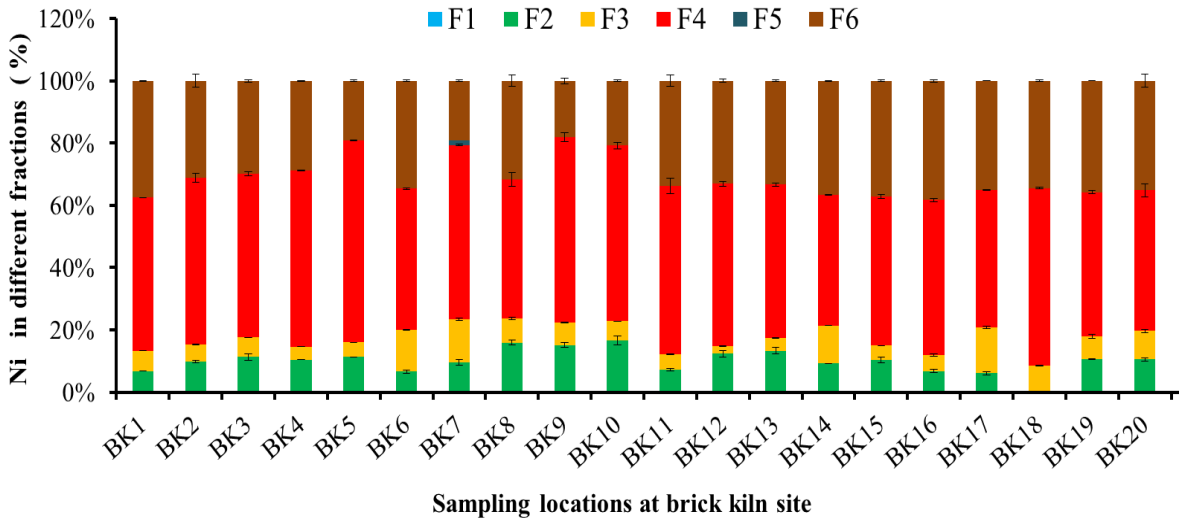

Fig. 4.22. Nickel in different fractions present in soils around brick kiln industry, Napaam, Tezpur.

4.4.2. Spatial distribution of the different metals

The patterns that emerged from spatial mapping of Cr, Mn, Cd, Cu, Ni, and Zn revealed distinct facets of their distribution. Thus, high concentrations of Cr near the brick kilns was revealed by continuous spatial patterns; whereas two discontinuous spartial pattern from rice fields, lying south of the kiln indiacting higher Cr concentration (Fig. 4.23). Fly ash dispersion, deposition, and subsequent disruption of fertile crop lands were implied by spatial analysis of Cr increment in the outlying sampling locations (BK 15 and BK16). Spatial mapping patterns of Mn, showed significantly high concentrations from agriculture fields on the eastern side of the brick kiln, and parts of the sampling location, BK15. The patterns underscored the fact that Mn is an essential trace element required for plant growth and commonly found in fertilizers. Concurrently, an interesting spatial distribution pattern for Cd was visible; it was very low in the east of the brick kiln, in contrast to the higher Cd contamination, west of the kiln. The eastern part, dominated by rice cultivation, supported elevated Mn concentration in the soil, which in turn is reported to reduce Cd uptake in the rice plant (Huang et al., 2021). This is primarily attributed to the competition

between Mn and Cd, facilitated by the transporter gene OsNramp5 (natural resistance-associated macrophage protein 5). The reduction of Cd in rice is vital, as the ingestion of rice (*Oryza sativa* L.) is the main route of human exposure to Cd. In the western part, the higher Cd levels showcased the contamination arising from proximity of sampling locations BK9 and BK10, which were closer to the brick kiln and to human habitation. These observations raise the level of potential threat to human health, since lower concentrations of Cd was observed by Mondal et al. (2017) in areas adjacent to brick kilns in Assam.

Spatial analysis of Cu revealed a higher concentration further away from the kiln, in the southern area (Fig. 4.23), thus suggesting alternative sources of origin; fertilizers, containing Cu an essential component is considered a prominent source. Ni, one of the most carcinogenic metals, was mainly concentrated near the brick kiln and sites adjacent to sampling site BK16. The latter is in the agricultural area, raising the possibility of Ni contamination. Spatial analysis revealed that the north western part of the site had higher contaminations of Zn; which gradually increased towards the rural settlements on the western side of the BI.

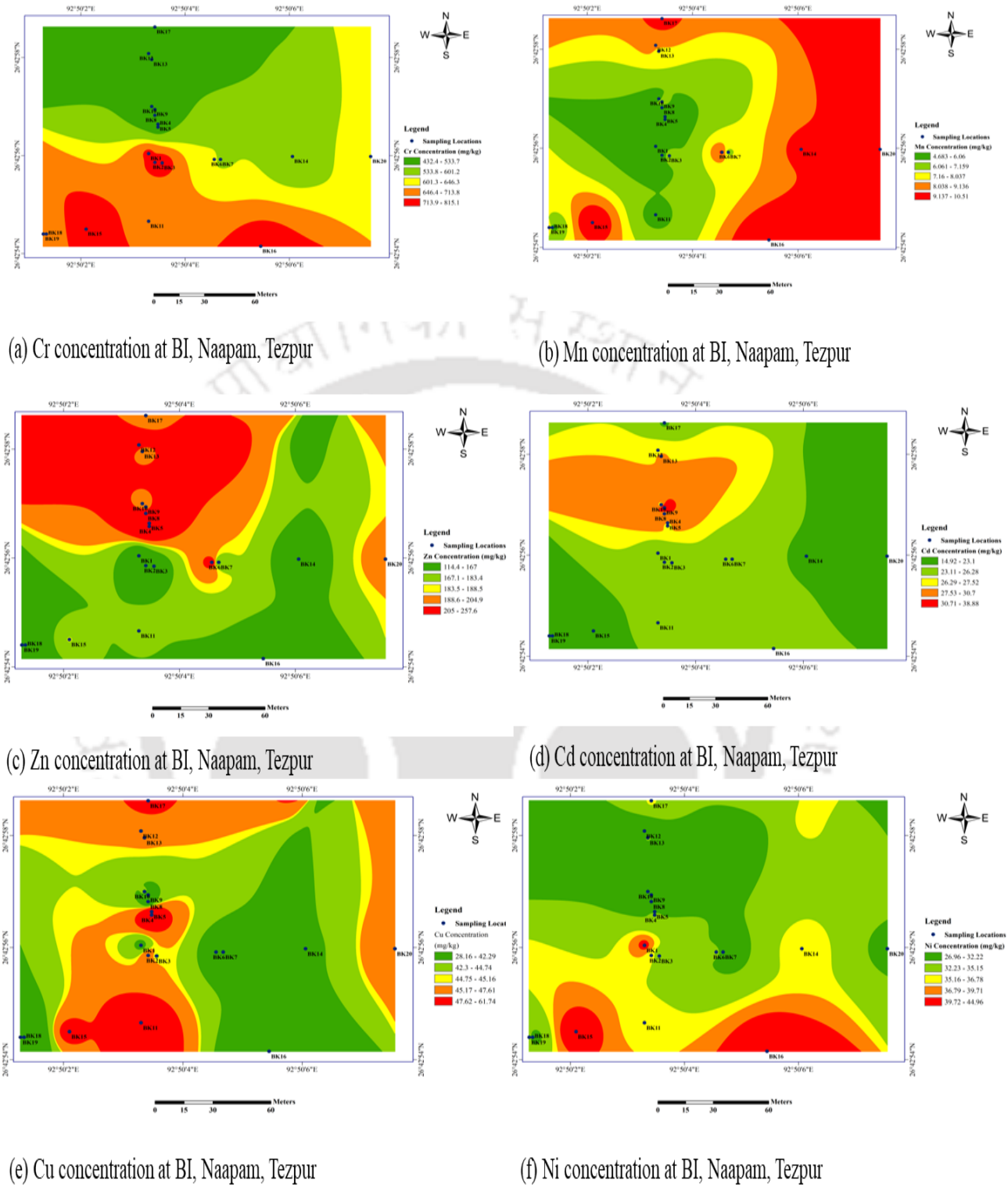

Fig. 4.23. Spatial distribution of the HMs in the soils around brick kiln industry, Naapam, Tezpur Assam.

4.4.3. Environmental indices for ecological risk assessment

Geo-accumulation index (I_{geo})

I_{geo} is the quantitative measure used to assess contamination level in the soil (Fig 4.24). For Cr, all the sampling locations (BK1-BK20) were within the moderately to heavily polluted category ($3 < I_{geo} \leq 4$). Mn pollution was negligible and classified as not polluted ($I_{geo} < 0$). Likewise, the level of contamination for Zn and its indices of geo-accumulation fell in the unpolluted (0-1) category.

Notably, Cd pollution in the present study area of the brick kiln industry, was in the extremely polluted ($I_{geo} > 5$) category for all sampling locations; attributed to the firing operations during brick manufacturing process. Higher contamination in the present study also corroborated previous data reported for Assam (Mondal et al., 2017). Cd is also usually considered as a marker of agricultural activities that use pesticides, chemical fertilizers, and other chemicals (Cai et al., 2019). For Cu and Zn, all the sampling locations fell under the unpolluted category ($I_{geo} < 0$).

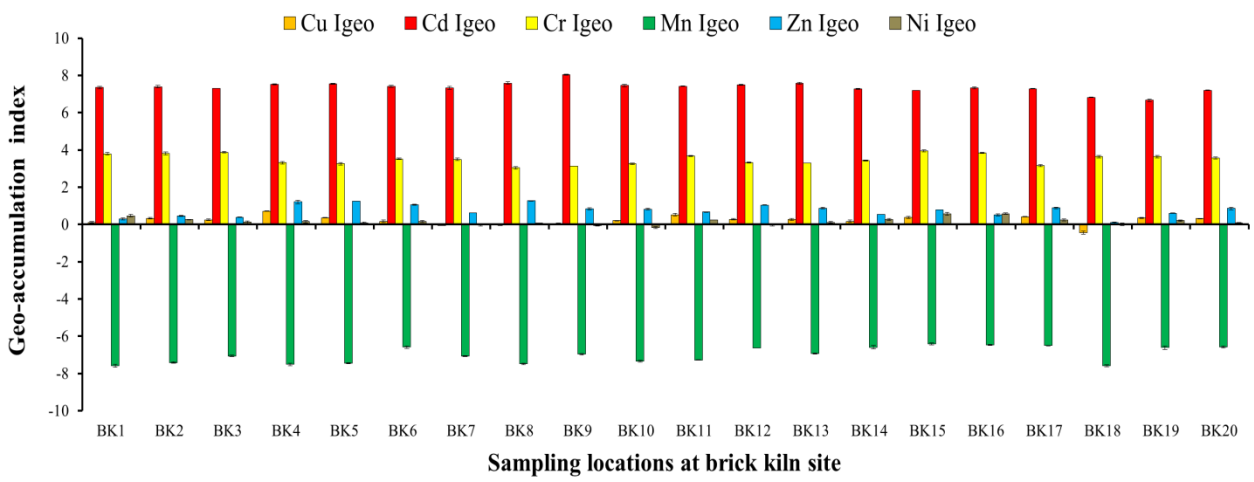

Fig. 4.24. Geo-accumulation index (I_{geo}) at brick kiln industry site, Napaam, Tezpur.

Pollution load index (PLI)

PLI represents the number of times the HM concentration in the soil exceeded the background concentration, and it provides a summative indication of the overall heavy metal level. The *PLI* index is indicated as ≤ 0.1 clean; 0.7-1 warning limit; 1-2 slight pollution; 2-3 moderate pollution; ≥ 3 heavy pollution. Thus, Site-2 has a warning limit for Cr metal contamination (1≤ *PLI* ≥ 0.7), whereas it is not visibly contaminated with the Mn and Ni (*PLI* < 0.1) (Fig. 4.25). 55% of the sampling locations came under the warning limit (0.7 -1) for Cu, while the remaining 45% were within the clean category (<0.1). Likewise, for Ni, 85% of the sampling locations were below the warning limit and 15% under the clean category. Among all studied HMs, only Cd, pollution levels breached the heavily polluted category (≥ 3). A decreasing trend of the soil pollution level was observed as the distance from the brick kiln increased. Therefore, unregulated expansion of brick kiln activities in rural areas, increases pollution load, and poses great risk to the surrounding agro-ecosystem. Regarding combined pollution effects from studied HMs, *PLI* showed a very high pollution load due to Cd contamination, followed by Ni and Zn. Similar results indicating higher pollution load was also reported by Proshad et al. (2017).

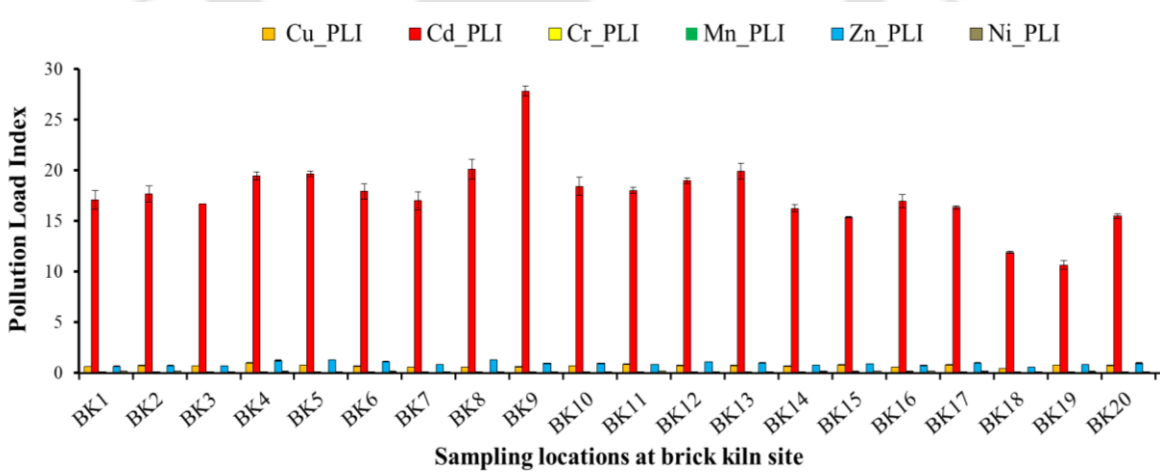

Fig. 4.25. Pollution load index **(***PLI*) at brick kiln industry site, Napaam, Tezpur.

Potential ecological risk index (PERI)

PERI illustrates the relative sensitivity of the biological community to toxic substances (Hakanson, 1980). Among the HMs evaluated, the average potential risk to the surrounding ecosystem, followed the trend Cd > Cu > Zn > Ni > Cr > Mn (Fig. 4.26). Notably, the above analysis showed a close agreement with research indicating higher ecological risk from Cd (Mondal et al., 2017). The *PERI* values for Cd in the MSW soil samples were higher than 320 with a maximum weight of 835.10, indicating severe ecological risk across all the sampling locations. Sources of HMs around the brick kiln, could be derived from multiple activities like associated industrial activities, combustion of fuel and coal, burning of wood, tires, and brick kiln oils. Brick kilns release elements potentially capable of causing high levels of pollution in the soils, thereby escalating soil toxicity. Therefore, accumulation of these hazardous elements in the soil, amplifies their potential risk in the soil ecosystems. The combined ecological risk index (*RI*) revealed a very high environmental risk. In 10% of the sampling locations, HMs exhibited very high risk ($RI \geq 600$), whereas the remaining 90% of the sampling locations demonstrated high risk ($600 \leq PLI \geq 300$). Predominantly, the soil in the brick kiln site indicated the higher ecological risk; the concomitant increased concentration of Cd, reiterated the same danger.

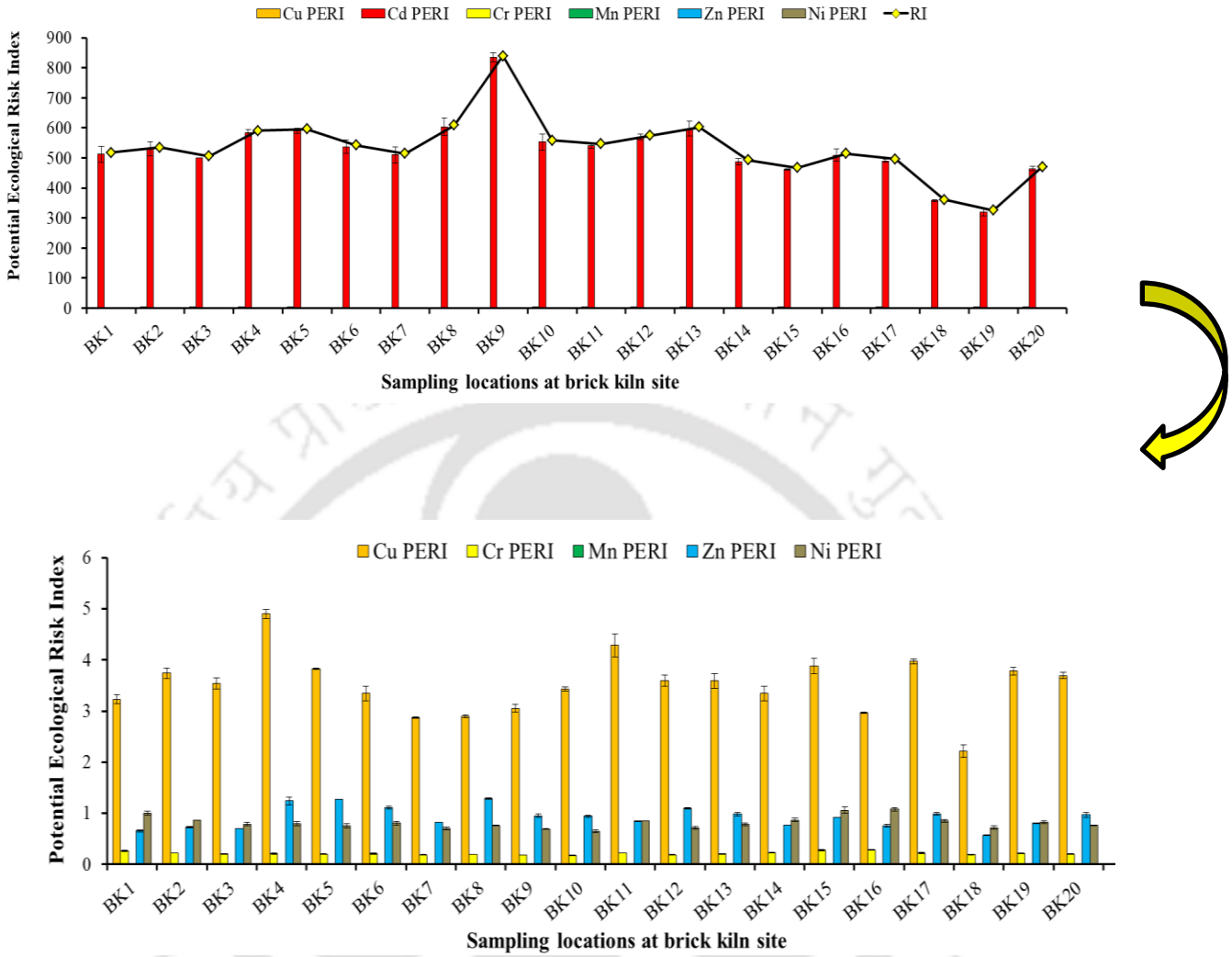

Fig. 4.26. Potential ecological risk index (*PERI)* at brick kiln industry site, Napaam, Tezpur.

Enrichment factor

Enrichment factor (*EF*) helps to elucidate the influence of anthropogenic activities on the soil. For Cr, all sampling locations of Site-2 fell under the category of severe enrichment ($10 \leq EF \leq 25$). Likewise, for Mn, all the sampling locations from BK1 to BK20 fell under the minor enrichment category ($1 \leq EF \leq 3$). BK6 situated on the brick industry's eastern side, exhibited severe enrichment ($10 \leq EF \leq 25$) for Zn. Simultaneously, 75% of sampling locations had only moderate, extreme enrichment ($5 \leq EF \leq 10$) for Zn. Moreover, moderate Zn enrichment ($3 \leq EF \leq 5$) was

observed at sampling locations BK1, BK2, BK3, BK3, BK16 and BK18, respectively. In the case of Cd, extremely severe enrichment was observed in all sampling locations (*EF* > 50). Cu, exhibited minor enrichment (1 < *EF* < 3); it is also considered a non-toxic and non-carcinogenic element. While Ni, known to be a highly carcinogenic HM, showed minor and low anthropogenic contributions in all sampling locations.

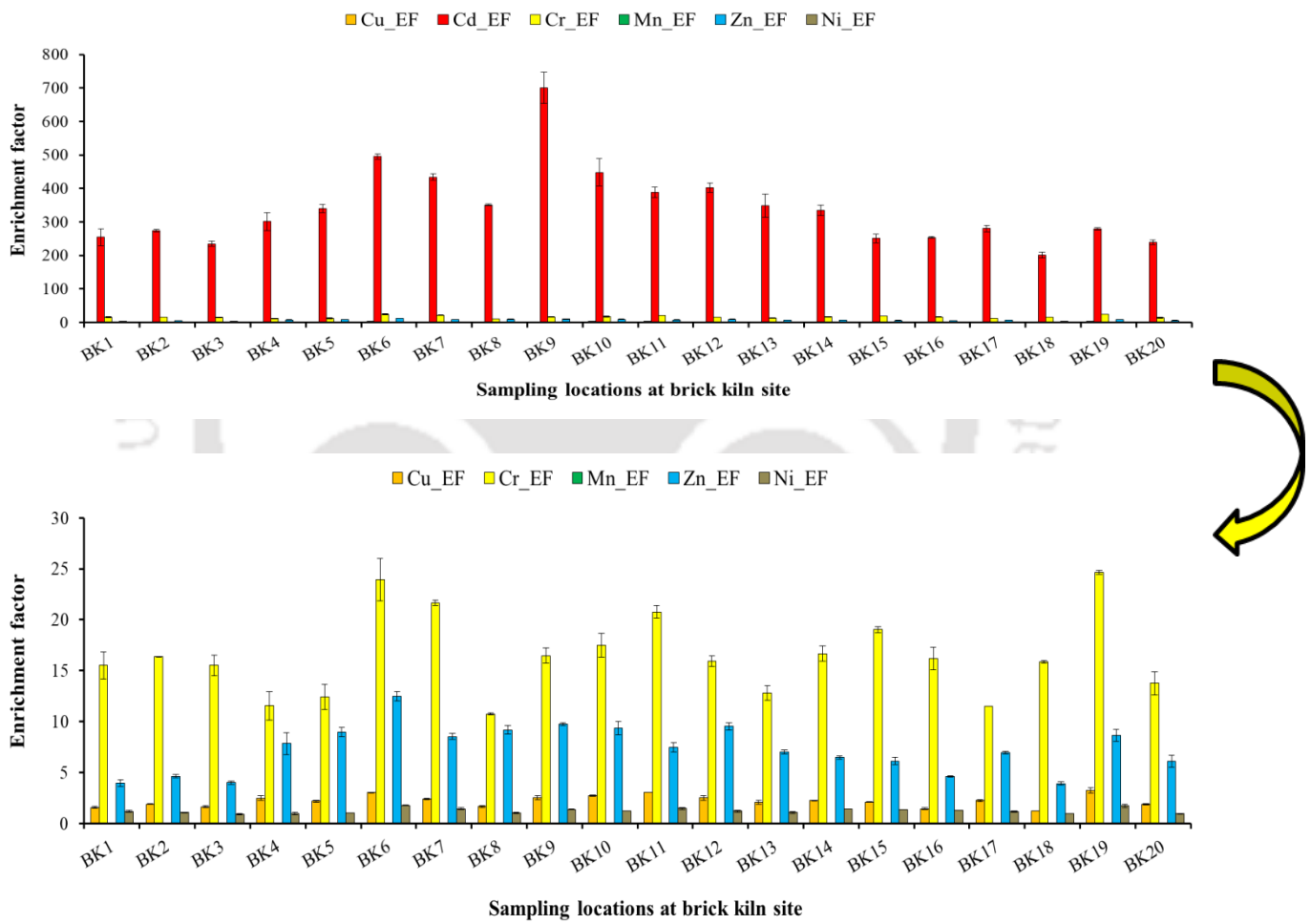

Fig. 4.27. Enrichment Factor (*EF*) at brick kiln industry site, Napaam, Tezpur.

Mobility factor

The *MF* indicates that metals in the earth matrix can be bioavailable. Very low mobility of Cr, were reported particularly from the sampling location of BK4, BK5, BK8, BK9, and BK10, which made it less bioavailable (7.23% - 18.84%). The low mobility of Cr was reported from rest sampling locations, contributing about 85% (20.14% - 35.44%). Mn varied from 36.24% to 91.25%, which showed that a considerable amount of Mn could be in the mobile phase and thus more bioavailable. 20% of the sampling locations belonged to the very high mobility category, while 25% of the sampling locations were within the under increased mobility category. For Zn, 55% of the sampling locations had low mobility (21-40%), whereas the remaining 45% showed moderate mobility (41-60%). The pattern of mobility was dependent on the specific areas and surrounding environment. Very high mobility was observed for Cd in all sampling locations except BK9 and BK11 (Fig. 4.28). Higher mobility was found in locations closer to the brick kiln. Cd is a residual element emanating from the kiln during firing operations. High mobility of Cu was observed in location BK18 and BK19, which were nearer to the agriculture fields in comparison to the other sampling locations. Moderate and low mobility of Cu was detected in 65% and 25% of sampling locations of brick kiln site, respectively. Impaired mobility of Ni was observed in locations BK1 to BK20. Overall, the average mobility factor (*MF*) for HMs in the Site-2 were in the following order of Cd (90.73%) > Mn (64.75%) > Cu (46.41%) > Zn (40.14%) > Cr (23.24%) > Ni (17.30%).

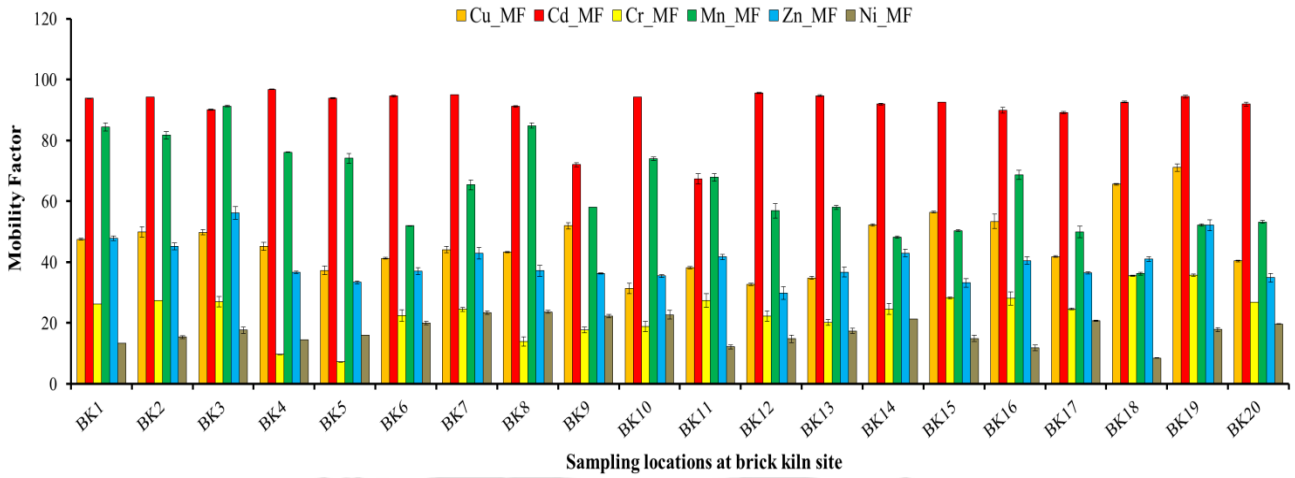

Fig. 4.28. Mobility Factor (*MF*) at brick kiln industry site, Napaam, Tezpur.

Individual contamination factor

ICF and *GCF* provide considerable data to evaluate the degree of contamination of HMs. These is factors also indicates the degree of potential ecological risk to the aquatic environment concerning the retention time. *ICF* of the Cr is not calculated since no residual concentration was found. Based on *ICF*, the Cd possessed a higher contamination level (*ICF* > 6) (Fig. 4.29). This high contamination prevailed in the entire study area, irrespective of the sampling locations. Higher *ICF* was reported at BK7 and BK12, which correspond to the higher deposition of the soot particle. The higher contamination value of the IFC showed an apparent corresponding relationship between the higher *MF%* and I_{geo}, suggesting a greater risk of contamination to the surrounding ecosystem over time with Cd. Notably, the the higher risk category of Cd, might be attributed to the use of the cheaper fuels like firewood and old rubber tires, discarded motor oil, plastic, used lubricant oils, poultry farm droppings, dung cakes, and agricultural residue, for firing the brick kin

(Kamal et al., 2014). *ICF* of the Mn indicated higher contamination (*ICF* > 6) which accounted for 75% of the sampling locations, whereas remaining 25% of locations displayed considerable level of contamination (3 < *ICF* < 6). Mn is among the nontoxic HMs, and found mainly in the chemical fertilizers, therefore its higher level of contamination, may not indicate a heightened level of risk. Cu and Zn followed a similar trend, and about 85% sampling locations showed moderate contamination, and only 15% fell under the considerable contamination category. For Ni, 80% of the sampling locations belonged to the moderate category, and the remaining 20% belonged to the considerable category (3 < *ICF* < 6).

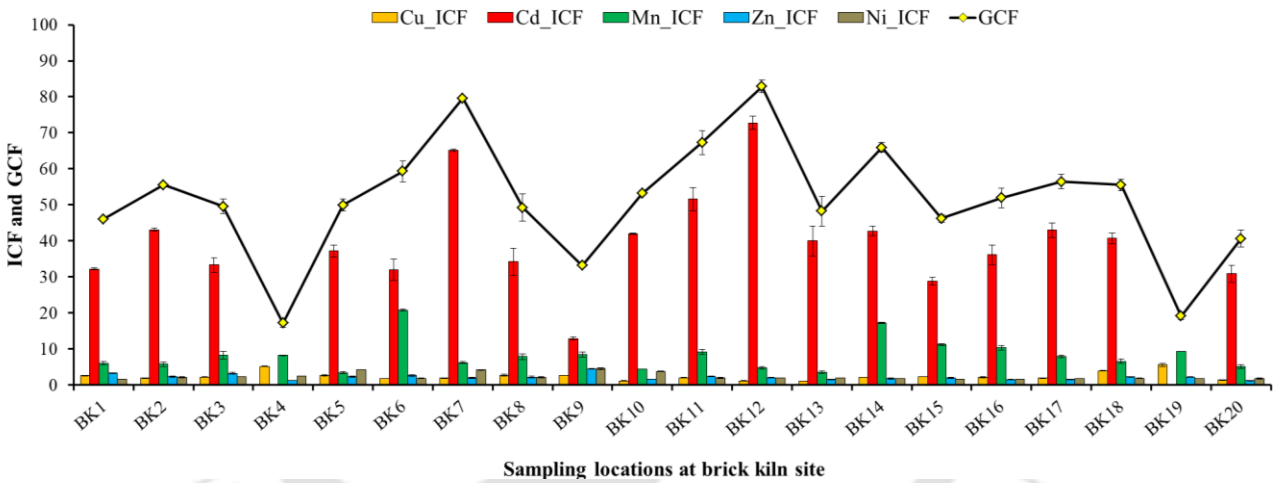

Fig. 4.29. *ICF* and *GCF* at brick kiln industry site, Napaam, Tezpur.

4.4.4. Human health risk assessment

Non-carcinogenic risks

Health risk assessment gives us insights into possible pathways of pollutants gaining access into the body and its associated risks. The exposure of the HMs in the form of average daily doses (ADDs) was higher for the Cr followed by Cd (Fig. 4.30). Non-carcinogenic and carcinogenic risks due to the metals in soil contaminated with BI are presented in Table 4.2. In this study non-

carcinogenic risks associated with Cr were ordered ingestion (0.16) > dermal (0.03) > inhalation (0.002) in adult and ingestion (1.35) > dermal (0.18) > inhalation (0.003) in children. Similar pattern of non-carcinogenic risk was found for Zn with ingestion (0.0001) > dermal (1.07×10^{-5}) > inhalation (7.9×10^{-8}) in adult and ingestion (0.004) > dermal (6.0×10^{-5}) > inhalation (1.2×10^{-7}) in children. Further, Mn also corroborates existing results that report higher ingestion (0.000) > dermal (2.0×10^{-5}) > inhalation (2.90×10^{-5}) in adult and ingestion (0.004) > dermal (6.0×10^{-5}) > inhalation (1.2×10^{-7}) in children. Likewise, the other HMs followed a similar trend. The average *HQ* (Hazard Quotient) value for adults via ingestion of Cd, Cu and Ni were 0.038, 0.0001 and 0.001, respectively; while via inhalation, the *HQ* values were 5.63×10^{-6}, 2.6×10^{-7} and 1.5×10^{-7} and through dermal it was 0.015, 2.73×10^{-5} and 1.36×10^{-5}, respectively. Additionally, the average *HQ* values for children through ingestion were 0.306, 0.008 and 0.014, inhalation 8.5×10^{-6}, 2.28×10^{-7}, 4.02×10^{-7} and dermal 0.085, 7.63×10^{-5} and 0.0001 of Cd, Cu and Ni respectively.

Among all metals studied, the contribution of Cr to the total *HI* (total risk for non-carcinogenic effects) was highest, with values as high as 78% for adult and 79% for children, followed by Cd with 20% (Fig. 4.31). Overall, similar observations were reported by the other researchers (David et al., 2020; Jahan et al., 2016). Earlier, (David et al., 2020) also reported a higher threat to human health due to Cr from brick kiln sites, particularly the children. A hazard quotient (*HQ*) less than a threshold value of 1 indicates that there is no significant risk associated with the non-carcinogenic effect, whereas *HQ* higher than > 1 indicates significant non-carcinogenic risk (USEPA, 2001). It was found that HQ_{ing} associated with Cr in children was comparatively much higher than in adults. These results showed that children are more prone to risks associated with Cr present in the soil and the major path of contamination risks is through ingestion. Cr alters the energy production,

carbohydrate tolerance, and normal metabolic process of the body. Further, reactions between Cr, thiols and ascorbate result in the formation of ROS, which ultimately results in DNA and protein damage (David et al., 2020). At the study site, as children are often involved in the BI, they are exposed to greater health risks. In this study Cr exhibited almost seven times higher hazard index (*HI*) for children (1.55) than for adults (0.206). However, no health risks were found due to Cu, Cd, Mn, Ni, and Zn as their *HI* were below 1.0.

Carcinogenic risks

Generally, Cu, Zn and Mn are considered as non-carcinogenic according to the international agency for research on cancer (IARC, 2018), therefore carcinogenic risk (CR) for only Cr, Cd and Ni were computed using standard formula and represented in Table 4.2.

The cancer risks or carcinogenic risk (CR) for Cr values in soil for the adult were 0.021 (Cr_{ing}), 3.12×10^{-6} (Cr_{inh}), 8.5×10^{-5} (Cr_{der}), and 0.170 (Cr_{ing}), 4.7×10^{-6} (Cr_{inh}) and 0.0001 (Cr_{der}) for children. Similarly, The CR values of Cd for adults are 0.002 (Cr_{ing}), 3.55×10^{-7} (Cr_{inh}), 9.62×10^{-6} (Cr_{der}); for children it was observed as 0.019 (Cr_{ing}), 5.39×10^{-7} (Cr_{inh}), 5.4×10^{-5} (Cr_{der}). The CR values of the Ni for adults were 0.003 (Cr_{ing}), 4.57×10^{-7} (Cr_{inh}), 1.24×10^{-5} (Cr_{der}) and 0.024 (Cr_{ing}), 6.95×10^{-7} (Cr_{inh}) and 6.96×10^{-5} (Cr_{der}) for children. CR value through ingestion and dermal contact in children were 10 times higher than that for adults. Overall, the mean values of the CR of Cr in the soils contaminated with BI were 0.021 for adult and 0.171 for children. From the Cr value, it could be inferred that carcinogenic risk mainly occurs through the ingestion pathway followed by dermal contact. Ingestion of Cr and Cd decreases the body mass index (BMI) of children (David et al., 2020). Also, an elevated level of Cd would result in iron deficiency, and this problem is more severe in the children living in the vicinity of the BI industry. Additionally,

the Ni exposure also poses a higher impact in children; Ni is haematotoxic, reprotoxic, immunotoxic, genotoxic, neurotoxic, and carcinogenic. Furthermore, it has a more significant effect on reproductive disorders (Lu et al., 2005). In general, the CR value was higher than 10^{-4}, indicating that carcinogenic risk from Cr in contaminated soil is very high, and it poses a severe threat to human health. In the study site, children from the adjacent village, aged between 15-16 years were engaged in the BI. Thus, children are exposed to severe health risk in term of physical and mental well-being, by their association with the BI.

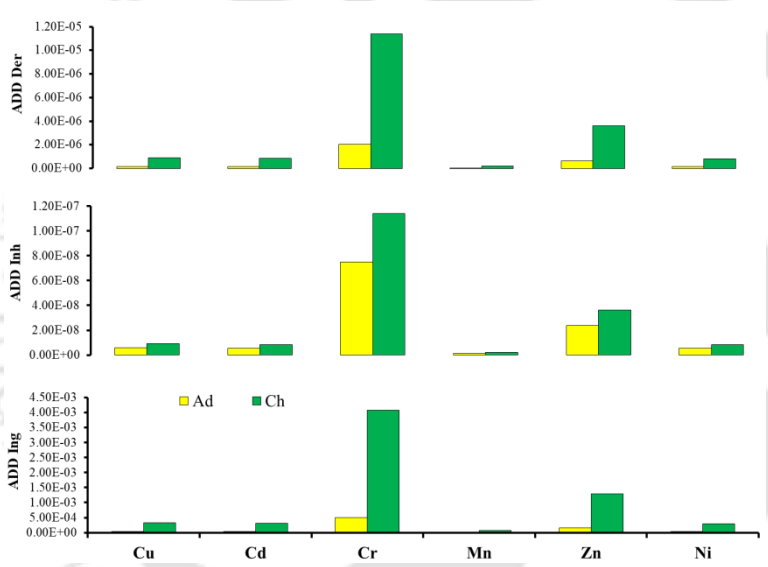

Fig. 4.30. Average daily doses (ADDs) of the pollutant exposure to the human health.

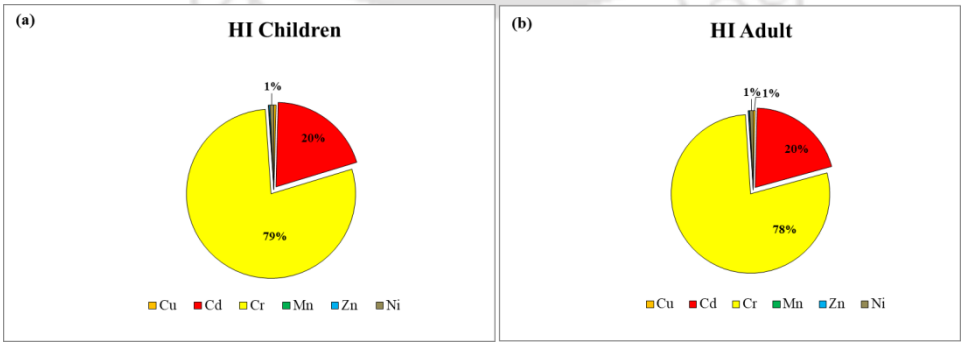

Fig. 4.31. Percentage contribution of HMs to the HI in both children and adult at Site-2.

Table 4 2. Human health risk assessment for carcinogenic and non-carcinogenic risk at Site-2.

		Non-carcinogenic risks											
		Chromium		**Manganese**		**Zinc**		**Cadmium**		**Nickel**		**Copper**	
		Adult	Children	Adult	Children	Adult	Children	Adult	Children	Adult	Children	Adult	Children
HQ $_{ing}$	Min	0.064	0.518	0.000	0.000	0.000	0.002	0.022	0.177	0.001	0.000	0.000	0.005
	Max	0.256	2.051	0.000	0.002	0.000	0.007	0.058	0.470	0.002	0.019	0.001	0.015
	Mean	0.169	**1.356**	0.000	0.001	0.000	0.004	0.038	0.306	0.001	0.014	0.000	0.008
HQ $_{inh}$	Min	0.000	0.001	1.63E-05	2.48E-05	4.77E-08	7.25E-08	3.25E-06	4.95E-06	2.04E-07	3.1E-07	9.99E-08	1.52E-07
	Max	0.003	0.006	4.59E-05	6.98E-05	1.35E-07	2.05E-07	8.64E-06	1.31E-05	3.45E-07	5.24E-07	2.79E-07	4.25E-07
	Mean	0.002	0.003	2.90E-05	4.42E-05	7.91E-08	1.20E-07	5.63E-06	8.56E-06	2.64E-07	4.02E-07	1.5E-07	2.28E-07
HQ $_{der}$	Min	0.012	0.072	1E-05	7E-05	6.47E-06	3.63E-05	0.008	0.049	2.11E-05	0.000	9.03E-06	5.07E-05
	Max	0.051	0.287	3E-05	0.000	1.83E-05	0.000	0.023	0.131	3.57E-05	0.000	2.53E-05	0.000
	Mean	0.033	0.189	2E-05	0.000	1.07E-05	6.02E-05	0.015	0.085	2.73E-05	0.000	1.36E-05	7.63E-05
HI	Min	0.078	0.588	0.000	0.001	0.000	0.002	0.030	0.226	0.001	0.000	0.000	0.005
	Max	0.311	2.344	0.000	0.002	0.000	0.007	0.082	0.601	0.002	0.019	0.001	0.015
	Mean	0.206	**1.550**	0.000	0.001	0.000	0.004	0.053	0.392	0.001	0.014	0.001	0.0082
		Carcinogenic risks											
CR $_{ing}$	Min	0.008	0.064	-	-	-	-	0.001	0.011	0.002	0.019	-	-
	Max	0.032	0.258	-	-	-	-	0.003	0.029	0.004	0.032	-	-
	Mean	0.021	**0.170**	-	-	-	-	0.002	0.019	0.003	0.024	-	-
CR $_{inh}$	Min	1.19E-06	1.81E-06	-	-	-	-	2.05E-07	3.12E-07	3.53E-07	5.36E-07	-	-
	Max	4.75E-06	7.22E-06	-	-	-	-	5.44E-07	8.28E-07	5.96E-07	9.06E-07	-	-

	Mean	3.12E-06	4.78E-06	-	-	-	-	3.55E-07	5.39E-07	4.57E-07	6.95E-07	-	-
CR_{der}	Min	3.24E-05	0.000	-	-	-	-	5.56E-06	3.12E-05	9.57E-06	5.37E-05	-	-
	Max	0.000129	0.000	-	-	-	-	1.48E-05	8.29E-05	1.62E-05	9.08E-05	-	-
	Mean	8.53E-05	0.000	-	-	-	-	9.62E-06	5.4E-05	1.24E-05	6.96E-05	-	-
CR	Min	0.008	0.065	-	-	-	-	0.001	0.011	0.002	0.019	-	-
	Max	0.032	0.259	-	-	-	-	0.003	0.029	0.004	0.032	-	-
	Mean	0.021	**0.171**	-	-	-	-	0.002	0.019	0.003	0.024	-	-

HQing=Hazard Quotient ingestion; HQinh=Hazard Quotient inhalation; HQdermal= Hazard Quotient dermal; HI=Hazard index; CRing=Carcinogenic risk ingestion; CRinh=Carcinogenic risk inhalation; CRder=Carcinogenic risk dermal.

** $CR>10^{-4}$ indicate higher carcinogenic risk.

* HQ>1 indicate higher non-carcinogenic risk

4.5. Conclusion

Geochemical fractionation demonstrated that at Site-1, Cr and Zn were associated with the Fe- Mn oxide bound (F4) fraction, accounting for 44.23% and 30.68%, respectively, whereas Mn (52.55%) was associated with the exchangeable fraction (F2). Cd (54.59%) was primarily associated with the carbonate bound fraction (F3), while 25.53% of Cu and 40.60% Ni were associated with the exchangeable fraction (F2). Likewise, at Site-2, Cr was mainly associated with organic bound fraction (F5). Mn and Zn were associated with exchangeable and residual fraction accounting for 49.47% and 32.54%, respectively. Cd and Cu were mainly associated with carbonate bound fraction (F3), accounting for 55.78% and 32.80%, respectively, whereas Ni was associated with F4 fraction (51.32%). The result showed that the at Site-1 anthropogenic enrichment of Cr, Cd, and Ni is higher due to the paints, Ni-Cd batteries, PCBs, and coloured glass wastes present in the MSW. At Site-2, the higher contamination of Cd might be due to tires and polymeric materials used in firing operations and deposition of the bottom ash in agricultural fields. Higher mobility, higher enrichment, and higher contamination factors were found for Cd and Cr. In both the sites higher I_{geo}, *PERI* and *PLI* were higher for Cd. In both the sites, higher non-carcinogenic risks were marked in children due to Cr. In contrast, in Site-1, the carcinogenic risk due to Cd was higher in children, and for Ni in both adult and children. Cr posed higher risk in children only in Site-2. The wealth of *in situ* data supporting the intense HM contamination in both the study areas, and the severity of ecological and health risks, warrant urgent mitigation mechanisms and reforms in policies for soil quality management.

References

Achakzai, K., Khalid, S., Bibi, A., 2015. Determination of Heavy Metals in Agricultural Soil Adjacent to Functional Brick Kilns : A Case Study of Rawalpindi. Sci. Technol Develop. 34, 122–129.

Adimalla, N., Li, P., 2019. Occurrence, health risks, and geochemical mechanisms of fluoride and nitrate in groundwater of the rock-dominant semi-arid region, Telangana State, India. Hum. Ecol. Risk Assess. Inter. J. 25, 81-103.

Ahmad, K., Muhammad, S., Ali, W., Jadoon, I.A., Rasool, A., 2020. Occurrence, source identification and potential risk evaluation of heavy metals in sediments of the Hunza River and its tributaries, Gilgit-Baltistan. Environ. Technol. Inno. 18, 100700.

Alam, P., Sharholy, M., Ahmad, K., 2020. A study on the landfill leachate and its impact on groundwater quality of Ghazipur area, New Delhi, India, in: Recent Developments in Waste Management. Springer, Singapore, pp. 345-358.

Alloway, B.J., 2012. Sources of heavy metals and metalloids in soils in: Alloway, B.J. (Ed.), Heavy Metals in Soils: Trace Metals and Metalloids in Soils and Their Bioavailability, Environmental Pollution, vol. 22. Springer, Dordrecht, pp. 11-50.

Al-Mur, B.A., 2020. Geochemical fractionation of heavy metals in sediments of the Red Sea, Saudi Arabia. Oceanologia 62, 31-44.

Ancic, M., HuCek, A., Rihtaric, I., Cazar, M., Bacun-Druzina, V., Kopjar, N., Durgo, K., 2020. Physico chemical properties and toxicological effect of landfill groundwaters and leachates. Chemosphere 238, 24574.

ATSDR (Agency for Toxic Substance and Disease Registry), 2004. Draft Evaluation of the Toxicology of Chemical Mixtures Commonly Found at Hazardous Waste Sites US Public Health Service. US Department of Human Services, Atlanta, GA. https://www.atsdr.cdc.gov/toxprofiles/tp124.pdf. (Accessed 24 October 2019).

ATSDR (Agency for Toxic Substances and Disease Registry), 2011. Toxic substances portal, cadmium. https://www.atsdr.cdc.gov/substances/toxsubstance.asp? Toxid=15. (Accessed 23 January 2020).

Blewett, T.A., Leonard, E.M., 2017. Mechanisms of nickel toxicity to fish and invertebrates in marine and estuarine waters. Environ. Pollut. 223, 311-322.

Borah, P., Paul, A., Bora, P., Bhattacharyya, P., Karak, T., Mitra, S., 2017. Assessment of heavy metal pollution in soils around a paper mill using metal fractionation and multivariate analysis. Int. J. Environ. Sci. Technol. 14, 1-14.

Borah, P., Singh, P., Rangan, L., Karak, T., Mitra, S., 2018. Mobility, bioavailability and ecological risk assessment of cadmium and chromium in soils contaminated by paper mill wastes. Groundwater Sust. Dev. 6, 189-199.

Borah, P., Gujre, N., Rene, E.R., Rangan, L., Paul, R.K., Karak, T., Mitra, S., 2020. Assessment of mobility and environmental risks associated with copper, manganese and zinc in soils of a dumping site around a Ramsar site. Chemosphere 254, 126852.

Cai, L., Wang, Q., Wen, H., Luo, J., Wang, S., 2019. Heavy metals in agricultural soils from a typical township in Guangdong Province, China: Occurrences and spatial distribution. Ecotoxicol. Environ. Saf. 168, 184–191.

CCME (Canadian Council of Ministers of the Environment), 2007. Canadian Soil Quality Guidelines for the Protection of Environmental and Human Health: Summary Tables. In: Canadian Environmental Quality Guidelines, 1999. Canadian Council of Ministers of the Environment, Winnipeg. Updated September. 2007. http://esdat.net/Environmental %20Standards/Canada/SOIL/rev_soil_summary_tbl_7.0_e.pdf. (Accessed 13 October 2019).

Cao, S., Duan, X., Zhao, X., Ma, J., Dong, T., Huang, N., Sun, C., He, B., Wei, F., 2014. Health risks from the exposure of children to As, Se, Pb and other heavy metals near the largest coking plant in China. Sci. Total Environ. 472, 1001-1009.

Caparros-Gonzalez, R.A., Gimenez-Asensio, M.J., Gonzalez-Alzaga, B., Aguilar-Carduno, C., LorcaMarín, J.A., Alguacil, J., Gomez-Becerra, I., Gomez-Ariza, J.L., García-Barrera, T., Hernandez, A.F., Lopez-Flores, I., 2019. Childhood chromium exposure and neuropsychological development in children living in two polluted areas in southern Spain. Environ. Pollut. 252, 1550-1560.

Chabukdhara, M., Nema, A.K., 2013. Heavy metals assessment in urban soil around industrial clusters in Ghaziabad, India: probabilistic health risk approach. Ecotoxicol. Environ. Saf. 87, 57-64.

Chen, C.W., Kao, C.M., Chen, C.F., Dong, C.D., 2007. Distribution and accumulation of heavy metals in the sediments of Kaohsiung Harbor, Taiwan. Chemosphere 66, 1431-1440.

Christophoridis, C., Evgenakis, E., Bourliva, A., Papadopoulou, L., Fytianos, K., 2020. Concentration, fractionation, and ecological risk assessment of heavy metals and phosphorus in surface sediments from lakes in N. Greece. Environ. Geochem. Health 13, 1-23.

Dash, S., Borah, S.S., Kalamdhad, A., 2019. A modified indexing approach for assessment of heavy metal contamination in Deepor Beel, India. Ecol. Indicat. 106, 105444.

David, M., Turi, N., Ain, Q. ul, Rahman, H., Jahan, S., 2020. Evaluation of environmental effects of heavy metals on biochemical profile and oxidative stress among children at brick kiln sites. Arch. Environ. Occup. Heal. 0, 1–9. https://doi.org/10.1080/19338244.2020.1854645

De Miguel, E., Iribarren, I., Chacon, E., Ordonez, A., Charlesworth, S., 2007. Riskbased evaluation of the exposure of children to trace elements in playgrounds in Madrid (Spain). Chemosphere 66, 505-513.

Dehghani, S., Moore, F., Keshavarzi, B., Beverley, A.H., 2017. Health risk implications of potentially toxic metals in street dust and surface soil of Tehran, Iran. Ecotoxicol. Enviorn. Saf. 136, 92-103.

Dey, S., Dey, M., 2017. Soil fertility loss and heavy metal accumulation in and around functional brick kilns in Cachar district, Assam, india: a multivariate analysis. J. Bio. Innov. 6 ,768-781.

El Azhari, A., Rhoujjati, A., El Hachimi, M.L., Ambrosi, J.P., 2017. Pollution and ecological risk assessment of heavy metals in the soil-plant system and the sediment-water column around a former Pb/Zn-mining area in NE Morocco. Ecotoxicol. Environ. Saf. 144, 464-474.

Ellis, J.B., Revitt, D.M., 2008. Quantifying diffuse pollution sources and loads for environmental quality standards in urban catchments. Water, Air, Soil Pollut. 8, 577-585.

Forstner, U., Wittmann, G.T., 2012. Metal Pollution in the Aquatic Environment. Springer Science & Business Media.

Gan, Y., Huang, X., Li, S., Liu, N., Li, Y.C., Freidenreich, A., Wang, W., Wang, R., Dai, J., 2019. Source quantification and potential risk of mercury, cadmium, arsenic, lead, an chromium in farmland soils of Yellow River Delta. J. Clean. Prod. 221, 98-107.

Gill, R.A., Ali, B., Islam, F., Farooq, M.A., Gill, M.B., Mwamba, T.M., Zhou, W., 2015. Physiological and molecular analyses of black and yellow seeded *Brassica napus* regulated by 5-aminolivulinic acid under chromium stress. Plant Physiol. Biochem. 94, 130-143.

Gujre, N., Mitra, S., Soni, A., Agnihotri, R., Rangan, L., Rene, E.R., Sharma, M.P., 2021a. Speciation, contamination, ecological, and human health risks assessment of heavy metals in soils dumped with municipal solid wastes. Chemosphere, 262, 128013.

Hakanson, L., 1980. Ecological risk index for aquatic pollution control. A sedimentological approach. Water Res. 14, 975-1001.

Halwani, D.A., Jurdi, M., Salem, F.K.A., Jaffa, M.A., Amacha, N., Habib, R.R., Dhaini, H.R., 2020. Cadmium health risk assessment and anthropogenic sources of pollution in Mount-Lebanon springs. Expos. Health 12, 163-178.

Huang, G., Ding, C., Guo, N., Ding, M., Zhang, H., Kamran, M., Zhou, Z., Zhang, T. and Wang, X., 2021. Polymer-coated manganese fertilizer and its combination with lime reduces cadmium accumulation in brown rice (*Oryza sativa* L.). J. Hazard. Mater., 125597.

IARC, 1993. IARC Monographs on the Evaluation of the Carcinogenic Risks to Humans: Beryllium, Cadmium, Mercury, and Exposures in the Glass Manufacturing Industry World Health Organization, vol. 58.

IARC, 2018. Chromium (IV) compounds. IARC monograph 100C. https://monographs.iarc.fr/wp-content/uploads/2018/06/mono100C-9.pdf (accessed 24 January 2020).

Ikem, A., Egiebor, N.O., Nyavor, K., 2003. Trace elements in water, fish and sediment from Tuskegee Lake, Southeastern USA. Water, Air, Soil Pollut. 149, 51-75.

Ismail, M., Muhammad, D., Khan, F.U., Munsif, F., Ahmad, T., Ali, S., Khalid, M., Haq, N.U. and Ahmad, M., 2012. Effect of brick kilns emissions on heavy metal (Cd and Cr) content of contiguous soil and plants. Sarhad J. Agric. 28, 403-409.

Jahan, S., Falah, S., Ullah, H., Ullah, A., Rauf, N., 2016. Antioxidant enzymes status and reproductive health of adult male workers exposed to brick kiln pollutants in Pakistan. Environ. Sci. Pollut. Res. 23, 12932–12940.

Ji, H., Li, H., Zhang, Y., Ding, H., Gao, Y., Xing, Y., 2018. Distribution and risk assessment of heavy metals in overlying water, porewater, and sediments of Yongding River in a coal mine brownfield. J. Soils Sediments 18, 624-639.

Jin, Y., O'Connor, D., Ok, Y.S., Tsang, D.C., Liu, A., Hou, D., 2019. Assessment of sources of heavy metals in soil and dust at children's playgrounds in Beijing using GIS and multivariate statistical analysis. Environ. Int. 124, 320-328.

Kamal, A., Malik, R.N., Martellini, T., Cincinelli, A., 2014. Cancer risk evaluation of brick kiln workers exposed to dust bound PAHs in Punjab province (Pakistan). Sci. Total Environ. 493, 562-570.

Karak, T., Paul, R.K., Das, S., Das, D.K., Dutta, A.K., Boruah, R.K., 2015. Fate of cadmium at the soil-solution interface: a thermodynamic study as influenced by varying pH at South 24 Parganas, West Bengal, India. Environ. Monit. Assess. 187, 713.

Khairy, M.A., Barakat, A.O., Mostafa, A.R., Wade, T.L., 2011. Multi-element determination by flame atomic absorption of road dust samples in Delta Region Egypt. Microchem. J. 97, 234-324.

Khan, M.A., Khan, S., Khan, A., Alam, M., 2017. Soil contamination with cadmium, consequences and remediation using organic amendments. Sci. Total Environ. 601, 1591-1605.

Kubier, A., Wilkin, R.T., Pichler, T., 2019. Cadmium in soils and groundwater: a review. Appl. Geochem. 108, 104388.

Lane, D.J., Hartikainen, A., Sippula, O., L€ahde, A., Mesceriakovas, A., Per€aniemi, S., Jokiniemi, J., 2020. Thermal separation of zinc and other valuable elements from municipal solid waste incineration fly ash. J. Clean. Prod. 253, 120014.

Leharne, S., Charlesworth, D., Chowdhry, B., 1992. A survey of metal levels in street dusts in an inner London neighbourhood. Environ. Int. 18, 263-270.

Li, Z., Ma, Z., van der Kuijp, T.J., Yuan, Z., Huang, L., 2014. A review of soil heavy metal pollution from mines in China: pollution and health risk assessment. Sci. Total Environ. 468, 843-853.

Li, Y., Liu, K., Zhu, J., Jiang, Y., Huang, Y., Zhou, Z., Chen, C., Yu, F., 2019. Manganese accumulation and plant physiology behavior of *Camellia oleifera* in response to different levels of nitrogen fertilization. Ecotoxicol. Environ. Saf. 184, 109603.

Liu, L., Ouyang, W., Wang, Y., Tysklind, M., Hao, F., Liu, H., Su, L., 2020. Heavy metal accumulation, geochemical fractions, and loadings in two agricultural watersheds with distinct climate conditions. J. Hazard Mater. 389, 122125.

Lu H, Shi X, Costa M, Huang, C., 2005. Carcinogenic effect of nickel compounds. Mol Cell Biochem. 279, 45–67.

Luo, X.S., Ding, J., Xu, B., Wang, Y.J., Li, H.B., Yu, S., 2012. Incorporating bioaccessibility into human health risk assessments of heavy metals in urban park soils. Sci. Total Environ. 424, 88-96.

Luo, Y., Yao, A., Tan, M., Li, Z., Qing, L., Yang, S., 2020. Effects of manganese and zinc on the growth process of Phytophthora nicotianae and the possible inhibitory mechanisms. PeerJ 8, 8613.

Ma, W., Tai, L., Qiao, Z., Zhong, L., Wang, Z., Fu, K., et al., 2018. Contamination source apportionment and health risk assessment of heavy metals in soil around municipal solid waste incinerator: a case study in North China. Sci. Total Environ. 631-632, 348-357.

McMahon, P.B., Belitz, K., Reddy, J.E., Johnson, T.D., 2019. Elevated manganese concentrations in United States groundwater, role of land surface soil aquifer connections. Environ. Sci. Technol. 53, 29-38.

Memoli, V., Esposito, F., Panico, S., De, A., Barile, R., Maisto, G., 2019. Evaluation of tourism impact on soil metal accumulation through single and integrated indices. Sci. Total Environ. 682, 685-691.

MoHFW (Ministry of Health and FamilyWelfare), 2010. Annual report to the people on Health. http://mohfw.nic.in/WriteReadData/l892s/9457038092. (Accessed 15 March 2019).

Mondal, A., Das, S., Kumar, R., Bhattacharyya, P., Sundar, S., 2017. Environmental footprints of brick kiln bottom ashes: Geostatistical approach for assessment of metal toxicity. Sci. Total Environ. 609, 215–224.

Mondal, P., Schintu, M., Marras, B., Bettoschi, A., Marrucci, A., Sarkar, S.K., Chowdhury, R., Jonathan, M.P., Biswas, J.K., 2020. Geochemical fractionation and risk assessment of trace elements in sediments from tide-dominated Hooghly (Ganges) River Estuary, India. Chem. Geol. 532, 119373.

Mozumder, C., Tripathi, N.K., 2014. Geospatial scenario-based modelling of urban and agricultural intrusions in Ramsar wetland Deepor Beel in Northeast India using a multi-layer perceptron neural network. Int. J. Appl. Earth Obs. 32, 92-104.

Müller, G., 1969. Index of geo-accumulation in the sediments of the rhine river. Geojournal 2, 108-118.

Narwal, R.P., Singh, B.R., 1998. Effect of organic materials on partitioning, extractability and plant uptake of metals in an alum shale soil. Water, Air, Soil Pollut. 103, 405-421.

Negra, C., Ross, D.S., Lanzirotti, A., 2005. Oxidizing behavior of soil manganese. Soil Sci. Soc. Am. J. 69, 87-95.

Nkinahamira, F., Suanon, F., Chi, Q., Li, Y., Feng, M., Huang, X., Yu, C.P., Sun, Q., 2019. Occurrence, geochemical fractionation, and environmental risk assessment of major and trace elements in sewage sludge. J. Environ. Manag. 249, 109427.

Olajire, A.A., Ayodele, E.T., Oyedirdan, G.O., Oluyemi, E.A., 2003. Levels and speciation of heavy metals in soils of industrial southern Nigeria. Environ. Monit. Assess. 85, 135-155.

Ouattara, A.A., Yao, K.M., Kinimo, K.C., Trokourey, A., 2020. Assessment and bioaccumulation of arsenic and trace metals in two commercial fish species collected from three rivers of C^ote d'Ivoire and health risks. Microchem. J. 154, 104604.

Panwar, R.M., Ahmed, S., 2018. Assessment of contamination of soil and groundwater due to e-waste handling. Curr. Sci. 114, 166-173.

Plum, L.M., Rink, L., Haase, H., 2010. The essential toxin: impact of zinc on human health. Int. J. Environ. Res. Publ. Health 7, 1342-1365.

Pobi, K.K., Nayek, S., Gope, M., Rai, A.K., Saha, R., 2020. Sources evaluation, ecological and health risk assessment of potential toxic metals (PTMs) in surface soils of an industrial area, India. Environ. Geochem. Health 1-22.

Poznanovic Spahic, M.M., Sakan, S.M., Glavas-Trbic, B.M., Tancic, P.I., Skrivanj, S.B., Kovacevic, J.R., Manojlovic, D.D., 2019. Natural and anthropogenic sources of chromium, nickel and cobalt in soils impacted by agricultural and industrial activity (*Vojvodina, Serbia*). J. Environ. Sci. Health 54, 219-230.

Prartono, T., Sanusi, H.S., Nurjaya, I.W., 2016. Seasonal distribution and geochemical fractionation of heavy metals from surface sediment in a tropical estuary of Jeneberang River, Indonesia. Mar. Pollut. Bull. 111, 456-462.

Proshad, R., Ahmed, S., Rahman, M., Kumar, T., 2017. Apportionment of Hazardous Elements in Agricultural Soils Around the Vicinity of Brick Kiln in Bangladesh. J. Environ. Anal. Toxicol. 07. https://doi.org/10.4172/2161-0525.1000439

Qiao, D., Wang, G., Li, X., Wang, S., Zhao, Y., 2020. Pollution, sources and environmental risk assessment of heavy metals in the surface AMD water, sediments and surface soils around unexploited Rona Cu deposit, Tibet, China. Chemosphere 248, 125988.

Rahman, S.M., Kippler, M., Tofail, F., Bolte, S., Derakhshani Hamadani, J., Vahter, M., 2017. Manganese in drinking water and cognitive abilities and behavior at 10 years of age: a prospective cohort study. Environ. Health Perspect. 125, 057003.

Sandra, L.R., Covadonga, C., Juan, J.L., 2012. Novel chelating agents as manganese and zinc fertilisers: characterisation, theoretical speciation and stability in solution. Chem. Speciat. Bioavailab. 24, 147-158.

Sekine, R., Marzouk, E.R., Khaksar, M., Scheckel, K.G., Stegemeier, J.P., Lowry, G.V., Donner, E., Lombi, E., 2017. Aging of Dissolved Copper and Copper-based Nanoparticles in Five Different Soils: Short-term Kinetics vs. Long-term Fate. J. Environ. Qual. 46, 1198-1205.

Sharma, R.K., M. Agrawal, F.M. Marshall, 2007. Heavy metal contamination of soil and vegetables in suburban areas of Varanasi, India. Ecotoxicol. Environ. Safe. 66, 258-266.

Shi, G., Chen, Z., Bi, C., Wang, L., Teng, J., Li, Y., Xu, S., 2011. A comparative study of health risk of potentially toxic metals in urban and suburban road dust in the most populated city of China. Atmos. Environ. 45, 764-771.

Singh, K.R., Dutta, R., Kalamdhad, A.S., Kumar, B., 2019. An investigation on water quality variability and identification of ideal monitoring locations by using entropy-based disorder indices. Sci. Total Environ. 647, 1444-1455.

Singh, P., Purakayastha, T.J., Mitra, S., Bhowmik, A., Tsang, D.C., 2020. River water irrigation with heavy metal load influences soil biological activities and risk factors. J. Environ. Manage. 270, 110517.

Soledad Morales-Garcia, S., Meza-Olvera, E., Shruti, V.C., Sedeno-Diaz, J.E., 2020. Assessment of metal contamination and their ecological risks in wetland sediments of the former Texcoco saline lake, Mexico. J. Soils Sediments. https:// doi.org/10.1007/s11368-020-02613-3.

Stepniewska, Z., Bucior, K., Bennicelli, R.P., 2004. The effects of MnO_2 on sorption and oxidation of Cr (III) by soils. Geoderma 122, 291-296.

Tardif, S., Cipullo, S., Sø, H.U., Wragg, J., Holm, P.E., Coulon, F., Brandt, K.K., Cave, M., 2019. Factors governing the solid phase distribution of Cr, Cu and as in contaminated soil after 40 years of ageing. Sci. Total Environ. 652, 744-754.

Taylor, S.R., 1964. Trace element abundances and the chondritic earth model. Geochem. Cosmochim. Acta 28, 1989-1998.

Tessier, A., Campbell, P.G.C., Bisson, M., 1979. Sequential extraction procedure for the speciation of particulate traces metals. Anal. Chem. 51, 844-851.

Thakur, S., Dhyani, S., Bramhanwade, K., Pandey, K.K., Bokade, N., Janipella, R., Pujari, P., 2020. Non-invasive biomonitoring of mercury in birds near thermal power plants: lessons from Maharashtra, India. Environ. Monit. Assess. 192.

Tian, K., Huang, B., Xing, Z., Hu, W., 2017. Geochemical baseline establishment and ecological risk evaluation of heavy metals in greenhouse soils from Dongtai, China. Ecol. Indicat. 72, 510-520.

Tume, P., Gonzalez, E., King, R.W., Monsalve, V., Roca, N., Bech, J., 2018. Spatial distribution of potentially harmful elements in urban soils, city of Talcahuano, Chile. J. Geochem. Explor. 184, 333-344.

Turner, A., Simmonds, L., 2006. Elemental concentrations and metal bioaccessibility in UK household dust. Sci. Total Environ. 371, 74-81.

US EPA (United States Environmental Protection Agency), 2001. Supplemental Guidance for Developing Soil Screening Levels for Superfund Sites. OSWER, vol. 9355. US Environmental Protection Agency, Washington, DC, pp. 4-24, 2001. Office of SolidWaste and Emergency Response. http://www.epa.gov/superfund/resources/soil/ssgmarch01.pdf. (Accessed 12 March 2019).

US EPA (US Environmental Protection Agency), 1989. Risk Assessment Guidance for Superfund Human Health Evaluation Manual, vol. I. US Environmental Protection Agency, Washington, DC. EPA/540/1-89/002.

USDoE (US Department of Energy), 2011. The Risk Assessment Information System (RAIS). U.S. Department of Energy's Oak Ridge Operations Office (ORO). https:// rais.ornl.gov/. (Accessed 25 March 2019).

Verbinnen, B., Billen, P., Van Coninckxloo, M., Vandecasteele, C., 2013. Heating temperature dependence of Cr (III) oxidation in the presence of alkali and alkaline earth salts and subsequent Cr (VI) leaching behavior. Environ. Sci. Technol. 47, 5858-5863.

Wang, X., Dan, Z., Cui, X., Zhang, R., Zhou, S., Wenga, T., Yan, B., Chen, G., Zhang, Q., Zhong, L., 2020a. Contamination, ecological and health risks of trace elements in soil of landfill and geothermal sites in Tibet. Sci. Total Environ. 715, 136639.

Wang, Q., Hong, H., Yang, D., Li, J., Chen, S., Pan, C., Lu, H., Liu, J., Yan, C., 2020b. Health risk assessment of heavy metal and its mitigation by glomalin-related soil protein in sediments along the South China coast. Environ. Pollut. 114565.

Wu, W., Liu, X., Zhang, X., Zhu, M., Tan, W., 2018. Bioleaching of copper from waste printed circuit boards by bacteria-free cultural supernatant of ironesulfuroxidizing bacteria. Bioresour. Bioprocess 5, 10.

Xia, B., Guo, P., Lei, Y., Zhang, T., Qiu, R., Knorr, K.H., 2016. Investigating speciation and toxicity of heavy metals in anoxic marine sediments- case study from a mariculture bay in Southern China. J. Soils Sediments 16, 665-676.

Xiong, X., Liu, X., Iris, K.M., Wang, L., Zhou, J., Sun, X., Rinklebe, J., Shaheen, S.M., Ok, Y.S., Lin, Z., Tsang, D.C., 2019. Potentially toxic elements in solid waste streams: fate and management approaches. Environ. Pollut. 253, 680-707.

Xu, Y., Li, J., Liu, L., 2016. Current status and future perspective of recycling copper by hydrometallurgy from waste printed circuit boards. Procedia Environ. Sci. 31,162-170.

Yang, D., Liu, J., Wang, Q., Hong, H., Zhao, W., Chen, S., Yan, C., Lu, H., 2019. Geochemical and probabilistic human health risk of chromium in mangrove sediments: a case study in Fujian, China. Chemosphere 233, 503-511.

Ye, Y., Cota-Ruiz, K., Hernandez-Viezcas, J.A., Valdes, C., Medina-Velo, I.A., Turley, R.S., Peralta-Videa, J.R., Gardea-Torresdey, J.L., 2020. Manganese nanoparticles control salinity-modulated molecular responses in Capsicum annuum L. through priming: a sustainable approach for agriculture. ACS Sustain. Chem. Eng. 8, 1427-1436.

Zhang, J., Liu, C.L., 2002. Riverine composition and estuarine geochemistry of particulate metals in China -weathering features, anthropogenic impact and chemical fluxes. Estuar. Coast Shelf Sci. 54, 1051-1070.

Zhang, J., Hua, P., Krebs, P., 2017a. Influences of land use and antecedent dry weather period on pollution level and ecological risk of heavy metals in road-deposited sediment. Environ. Pollut. 228, 158-168.

Zhang, Y., Liu, P., Wang, C., Wu, Y., 2017b. Human health risk assessment of cadmium via dietary intake by children in Jiangsu Province, China. Environ. Geochem. Health 39, 29-41.

Zhang, J., Li, H., Zhou, Y., Dou, L., Cai, L., Mo, L., You, J., 2018. Bioavailability and soil-to-crop transfer of heavy metals in farmland soils: A case study in the Pearl River Delta, South China. Environ. Pollut. 235, 710-719.

Zheng, N., Liu, J., Wang, Q., Liang, Z., 2010. Health risk assessment of heavy metal exposure to street dust in the zinc smelting district, Northeast of China. Sci.Total Environ. 408, 726-733.
Zoller, W.H., Gladney, E.S., Duce, R.A., 1974. Atmospheric concentrations and sources of trace metals at the South Pole. Science 83, 198-200.

CHAPTER 5

Preparation and characterization of biochar from locally available plant materials

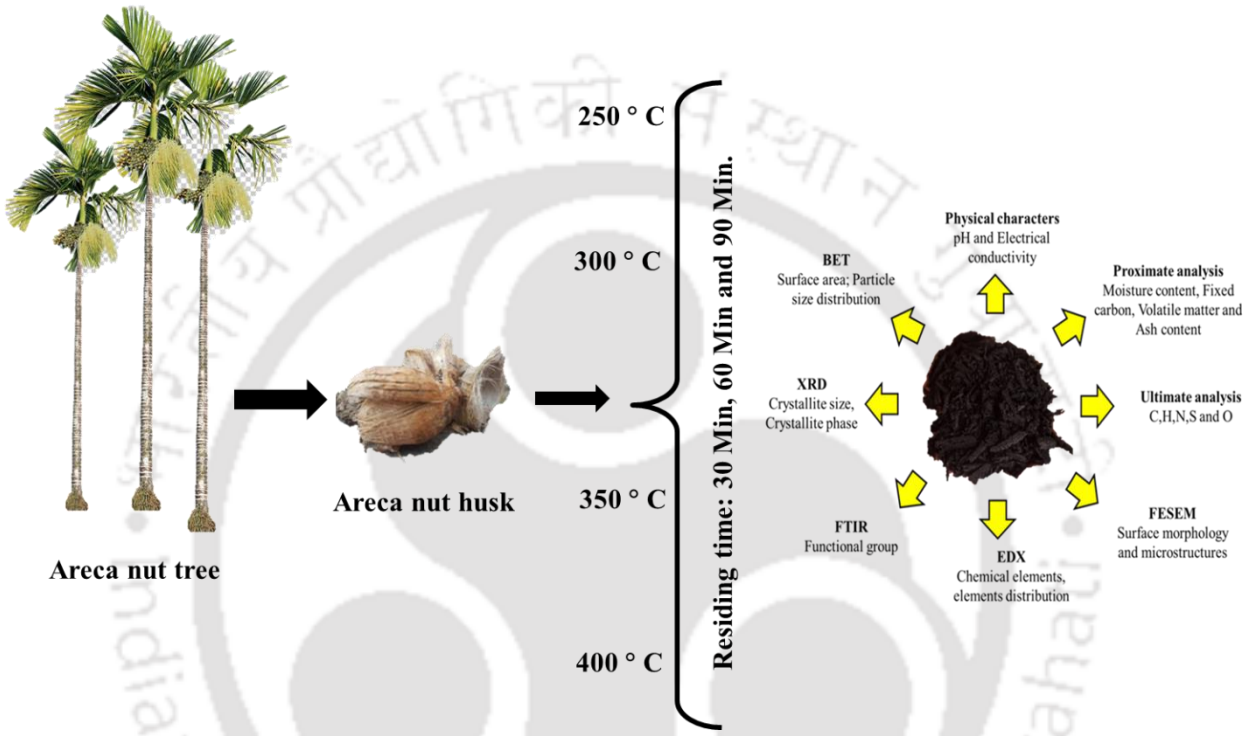

"This chapter deals with the preparation of the biochar from locally available plant material, i.e., areca nut husk. Further, it also discusses on the characteristics of the prepared biochars for larger soil applications."

5. Preparation and characterization of biochar from locally available plant materials

5.1. Introduction

Areca nut husk (AH), is the outer covering of a palm nut or fruit, *Areca catechu*, belonging to the Arecaceae family. The dehusked nut is widely chewed with or without the leaves of the betel vine in South East Asian countries; in India it is also used in religious and social rituals. India is the largest consumer and producer (57%) of areca nut; in 2017-2018, 833,000 tons were harvested from an area of 497,000 ha within the country which rise to about 901,000 tons in 2019 (Rajan et al., 2017; Deshmukh et. al., 2019) (Fig. 5.1). Areca nut trees are mainly planted in the backyard gardens in rural areas, where the husk of the fruit is predominantly utilized as a solid fuel for cooking, though a large portion remains unused. The husk that covers the monocot seed or fruit is a natural lignocellulosic material, which contributes to the 60-80% of the dry mass of the fruit (Singh et al., 2017). Two types of fibers (course and fine) constitute the husk; with an average length 4 cm, the fibers are thus smaller than that of the coconut. Cellulose, hemicellulose (35-64.8%), lignin (13-26%), pectin and protopectin are the principal fiber components.

Fig. 5.1. Global production of areca nut (year 2019; Source: https://www.tridge.com/intelligences/areca-nut/production, Accessed on 25 March 2021).

Despite being extremely resistant to chemical and biological degradation, the husk remains mostly unused or dumped. The state of Assam holds the third position in total areca nut production in India (Fig. 5.2). The basic cellulosic nature of the husk renders it recalcitrant, and preempts its incorporation into the soil in a non-pyrolytic form in the soil. Therefore, pyrolytic conversion of AH to biochar (BC) presents sustainable strategy for the management and valorization of the unused residue.

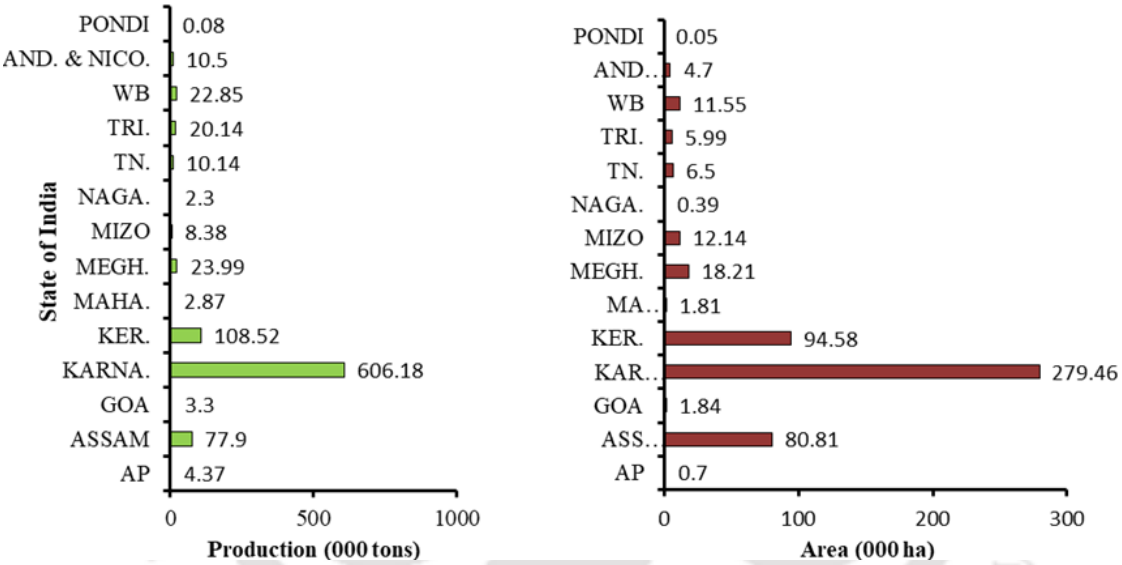

Fig. 5.2. Areca nut production and area under cultivation, India (2017-2018). (Source: DASD, 2019)

BC can be used as promising and cost-effective soil amendment technique which improves crop productivity with its greater surface area, highly porous structure, added oxygen functional groups and higher cation exchange capacity (CEC) (Dai et al., 2020). BC properties are influenced by the retention time, temperature, and feedstock (Pariyar et al., 2020). BC produced from AH enhances carbon storage and fertility of the soil, thereby reducing the soil degradation. Ideally, farm level

preparation and valorization of BC from the areca nut husk would be a suitable option. However, for more sustained amelioration of targeted soils by AHB application, its properties must be carefully assessed (Dai et al., 2020). The fact that an areca nut garden yields about 5.5-6 t ha^{-1} $year^{-1}$ of AH, supply of husks for biochar preparation is well assured.

Globally, soil quality plays an essential role in the economies of nations, yet soil pollution is a prevalent and persistent problem. The soil quality has a direct relationship with the yield of crops and its productivity. BC as a soil amendment is one of the best possible solutions to speed up the restoration and rejuvenation process of degraded land. Despite its high availability, the lack of monetary incentive ensures that most of the AH is discarded as solid waste. Our study therefore aimed to take advantage of this natural bounty of AH biomass for the preparation of AHB, and assess its effet on soil quality in conjuhation with vetiver. BC application for managing soil biota and conserving soil quality is a theme of burgeoning interest; though the exact soil alteration processes by AHB are not well understood. Thus, an attempt has been made to develop and characterize the BC and test its applications for soil quality improvement. Along with the wider perspectives of BC properties on the various agronomical and environmental backgrounds, one of the objectives of the present research was to explore different aspects of prepared BC, their limitations, and present knowledge, in soil quality improvement.

5.2. Materials and methods

5.2.1. Procurement of raw material and biochar preparation

Husks from matured areca nuts were procured from Rampur village, Guwahati, Assam and air dried for 4-5 days. The AHB was prepared under a limited air supply, using a tubular furnace (35 × 7 cm, length ×diameter) with a cooling chamber in the lid. As the objective was to scale up a simple, and cheap pyrolysis procedure, easily adaptable by the local farmers, nitrogen was not

used in the preparation of AHB in the tubular furnace. Known quantity of the air-dried material was used for the preparation of the AHB heated in tubular furnace at different temperature (250, 300, 350, 400 °C) and residence time (30, 60 and 120 min). After pyrolysis the AHB yield was computed according to Eq. (1)

$$Biochar\ \ yield\ (wt\%) = \frac{Weight\ of\ \ biochar\ collected\ (g)}{Weight\ of\ \ feed\ biomass(g)} \times\ 100 \quad (1)$$

pH and EC were measured on a 1:2.5 (*w/v*) water suspension of the biochar samples, after stirring for 1 h at 25°C, using Hanna pH and EC meter. Oxidizable OC of the prepared AHB was determined using potassium dichromate oxidation method (Walkley and Black, 1934). This process was generally used to investigate the labile fraction of carbon present in BC (Calvelo Pereira et al., 2011). Loss on ignition (LOI) of AHB was determined using ASTM method (D-1762-84). The ratio of OC and LOI was employed for calculating Carbon lability index (Blair et al., 1995). Similarly, stable organic matter (SOM) was calculated as:

$$SOM = LOI - (OC \times\ 1.724) \quad (2)$$

Where, 1.724 was used as conversion factor to convert organic carbon into organic matter. Using SOM, the stable organic matter yield index was computed using the following equation (Eq. 3):

$$SOMYI = \left(\frac{Char\ yield}{100}\right) \times\ SOM \quad (3)$$

Moisture content (MC), ash (AC), and volatile matter (VM) content of the AHB were determined by ASTM D 3173, ASTM D 3174 and ASTM D 3175 standards, respectively.

Whereas, fixed carbon (FC) was computed by subtracting the percentage of moisture, ash and volatile matter content of the AHB from 100.

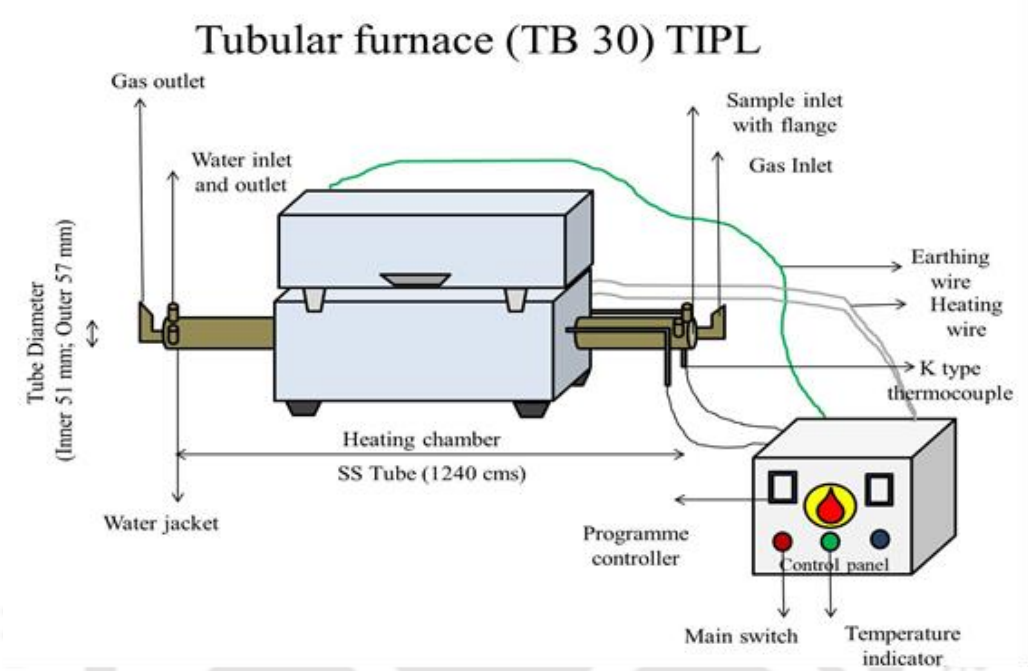

Fig. 5.3. Schematic diagram of tubular furnace used for biochar preparations.

5.2.2. Characterization of the prepared biochar

Elemental analysis was carried out using CHN elemental analyzer (Perkin Elmer, 2400 Series II) via high-temperature-catalyzed combustion. The surface morphology of the sample was analyzed by field emission scanning electron microscopy (FESEM) (Carl Zeiss-Sigma 300, Germany), at Central Instrumentation Facility, IIT Guwahati using a gold coating. The sample was pre-dried for 24 h in the oven, and kept in a desiccator to remove the moisture. The energy dispersive X-ray spectroscopy (EDX) is the most widely used qualitative estimation technique for the elemental analysis with a sampling depth of 1-2 μm. Fourier transform infrared (FTIR) spectroscopy was performed to assess the surface functional groups of BC. Crystalline size of the AHB was

determined using the Micromax-007HF, Rigaku X-ray diffractometer. Particle size analysis was carried out by dynamic light scattering (DLS) method using Anton Paar Litesizer 500. For the thermochemical assessment, differential scanning calorimetry (DSC), and thermo gravimetric analysis (TGA) were carried out using NetschModel STA449F3A00, where the AHB samples were heated up to 800°C with heating rate of 10.0 K min^{-1}.

5.3. Results and discussion

5.3.1. Physical properties of AHBs.

The pH values of different AHB varied remarkably from 8.01 to 10.52, and the positive correlation with increasing pyrolysis temperature was attributed to the separation of alkali salts (Ca, Mg, Na and K) from organic materials (Pariyar et al., 2020; Roy et al., 2019). Though the higher pH helps to reduce the acidity and neutralize the soil, the BC prepared at the low temperatures tend to be more effective for agricultural purposes, enhancing the dry matter yield of the crop (Prasad et al., 2018). The electrical conductivity (EC) is an indication of the salinity of the BC. In the present study EC of the AHB ranged from 2.10 to 9.51 mS cm^{-1} (Table 5.1.). Application of BC with higher EC values, might induce undesirable changes in soil salinity, plant growth patterns and retard microbial growth. The microbial population has been negatively correlated with the BC possessing higher EC, suggesting that higher salinity retards the microbial growth (Zhang et al., 2018a). Therefore, in the present study AHB with lower EC values were selected for soil applications.

5.3.2. Proximate and ultimate analysis of AHBs.

The AH was thermally treated at 250, 300, 350 and 400 °C under three different residence times (30, 60 and 90 minutes) to obtain AHBs a carbonized product. The ash content in different biochar varied from 7.46 to 9.89%. The results were consistent with the existing studies conducted by Gogoi et al. (2017), where higher pyrolysis temperature caused a substantial increase in ash content. The AHBs exhibited lower ash content which might be due to the lower mineral content of the AH. Moisture content in the different AHBs ranged from 5.42 to 6.87%, and a decreasing trend was observed with an increase in pyrolysis temperature and time (Table 5.1). In biomass, moisture is chiefly present in two forms, i.e., capillary or free water in the lumens, and hygroscopic water on the cell walls (Pariyar et al., 2020). It was reported that the moisture content in the plant-derived biochar is comparatively more than sludge or waste-derived BC. The volatile matter percentage for AHB was 19.29 to 26.87%, respectively (Table 5.1). The percentage of volatile content mainly is depended on temperature, residential time, and oxygen during pyrolysis (Spokas et al., 2011). Lower temperature BC had higher VM and organic acids, which supported increased levels of hydrolytic soil enzymes and microbial activitiy, in comparision to the high-temperature biochar (Gul and Whalen, 2016). Fixed carbon in biochar is that part that remains for long periods in soil, and it is highly recalcitrant in nature. In the present study, the fixed carbon showed slight variation with residence time, although it chiefly depends upon the type of feedstock in many other cases. AHBs have fixed carbon ranging from 58.81 to 65.41%; present results also corroborate with the study conducted by Gogoi et al. (2017). Generally, it was observed that BC having higher fixed carbon had lower ash content or vice versa (Table 5.1).

Ultimate analysis (C, H, N, and O) was performed to know the elemental composition and to choose the most stable biochar for suitable soil applications. Elemental analyses of different BC produced in the study are provided in Table 5.1. Slight change in the elemental compositions was

observed with change in pyrolysis temperature. AHB in this study had a carbon content between 19.28% and 58.75%. Highest carbon content was observed at 250 °C at 60 min, suggesting the dominance of carbon containing functional groups. The BC with higher carbon content tends to be more environmentally stable (Moradi-Choghamarani et al., 2019). However, the carbon content of the BC depends upon type of biomass, pyrolysis temperature, and residential time. Biomass such as pine saw dust, rice husk, and food waste, have higher carbon content and are thus suitable for soil applications, and remediation of HMs (Pariyar et al., 2020). Increasing pyrolysis temperature coupled with decreasing hydrogen content suggests cleavage and cracking of weak bonds, contributing to production of water, oil and other syngas (H_2, CO_2, N_2O, and CH_4). The N content reduction with increase in pyrolysis temperature, in the present study corroborates previous BC characterizations (Han et al., 2017; Kumar et al., 2013; Moradi-Choghamarani et al., 2019; Nikravesh et al., 2017; Pariyar et al., 2020). It is noteworthy that plant derived BC had lower N content as compared to the waste based BCs (Hossain et al., 2011).

The O/C and H/C ratio are helpful in knowing degree of aromaticity, and polarity (Lehmann and Joseph, 2015). The lower H/C (0.05 to 0.09) and O/C ratio (0.65 to 2.52) suggests greater degree of aromaticity and stability of BC. The H/C ratio is generally used as an indicator of carbonization. Decreased H/C ratios of all the BC (made at the different temperatures) indicated they lost more water and ‘O’ containing functional groups, and formed more aromatic and graphic structures to condense C. The increased pyrolytic temperature fused the aromatic C rings and facilitated transformation from the amorphous to the turbostratic state; thus, offering greater affinity for microbes and remediation of PAH contaminated soil (Zhang et al., 2018a). In the present study, higher O/C ratio with increasing pyrolysis temperature, implied the less labile nature of AHB or plant derived BC, due to large aromatic structures present in the feedstocks (Jindo et

al., 2014). The lowest O/C was obtained at temperature 250 °C for 60 min, which suggested a BC half-life of < 100 year (IBI, 2014; Spokas, 2010).

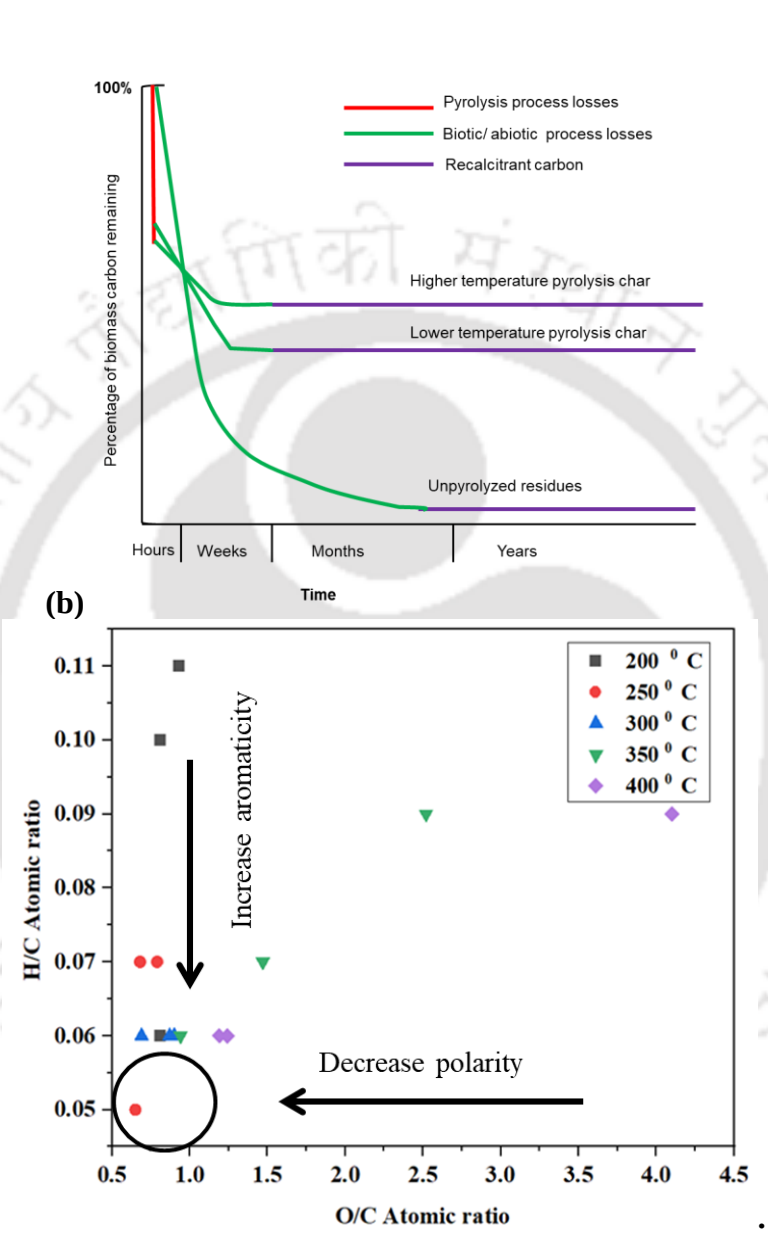

Fig. 5.4. (a) Percentage of biomass carbon in different char (b) Van krevelen diagram showing O/C and H/C atomic ratio of AHBs prepared at different temperature and residence time.

Table 5.1.

Proximate and elemental analysis of different type of AHBs.

Temperature	**250 °C**			**300 °C**			**350 °C**			**400 °C**		
Proximate and Elemental analysis	30 min.	60 min.	90 min.	30 min.	60 min.	90 min.	30 min.	60 min.	90 min.	30 min.	60 min.	90 min.
pH (H_2O)	8.01	8.07	8.53	8.86	9.15	9.19	10.43	10.51	10.4	10.41	10.43	10.52
EC (µS/cm)	2.17	2.59	3.78	2.10	2.14	3.19	5.89	5.94	6.64	9.14	9.27	9.51
MC (%)	6.87	6.85	6.86	6.43	6.36	6.22	6.10	5.89	5.78	5.56	5.47	5.42
VM (%)	26.87	26.30	25.10	24.10	23.53	22.76	21.31	21.25	20.43	19.52	19.45	19.29
AC (%)	7.46	7.70	7.90	8.04	8.03	8.40	8.67	8.81	9.16	9.50	9.89	9.89
FC (%)	58.81	58.81	58.81	61.42	62.08	62.62	63.92	64.06	64.62	65.41	65.19	65.39
C	57.29	58.75	52.78	56.97	50.81	50.41	50.11	39.33	27.67	43.6	43.96	19.28
H	3.86	2.99	3.69	3.54	3.07	3.27	2.89	2.69	2.58	2.4	2.79	1.76
N	BDL	BDL	1.74	BDL	1.85	0.7	BDL	0.16	BDL	BDL	1.04	BDL
O	38.85	38.26	41.79	39.49	44.27	45.62	47	57.82	69.75	54	52.21	78.96
H/C ratio	0.07	0.05	0.07	0.06	0.06	0.06	0.06	0.07	0.09	0.06	0.06	0.09
O/C ratio	0.68	0.65	0.79	0.69	0.87	0.9	0.94	1.47	2.52	1.24	1.19	4.1

* Values shown here are the averages of the three replicates
EC= Electrical conductivity; MC=Moisture content; VM= Volatile matter; AC=Ash content; FC=Fixed carbon; C=Carbon%; H=Hydrogen%; N=Nitrogen%; O=Oxygen%

5.3.3. Agronomic characterization of AHBs for soil application.

The increasing pyrolysis temperature and residence time lowered AHB yield and increased the ash content time (Fig. 5.5). The significantly lower yield of AHB at temperatures above 350 °C is a result of dehydration, loss of volatile matter and non-condensable gases like CO_2, H_2 and CH_4 (Niazi et al., 2018). The increased ash content beyond 300 °C (28.91% to 34.91%) lowered SOM and LOI in AHB (Fig. 5.5). The lowered LOI observed is in close agreement with the studies carried out by Kumar et al., (2013) and Masto et al., (2013). Lower LOI reflects the higher ash content of the AHB, formed after 300 °C which ranged from 28.91% to 34.91%. Concurrently, the AHB carbon liability index which is the ratio of OC/LOI also decreased with increasing pyrolysis temperature and residence time.

The soil amendment potential of BC is rendered recalcitrant, unsuitable and particularly unstable over time, when it is produced at temperatures higher than 250 °C. BC with higher stability is required to mediate soil rejuvenation through augmented adsorption of nutrients and carbon sequestration.

In present study, though maximum SOM was observed at 250 °C and 30 min duration, the yield of AHB was lower than higher temperatures. Consequently, SOMYI was employed to assess the higher yield and greater stability of BC, as both parameters are essential for viable and wider soil applications. SOMYI is a widely used parameter to investigate the higher yield, higher carbon and BC prepared in low temperature (Vijayanand et al., 2016; Han et al., 2017; Kumar et al., 2013; Masto et al., 2013; Nikravesh et al., 2017). The SOMYI of AHB showed a clear correlation with temperature and residence time; it increased up to 250 °C, and subsequently, decreased at 300 °C (Fig. 5.5); a positive indication of optimum SOM yield at moderate pyrolysis conditions. Therefore, based on the RSM, AHB produced at 250 °C for 60 min (Fig. 5.6) had the requisite yield and stability for AHB production for bulk soil applications. This could enable utilization of locally available residue and appropriate technologies to improve soil fertility. A similar preference for low temperature char with maximum stable C yield was also supported by other investigators (Masto et al., 2013). In addition, it was observed that BC derived from lower temperatures, possessed negatively charged functional groups (C=O and C-H), which serve as sites for nutrient exchange (Bolster and Abit, 2012).

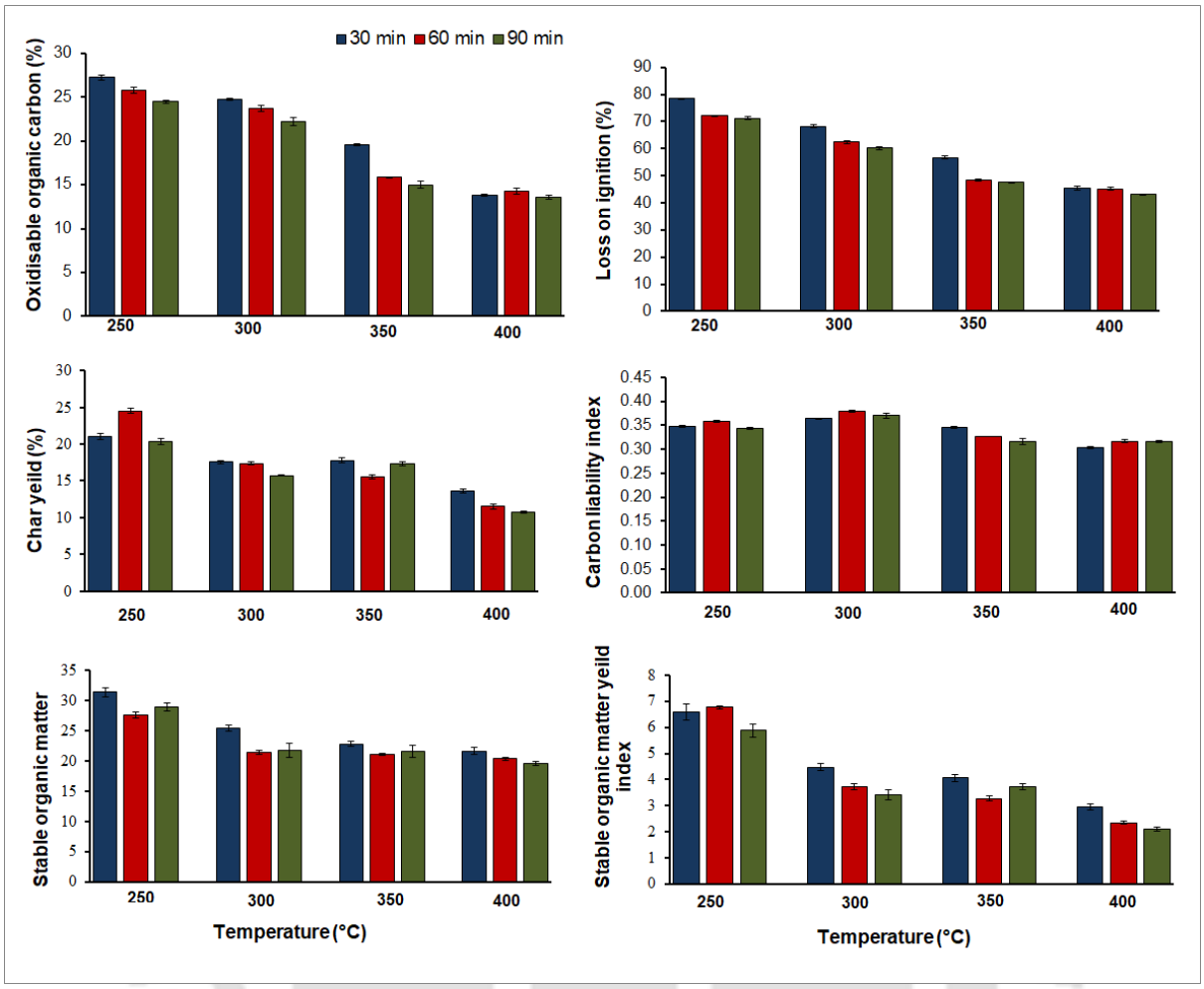

Fig. 5.5. Effect of different pyrolysis temperature and residence time on biochar yield, and other parameters.

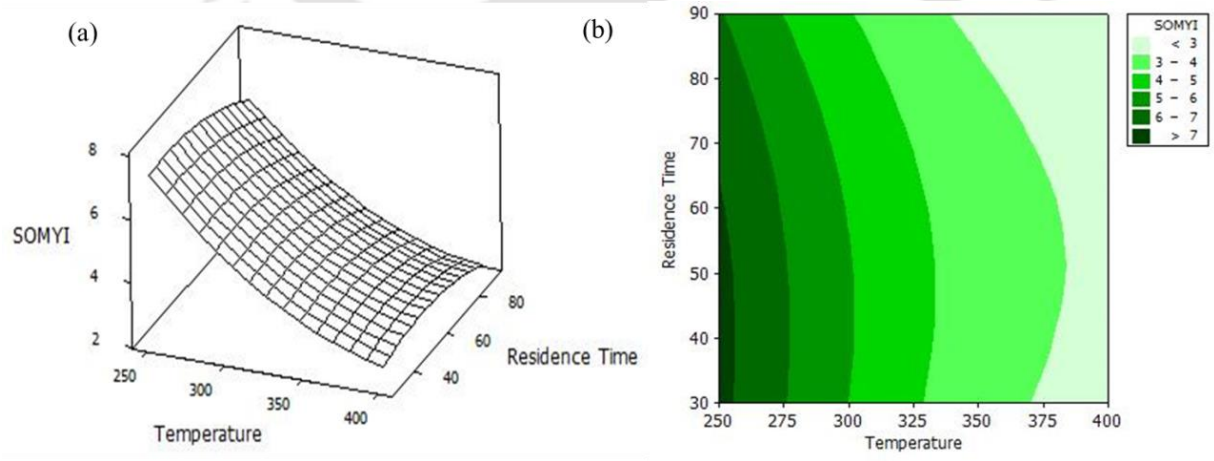

Fig. 5.6. Response surface and contour plot of stable organic matter yield index (SOMYI) of areca nut husk biochar (AHB).

5.3.4. Morphological analysis of AHB

The surface morphology of the AHB obtained at 250 °C with 60 min residence time was further studied using field emission scanning electron microscope (FESEM). The oval shaped micro-porous structure with diameter ranging from 2.13 to 3.81 µm was seen in the the FESEM micrograph (Fig. 5.7). At 2.0 Kx magnification the honeycomb structure was clearly visible which could be due to the volatilization of organic compound and biological capillary structure of the biomass (Gupta et al., 2018). Micrograph of AHB revealed the large pore size present on the surface of BC, which might act as a suitable habitat for the soil biota (Gujre et al., 2021).

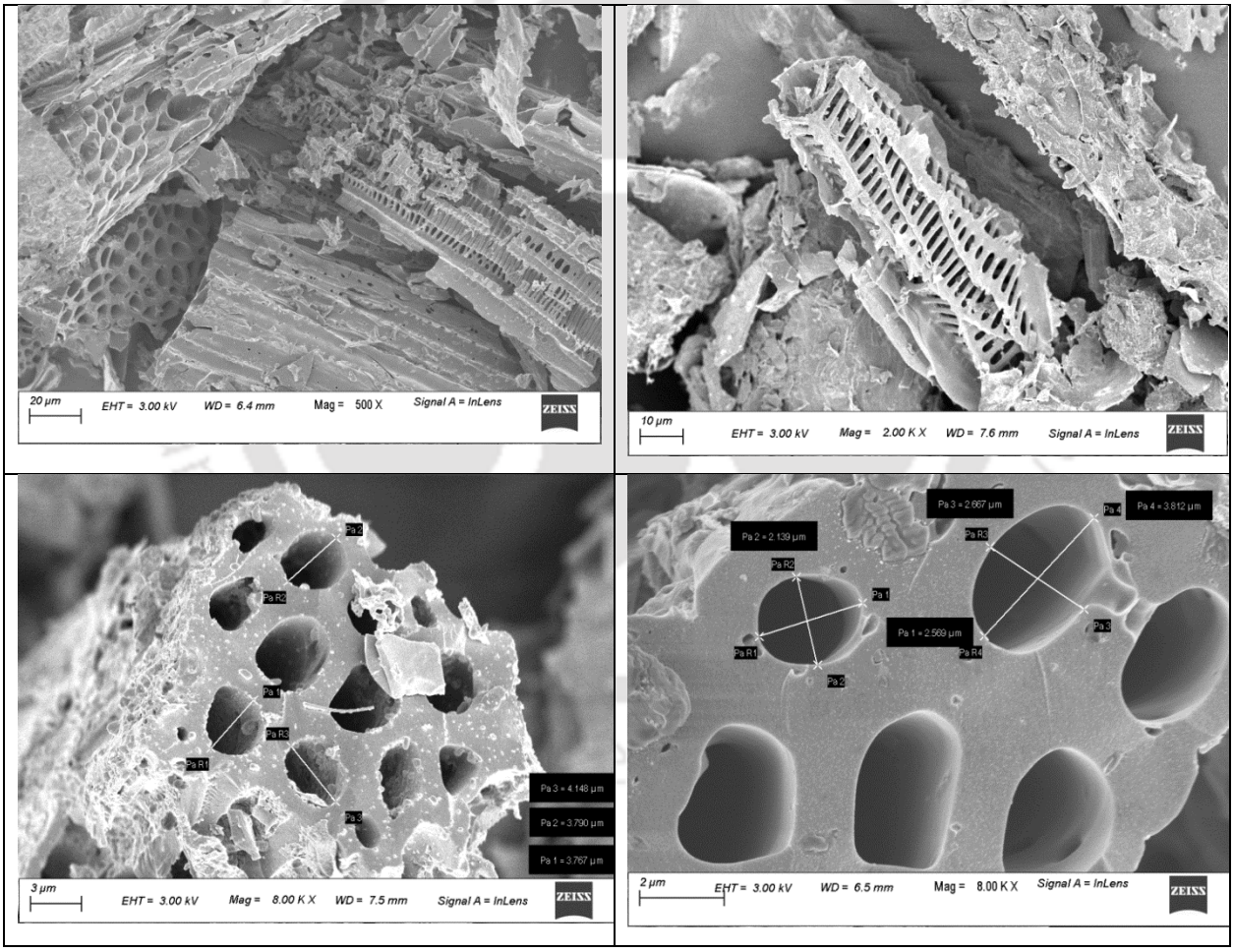

Fig. 5.7. FESEM micrograph of the AHB at 500 X, 2.00 KX and 8.00 KX.

Biochar's particle size, shape, and internal structure played critical roles in controlling soil water storage as they alter pore characteristics. BC has pores inside of particles known as intrapores, which may provide additional space for water storage. Likewise, beyond the pore space between particles is known as interpores. Particle size may influence both intrapores and interpores through different processes. Further, size of biochar particle has the potential to alter soil hydrology and to regulate the amount of water stored in soils. The hydrodynamic diameter of the AHB is 1191.6 nm, and its surface particles are widely divergent in size. Thus, in terms of surface area, 70.11% has 883.1(± 430.8) nm particles, 20.69% contains particles sized 207.0 (±45.38) nm, and only 10% has large particles of 3580 (± 988.7) nm (Fig. 5.8). The BC intrapore extend the water storage capacity of the soil, beyond its inherent porosity. Variable BC particles may enhance soil macroporosity, facilitating oxygen diffusion into the soil and reducing soil resistance to root penetration (Downie et al., 2012). BC with a high intraporosity and irregular shapes will most effectively increase water storage in the coarse soil (Liu et al., 2017).

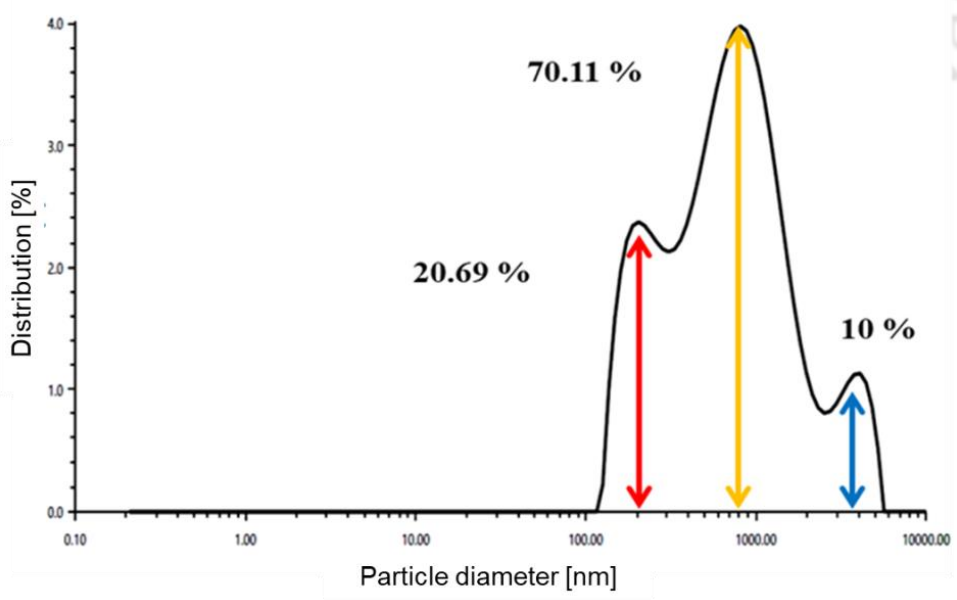

Fig. 5.8. Percentage of particle size distribution on AHB surface.

For soil applications, another essential property of the BC is the specific surface area (SSA). It is having a notable effect on the interactions between biochar and soil matrix. The larger the surface area, more is the interaction effects. SSA of the biochar was determined using N_2 adsorption-desorption isotherm through Brunauer-Emmett-Teller (BET) method. Result revealed that the AHB has an SSA of 2.6608 m^2 g^{-1}. Generally, it has been observed that the BET surface area of lower temperature biochar lies close to the 1 m^2 g^{-1}, which might be attributed to the macropores structure of biochar. Higher BET surface area can be obtained using a different type of activation process, which facilitates the formation of micropores in the carbon structure. Likewise, the pore size distribution was obtained from the desorption branch of the isotherm using the Barrett-Joyner-Halender (BJH) model. Biochar with a well-developed pore structure helps adsorb the soil organic matter into the pores. This effectively prevents its consumption by microorganisms and other biota and their extracellular enzymes (Zimmerman et al., 2011). Type-II isotherm is observed in AHB, indicating the material with diameters exceeding micropore (>2 nm). No hysteresis observed in the isotherm, indicating the absence of capillary condensation (Fig. 5.9). In the present study, the AHB has a pore size of 9.2981 nm, suggesting the prepared AHB's mesoporous nature.

According to several researchers, biochar can be divided into three types based on pores which include micropores (< 2 nm dia), mesopores (2-50 nm dia) and macropores (>200 nm). For adsorption applications, the biochar with a pore size of < 2 nm diameter would be suitable, whereas mesopores and macropores would be preferable for soil quality applications. The larger pore size offers easier penetration for the fungal hyphae, thereby helping the plants acquire nutrients.

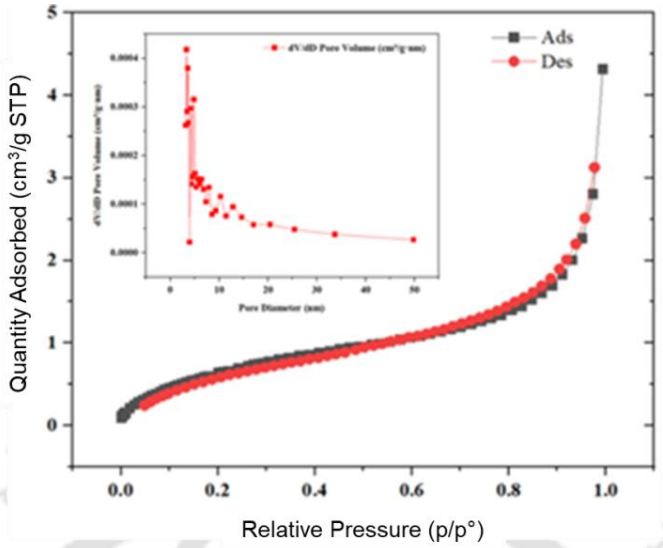

Fig. 5.9. Adsorption-desorption isotherm for pore size analysis of the AHB.

5.3.5. Elemental and functional group assessment of AHB

SEM-Energy Dispersive X-Ray Analysis (EDX) is an x-ray technique used to identify the elemental composition of materials. The elemental composition of the major elements in AHB are C (63.4%) > O (34.8%) > Al (0.9%) > N (0.7%) > Cu (0.1%). Results showed that the carbon and oxygen accounted for 97.2% on the surface of AHB, which might be due to the carbon content of the AH and the presence of oxygen containing functional groups (5.10). Fourier transform infrared (FTIR) spectroscopy was employed to examine the surface functional groups of the AHB. For the functional group assessment, FTIR spectra of the prepared BC were analyzed with various peaks depicting different functional groups (Fig. 5.11). The peaks around 3700 cm^{-1} for the BC, correspond to the –O-H carboxylic stretching vibrations (Saikia et al., 2017). This vibration indicates the presence of oxygen containing functional groups such as phenols, carboxyl, hydroxyl, and carbonyl (Dandamudi et al., 2021). Peak appearing at around 2225 cm^{-1}, indicates C ≡ C alkyl group present on the BC surface. The presence of carbonyl group along with amide group,

specifically carboxyamide –C(=O) N= was observed in the region around 1558 cm^{-1}. The vibration at 1458 cm^{-1} suggests the aliphatic C—H stretch, which was observed from the phenolic group transformation. The peaks at 1006 cm^{-1} corresponds to the C—O stretching typically associated with bend cellulose, hemicelluloses, and lignin and aromatic —CH scissoring (Saikia et al., 2017). 893 cm^{-1} and 617 cm^{-1} weak peaks correspond to the aromatic ring bending of C-H groups. FTIR analysis revealed the presence of hydroxyl, alkenes, and alkyl groups on the surface of AHB. For soil applications, surface chemistry and hydrophobicity are important factors. The BC obtained at lower pyrolysis temperature contains aliphatic functional groups, which increases the hydrophobicity of the BC (Edeh and Buss, 2020). Low temperature pyrolyzed BC are more efficient for remediating the inorganic contaminants like Cr (IV), which might be attributed to the hydroxyl and carboxyl functional groups attached on its surface (Zhang et al., 2018b). Earlier, researchers also indicated that BC prepared in lower temperature is helpful in removal of polar insecticides and herbicides such as 1-naphthol, norflurazon and fluridone (Oliveira et al., 2017). The functional groups attached to the surface promote the complex formation and improve the binding ability of the BC (Yuan et al., 2019). Additionally, BC amendment can improve the activities of distinct functional group thus affecting the soil enzyme and microbial activities (Yuan et al., 2019; Zhang et al., 2019) .

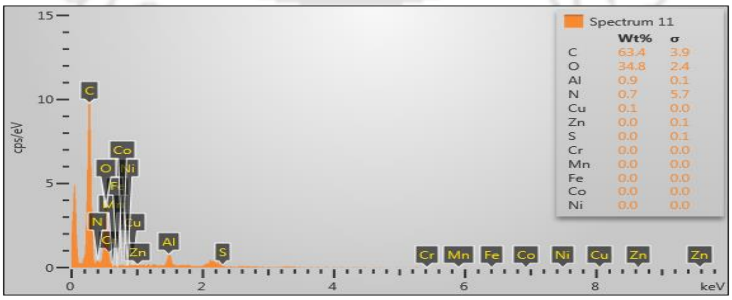

Fig.5.10. EDX picture of the AHB showing different elements.

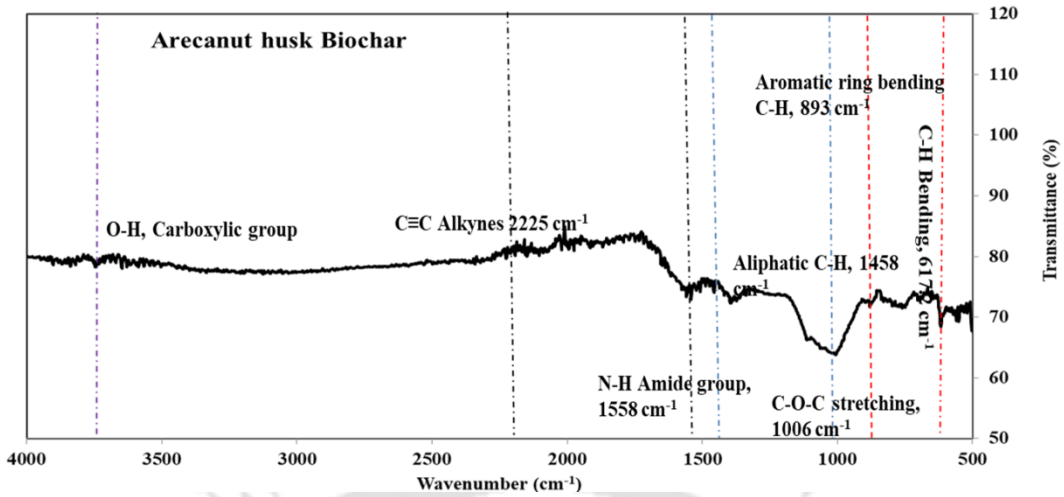

Fig.5.11. FT-IR spectra of the AHB showing different functional groups.

5.3.6. Size and thermochemical assessment of AHB

X-Ray Diffraction (XRD) measurements were performed to assess different crystallite size of AHB. Crystallite size is most likely the smallest single crystal in powder form. The crystallite size is commonly determined by XRD using the Scherrer equation which is as follows:

$$D = \frac{k\lambda}{\beta \cos\theta}$$

Where, D= Crystallites size (nm), K= 0.9 (Scherrer constant), λ= 1.54184 A^0, $\beta^=$ Full width at half maximum (FWHM) (radians), θ= Peak position (radians).

The average crystallite size of the AHB is 33.13 nm. High crystallite size increases the particle size of the BC and also the absorption capacity of a particular BC. Further, it has been reported that rice husk BC produced in low temperature have higher stability and turbostatic crystallites which significantly contributed in enhancing the recalcitrant nature of BC (Wu et al., 2012).

Thermo gravimetric analysis (TGA) offers insight into the thermal degradation and thermal stability properties of the BC (Kumar et al., 2013). TGA of the AHB prepared at 250 °C was used

to verify the thermal stability, the TG, DTG and DSC profiles of AHB have been shown in Fig. 5a. In the present study three regions of weight loss and associated heat flow are apparent. The first region (WL_1) of the weight loss (RT- 260°C) is associated with the release of physisorbed and non-structural water from the surface and pores of the BC (Pariyar et al., 2020). The TG profile showed an initial weight loss of 4.92% up to 260 °C, which might be attributed to the small amount of moisture adsorption on its surface. The second region of weight loss (WL_2) was more prominent at temperatures between 260-620 °C. The major weight loss of the AHB was observed in this region accounting for 27.72%; the WL_2 in this region is typically associated with the decomposition of hemicellulose and cellulose. Decline in the TG curve around 300 °C suggests that the main weight loss took place after 300 °C. This indicates the incomplete decomposition of cellulose and higher content of lignin. After 400 °C, the cellulose present in the BC is converted into condensable vapour and non-condensable gases. Concurrently, with a consistent weight loss, an exothermic peak was also observed in the region from 300- 350 °C which could be due to the thermal oxidation of the organic compounds. The BC obtained at higher temperature (> 350 °C), progressed through the process of thermal oxidation turning the BC more recalcitrant in comparison to the BC prepared at lower temperature (Harvey et al., 2012). Further, the third region of weight loss (WL_3) continued from 620 °C till 800 °C suggesting the slow decomposition of lignin which accounted for 32.15%, whereas about 67.85% of mass residue still remained intact. Lignin is an important constituent of the fibres of the areca nut husk (Kumar et al., 2013; Masto et al., 2013). Therefore, after analysing the three different weight loss regions of AHB, its thermal stability index (WL_3/WL_2) and weight loss associated organic matter combustion ($W_{org} = WL_2 + WL_3$) were computed. The result revealed that the thermal stability index of the AHB was 1.15 which suggested the recalcitrant nature of the prepared BC which has the potential in improving

soil-plant continuum, thereby increasing plant growth (Woolf et al., 2010). However, the obtained thermal stability index is comparatively lower than water hyacinth BC prepared at 300 °C (3.31), suggesting lower recalcitrant nature of AHB (Masto et al., 2013). In soil matrix, BC prepared at low temperatures are less aromatic (lower recalcitrant), thereby helpful in growth of the bacteria and fungi.

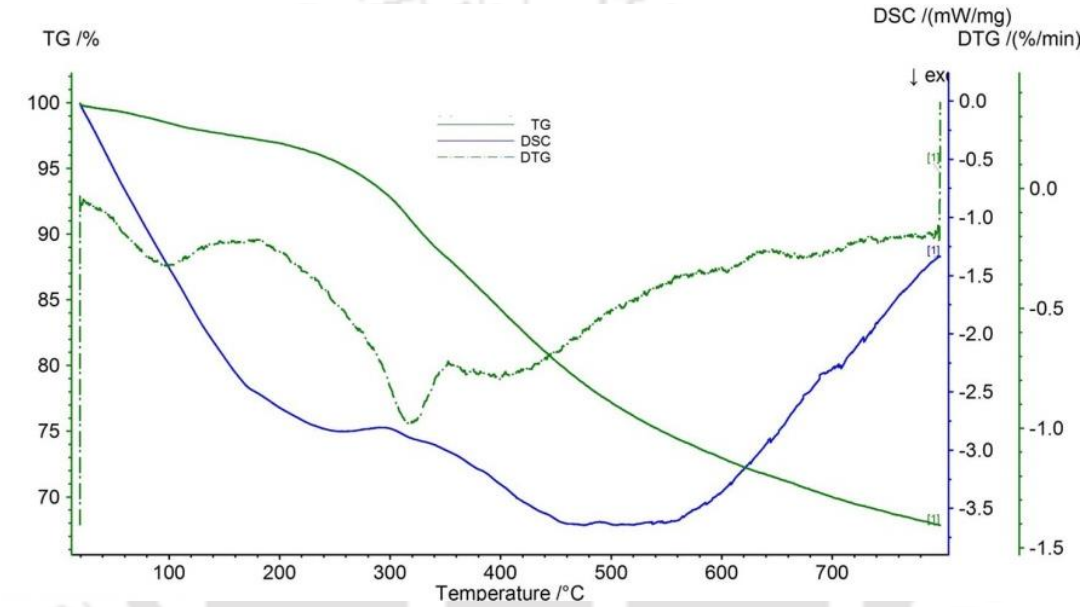

Fig.5.12. TGA-DTG and DSC curves of AHB.

5.4. Conclusion

With the aim of waste valorization and soil quality improvement in the present study, AHB was prepared and characterized. This study depicts the lower H/C and O/C ratio, ranging from 0.05 to 0.09 and 0.65 to 2.52. A lower ratio suggests a greater degree of aromaticity and stability of BC. The lowest O/C was obtained at temperature 250 °C for 60 min, which suggested a BC half-life of < 100 years. It was observed that the AHB prepared at a lower temperature was suitable for soil

quality applications. The AHB prepared at low-temperature (250 °C) obtained the highest SOMYI (6.78) and 'O' containing surface functional groups. Result revealed that the thermal stability index of the AHB prepared at 250 °C was 1.15. Lower thermal stability reflects lesser recalcitrant aromatic C, which is favourable for microbial and soil enzymatic activities. Further, a micrograph of AHB revealed that larger pores are present on the surface of BC, which might act as a suitable habitat for the soil biota. AHB has variable particle size, enhancing soil macro porosity and oxygen diffusion into the soil and reducing soil resistance to root penetration.

References

Blair, G.J., Lefroy, R.D., Lisle, L., 1995. Soil carbon fractions based on their degree of oxidation, and the development of a carbon management index for agricultural systems. Aust. J. Agric. Res. 46, 1459–1466.

Bolster, C.H., Abit, S.M., 2012. Biochar Pyrolyzed at Two Temperatures Affects *Escherichia coli* Transport through a Sandy Soil. J. Environ. Qual. 41, 124–133.

Calvelo Pereira, R., Kaal, J., Camps Arbestain, M., Pardo Lorenzo, R., Aitkenhead, W., Hedley, M., Macías, F., Hindmarsh, J., Maciá-Agulló, J.A., 2011. Contribution to characterisation of biochar to estimate the labile fraction of carbon. Org. Geochem. 42, 1331–1342.

Dai, Y., Zheng, H., Jiang, Z., Xing, B., 2020. Combined effects of biochar properties and soil conditions on plant growth : A meta-analysis. Sci. Total Environ. 713, 136635.

Dandamudi, K.P.R., Murdock, T., Lammers, P.J., Deng, S., Fini, E.H., 2021. Production of functionalized carbon from synergistic hydrothermal liquefaction of microalgae and swine manure. Resour. Conserv. Recycl. 170, 105564.

DASD (Directorate of Arecanut and Spices Development) 2019. Statewise area, production and productivity of Arecanut in India. https://www.dasd.gov.in/adminimage/Arecanut_area_and_production_2020.pdf (Accessed on 24 March 2021).

Deshmukh, P.S., Patil, P.G., Shahare, P.U., Bhanage, G.B., Dhekale, J.S., Dhande, K.G., Aware, V. V., 2019. Effect of mechanical and chemical treatments of areca nut (*Areca catechu* L.) fruit

husk on husk and its fibre. Waste Manag. 95, 458–465.

Downie, A., Crosky, A., Munroe, P., 2012. Physical properties of biochar, in: Biochar for Environmental Management: Science and Technology. Routledge, pp. 13–32.

Edeh, I.G., Buss, W., 2020. A meta-analysis on biochar ' s effects on soil water properties – New insights and future research challenges. Sci Total Environ.714, 136857.

Gogoi, D., Bordoloi, N., Goswami, R., Narzari, R., Saikia, R., Sut, D., Gogoi, L., Kataki, R., 2017. Effect of torrefaction on yield and quality of pyrolytic products of areca nut husk: An agro-processing wastes. Bioresour. Technol. 242, 36–44.

Gujre, N., Soni, A., Rangan, L., Tsang, D.C.W., Mitra, S., 2021. Sustainable improvement of soil health utilizing biochar and arbuscular mycorrhizal fungi: A review. Environ. Pollut. 268, 115549.

Gul, S., Whalen, J.K., 2016. Biochemical cycling of nitrogen and phosphorus in biochar-amended soils. Soil Biol. Biochem. 103, 1-15.

Gupta, S., Kua, H.W., Koh, H.J., 2018. Application of biochar from food and wood waste as green admixture for cement mortar. Sci. Total Environ. 619–620, 419–435.

Han, L., Sun, H., Ro, K.S., Sun, K., Libra, J.A., Xing, B., 2017. Removal of antimony (III) and cadmium (II) from aqueous solution using animal manure-derived hydrochars and pyrochars. Bioresour. Technol. 234, 77–85.

Harvey, O.R., Kuo, L.J., Zimmerman, A.R., Louchouarn, P., Amonette, J.E., Herbert, B.E., 2012. An index-based approach to assessing recalcitrance and soil carbon sequestration potential of engineered black carbons (biochars). Environ. Sci. Technol. 46, 1415–1421.

Hossain, M.K., Strezov Vladimir, V., Chan, K.Y., Ziolkowski, A., Nelson, P.F., 2011. Influence of pyrolysis temperature on production and nutrient properties of wastewater sludge biochar. J. Environ. Manage. 92, 223–228.

IBI, 2012. IBI Biochar Standards. International Biochar Initiative. Available at: www.biochar-international.org/ (accessed 2 December 2021)

Jindo, K., Mizumoto, H., Sawada, Y., Sanchez-Monedero, M.A., Sonoki, T., 2014. Physical and chemical characterization of biochars derived from different agricultural residues. Biogeosciences 11, 6613–6621.

Kumar, S., Masto, R.E., Ram, L.C., Sarkar, P., George, J., Selvi, V.A., 2013. Biochar preparation from *Parthenium hysterophorus* and its potential use in soil application. Ecol. Eng. 55, 67–72.

Lehmann, J., Joseph, S., 2009. Biochar for environmental management: an introduction, in: Biochar for Environmental Management. Taylor & Francis, pp. 1–12.

Liu, Z., Dugan, B., Masiello, C.A., Gonnermann, H.M., 2017. Biochar particle size , shape , and porosity act together to influence soil water properties 1–19.

Masto, R.E., Kumar, S., Rout, T.K., Sarkar, P., George, J., Ram, L.C., 2013. Biochar from water hyacinth (*Eichornia crassipes*) and its impact on soil biological activity. Catena 111, 64–71.

Moradi-Choghamarani, F., Moosavi, A.A., Baghernejad, M., 2019. Determining organo-chemical composition of sugarcane bagasse-derived biochar as a function of pyrolysis temperature using proximate and Fourier transform infrared analyses. J. Therm. Anal. Calorim. 138, 331–342.

Niazi, N.K., Bibi, I., Shahid, M., Ok, Y.S., Burton, E.D., Wang, H., Shaheen, S.M., Rinklebe, J., Lüttge, A., 2018. Arsenic removal by perilla leaf biochar in aqueous solutions and groundwater: An integrated spectroscopic and microscopic examination. Environ. Pollut. 232.

Nikravesh, I., Boroomandnasab, S., Naseri, A.A., Mohammadi, A.S., 2017. Wheat Straw Biochar Application to Loam-Sand Soil : Impact on Yield Components of Summer Maize and Some Soil Properties 8, 54–60.

Oliveira, F.R., Patel, A.K., Kumar, S., Jaisi, D.P., Adhikari, S., Lu, H., 2017. Bioresource Technology Environmental application of biochar : Current status and perspectives. Bioresour. Technol. 246, 110–122.

Pariyar, P., Kumari, K., Kumar, M., Jadhao, P.S., 2020. Science of the Total Environment Evaluation of change in biochar properties derived from different feedstock and pyrolysis temperature for environmental and agricultural application. Sci. Total Environ. 713, 136433.

Prasad, M., Tzortzakis, N., McDaniel, N., 2018. Chemical characterization of biochar and assessment of the nutrient dynamics by means of preliminary plant growth tests. J. Environ. Manage. 216, 89–95.

Rajan, A., Kurup, J.G., Abraham, T.E., 2017. Biosoftening of areca nut fiber for value added products. Biochem. Eng. J. 25, 237–242.

Roy, S., Kumar, U., Bhattacharyya, P., 2019. Synthesis and characterization of exfoliated biochar from four agricultural feedstock.Environ. Sci. Pollut. Res.26, 7272–7276.

Saikia, R., Goswami, R., Bordoloi, N., Senapati, K.K., Pant, K.K., 2017. Removal of arsenic and fl uoride from aqueous solution by biomass based activated biochar : Optimization through response surface methodology. J. Environ. Chem. Eng. 5, 5528–5539.

Singh, R.D., Bhuyan, K., Banerjee, J., Muir, J., Arora, A., 2017. Hydrothermal and microwave

assisted alkali pretreatment for fractionation of areca nut husk. Ind. Crop. Prod. 102, 65–74.

Spokas, K.A., 2010. Review of the stability of biochar in soils : predictability of O : C molar ratios 1, 289–303.

Vijayanand, C., Kamaraj, S., Sriramajayam, S., Ramesh D., 2016. Biochar production from arecanut waste. Int. J. Farm Sci. 6, 43-48.

Walkley, A., Black, I., 1934. An examination of the Degtjareff method for determining soil organic matter and a proposed modification of the chromic acid titration method. Soil Sci. 37, 29–38.

Woolf, D., Amonette, J.E., Street-Perrott, F.A., Lehmann, J., Joseph, S., 2010. Sustainable biochar to mitigate global climate change. Nat. Commun. 1, 56.

Wu, W., Yang, M., Feng, Q., McGrouther, K., Wang, H., Lu, H., Chen, Y., 2012. Chemical characterization of rice straw-derived biochar for soil amendment. Biomass Bioenerg. 47, 268–276.

Zhang, L., Xiang, Y., Jing, Y., Zhang, R., 2019. Biochar amendment effects on the activities of soil carbon , nitrogen , and phosphorus hydrolytic enzymes : a meta-analysis 22990–23001.

Zhang, G., Guo, X., Zhu, Y., Liu, X., Han, Z., Sun, K., Ji, L., He, Q., Han, L., 2018a. The effects of different biochars on microbial quantity, microbial community shift, enzyme activity, and biodegradation of polycyclic aromatic hydrocarbons in soil. Geoderma 328, 100–108.

Zhang, X., Fu, W., Yin, Y., Chen, Z., Qiu, R., Simonnot, M., Wang, X., 2018b. Adsorption-reduction removal of Cr (VI) by tobacco petiole pyrolytic biochar : Batch experiment , kinetic and mechanism studies 268, 149–157.

Zimmerman, A.R., Ouyang, L., 2019. Priming of pyrogenic C (biochar) mineralization by dissolved organic matter and vice versa. Soil Biol. Biochem., 130, 105-112.

CHAPTER 6

Heavy metal remediation potential of biochar

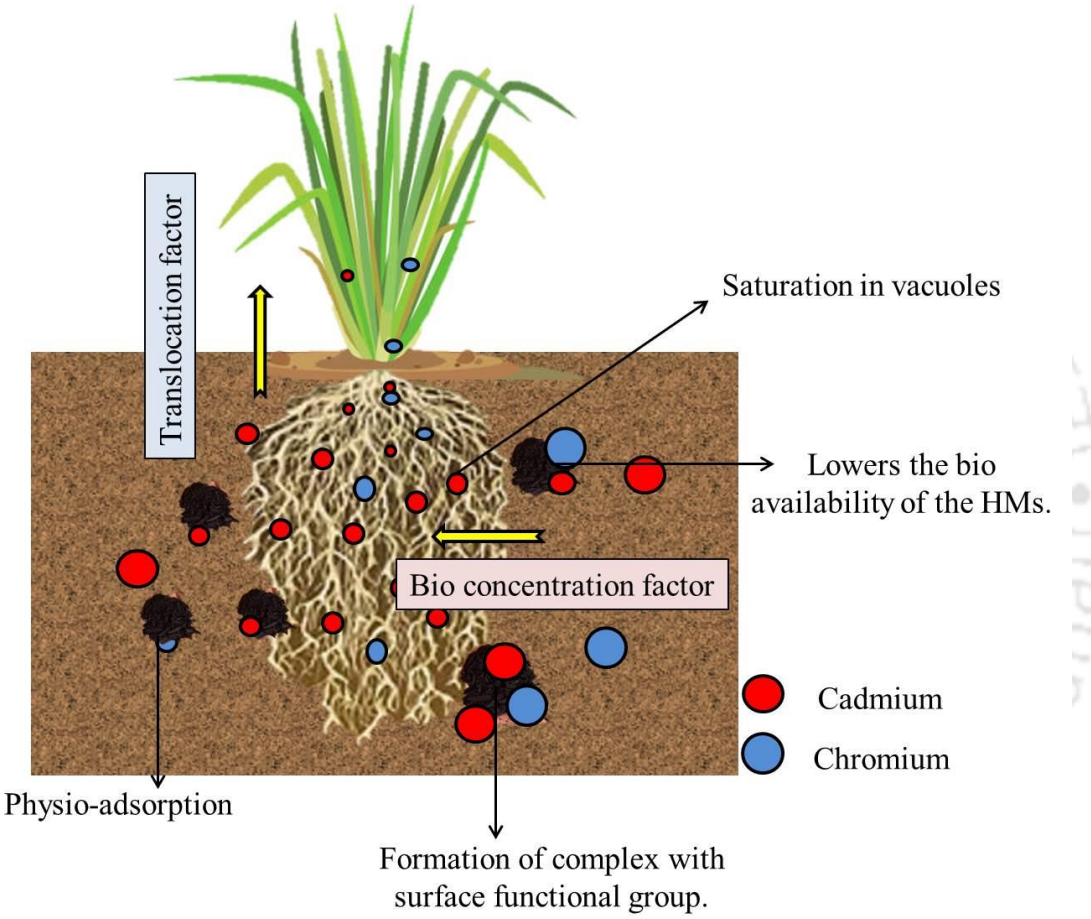

"The present chapter deals with application of biochar prepared from AH in soil contaminated with Cd and Cr, using vetiver grass for phytoremidiation. As a natural corollary, the HMs remediation potential of vetiver in conjunction with AHB is also investigated."

6. Heavy metal remediation potential of biochar

6.1. Introduction

For HMs remediation and soil quality improvement, phytoremediation is one of the best solutions. Globally, it is accepted that certain plant species are capable of effective and long-term HM remediation of the soil, thereby reducing the toxicity and rejuvenating soil quality. In the present study, vetiver grass (*Chrysopogon zizaniodes* L.), a perennial C4 grass of the Poaceae family, and native to India, was utilized for remediating soil contaminated with Cd and Cr. Vetiver is a fast growing plant, 1 to 2 m in height, with an extensive fibrous root system that exudes aromatic oils; it has distinct physiological, morphological, ecological characteristics and high biomass. Vetiver is used for different environmental management applications across the world, which primarily include mine reclamation, prevention of soil erosion, salinity management, and rejuvenation of the HMs contaminated sites (Banerjee et al., 2019; Gautam and Agrawal, 2017). However, its metal accumulation and metal tolerance ability, with higher root and shoot biomass, makes it the best choice for phytoremediation.

In addition to soil quality management, vetiver grass is potentially an effective and viable option for soil riverbank stabilization. The turbulent Brahmaputra, flowing through Assam causes severe river bank erosion. Several studies have claimed that use of appropriate agro-ecotechnology like vetiver can effectively arrest Brahmaputra's soil erosion. The dense and fibrous roots of vetiver can grow up to 7 m in depth in the soil (Grass et al., 2020); soil aggregation within its fibrous root network are postulated to assist in soil stabilization. Further, vetiver is locally known as "*Birina*", in Assam and is also traditionally used as a roofing material.

In the present study, high concentrations of Cd and Cr were detected in the studied soil due to anthropogenic activities. These HMs are known to be carcinogenic and toxic even at low concentrations. The permissible limit in agricultural soil for Cr and Cd are 64 mg kg^{-1} and 1.5 mg kg^{-1} respectively (CCME, 2007). Conventional and unilateral soil quality management strategies such as biological and chemical processes are widely employed for rejuvenation of the soil. Yet, such techniques are constrained by high application cost, field challenges, and ineffective remediation. Therefore, the present study used BC in conjunction with vetiver as a simple, clean, cost-effective, and ecofriendly technology; to decontaminate soils and enable integrated soil quality management, which is the need of the hour.

The primary mechanism in phytoremediation is phytostabilization, which generally immobilizes the HMs through a dense rhizosphere, reducing their bioavailability inside the soil system, and restricting their translocation in above-ground biomass. Further, a study revealed that vetiver roots and shoots could sequester approximately five times higher Zn and Cr present in the soil, than other similar rehabilitating species (Truong, 1999). The plant species is an apt choice for phytoremediation, as it displays both high tolerance and accumulation of HM, besides being a non-edible and non-grazing grass, with high biomass of shoot and roots. Despite many reports on vetiver and its HMs remediation potential, there is still a clear dearth of knowledge regarding behaviour and remediation potential in conjunction with BC. The present study thereby attempts to fill the existing gap of knowledge and explores the combined effect of vetiver and BC derived from areca nut husk or AHB on soil quality improvement.

6.2. Materials and methods

6.2.1. Pot experiment for assessment of the AHB

For assessment of impact of AHB, microcosm pot culture was established in completely randomized design (CRD) using vetiver (*Chrysopogon zizanioides* L.) for 90 days. The topsoil used in the experiment was collected from two contaminated sites. After removing small stones, plant materials and other wastes from contaminated soil, they were air dried and uniformly ground to a homogenous mass. Dried samples were sieved through a 2 mm mesh and mixed in a 1:1 proportion to obtain uniform soil combinations. Prepared and characterized AHB (250 °C; 60 min) was used for the microcosm pot culture. A total of 4 doses were selected on the basis of standard application protocol of biochar viz. 0 t ha^{-1}, 5 t ha^{-1}, 10 t $ha^{-1}$and 15 t ha^{-1}. The application doses were calculated for 10 kg of soil per pot and applied by mixing at rhizosphere zones of plant. This experiment was a 2 × 4 factorial design with addition of heavy metals and biochar amendment, and four replicates (Fig. 6.1). The experiment consisted of two soil substrates (contaminated and uncontaminated soils), and four biochar treatments (0, 5, 10, 15 t ha^{-1} which is designated as BC dose of 0, 1, 2, and 3 respectively). Vetiver plantlets were transferred from the field in plastic bags containing sterilized growth medium (a mixture of sand and compost, 5:1), and acclimitized kept in a rainproof net-house at the Agro-ecotechnology Laboratory, CRT, IIT Guwahati till further use. 10 kg of plastic pot was chosen for microcosm field experiment, labelled and tagged with aluminium tags.

Before the experiment was started, vetiver clumps were separated into individual tillers. The tillers, with 30 cm of the top part of the plant and 10 cm of the roots, were dipped into 5 cm of water for three to five days in the shade, to enhance root production before being transplanted into the pots (Fig. 6.2.). Pots were gravimetrically maintained at approximately 60% water holding capacity. All the plants were grown in a nethouse with ambient temperature of 20–35 °C and humidity was maintainted at about 60% during the 90 days of experimentation.

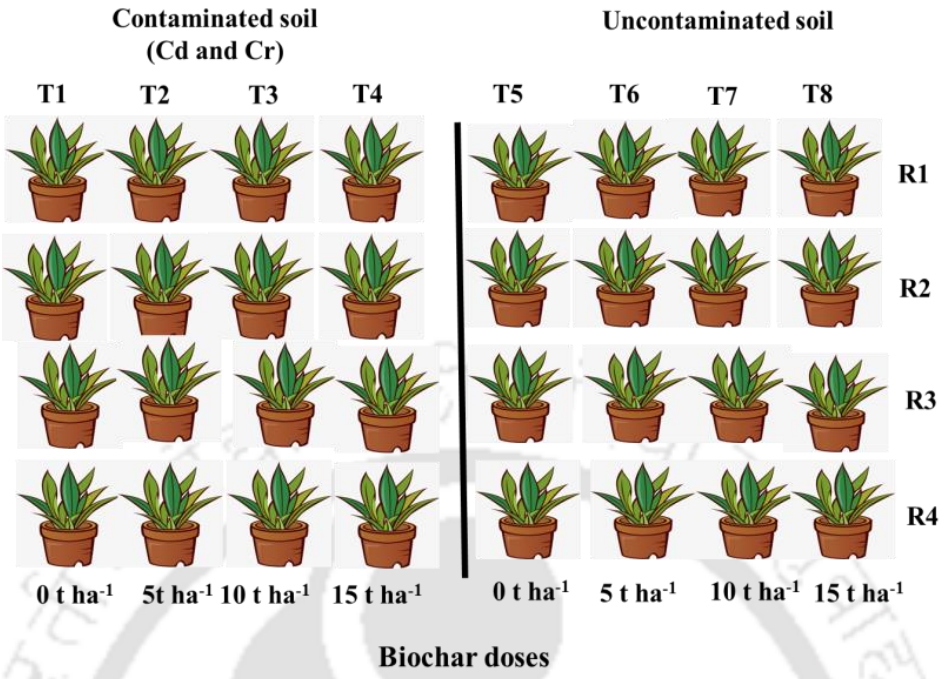

Fig. 6.1. AHB treatments used for the pot experiment.

Fig. 6.2. Schematic flowchart of the pot experiment.

6.2.2. Assessment of metal contents in soil and plant

After 90 days plants were harvested by hand, and the rhizosphere soil samples were collected. The plant samples were dried at 80 °C for 2 days to attain a constant weight in order to measure the dry weight of root and shoot. The dried plant samples were then used to determine the concentrations of Cd and Cr, after digestion in mixtures of HNO_3 and $HClO_4$ (2:1 *v/v*) by AAS (AAS Model: AA240, Agilent, Malaysia). The soil DTPA-extractable Cd and Cr concentration were prepared by (0.005 M diethylenetriaminepentaacetic acid (DTPA), 0.1 M triethanolamine (TEA) and 0.01 M $CaCl_2$) and determined using AAS (Lindsay and Norvell, 1978). Precision and accuracy of analysis of the samples were rigorously maintained through repeated assessment against standard reference material (SRM). The SRM used during the analysis is SRM 2706 and SRM-1515 procured from the National Institute of Standards and Technology, Standard Reference Materials, Madison, USA. Standard stock solution of 1000 mg L^{-1} was used for analysing the HMs. Blank and certified standards were run after every ten samples to calibrate the instrument. The results were found within ±2% of the certified value.

For evaluating the phytoextraction potential of vetiver grass under AHB effect two important indices, translocation factor (TF), and bio-concentration factor (BCF), were calculated (Qihang et al., 2011) using following two equations:

$$TF = \frac{Metal\ conc.in\ shoot}{Metal\ conc.in\ root} \quad (1)$$

$$BCF = \frac{Metal\ content\ in\ plant\ tissue}{Metal\ content\ in\ soil} \quad (2)$$

Where, the metal content in plant is in mg kg^{-1} and for metal content in soil the its bioavailable fractions are used.

6.3. Results and discussion

6.3.1. Metal concentration in different treatments

To assess the impact of AHB, microcosm pot culture was established. CRD (Complete Randomized Design) was used for this pot experiment. Vetiver (*Chrysopogon zizanioides* L.) was grown in the pots for 90 days. The initial bioavailable concentrations of Cr and Cd in the contaminated soils were 196.12 (± 2.81) mg kg^{-1} and 19.87 (± 0.77) mg kg^{-1}, respectively. Similarly, in the uncontaminated soil, Cr and Cd concentrations were 34.85 (± 1.00) mg kg^{-1} and 1.35 (± 0.45) mg kg^{-1}. After 90 days, it was observed that C. *zizanioides* facilitated phytostabilization of two HMs under investigation. The application of AHB generated an additive effect on plant growth and HM uptake, with substantially higher biomass, and lower Cd and Cr concentration in the soil. Cr concentration in the soil ranged from 21.00 (± 0.62) to 74. 70 (± 1.84) mg kg^{-1}, in the root from 10.89 (±0.71) to 44.60 (±1.09) mg kg^{-1} and in the shoot from 8.30 (±0.54) to 33.59 (±2.24) mg kg^{-1} (Fig. 6.3). Cd concentration in the soil ranged from 0.29 (±0.01) to 16.12 (±0.47) mg kg^{-1}, from 0.23 (±0.00) to 12.12 (±0.07) mg kg^{-1} in the root and from 0.15 (±0.00) to 10.55 (±0.03) mg kg^{-1} in the shoot (Fig. 6.4). Results showed vetiver had very high tolerance to Cd and could accumulate much more Cd in roots than in shoots. Higher concentrations of both Cr and Cd were detected in the root in comparison to the shoot in all treatments (Fig. 6.3 and Fig. 6.4); a preferred feature, even though vetiver is a non-grazing and non-edible plant species. For stabilizing metal-contaminated sites, a lower metal concentration in shoots is always preferred; this will arrest the movement of the metals in the shoot and finally into the ecosystem through the food chain (Yang et al., 2003). Vetiver being a metal tolerant species, several studies across the world have used the metal tolerant behaviour of vetiver for various reclamation practices (Akhzari

and Alipoor, 2019; Banerjee et al., 2019; Gautam and Agrawal, 2017; Roongtanakiat and Chairoj, 2001; Vargas et al., 2016; Zhang et al., 2014).

Interestingly, vetiver possesses an extensive root system with a maximum diameter of 20 cm and length of 5 m which facilitates the stabilisation of the soil, particularly in tailings and avoids erosion. Vetiver has unique morphological, physiological and ecological characteristics that enable it to tolerate a wide range of HMs, thus rejuvenating the contaminated soil (Bahraminia et al., 2016). Yang et al. (2003) carried out a comparative assessment of Pb, Zn, Cu, and Cd tolerance capacity of vetiver and demonstrated that it can accumulate a higher concentration of the metals in the roots than the shoots. Globally, to combat the hazardous effect of HMs, it is imperative to utilize plants that arrest the translocation of metals to the parts above the ground. Under the present circumstances, vetiver is the most suitable plant for managing soil degradation with multiple benefits. Also, addition of AHB enhances the sequestration of the HMs in soil, restricting its further mobility in soil.

The observed higher accumulation of HMs in root might be due to the ionic properties of the HMs. HM cations are preferentially absorbed by the negative charge sites of the root cell wall (Yang et al., 2003). Cd also forms immobile metal complexes in the roots, through cation exchange with ligands containing the sulfhydryl group (Topcuoglu, 2012). Lower availability of Cr in the shoot might be attributed to the saturation and accumulation in vacuoles and apoplast of root cells (Park et al., 2011). Increased BC concentration enhances the root biomass of vetiver, which in turn boosts the adsorption capacity of the roots. In addition, the soil minerals help the biochar to immobilise Cd in the soil, ultimately reducing its bioavailability in the soil (Qiu et al., 2020).

From the present study, it can be concluded that at an application rate of 15 t $ha^{-1}$of AHB, can effectively remediate about 39.4% and 67.1% of Cd and Cr, respectively. The experimental results

indicated that about 10 t ha^{-1} of AHB can remediate 34.7% and 66%; 5 t ha^{-1} can remediate 29.4% and 65.2% of Cd and Cr, respectively. Overall, the experimental dose of 15 t ha^{-1} AHB demonstrated better remediation potential for Cr than Cd. However, remediation potentials of AHB were significantly influenced by the presence of vetiver. In fact, AHB and vetiver complemented each other in remediating the HMs from the contaminated soils, and simultaneously enhanced the nutrient availability. Some studies suggested that BC derived from the sugarcane bagasse can remediate Cr and Cd up to 85 and 67% with an application rate of 1.5% or 30 t ha^{-1} (Bashir et al., 2018). For HM remediation, BC undergoes different mechanism like catalysis, precipitation, electrostatic adsorption, formation of metal ion complexes, sorption and competition between elements (Yadav and Karak, 2019).

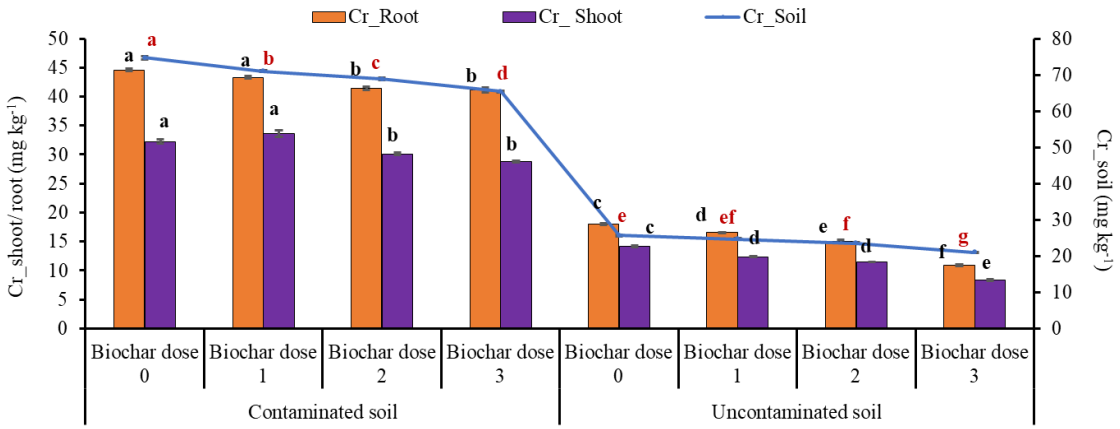

Fig. 6.3. Cr concentration in the soil, root and shoot of the vetiver under different doses of AHB.

Note: Bar showing mean values (± SE) with the similar letter are not significantly different at p > 0.05 level following DMRT; LSD (Soil =1.617; Root=1.450; Shoot=1.490).

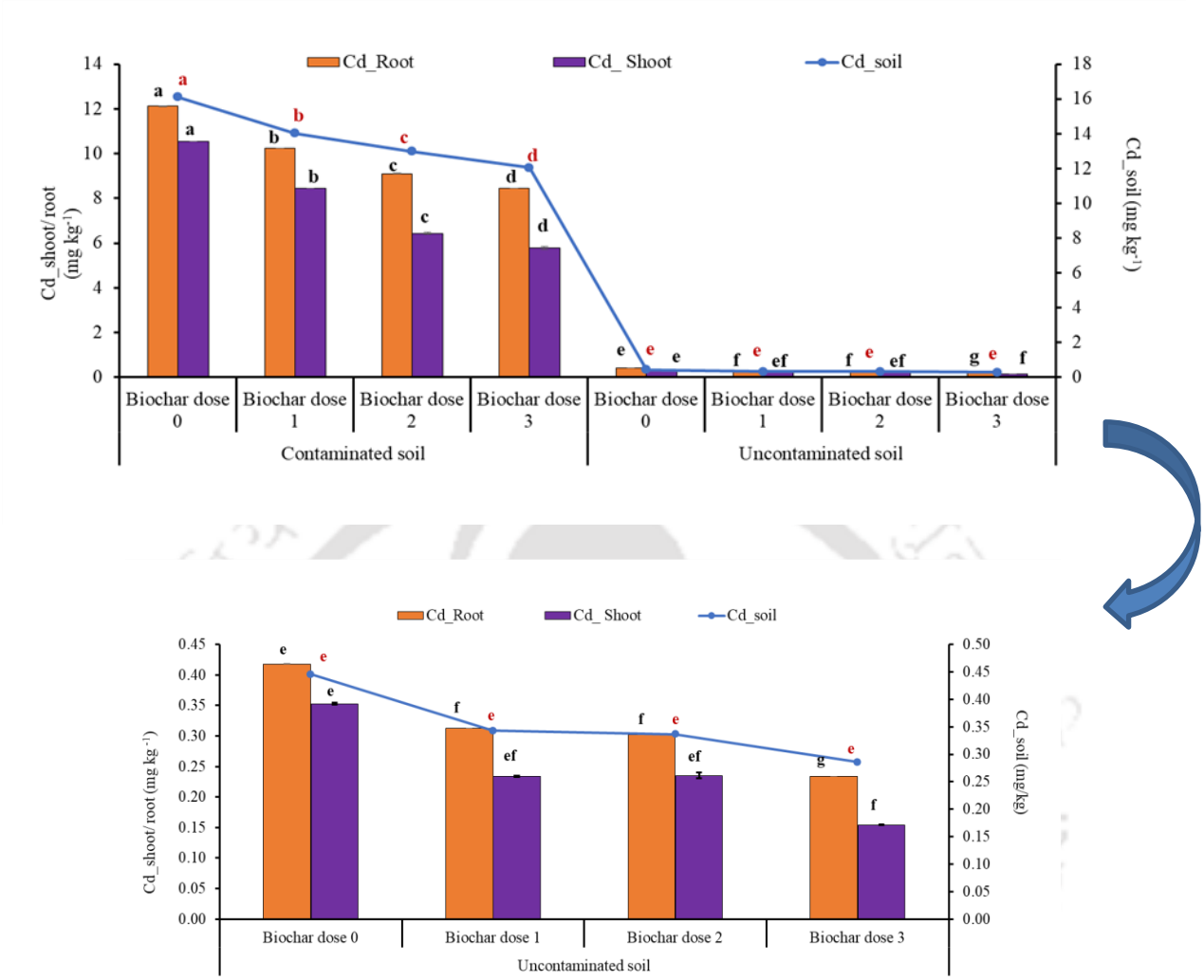

Fig. 6.4. Cd concentration in soil, root and shoot of the vetiver under different doses of AHB.

Note: Bar showing mean values (± SE) with the similar letter are not significantly different at p > 0.05 level following DMRT; LSD (Soil =0.618; Root=0.046; Shoot=0.161).

6.3.2. Bio-concentration factor (BCF) and translocation factor (TF) of Cr

The TF values observed in all of the treatments were smaller than 1, coupled with slight variation among different AHB doses. In contaminated soil, the lowest TF value (0.70) was observed with BC dose of 15 t ha^{-1}, suggesting higher remediation of Cr. Similarly, in uncontaminated soil, the lowest TF (0.75) was observed with an AHB dose of 5 t ha^{-1} (Fig. 6.5). It further indicated that in

contaminated soils, the AHB dose of 15 t ha^{-1} is more effective, whereas, in uncontaminated soils, the AHB dose of 5 t ha^{-1} would be optimal for applications. Further, TF values < 1 suggest that considerable amounts of Cr were absorbed by the roots, restricting its translocation to the shoot. AHB facilitated nutrient adsorption by vetiver, and thereby increased the root growth of vetiver. Significant reduction in TF values under AHB treatments could be due to the lower availability of metals in soil, as a result of absorption by the roots and increased translocation to the shoot. The findings of this study are in agreement with previous studies on iron ore mining which reported higher Fe, Al, Zn, Cr and Ni contents in roots than in shoot of vetiver grown in contaminated soil with less than 1 TF value (Banerjee et al., 2019).

Specialized features of vetiver grass such as fibrous root system, narrow and waxy leaves are also helpful in its metal tolerant behaviour. These features also reduce the evapotranspiration rate, resulting in restricted transport of metals to the shoot through the xylem (Boonyapookana et al., 2005). The lowest TF value suggests that Cr accumulated in the underground parts of vetiver. AHB can sequester Cr in the soil, prevent the roots from absorbing Cr, but it does not affect Cr transportation in the plant. The TF values are widely affected by the antagonistic and synergetic behaviour of different metals, which ultimately affect the metal uptake and distribution (Gautam and Agrawal, 2017).

Bio-concentration factor (BCF) is a quantitative factor representing the transfer of available metals from soil to different plant parts. A plant with a BCF value > 1 indicates its efficiency in taking up higher metal content from the soil, while a BCF value < 1 is a metal excluder (Yanqun et al., 2005). In the present study, BCF >1 suggested that vetiver under BC treatments have higher metal uptake efficiency under all BC doses. But, in uncontaminated soil, high AHB doses (15 t ha^{-1}) had lower BCF (< 1), suggesting metal excluding characteristics of vetiver plant. This might be

due to the higher dose of AHB, which stabilizes the available HMs within the soil. Low BCF values for studied metals in the plant, might also be attributed to a decrease in bioavailability of metal content, with an increase in soil pH (Castaldi et al., 2009).

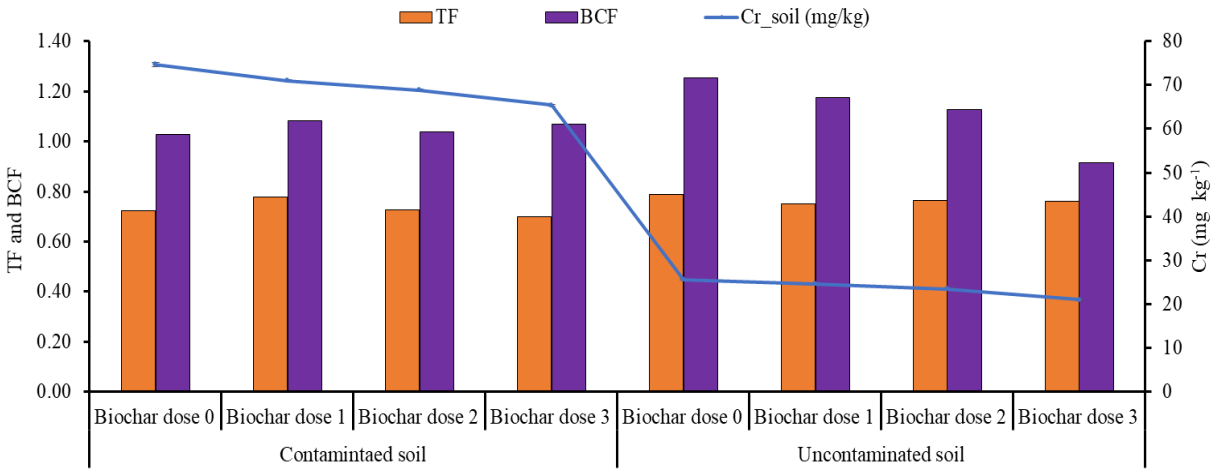

Fig. 6.5. TF and BCF of Cr in presence of vetiver and different AHB doses.

6.3.3. Bio-concentration factor (BCF) and translocation factor (TF) of Cd

Bio-concentration factor (BCF) and translocation factor (TF) are two valuable parameters for studying the metal accumulation and distribution within plant parts. The ability to translocate metals from root to shoot was assessed using TF, expressed as the [Metal] shoot/ [Metal] root ratio. BCF measures the potential of the plants to accumulate the HMs in their different parts, with respect to the metal concentrations present in the soil (Branquinho et al., 2007). TF measures the plant's potential to translocate heavy metals from roots to aerial shoots.

In contaminated and uncontaminated soil, the lowest TF values of 0.68 and 0.66 were observed with a BC dose of 15 t ha^{-1}, suggesting higher remediation of Cd along with increased BC dose. It further indicated that in Cd contaminated soil, the BC dose of 15 t ha^{-1} is more efficient in bioremediation (Fig. 6.6). TF values < 1 suggests that considerable amounts of Cd were absorbed

by the roots, restricting its translocation in the shoot. This is an outcome of increased vetiver root growth facilitated by BC enhanced nutrient adsorption

Earlier studies reported similar results for Cd accumulation in plant roots (Roongtanakiat and Chairoj, 2001). The restriction of metal translocation from root to shoot in *V. zizanioides* might be one of its intrinsic metal tolerance mechanisms. Another phytoremediation strategy is the attachment of HM cations to the negatively charged cell wall of the plant roots. Cd a transition metal, is highly toxic to biological systems, thus as reported in the present study, Cd addition in the food chain might have a disastrous effect on human health. The accumulation of absorbed metals (Cd) in plant tissues does not inflict any significant adverse impact on plant metabolism and productivity. The principal amount is retained in the roots, and only a fraction goes to the shoots. Such a restricted translocation of metals into shoots and confinement of a significant amount in roots, as observed in the present study on vetiver, is considered ideal for phytoremediation, to stabilize degraded and contaminated soils. BCF >1 suggested that vetiver has higher metal uptake efficiency under all BC doses. This implies that Cd is absorbed from the soil into the plant at a higher rate. Also, the BCF reported was comparatively lower (1.18) in the high BC doses of 15 t ha^{-1} suggesting that vetiver showed a slight shift towards excluder behaviour under higher BC dosage. BC could lead to soil alkalization, making HMs less bioavailable in the soil (Bian et al., 2014). Specialized features of vetiver grass such as fibrous root system and long, narrow and waxy leaves are also aid its metal tolerant behaviour. Such specialized features of vetiver reduce evapotranspiration rate, resulting in restricted transport of metals to shoot through xylem (Boonyapookana et al., 2005).

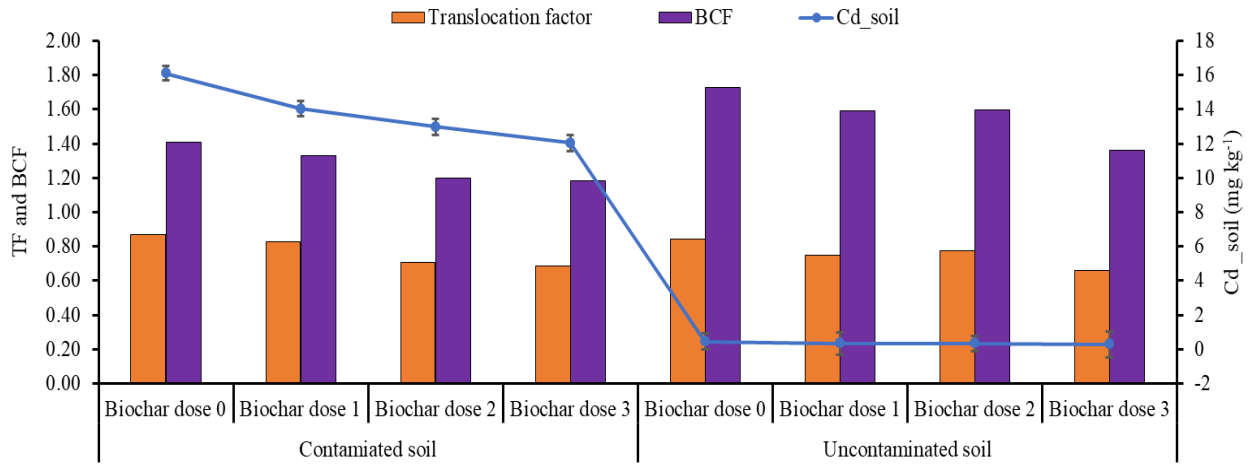

Fig. 6.6. TF and BCF of Cd in presence of vetiver and different AHB doses.

6.4. Conclusion

To evaluate the HMs remediation potential of AHB, a pot experiment was carried out using vetiver. Vetiver (*C. zizanioides* L.), is an aromatic, perennial and C4 plant, that prevents soil erosion, remediates HMs and tolerates a diverse pH range. Based on metal TF and BCF, vetiver is found to act as a potential metal tolerant plant, effective in phytostabilization of Cd and Cr in roots. Further, the BCF depicted the HM accumulating ability of vetiver under different AHB doses. TF showed that limited uptake of Cd and Cr by the shoot, lowers the risk of bio magnifications inside the plant body. It was also observed that under higher AHB doses (15 t ha^{-1}), vetiver works as Cr excluder, rather than an absorber, in uncontaminated soil. This suggests that excluders may allocate more energy to roots than shoots, resulting dense root system in uncontaminated soil. Combined application of AHB in conjunction with vetiver, facilitated HM immobilization, particularly in the roots as compared to the shoot.

References

Akhzari, D., Alipoor, N., 2019. Studying the quantitative and qualitative characteristics of vetiver grass (*Chrysopogon zizanioides* L.) under different compost and zeolite. Environ. Resour. Res. 7, 137–146.

Bahraminia, M., Zarei, M., Ronaghi, A., Ghasemi-, R., 2016. Effectiveness of arbuscular mycorrhizal fungi in phytoremediation of lead- contaminated soil by vetiver grass. Int. J. Phytoremediation 18, 730–737.

Banerjee, R., Goswami, P., Lavania, S., Mukherjee, A., Lavania, U.C., 2019. Vetiver grass is a potential candidate for phytoremediation of iron ore mine spoil dumps. Ecol. Eng. 132, 120-136.

Bashir, S., Zhu, J., Fu, Q., Hu, H., 2018. Cadmium mobility, uptake and anti-oxidative response of water spinach (*Ipomoea aquatic*) under rice straw biochar, zeolite and rock phosphate as amendments. Chemosphere 194, 579–587.

Bian, R., Joseph, S., Cui, L., Pan, G., Li, L., Liu, X., Zhang, A., Rutlidge, H., Wong, S., Chia, C., Marjo, C., 2014. A three-year experiment confirms continuous immobilization of cadmium and lead in contaminated paddy field with biochar amendment. J. Hazard. Mater. 272, 121-128.

Boonyapookana, B., Parkpian, P., Techapinyawat, S., DeLaune, R.D., Jugsujinda, A., 2005. Phytoaccumulation of lead by sunflower (*Helianthus annuus*), tobacco (*Nicotiana tabacum*), and vetiver (*Vetiveria zizanioides*). J. Environ. Sci. Health 40, 117-137.

Branquinho, C., Serrano, H.C., Pinto, M.J., Martins-Louçao, M.A., 2007. Revisiting the plant hyperaccumulation criteria to rare plants and earth abundant elements. Environ. Pollut. 146, 437-443.

CCME (Canadian Council of Ministers of the Environment), 2007. Canadian Soil Quality Guidelines for the Protection of Environmental and Human Health: Summary Tables. In: Canadian Environmental Quality Guidelines, 1999. Canadian Council of Ministers of the Environment, Winnipeg. Updated September. 2007. http://esdat.net/Environmental%20Standards/Canada/SOIL/rev_soil_summary_tbl_7.0_e.pdf. (Accessed 13 October 2019).

Castaldi, P., Melis, P., Silvetti, M., Deiana, P., Garau, G., 2009. Influence of pea and wheat growth on Pb, Cd, and Zn mobility and soil biological status in a polluted amended soil. Geoderma, 151, 241-248.

Gautam, M., Agrawal, M., 2017. Phytoremediation of metals using vetiver (*Chrysopogon zizanioides* (L.) Roberty) grown under different levels of red mud in sludge amended soil. J. Geochem. Explor. 182, 218-227.

Grass, V., Masinire, F.F., Adenuga, D.O., Tichapondwa, S.M., Evans, M.N., 2020. Remediation of Chromium (VI) Containing Wastewater Using *Chrysopogon zizanioides* (Vetiver Grass) 1–7. https://doi.org/10.3303/CET2079065

Lindsay, W.L., Norvell, W.A. 1978. Development of a DTPA soil for Zinc, Iron, Manganese, and Copper. Soil Sci Soc Am J, 42, 421-428.

Park, S., K.S. Kim, J.T. Kim, D. Kang, K. Sung. 2011. Effects of humic acid on phytodegradation of petroleum hydrocarbons in soil simultaneously contaminated with heavy metals. J. Env. Sci., 23,2034-2041

Qiu, Y., Zhang, Q., Gao, B., Li, M., Fan, Z., Sang, W., Hao, H., Wei, X., 2020. Removal mechanisms of Cr (VI) and Cr (III) by biochar supported nanosized zero-valent iron: Synergy of adsorption, reduction and transformation. Environ. Pollut. 265, 115018.

Qihang, W., Wang, S., Thangavel, P., Qingfei, L., Zheng, H., Jun, B., Qui, R., 2011. Phytostabilization of *Jatropha curcas* L. in polymetalic acid mine tailings. Int. J. Phytoremediation 13, 788–804.

Roongtanakiat, N., Chairoj, P., 2001. Vetiver Grass for the Remediation of Soil Contaminated with Heavy Metals. Kasetsart J. (Nat. Sci.) 35, 433 – 440.

Topcuoglu, B., 2012, September. The influence of humic acids on the metal bioavailability and phytoextraction efficiency in long-term sludge applied soil. In Conference on international research on food security, natural resource management and rural development (pp. 19-21).

Truong, P., 1999. Vetiver grass technology for mine rehabilitation. Bangkok: Office of the Royal Development Projects Board.

Vargas, C., Pérez-esteban, J., Masaguer, A., Moliner, A., Vargas, C., Moliner, A., 2016. Phytoremediation of Cu and Zn by vetiver grass in mine soils amended with humic acids. Environ. Sci. Pollut. Res. 13521–13530.

Yadav, N.N. V, Karak, D.M.T., 2019. Biochar amendment alters the relation between the Pb distribution and biological activities in soil. Int. J. Environ. Sci. Technol. https://doi.org/10.1007/s13762-019-02257-y

Yang, B., Shu, W.S., Ye, Z.H., Lan, C.Y., Wong, M.H., 2003. Growth and metal accumulation in vetiver and two Sesbania species on lead / zinc mine tailings. Chemosphere 52, 1593–1600.

Yanqun, Z., Yuan, L., Jianjun, C., Haiyan, C., Li, Q., Schvartz, C., 2005. Hyperaccumulation of Pb, Zn and Cd in herbaceous grown on lead–zinc mining area in Yunnan, China. Environ. Int. 31, 755-762.

Zhang, X., Gao, B., Xia, H., 2014. Effect of cadmium on growth , photosynthesis , mineral nutrition and metal accumulation of bana grass and vetiver grass. Ecotoxicol. Environ. Saf. 106, 102–108.

CHAPTER 7

Nutrient dynamics in plant and soil

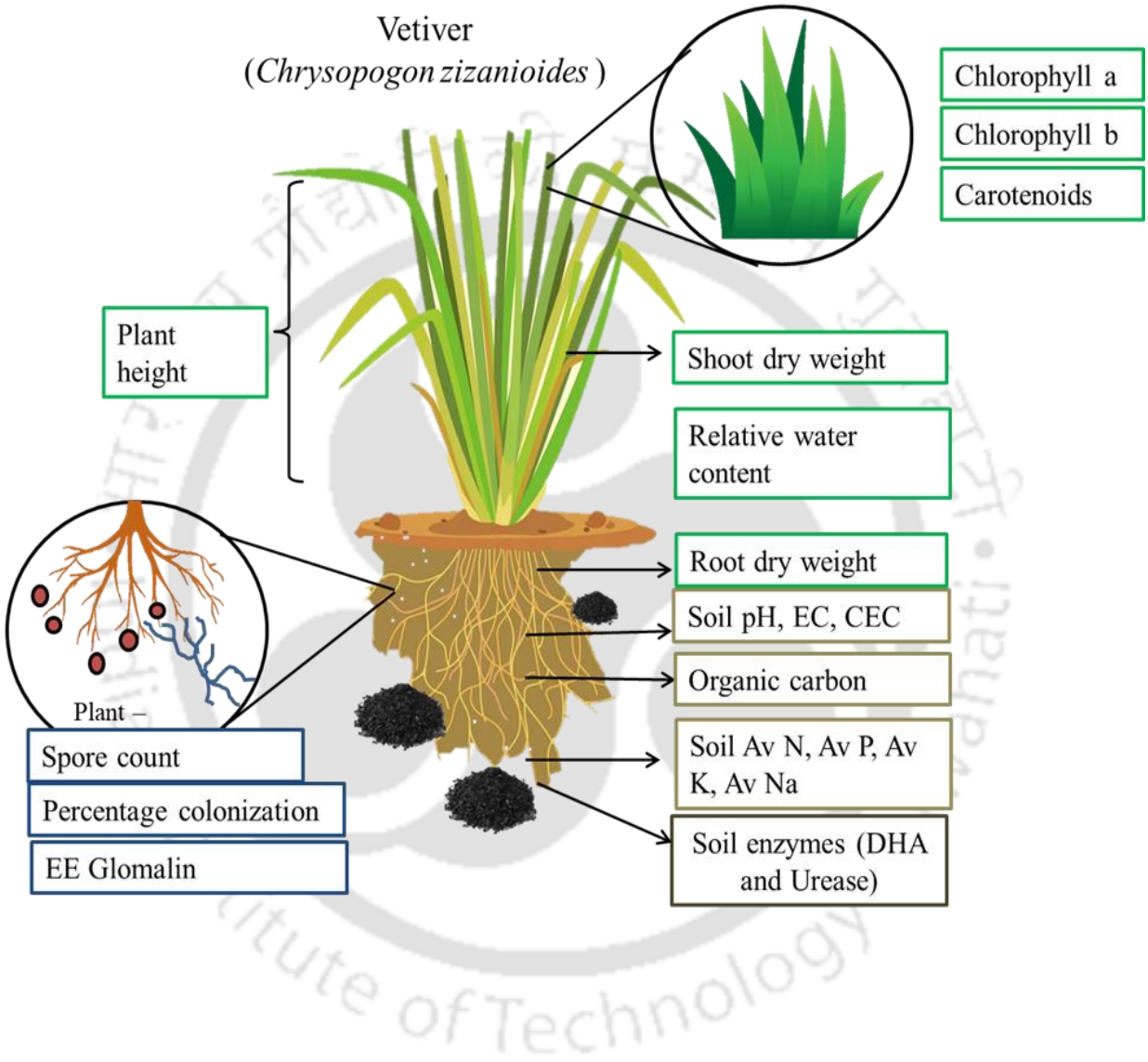

"The present chapter deals with application of the biochar prepared from the areca nut husk and its effect on soil, plant and arbuscular mycorrhizal fungi (AMF). It also explores the nutrient dynamics in different treatments of AHB."

7. Nutrient dynamics in plant and soil

7.1. Introduction

BC obtained through different feedstocks and its amendment in degraded soil has worldwide acceptance as a potential option to improve soil fertility and its ecosystem functioning (Yulin et al., 2020). BC has multifaceted benefits, primarily improving the pH, CEC, soil buffering, porosity, water retention capacity, and bulk density of contaminated soil (Yuan et al., 2019). The application of BC helps in regulating various biogeochemical processes in the soil, including the carbon (C), phosphorus (P), and nitrogen (N) cycle. BC assists in stabilizing the OC, and in converting organic nitrogen into ammonium and nitrate, which the plant can directly absorb. It has been reported that BC can potentially help sequester about > 12% of the greenhouse gases (CO_2, CH_4 and N_2O) emanating from different anthropogenic activities (Vithanage et al., 2015). In addition, BC prepared at high temperature is reported to have a surface adsorption mechanism, for nutrient enhancement, whereas the BC prepared at low-temperature enhances partitioning of residual organic matter.

Apart from various physico-chemical parameters, biochemical parameters which are sensitive and greatly influenced by alteration in management practices, act as a quick diagnostic tool for testing soil quality (Tang et al., 2020). One of our recent studies revealed that soil enzyme activities (SEAs) are transitionally impacted by the type of waste that has contaminated the soil (Datta et al., 2021) (Fig. 7.1). SEAs reflect prime microbial reactions involved in soil nutrient cycling, and determine the biogeochemical effect of soil amendments; particularly BC, on nutrient dynamics and plant growth. In the present study, we have investigated two major soil enzymes; soil dehydrogenase (SDH) and urease (UR).

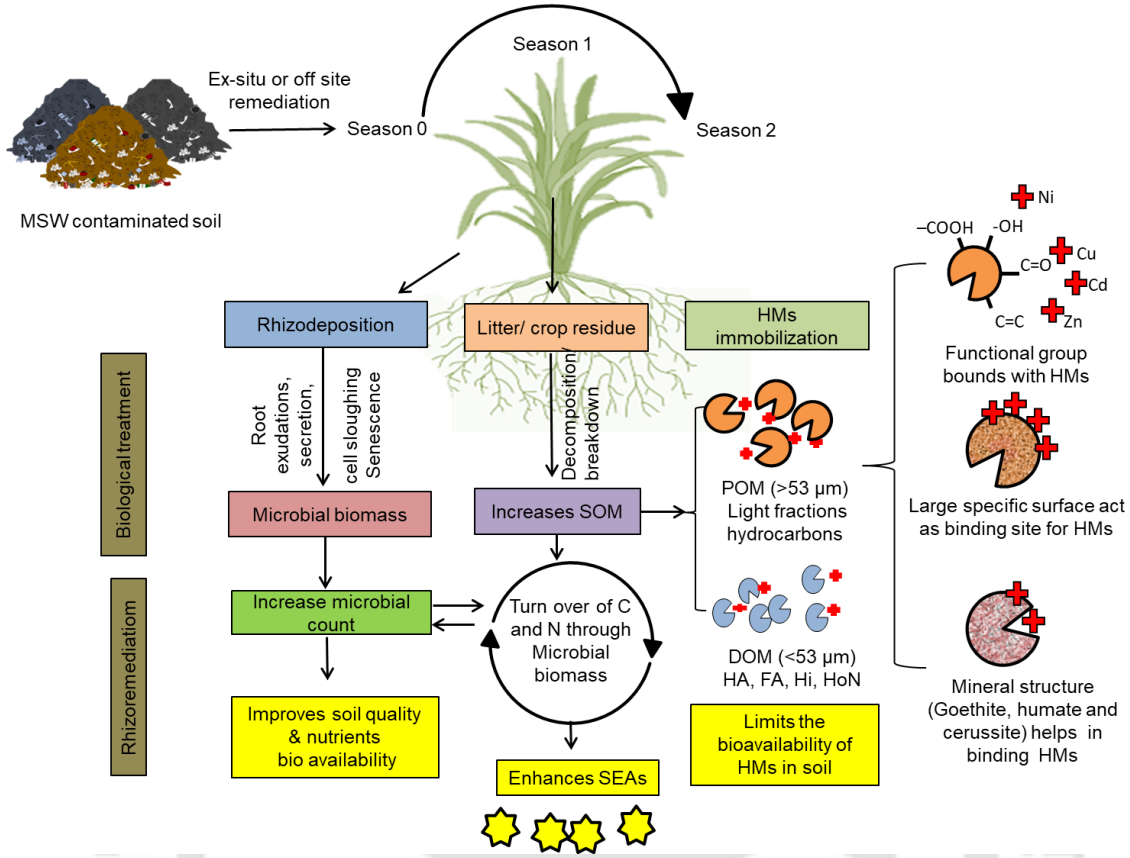

Fig. 7.1. Effect of the organic matter on SEAs in soil contaminated by MSW.

BC application in the soil directly or indirectly affects the N cycle, induces a reduction in N_2O emission, and promotes denitrifying rhizobia such as Bradyrhizobiaceae and Hyphomicrobiaceae (Anderson et al., 2011). With its large surface area, BC offers an increased reactive surface for N and P attachment in soil microbial biomass, which modulates N and P bioavailability in soil. Concurrently, functional groups attached to the surface of BC participate in the adsorption process of NO_3 (Huang et al., 2019). BC is also known to assist the regulation of mineralization, N_2 fixation, nitrification, ammonia volatilization, increasing NH_4 storage by enhancing CEC and denitrification (Gul and Whalen, 2016).

In contrast, a study suggested that the effect of BC is negligible on the available N in soil and plant tissue (Biederman and Harpole, 2013). The role of BC in the soil P cycle is regulated by biochar-mediated microbial enrichment, consequently impacting P use efficiency (PUE) of plants (Anderson et al., 2011). BC is used as a liming agent in acidic soil and renders the bound P bioavailable (Cui et al., 2011). Further, concomitant BC and P availability would be more beneficial in acidic soils of low latitudes, where agriculture is limited by P availability (Steiner et al., 2008). Leaf biochar had a significant effect on the P dynamics in the high altitude forests of *Cunninghamia lanceolata* (Chinese fir), mediated by P-solubilizing bacteria like, *Paraburkholderia*, *Planctomyces* sp., *Sphingomonas* sp. and *Singulisphaera* sp., which can indirectly improve P availability in soil (Zhou et al., 2020).

7.2 Materials and methods

7.2.1. Plant height, biomass and photosynthetic pigments

All the soil physico-chemical parameters were investigated using standard protocols discussed and elaborated in Chapter 3. Plant height was measured using the standard cm scale. To assess the effect of BC on plant growth, biomass of vetiver plants was determined. After 90 days of cultivation, the above-ground part and roots of vetiver were collected separately, and washed thoroughly with ultrapure water. The plant parts were then dried in an oven (70 °C) till constant weight was attained, and cooled to room temperature to determine the dry biomass as shoot dry weight (SDW) and root dry weight (RDW). Relative water content percentage (RWC %) was measured following the method of Chen et al. (2009) using the following equation as

$$RWC\ \% = [(FW-DW)/FW] \times 100 \qquad (1)$$

Where, FW=fresh weight of the sample (g); DW=dry weight of the sample (g).

The leaf samples of individual treatment from each plot were taken to determine chlorophyll a (Chl a), chlorophyll b (Chl b) and carotenoids before harvest. According to Arnon's (1949) method, chlorophyll and carotenoid extracts were determined by spectrophotometer at 663 and 645, 470 nm (D663, D645, D470) wavelength, respectively:

$$\text{Chla (mg g}^{-1}\text{ FW)} = (12.7 \times D663) - (2.69 \times D645) \quad (2)$$

$$\text{Chlb (mg g}^{-1}\text{ FW)} = (22.9 \times D645) - (4.68 \times D663) \quad (3)$$

$$\text{Carotenoids (mg g}^{-1}\text{ FW)} = (1000 \times D470 - 1.9 \times \text{chla} - 63.14 \times \text{chlb} / 214) \quad (4)$$

7.2.2. *Mycorrhizal Spore density, percentage colonization, glomalin and SEAs*

Various techniques were used to recover AMF propagules from the soil. The most basic of these is wet sieving and decanting (Gerdemann and Nicolson, 1963), to remove the clay and sand fractions of the soil while retaining spores and other similar-sized soil and organic matter particles on sieves of various sizes. The sieve sizes used during the wet sieving were 15, 30, 60, 100, 200 and 400 BSS.

Spore density was calculated using the following formula:

$$\text{Total spores/m L (TS)} = n / 20 \times 100$$

$$\text{Spores/ g= TS/ amount of soil (g)}$$

Where, n=Number of spores observed in 20 mL of suspension out of 100 mL of sieved solution. AMF colonization was assessed using Biermann and Linderman (1981) method (frequency distribution method), in which the colonization was assessed as proportion of root length colonized by mycorrhizal fungi using stereo microscope. Clearing was carried out using KOH, followed by bleaching with hydrogen peroxide. The roots were stained by trypan blue, followed by mounting

on slides, using lactoglycerol solution. The percentage of colonization was calculated by the following formula:

N= % of segments lengths colonized (0, 10,….100) × Frequency (no. of segment colonized)

Computed % of root length colonized=N/ Total number of segments under observation

Computed % of root length colonized = N/ Total number of segments under observation

Glomalin was extracted from soil following the standard method (Wright and Upadhyaya, 1996) with some modifications. Briefly, 1 g of soil sample was autoclaved with 8 mL of 50 mM sodium citrate (pH 8), at 121 °C for 60 minutes, and centrifuged at 15,000 rpm for 15 minutes. The supernatants were collected in a fresh Teflon tube. To ensure complete recovery of glomalin, each sample was repeatedly autoclaved for 60 min at 121 °C until the typical reddish-brown colour disappeared from the supernatant. A total of 8 extraction cycles were required for the complete recovery of GRSP from the soil. All extracts from each soil sample were then pooled and stored at ~4 °C until quantification. The supernatants were purified using 20% trichloroacetic acid (TCA). The quantification was carried out using the Bradford protein assay, using bovine serum albumin (BSA) as a reference standard. The extracts were diluted with phosphate-buffered saline, followed by the addition of Bio-Rad Bradford dye (Coomassie brilliant blue G-250). Absorbance was measured at 595 nm, using a spectrophotometer (Genesys 10S UV-Vis Spectrophotometer), and the concentration was calculated to mg GRSP g^{-1} soil.

SEAs like DHA activity was calculated using triphenyl-tetrazolium chloride (TTC) as a substrate, and expressed as µg TPF g^{-1} dry soil (Casida et al., 1964). Likewise, UR activity was determined according to Klose and Tabatabai (2000), as mg $NH_4^+ g^{-1}$ dry soil

7.3. Results and discussion

7.3.1. Impact of AHB on soil quality

The pronounced effect of AHB on soil pH might be due to the functional groups and concentration of alkaline salts like Ca^{2+}, Mg^{2+}, and K^{+}, present on its surface (Kumar et al., 2013). Higher AHB doses corresponded to the higher pH of the soil. The pH in the soil ranged from 6.93 ± 0.02 to 7.67 ± 0.02. The salinity effect is negligible in all treatments as it was less than the salinity threshold of 8 mS cm^{-1} (Fig. 7.2). EC is an indication of the total concentration of ionized constituents; higher AHB doses elicited higher EC, which might be attributed to the higher BC doses. In all soil treatments, the EC ranged from 0.56 ± 0.01 to 1.59 ± 0.20. The increased EC with the increasing BC doses, might be attributed to the Al and Cu present in AHB. EC depends on the amount and kind of clay, and organic matter present in the soil. Results showed that the AHB with a dose of 15 t ha^{-1} displayed higher CEC in both contaminated and uncontaminated soils, as compared to soils without AHB amendment. Over time, in soil, oxidation of BC results in the release of negative charge ions, thereby increasing CEC.

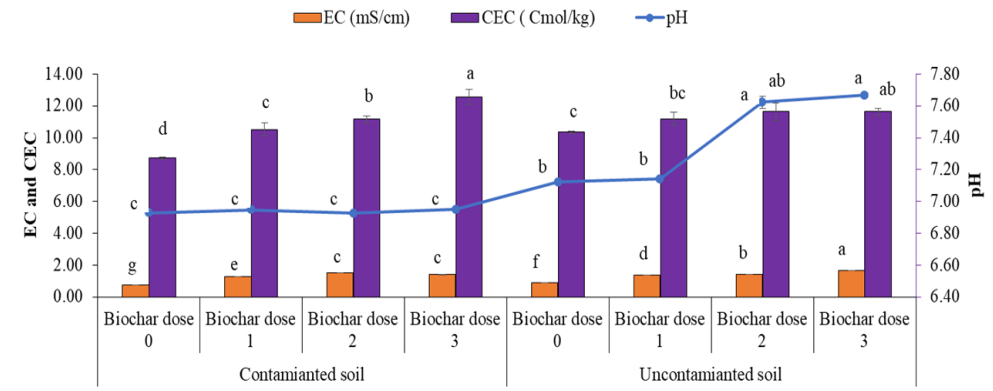

Fig. 7.2. pH, EC and CEC of the soil under different AHB doses.

Note: Bar showing mean values (± SE) with the similar letter are not significantly different at p > 0.05 level following DMRT; LSD (pH =0.04; EC=0.008; CEC=1.01).

The increase in OC might be due to high recalcitrant C content in AHB. Recent research suggest that BC obtained at lower temperature has lower total carbon (< 30%), compared to BC prepared at high temperature, which further enhances plant productivity (Dai et al., 2020). In all treatments, the OC values ranged from 24.41 ± 0.53 to 33.25 ± 0.53 (Fig. 7.3). In the pedosphere, SEAs are closely associated with soil properties, soil type, and environmental conditions. Several studies indicated that BC produced at higher temperature with very high BC load decrease C cycling enzymatic activities in the soil (Zhang et al., 2018a; Zhang et al., 2018b). This decrease might be attributed to the higher pH and aromatic C content of the BC produced at the higher temperature. Therefore, in the present study, we have used BC prepared at lower temperature for the soil applications. Subsequently, DHA and UR activities were found to be higher under 15 t ha^{-1} of BC dose. The increased SEAs could be attributed to the potential co-metabolism and the mineralization of OC in the presence of BC (Zhang et al., 2019) (Fig. 7.3). The present study also revealed that BC applications at 10–15 t ha^{-1} would increase the nutrient content in both contaminated, and uncontaminated soil (Fig. 7.4).

Results indicated that AHB enhanced the Av N content in the soil, ranging from 86.27 ± 0.64 to 194.12 ± 1.17 mg kg^{-1} (7.4). In soil, AHB works more as a nitrogen enhancer, than as an N supplier. It improves the nutrient binding ability, which depends on pH, surface area, and ion exchange capacities. The sorption and desorption of nutrients in BC are prime mechanisms that affect the N availability. Changes in soil mineralizable substrates and alteration in the process of nitrification and denitrification are the other mechanisms involved in the mineralization of N. (Dai et al., 2020). The Av P content in all treatments ranged from 86.75 ± 0.59 to 99.61 ± 2.40 mg kg^{-1} (Fig. 7.4.). Due to the liming effect and enhancement in soil physico-chemical properties, the N and P cycling enzyme activities improved significantly (Zhang et al., 2019). Moreover, a study

also revealed that BC with an application rate of 10 and 20 t ha^{-1}, certainly altered the soil phospholipid fatty acids (PLFA) concentrations, thereby altering the microbial community (Mitchell et al., 2015). Likewise, in the present study, Av K and Av Na ranged from 70.70 ± 1.27 to 121.28 ± 1.80 mg kg^{-1}, and 59. 59 ± 0.41 to 140.63 ± 1.25 mg kg^{-1}, respectively (Fig. 7.4). Biochar in soil enhances the availability of the different nutrients through different mechanisms, illustrated in Fig. 7.5.

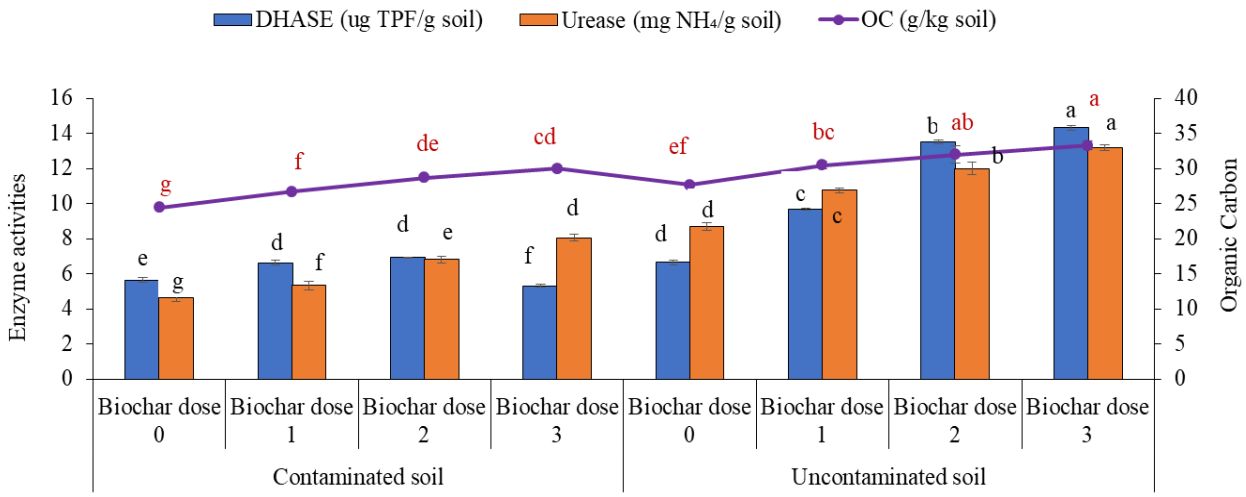

Fig. 7.3. OC, DHA and UR activities in the soil under different AHB doses.

Note: Bar showing mean values (± SE) with the similar letter are not significantly different at p > 0.05 level following DMRT; LSD (OC =1.66; DHA=0.05; CEC=0.66).

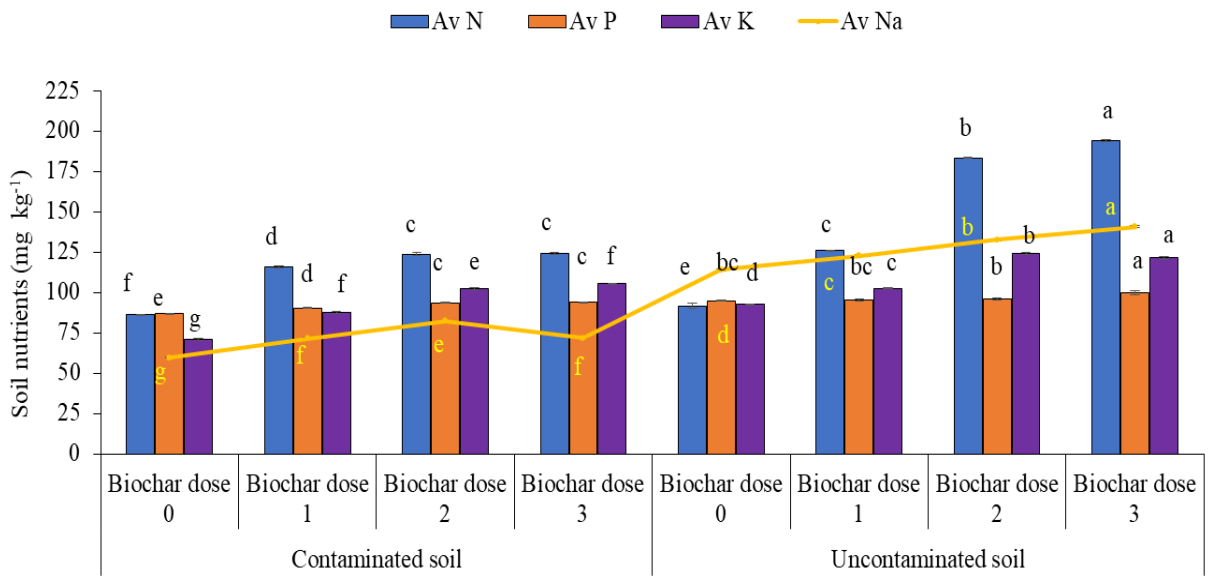

Fig. 7.4. Soil nutrient contents in the soil under different AHB doses.

Note: Bar showing mean values (± SE) with the similar letter are not significantly different at $p > 0.05$ level following DMRT; LSD (AvN =2.39; AvP=1.78; AvK=1.88; AvNa=1.53).

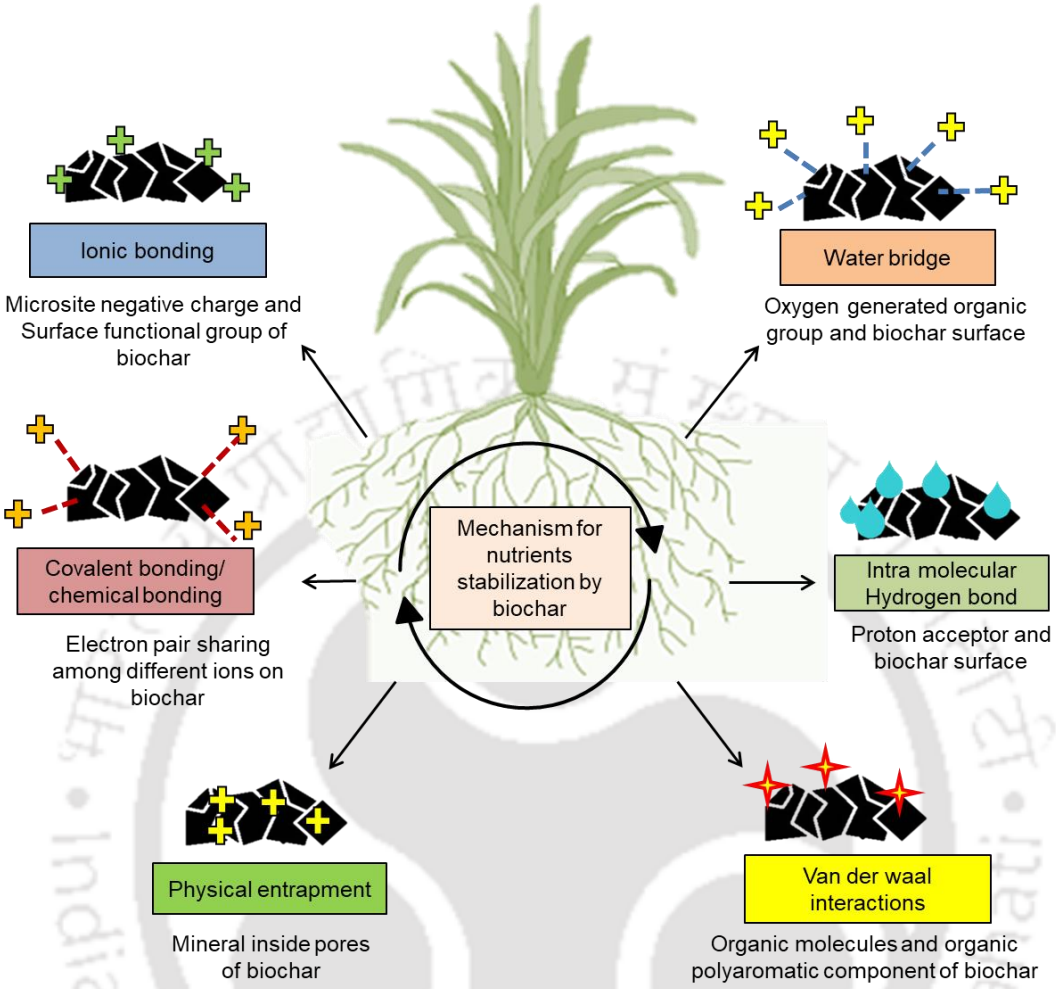

Fig. 7.5. Mechanism for nutrient stabilization by the AHB inside soil matrix.

7.3.2. Impact of AHB on vetiver plant

The photosynthetic pigments, which are chlorophyll a, chlorophyll b and total carotenoid in leaves of vetiver grown on contaminated and uncontaminated soil, are presented in Fig 7.6. After 90 days of growing in contaminated soil, the values of total chlorophyll and total carotenoid content decreased significantly. Investigating the photosynthetic pigment in the plant is a crucial parameter, reflecting photosynthetic and metabolic health; while its decline indicates physiological

stress in the plants. Results revealed that in uncontaminated soil, the effect of BC is more pronounced.

Although, comparatively lower chlorophyll content was observed in the contaminated soil due to Cd and Cr; HM generally have more severe impact on the chlorophyll and biomass of the plant. However, with the higher AHB doses, the HMs get immobilized in the soil, restricting its translocation to the shoot.

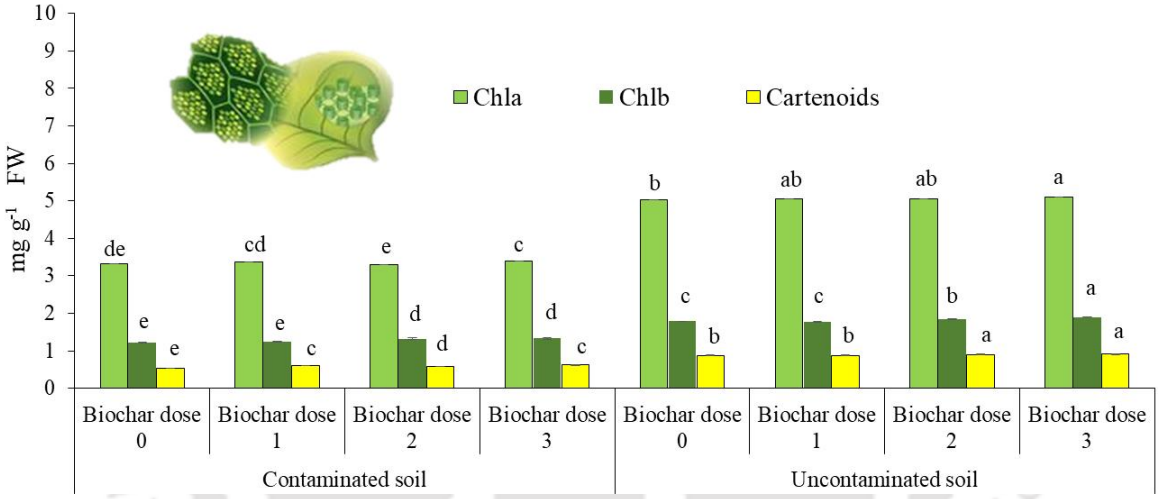

Fig. 7.6. Chlorophyll and carotenoid content in the vetiver under different AHB doses.

Note: Bar showing mean values (± SE) with the similar letter are not significantly different at $p > 0.05$ level following DMRT; LSD (Chla =0.05; Chlb=0.04; Car=0.01).

Plant biomass is the prime indicator of energy accumulation in plants. Alteration in the root to shoot biomass ratio depicts the plant strategies to allocate the resources to counter the HM stress. The RDW and SDW were comparatively higher in the BC dose of 15 t ha^{-1}. Plant biomass under AHB treatments was significantly higher than the uncontaminated soil, indicating that AHB helps in tolerance to the HMs in soil and their tissues (Chen et al., 2009). A gradual increase in RDW

was observed upto 15 t ha^{-1} of AHB treatment; whereas an insignificant change in shoot biomass was observed under a BC dose of 15 t ha^{-1}. Higher BC dose favours the biomass of vetiver, particularly, the fibrous root. The RDW of vetiver displayed highest increase in the contaminated soil, indicating vetiver grows better with a higher BC dose (15 t ha^{-1}) (Fig. 7.7). In the current study, HM pollution significantly enhanced the biomass ratio of root to shoot; this might be attributed to the higher allocation of energy to the roots for absorption of HMs and maintenance of normal functions under HMs stress, such as maintaining the soil water content (Zhang et al., 2014).

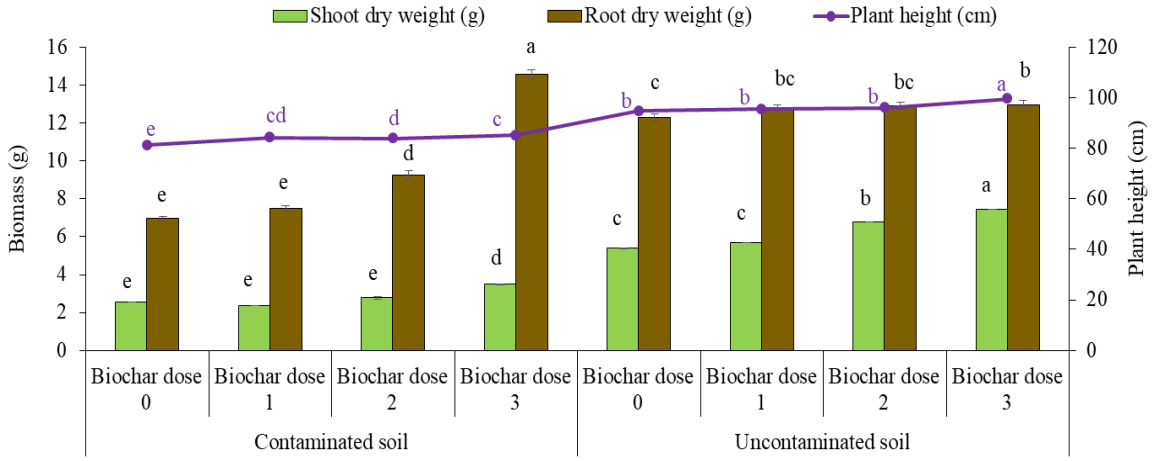

Fig. 7.7. RDW, SDW and plant height of the vetiver under different AHB doses.

Note: Bar showing mean values (± SE) with the similar letter are not significantly different at $p > 0.05$ level following DMRT; LSD (SDW =0.65; RDW=0.59; PH=1.20).

7.3.3. Impact of AHB on AMF

BC dose of 15 t ha^{-1}, in contaminated and uncontaminated soil, caused significant increase in spore density, in comparison to soil without any BC dosage; suggesting BC pores harbour habitats for

AMF spores (Fig. 7.8). Further, the specific AHB treatment of 15 tones ha^{-1}, provided suitable habitat for growth and enrichment of AMF spores, and yielded a higher AMF spore population; which was validated by the higher rate of colonization. These findings confirm that the BC acted as a refuge and ensured excellent compatibility between the roots of vetiver and AMF. It is noteworthy that BC also improves AMF colonization in inoculated roots and enhances P-uptake ability (Ra et al., 2020). In soil, AMF plays a pivotal role in soil C and N sequestration and soil aggregation.

Moreover, the present study also suggested that BC enhances the AMF colonization in vetiver roots, corroborating the results of extant studies (Vanek and Lehmann, 2015). In this study, the % colonization tended to be the highest, a AHB dose of 15 t ha^{-1}. Several researchers have also claimed that AMF mycelium consists of 20–30% of soil microbial biomass (Luo et al., 2017). Additionally, in the soil system, BC assist in forming soil macroaggregates, induced by BC interactions with the mineral present in the soil. With the increase in the AMF colonization, there is a concomitant enhancement in the glomalin content. Glomalin is the soil binding protein, and BC helps to enhance dense hyphae generation (Gujre et al., 2021a) (Fig. 7.9). Moreover, the natural adhesive qualities of glomalin related soil protein (GRSP) derived from AMF, have a strong reinforcing effect on soil aggregation, and could be used as a possible soil bioindicator. GRSP is a putative gene product of AMF produced on hyphal walls, once released into the soil following hyphal degradation, associates with stable C forms and humic acid-like compounds (Gujre et al., 2021b).

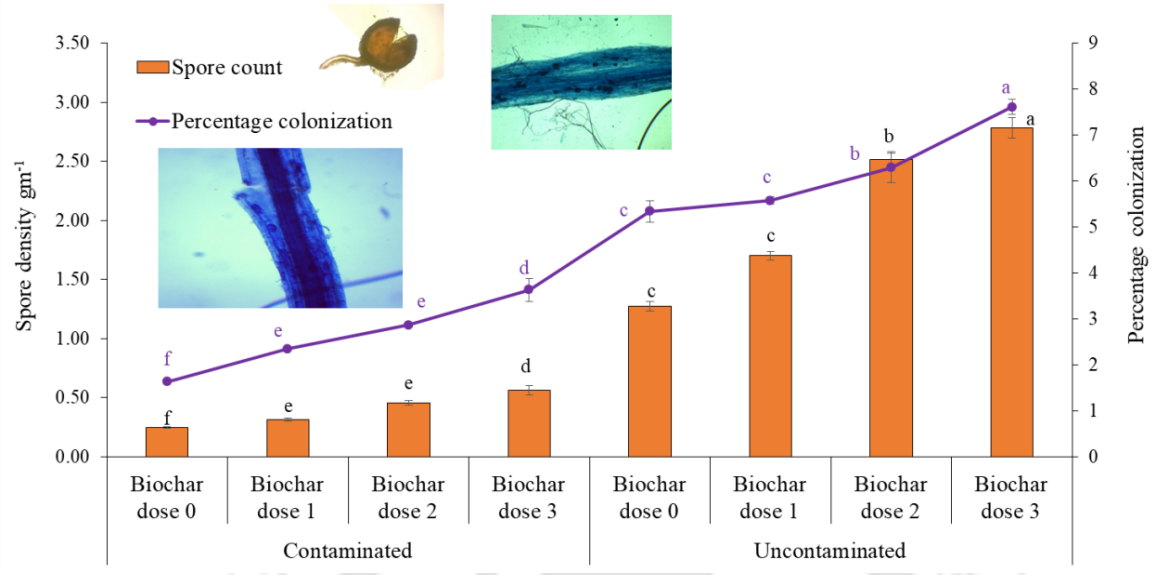

Fig. 7.8. AMF Spore density under different AHB doses.

Note: Bar showing mean values (± SE) with the similar letter are not significantly different at $p > 0.05$ level following DMRT; LSD (Spore density=0.136, Percentage colonization=0.523).

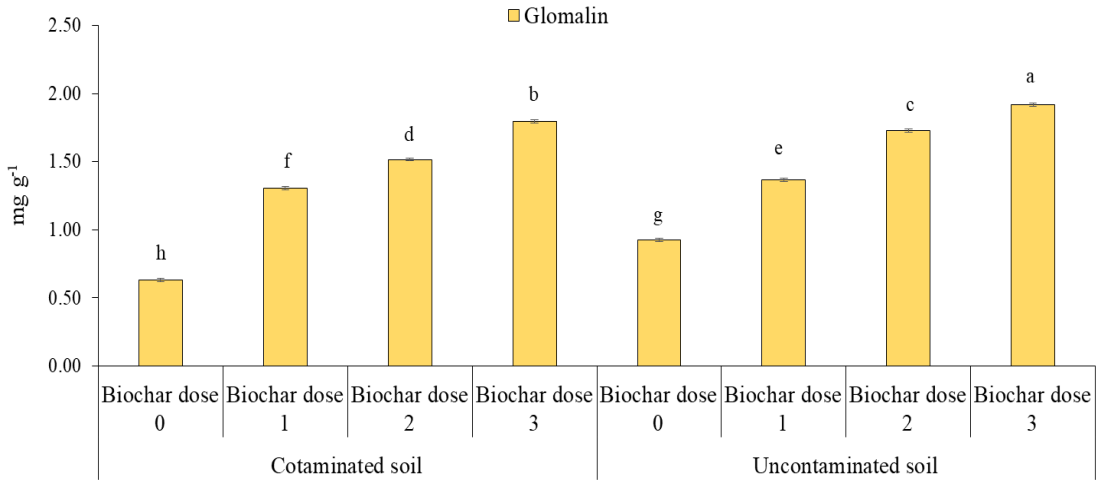

Fig. 7.9. Glomalin concentration under different AHB doses.

Note: Bar showing mean values (± SE) with the similar letter are not significantly different at $p > 0.05$ level following DMRT; LSD (Glomalin=0.039).

7.3.4. Principal component analysis of the soil and plant variables

The PCA provided two PCs with eigenvalues > 1, and together, they explained 92.77% of the variance. Soil variables were grouped into a two-component model using PC1, and PC2, that accounted for 81% and 12%. The PCA analysis showed that in PC1, OC, Av K, URE, Av N, Av P and DHA were the highest weighted variables. Under PC2, CEC and EC emerged as the highest weighted variables, with the rotated factor loadings of 0.66 and 0.45 (Fig. 7.10).

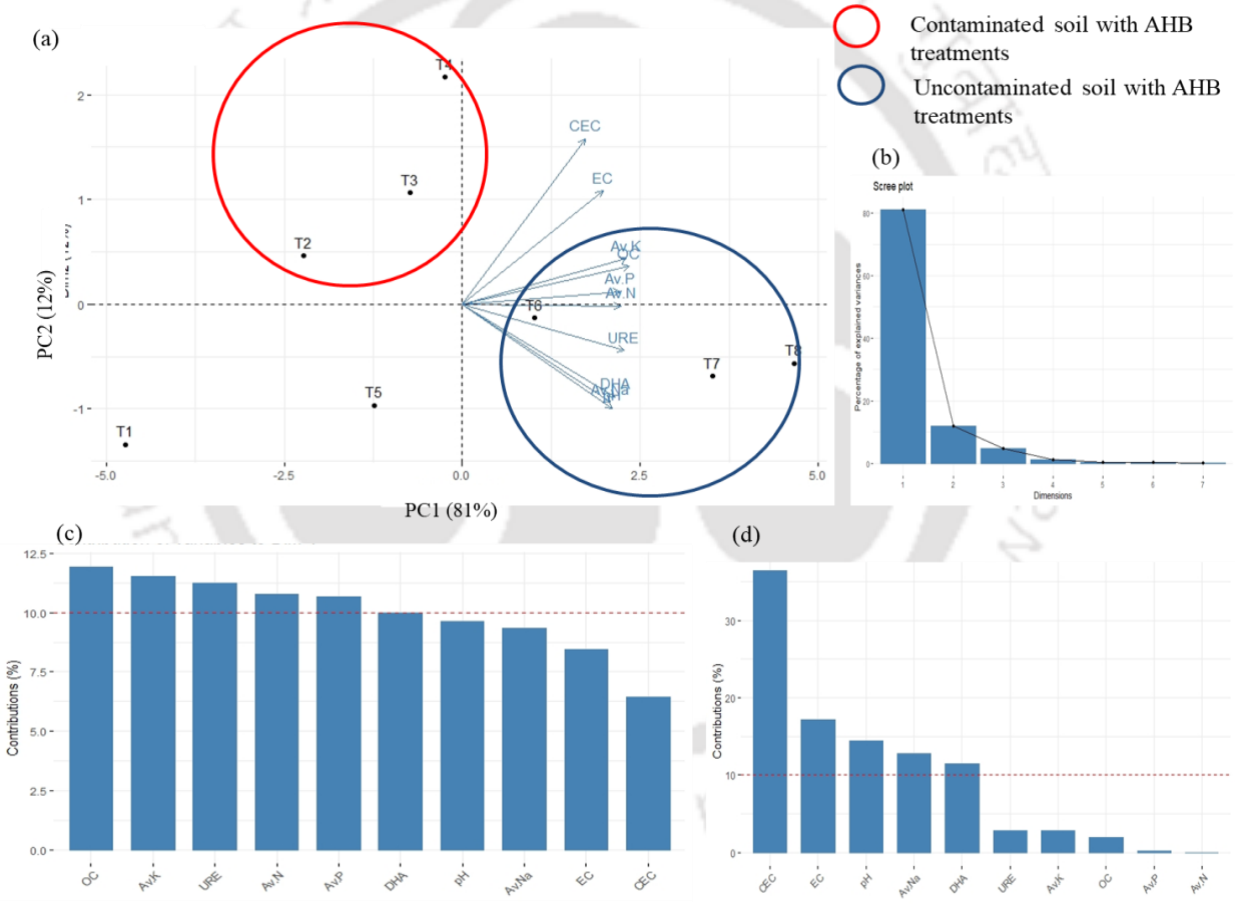

Fig. 7.10. PC analysis showing the soil variables (a) PCA biplot; (b) scree plot of the percentage variance; (c) Individual contribution of the variables in PC1; (d) Individual contribution of variables in PC2.

In the rotated component matrix, the first PC was dominated by the OC and Av K. OC in the soil might be due to the high recalcitrant C content in biochar. In soil, with time, oxidation of BC results in the release of negative charge ions, thereby increasing CEC. Further, the oxidised BC gets easily bound to the mineral matrix and facilitates adsorption of the organic compounds, through soil-biochar complex (Ogbonnaya and Semple, 2013).

PCA provided two PCs with eigenvalues > 1, and together, they explained 93.55% of the variance. Soil variables were grouped into a two-component model using PC1 and PC2 that accounted for 74.6% and 19%. The PCA analysis showed that in PC1, Chlb, SDW, PH, Car., the highest weighted variables were obtained for Chla. Under PC2, RWCR and RDW emerged as the highest variables with the rotated factor loadings of 0.98 and 0.57. In the rotated component matrix, the first PC was dominated by Chlb; the SDW which might have attributed to the potential growth of vetiver under BC treatments. The PCA biplot depicting the treatment in contaminated soil T4 (15 t ha^{-1}) worked better. In soil, increased BC doses facilitated the availability of the nutrients, and supported the growth of vetiver. Although, some studies have suggested that BC could significantly reduce the mobility and bioavailability of the HMs (Yang et al., 2016) (Fig. 7.11).

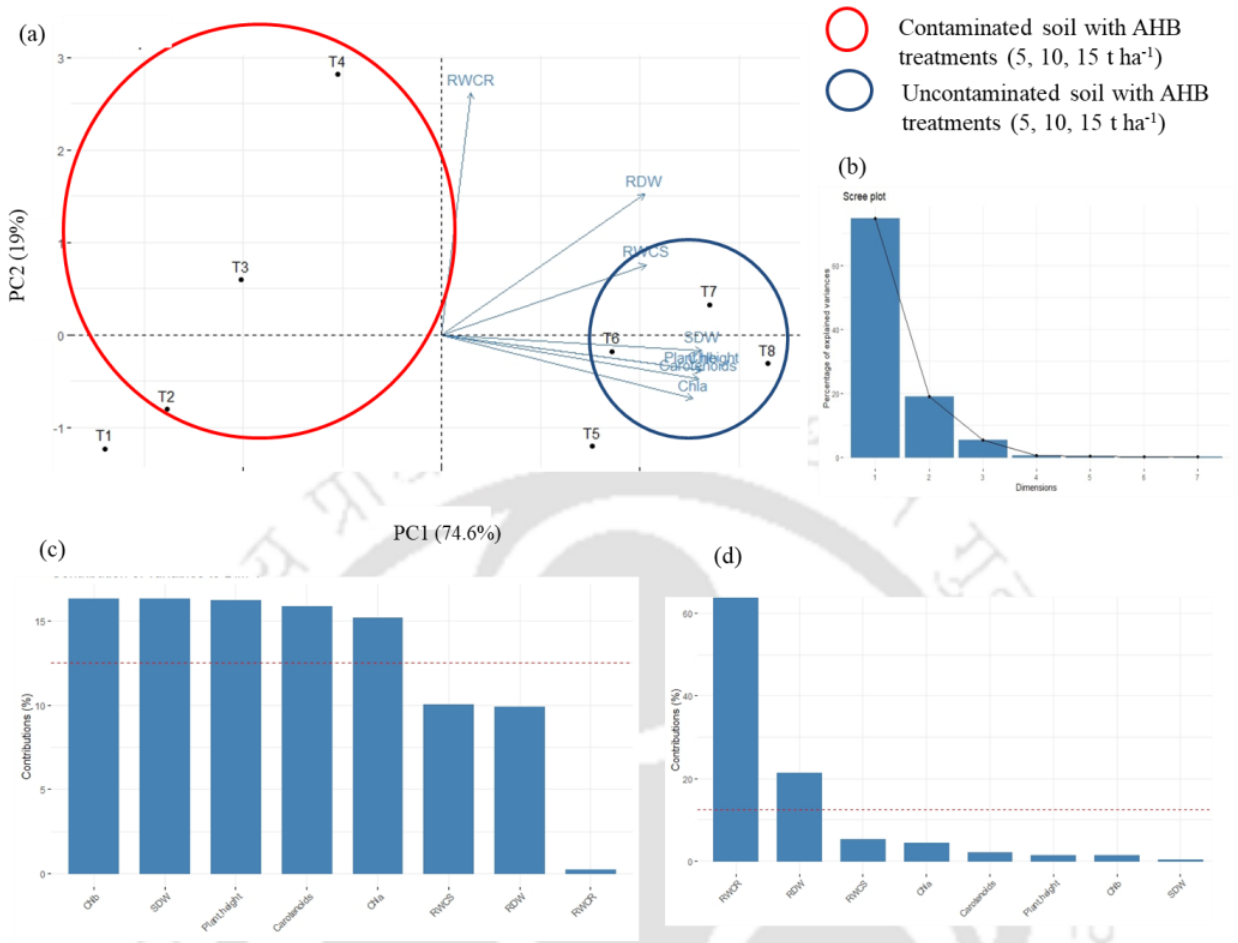

Fig. 7.11. PC analysis showing the plant variables (a) PCA biplot; (b) Scree plot of the percentage variance; (c) Individual contribution of the variable in PC1; (d) Individual contribution of variable in PC2.

Table 7.1.
Rotated principal component matrix and two-way ANOVA for physico-chemical, soil enzymes and heavy metals.

Soil parameters			**Plant parameters**		
Factors	**PC1**	**PC2**	**Factors**	**PC1**	**PC2**
pH	**0.883**	-0.415	PH	**0.984**	-0.144
EC	**0.827**	0.453	RWCS	0.773	0.285
CEC	0.721	0.660	RWCR	0.111	**0.982**
Av N	**0.933**	-0.006	SDW	**0.986**	-0.063
Av P	**0.929**	-0.050	RDW	0.768	0.570

Av K	**0.966**	0.181	Chla	**0.951**	-0.259
Av Na	**0.870**	-0.390	Chlb	**0.986**	-0.144
DHA	**0.898**	-0.370	CAR	**0.972**	-0.177
UR	**0.954**	-0.184	-	-	-
OC	**0.983**	-0.151		-	-
Eigen value	8.09	1.19		5.96	1.51
% variance	80.99	11.97		74.59	18.96
Cumulative %	80.99	92.97		74.59	93.55

Note: PCA loadings N > 0.8 shown in bold; p < 0.001

7.4. Conclusions

BC doses showed a significant effect on soil physico-chemical properties. The plant growth parameters like plant height, chlorophyll content, and biomass of vetiver plants slightly increased with BC doses. Further, the spore density, colonization, and glomalin also depended upon BC doses. Overall, most reports suggested that BC prepared at higher temperature (> 500) had more surface area and better functional groups arrangement. Still, for a more comprehensive agricultural application, we recommended BC prepared at lower temperature, which also works well along with vetiver. From the results of PCA analysis of plant variables, it is clear that Chla, and SDW, plant height was strongly affected by AHB doses. Whereas, in case of soil parameters OC, Av k, URE and Av N were mainly influenced by AHB. Vetiver under the influence of BC helps in remediating the soil quality and provides excellent stability and strength to the soil. Overall, the present research has assessed the soil quality status of two areas with divergent pollution profiles, and attempted to find the solutions for its remediation.

References

Anderson, C.R., Condron, L.M., Clough, T.J., Fiers, M., Stewart, A., Hill, R.A., Sherlock, R.R., 2011. Biochar induced soil microbial community change: implications for biogeochemical cycling of carbon, nitrogen and phosphorus. Pedobiologia, 54, 309-320.

Arnon, DI., 1949. Copper enzymes in isolated chloroplasts. Polyphenoloxidase in *beta vulgaris*. Plant Physiol. 24, 1.

Biederman, L.A., Harpole, W.S., 2013. Biochar and its effects on plant productivity and nutrient cycling: a meta-analysis. GCB bioenergy, 5, 202-214.

Biermann, B., Linderman, R.G., 1981. Quantifying vesicular-arbuscular mycorrhizae: a proposed method towards standardization. New Phytologist, 87, 63-67.

Casida, L.E., 1977. Microbial metabolic activity in soil as measured by dehydrogenase determinations. Appl. Environ. Microbiol. 34, 630–636.

Chen, J., Shiyab, S., Han, F.X., Monts, D.L., Waggoner, C.A., Yang, Z., Su, Y., 2009. Bioaccumulation and physiological effects of mercury in *Pteris vittata* and *Nephrolepis exaltata*. Ecotoxicology 18, 110–121.

Cui, L., Li, L., Zhang, A., Pan, G., Bao, D., Chang, A., 2011. Biochar amendment greatly reduces rice Cd uptake in a contaminated paddy soil: a two-year field experiment. BioResources, 6, 2605-2618.

Dai, Y., Zheng, H., Jiang, Z., Xing, B., 2020. Combined effects of biochar properties and soil conditions on plant growth : A meta-analysis. Sci. Total Environ. 713, 136635.

Datta, A., Gujre, N., Gupta, D., Agnihotri, R., Mitra, S., 2021. Application of enzymes as a diagnostic tool for soils as affected by municipal solid wastes. J. Environ. Manage. 286, 112169.

Gerdemann, J.W., Nicolson, T.H., 1963. Spores of mycorrhizal Endogone species extracted from soil by wet sieving and decanting. Transactions of the British Mycological society, 46, 235-244.

Gujre, N., Soni, A., Rangan, L., Tsang, D.C., Mitra, S., 2021a. Sustainable improvement of soil health utilizing biochar and arbuscular mycorrhizal fungi: A review. Environ. Pollut. 115549.

Gujre, N., Agnihotri, R., Rangan, L., Sharma, M. P., Mitra, S., 2021b. Deciphering the dynamics of glomalin and heavy metals in soils contaminated with hazardous municipal solid wastes. J. Hazard. Mater. 416, 125869.

Gul, S., Whalen, J.K., 2016. Biochemical cycling of nitrogen and phosphorus in biochar-amended soils. Soil Biol Biochem. 103, 1-15.

Huang, M., Li, Z., Luo, N., Yang, R., Wen, J., Huang, B., Zeng, G., 2019. Application potential of biochar in environment : Insight from degradation of biochar-derived DOM and complexation of DOM with heavy metals. Sci. Total Environ. 646, 220–228.

Klose, S., Tabatabai, M.A., 2000. Urease activity of microbial biomass in soils as affected

by cropping systems. Biol. Fertil. Soils 31, 191–199.
Kumar, S., Masto, R.E., Ram, L.C., Sarkar, P., George, J., Selvi, V.A., 2013. Biochar preparation from *Parthenium hysterophorus* and its potential use in soil application. Ecol. Eng. 55, 67–72.
Luo, S., Wang, S., Tian, L., Li, S., Li, X., Shen, Y., Tian, C., 2017. Long-term biochar application in fl uences soil microbial community and its potential roles in semiarid farmland. Appl. Soil Ecol. 117–118, 10–15.
Mitchell, P.J., Simpson, A.J., Soong, R., Simpson, M.J., 2015. Shifts in microbial community and water-extractable organic matter composition with biochar amendment in a temperate forest soil. Soil Biol. Biochem. 81, 244-254.
Ogbonnaya, U., Semple, K.T., 2013. Impact of biochar on organic contaminants in soil: a tool for mitigating risk? Agronomy, 3, 349-375.
Ra, M., Ortas, I., Rizwan, M., Javed, H., Raza, A., Farooq, M., Munis, H., 2020. Residual effects of biochar and phosphorus on growth and nutrient accumulation by maize (*Zea mays* L .) amended with microbes in texturally different soils. Chemosphere 238. https://doi.org/10.1016/j.chemosphere.2019.124710
Steiner, C., 2008. Biochar carbon sequestration. University of Georgia, Biorefining and Carbon Cycling Program, Athens, GA, 30602.
Tang, J., Zhang, L., Zhang, J., Ren, L., Zhou, Y., Zheng, Y., Luo, L., Yang, Y., Huang, H., Chen, A., 2020. Physicochemical features , metal availability and enzyme activity in heavy metal-polluted soil remediated by biochar and compost. Sci. Total Environ. 701, 134751.
Vanek, S.J., Lehmann, J., 2015. Phosphorus availability to beans via interactions between mycorrhizas and biochar. Plant Soil 395, 105–123.
Vithanage, M., Rajapaksha, A.U., Zhang, M., Thiele-Bruhn, S., Lee, S.S., Ok, Y.S., 2015. Acid-activated biochar increased sulfamethazine retention in soils. Environ. Sci. Pollut. Res. 22, 2175-2186.
Wright, S.F., Upadhyaya, A., 1996. Extraction of an abundant and unusual protein from soil and comparison with hyphal protein of arbuscular mycorrhizal fungi. Soil Sci. 161, 575-586.
Yang, X., Liu, J., Mcgrouther, K., Huang, H., Lu, K., Guo, X., He, L., Lin, X., Che, L., Ye, Z., Wang, H., 2016. Effect of biochar on the extractability of heavy metals (Cd , Cu , Pb , and Zn) and enzyme activity in soil. Environ Sci. Pollut. Res. 23, 974–984.
Yuan, P., Wang, J., Pan, Y., Shen, B., Wu, C., 2019. Review of biochar for the management of contaminated soil : Preparation , application and prospect. Sci. Total Environ. 659, 473–490.
Yulin, J., Yuhu, Z., Ihnsup, H., Peng, W., Qiwen, M., Yunjie, H., 2020. Effects of different straw biochars on soil organic carbon , nitrogen , available phosphorus, and enzyme activity in paddy soil. Sci. Rep. 10, 1–12. 2
Zhang, G., Guo, X., Zhu, Y., Liu, X., Han, Z., Sun, K., Ji, L., He, Q., Han, L., 2018a. The effects of different biochars on microbial quantity, microbial community shift, enzyme activity, and biodegradation of polycyclic aromatic hydrocarbons in soil. Geoderma 328, 100–108.

Zhang, L., Jing, Y., Xiang, Y., Zhang, R., Lu, H., 2018b. Responses of soil microbial community structure changes and activities to biochar addition: A meta-analysis. Sci. Total Environ. 643, 926–935.

Zhang, L., Xiang, Y., Jing, Y., Zhang, R., 2019. Biochar amendment effects on the activities of soil carbon , nitrogen , and phosphorus hydrolytic enzymes : a meta-analysis. Environ Sci. Pollut. Res. 26, 22990–23001.

Zhang, X., Gao, B., Xia, H., 2014. Effect of cadmium on growth , photosynthesis , mineral nutrition and metal accumulation of bana grass and vetiver grass. Ecotoxicol. Environ. Saf. 106, 102–108.

Zhou, C., Heal, K., Tigabu, M., Xia, L., Hu, H., Yin, D., Ma, X., 2020. Biochar addition to forest plantation soil enhances phosphorus availability and soil bacterial community diversity. For. Ecol. Manag. 455, 117635.

CHAPTER 8

Summary and future recommendations

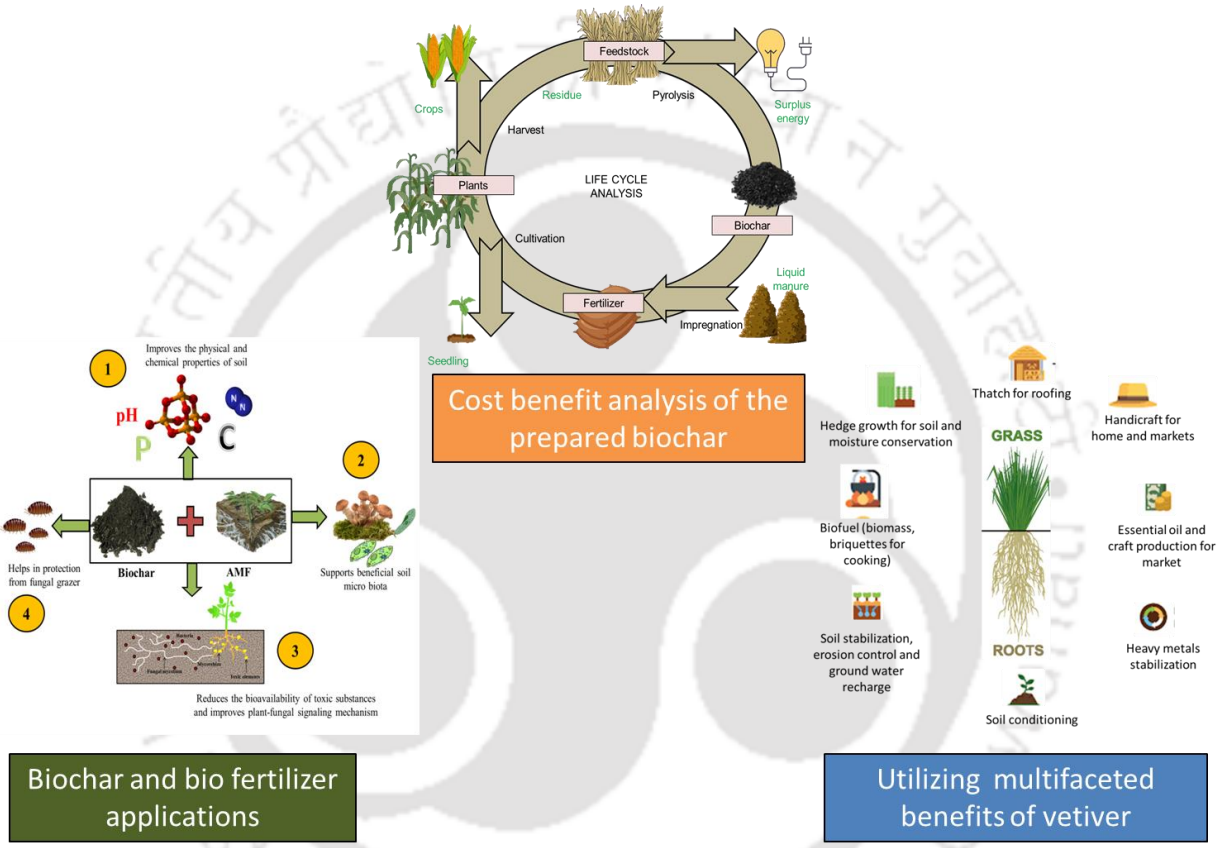

"The present chapter deals with the challenges and future recommendations out of the present study. Further it also summarizes major findings of the present work."

8. Summary and future recommendations

The present research was a comprehensive attempt to assess the soil quality of the areas contaminated with organic and inorganic wastes. It also explored the potential of local available plant material like areca nut husk for BC preparation and its applications in soil quality enhancement. Overall, this study reports extensive evidences to demonstrate the severity of soil pollution around the MSW dumping site and a brick kiln industry. Consequently, six environmentally important HMs (Cr, Mn, Zn, Cd, Ni and Cu) with respect to their effects on soil contamination, ecological and health risks have been documented, analyzed, and evaluated. The highest pollution load index was observed for Cr and Cd. I_{geo} values for Cr and Cd varied from strongly to extremely polluted category at both the sites. According to the health risk assessment results, the non-carcinogenic risk due to Zn, Cu, Ni and Mn were insignificant while Cr and Cd posed higher carcinogenic and non-carcinogenic risks in case of both adults and children. Children were found to be more vulnerable to heavy metal toxicity. The level of HM contamination in the study area and the severity of ecological and health risks provided adequate evidence, and underscored the urgency to adopt safe and effective disposal and management of waste. At Site-1, the electronics waste like Ni-Cd batteries, electrical PCBs, and glass wastes contributed to substantial contamination. Whereas, at Site-2 anthropogenic enrichment was higher due to bottom ash and raw materials used during the firing operation.

Therefore, with the target of waste valorization and soil quality improvement, application of AHB as a soil amendment was, characterized and evaluated. A novel agro-ecotechnological approach of applying AHB along with ecologically important vetiver grass was attempted in this study. AHB prepared at lower temperature was found to be more suitable for soil quality improvement. AHB, produced at low temperature (250 °C) demonstrated the highest SOMYI (6.78), along with oxygen containing surface functional groups. Concurrently, the effect of AHB

doses on the soil physico-chemical, biochemical and plant properties in both contaminated and uncontaminated soils were appraised in detail. The results suggested that higher AHB doses enhanced vetiver rhizosphere, thereby helping Cd and Cr remediation from the soil. Further, the comparatively higher value of RDW in comparison to SDW, suggested enhanced energy allocation to root in relation to the shoot, as a response to HM stress by vetiver plant species. Application of AHB with dose of 15 t ha^{-1} enhanced the concentrations of Av N, Av P, Av K and OC in both contaminated and uncontaminated. PCA demonstrated significant positive correlations between soil and plant growth factors. It also revealed that UR and OC are the leading variables suggesting the effect of AHB on soil nutrient enrichment. In brief, the present results suggested that AHB prepared at lower temperature and with an application rate of 15 t ha^{-1} displayed had significant impact on the soil quality. AHB can be recommended for field-based application, along with vetiver grass, which is known as an agent for soil aggregation and overall quality improvement. BC amendment is a relatively new and evolving, green agro-technology, germane to sustainable agriculture. Thus, the present assessment is critical in knowledge development for agricultural uses of BC. The present study assessed the status of the HMs and the potential of AHB for soil quality improvement. The practical approach of BC preparation utilizing local feedstock (AH), will help the rural people to effectively utilize the dumped agro-wastes, for soil quality improvement. With its potential as soil amender, AHB along with vetiver grass has multifaceted benefits. However, as an alternative and effective agro-technology, several aspects still need to be developed and evaluated due to different variables that determine the characteristics and applications of AHB. Despite its outstanding potential, BC is not yet widely implemented due to a lack of acceptability about the benefits of BC among various stakeholders. The present research has a strong technical focus on the soil quality assessment and its remediation using AHB, which mainly investigates the

dynamics inside soil and plant. Social-economic and cultural aspects of BC technologies are equally important yet remain unexplored. Today, there is a need for more interdisciplinary research that caters to successful BC usages. Further research is needed in the following directions:

- Minimizing the gaseous aerosol emissions during the pyrolysis and lowering air pollution impact.
- Optimization of pyrolysis temperature and energy-efficient mode of BC production, to reduce the energy inputs.
- Framing the application guidelines for BC, since fine ash contained in the BC, might cause respiratory problems in adults with respiratory disorders. Also, appropriate policies should be framed to encounter air and water loss during BC application.
- Life cycle assessment of BC should be carried out for its large-scale production, storage and transportation.

From a global perspective, AHB aids the policymaker by tackling crop improvement and soil quality management. Its application would further reduce the dependence on chemical fertilizers and initiate the way forward for sustainable agricultural practices. For more effective strategies, AHB should be coupled with bacterial and AMF based bio fertilizers. Interestingly, the empirical foundation of AHB and vetiver grass is not very broad. The presented framework of AHB and vetiver grass addresses the Indian milieu of soil quality rejuvenation. However, the present study offers tools that allow a novel and sustainable way of exploring new horizons in BC technologies.

Annexure-1

List of publications

Peer reviewed journals

- **Gujre, N**., Rangan, L., Mitra, S., 2021. Occurrence, geochemical fraction, ecological and health risk assessment of cadmium, copper and nickel in soils contaminated with municipal solid wastes. ***Chemosphere***, 129573. [IF: 7.086]
- **Gujre, N.,** Mitra, S., Soni, A., Agnihotri, R., Rangan, L., Rene, E. R., Sharma, M. P., 2021. Speciation, contamination, ecological and human health risks assessment of heavy metals in soils dumped with municipal solid wastes. ***Chemosphere***, 128013. [IF: 7.086]
- **Gujre, N**., Agnihotri, R., Rangan, L., Sharma, M.P., Mitra, S., 2021. Deciphering the dynamics of glomalin and heavy metals in soils contaminated with hazardous municipal solid wastes. ***Journal of Hazardous Materials,*** 416, 125869. [IF: 10.588]
- **Gujre, N.**, Soni, A., Rangan, L., Tsang, D.C., Mitra, S., 2020. Sustainable improvement of soil health utilizing biochar and arbuscular mycorrhizal fungi: A review. ***Environmental Pollution,*** 115549. [IF: 8.071]
- **Gujre, N.,** Mitra, S., Agnihotri, R., Sharma, M.P., Gupta, D., 2021. Novel agro-technological intervention for soil amendment through areca nut husk biochar in conjunction with vetiver grass. ***Chemosphere*** (Reviewer comments received and under revision). [IF: 7.086]

Conference attended / proceedings

- **Gujre, N.,** Mitra, S. (2018, January). Rejuvenating and enhancing agro-ecosystem through bio fertilizer. Poster presented at the International symposium on biodiversity and biobanking. Biodiverse 2018, January 27th-29th, 2018, IIT, Guwahati, Assam. pp 122.
- **Gujre, N.,** Mitra, S. (2019, February). Assessing environmental impact of brick kiln activities on surrounding soil quality at Napaam, Tezpur, Assam. Poster presented at the XIV Agricultural Science Congress (ASC), February 20-23rd, 2019, NASC and ICAR-IARI, New Delhi. pp 191.
- **Gujre, N.,** Soni, A., Mitra, S. (2019, November). Way toward sustainable waste utilization for potential applications in agricultural soil in Assam, Northeast, India. Poster presented at Young Scientist Conference, India International Science Festival, November 5-8th, 2019, Biswa Bangla Convention Center, Kolkata.
- **Gujre, N.,** Mitra, S. (2019, March). Assessing environmental impact of brick kiln activities on surrounding soil quality at Napaam, Tezpur, Assam. Oral presentation at Research conclave 2018, March 14-17th, 2018, IIT, Guwahati.

Chemosphere 262 (2021) 128013

Contents lists available at ScienceDirect

Chemosphere

journal homepage: www.elsevier.com/locate/chemosphere

Speciation, contamination, ecological and human health risks assessment of heavy metals in soils dumped with municipal solid wastes

Nihal Gujre [a], Sudip Mitra [a, *], Ankit Soni [a], Richa Agnihotri [b], Latha Rangan [a, c], Eldon R. Rene [d], Mahaveer P. Sharma [b]

[a] Agro-ecotechnology Laboratory, Centre for Rural Technology, Indian Institute of Technology Guwahati (IITG), Guwahati, Assam 781039, India
[b] ICAR-Indian Institute of Soybean Research, Khandwa Road, Indore, Madhya Pradesh 452001, India
[c] Department of Biosciences and Bioengineering, Indian Institute of Technology Guwahati (IITG), Guwahati, Assam 781039, India
[d] Department of Environmental Engineering and Water Technology, IHE Delft Institute for Water Education, 2601 DA Delft, the Netherlands

HIGHLIGHTS

- Soil contamination, ecological and health risks were evaluated for a dumping site.
- 80% of the sampling sites fell under the category of heavily polluted category for Cr.
- Presence of Cr resulted in high soil contamination and low ecological risks.
- Cr posed health hazards to children and adults.
- Children were found to be more prone to heavy metal contamination.

GRAPHICAL ABSTRACT

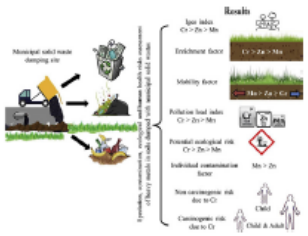

ARTICLE INFO

Article history:
Received 26 May 2020
Received in revised form
3 August 2020
Accepted 12 August 2020
Available online 18 August 2020

Handling Editor: T Cutright

Keywords:
Municipal solid waste
Heavy metals
Pollution indices
Ecological risks
Health risks

ABSTRACT

The main aim of this work is to assess the extent of soil contamination, potential ecological and health risks associated with the disposal of municipal solid waste (MSW) near a Ramsar site in Assam, India. Soil samples were collected and analysed for three heavy metals (HMs), namely, chromium (Cr), manganese (Mn) and zinc (Zn). The sources of HMs and their pollution levels were evaluated using different indices. The results demonstrated that Cr contamination was high near the metal scrap segregations unit within the dumping site, otherwise, the ecological risks associated with Zn and Mn were found to be low. The speciation of Cr and Zn were associated with the Fe–Mn oxide bound (F4) fraction, accounting 44.23% and 30.68%, respectively, whereas Mn (52.55%) was associated with the exchangeable fraction (F2). The fate and origin of HMs were assessed using mobility and enrichment factors and 16 out of the 20 sampling sites fell under the category of heavily polluted category for Cr, while others which were nearby the metal segregation units fell under the strongly to extremely polluted category. In few sites, significant enrichment was observed for Zn and minimal to moderate enrichment for Mn, respectively. Health risk assessment results indicated that Cr posed higher threat to human health through ingestion.

Chemosphere 271 (2021) 129573

Contents lists available at ScienceDirect

Chemosphere

journal homepage: www.elsevier.com/locate/chemosphere

Occurrence, geochemical fraction, ecological and health risk assessment of cadmium, copper and nickel in soils contaminated with municipal solid wastes

Nihal Gujre [a], Latha Rangan [a, b], Sudip Mitra [a, *]

[a] Agro-ecotechnology Laboratory, Centre for Rural Technology, Indian Institute of Technology Guwahati (IITG), Assam, 781039, India
[b] Applied Biodiversity Laboratory, Department of Biosciences and Bioengineering, Indian Institute of Technology Guwahati (IITG), Assam-781039, India

HIGHLIGHTS

- MSW dumping site has resulted in considerable environmental and health risk.
- Geochemical fractions of HMs were examined using sequential extraction procedure.
- 55% of Cd is associated with the carbonate bound fraction.
- I_{geo}, *PLI* and *PERI* indicated significant pollution load due to Cd.
- Higher human health risks are associated with Cd and Ni.

GRAPHICAL ABSTRACT

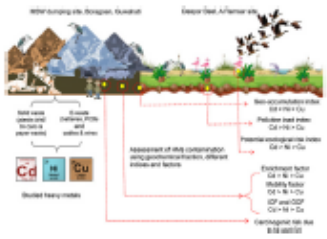

ARTICLE INFO

Article history:
Received 16 September 2020
Received in revised form
25 December 2020
Accepted 3 January 2021
Available online 7 January 2021

Handling Editor: Derek Muir

Keywords:
Municipal solid wastes
Dumping site
Heavy metals
Geochemical fractionation
Ecological risks
Health risks

ABSTRACT

Unscientific municipal solid waste (MSW) dumping provokes heavy metal (HM) associated ecological and human health hazards through heightened bioavailability and bioaccumulation. In this study, we focused on three important HMs Cadmium (Cd), Copper (Cu) and Nickel (Ni) and their geochemical fractions, to enable clutter free data management, analysis and interpretation. Stratified random soil sampling was carried out from twenty different locations around a Ramsar site (Deepor Beel) in Guwahati, India. The spatial concentration profiles of Cd, Cu and Ni were determined by data elicited from geochemical fractionation and the Geographic Information System (GIS). Ecological and health risks indices were used to evaluate the severity of soil pollution and assess the level of health risks. All the three HMs thus evaluated, conformed to the potential bioavailable category. Cd (54.59%) was associated mostly with the carbonate bound fraction (F3), while 25.53% of Cu and 40.60% Ni were associated with the exchangeable fraction (F2). Significant contamination levels and higher ecological risks posed by these metals were in the order Cd > Ni > Cu. Children were found to be more vulnerable towards Cd associated health risks whereas, Ni posed threats to both adults and children. Cu posed no risk to human health. Geochemical fractionation and different indices played a critical role in the integrated assessment of soil pollution, ecological and health risk assessment, and provided an empirical basis for the sustainable future planning and comprehensive adaptive management practices for MSW.

1. Introduction

Wetlands are highly productive ecosystems (Singh and Sinha, 2020), that render vital ecosystem services and functions. They

* Corresponding author.
E-mail addresses: sudipmitra@yahoo.com, sudipmitra@iitg.ac.in (S. Mitra).

https://doi.org/10.1016/j.chemosphere.2021.129573
0045-6535/

Environmental Pollution 268 (2021) 115549

Contents lists available at ScienceDirect

Environmental Pollution

journal homepage: www.elsevier.com/locate/envpol

Review

Sustainable improvement of soil health utilizing biochar and arbuscular mycorrhizal fungi: A review

Nihal Gujre [a, 1], Ankit Soni [a], Latha Rangan [b], Daniel C.W. Tsang [c], Sudip Mitra [a, 1, *]

[a] Agro-ecotechnology Laboratory, Centre for Rural Technology, Indian Institute of Technology Guwahati (IITG), Guwahati, Assam 781039, India
[b] Department of Biosciences and Bioengineering, Indian Institute of Technology Guwahati (IITG), Guwahati, Assam 781039, India
[c] Department of Civil and Environmental Engineering, The Hong Kong Polytechnic University, Hung Hom, Kowloon, Hong Kong, China

ARTICLE INFO

Article history:
Received 8 April 2020
Received in revised form
18 July 2020
Accepted 8 August 2020
Available online 28 August 2020

This paper has been recommended for acceptance by Jörg Rinklebe.

Keywords:
Arbuscular mycorrhizal fungi
Biochar
Soil amendment
Soil quality
Sustainable agriculture

ABSTRACT

Conservation of soil health and crop productivity is the central theme for sustainable agriculture practices. It is unrealistic to expect that the burgeoning crop production demands will be met by a soil ecosystem that is increasingly unhealthy and constrained. Therefore, the present review is focused on soil amendment techniques, using biochar in combination with arbuscular mycorrhizal fungi (AMF), which is an indispensable biotic component that maintains plant-soil continuum. Globally significant progress has been made in elucidating the physical and chemical properties of biochar; along with its role in carbon sequestration. Similarly, research advances on AMF include its evolutionary background, functions, and vital roles in the soil ecosystem. The present review deliberates on the premise that biochar and AMF have the potential to become cardinal to management of agro-ecosystems. The wider perspectives of various agronomical and environmental backgrounds are discussed. The present state of knowledge, different aspects and limitations of combined biochar and AMF applications (BC + AMF), mechanisms of interaction between biochar and AMF, effects on plant growth, challenges and future opportunities of BC + AMF applications are critically reviewed. Given the severely constrained nature of soil health, the roles of BC + AMF in agriculture, bioremediation and ecology have also been examined. In spite of the potential benefits, the functionality and dynamics of BC + AMF in soil are far from being fully elucidated.

1. Introduction

The life-sustaining role of soil in agriculture and food security is undermined by the rapid worldwide degradation of surface soil through increased erosion, salinity, acidification, and compaction (Scholes et al., 2018). Degradation is primarily driven by soil pollution, improper management practices, extreme climate events, lack of technological innovations and resilience systems (Shao et al., 2019; Van Leeuwen et al., 2019). The consequent economic and social ramifications result in slower economic growth, heightened food insecurity, increased poverty, and livelihood vulnerability; thus disrupting sustained agricultural production in the developing regions, especially in the tropical regimes (Lomba et al., 2019; Shao et al., 2019; Smetanova et al., 2019). In India, for example, humungous pressure is brought to bear on 2.4% of land area occupied by 18% and 15% of global human and livestock population, respectively (Pal et al., 2019). A decrease in crop production efficiency is also confronted in China due to heavy metals (HMs) contamination of more than 2×10^7 ha of farmland; 16.1% of this area exceeds designated limits for soil pollution (Palansooriya et al., 2020). These examples of challenging circumstances, from the world's most densely populated countries, endorse the deployment of environmentally friendly, economically viable, and sustainable technologies. Biochar along with AMF is a potentially achievable, appropriate, and advantageous amendment for soil quality remediation and improvement (Fang et al., 2018; O'Connor et al., 2018). Across the globe, BC + AMF have gained much attention for their wide range of applications particularly in improving nutrients cycling (Castañeda et al., 2020; Moland et al., 2018), drought-resistant (Hashem et al., 2019) and restoration of soil quality (González-Chávez et al., 2017; Ohsowski et al., 2018). Numerous experiments have been carried out to assess the BC + AMF effects on crops which can be influenced by various biochar properties, i.e.,

* Corresponding author.
E-mail addresses: sudipmitra@yahoo.com, sudipmitra@iitg.ac.in (S. Mitra).
[1] Equal contribution.

https://doi.org/10.1016/j.envpol.2020.115549
0269-7491/

Journal of Hazardous Materials 416 (2021) 125869

Contents lists available at ScienceDirect

Journal of Hazardous Materials

journal homepage: www.elsevier.com/locate/jhazmat

Deciphering the dynamics of glomalin and heavy metals in soils contaminated with hazardous municipal solid wastes

Nihal Gujre [a,1], Richa Agnihotri [b,1], Latha Rangan [c], Mahaveer P. Sharma [b], Sudip Mitra [a,*,2]

[a] Agro-ecotechnology Laboratory, Centre for Rural Technology, Indian Institute of Technology Guwahati (IITG), Assam 781039, India
[b] ICAR, Indian Institute of Soybean Research, Khandwa Road, Indore, Madhya Pradesh 452001, India
[c] Applied Biodiversity Laboratory, Department of Biosciences and Bioengineering, Indian Institute of Technology Guwahati (IITG), Assam 781039, India

ARTICLE INFO

Editor: Dr. Rinklebe Jörg

Keywords:
Arbuscular mycorrhizal fungi
Glomalin related soil protein
Solid wastes
Heavy metals
Soil organic carbon

ABSTRACT

Heavy metals (HMs) accumulation in the soils poses risks towards the environment and health. Glomalin related soil protein (GRSP) produced by arbuscular mycorrhizal fungi (AMF) has metal-sorption and soil aggregation properties and is critical in the survival of plants and AMF. For the first time, this study attempted to examine the GRSP mediated bio-stabilization of HMs in soils contaminated with municipal solid wastes (MSW). The content and interrelationship of GRSP and HMs, along with soil physicochemical properties were studied in 20 different soil samples from the dumping site. Higher amount of GRSP indicated potential bio-stabilization of HMs at some sites. GRSP exhibited weak positive correlation with essential (Zn, Cu) and toxic HMs (Cd, Ni). Cr and Mn were possibly sequestered in AMF structures and thus found to be negatively correlated with GRSP. The positive correlation observed between GRSP and soil nutrients like N, P and soil organic carbon (SOC) indicating potential of AMF-GRSP in sustaining soil health. Results revealed that AMF residing at contaminated sites produced higher amount of GRSP potentially to bio-stabilize the HMs, and reduce their bioavailability and also facilitate SOC sequestration.

1. Introduction

In recent years, heavy metals (HMs) contamination in soils has become one of the world's significant environmental challenges. Extensive anthropogenic activities coupled with rapid industrialization and urbanization have contributed significantly to soil contamination through HMs (Bhatti et al., 2018). Among the several anthropogenic activities, non-scientific disposal of municipal solid waste (MSW) is a significant contributor to the HMs in the soil (Gujre et al., 2021a). Inadequate treatment of waste, a lack of disposal facilities, and source segregation are some of the major reasons for open dumping of solid waste, causing soil pollution. Moreover, because of their bioavailability and mobility, HMs enter the food chain resulting in biomagnification (Bhatti et al., 2018). HMs typically have high toxicity, low degradation potential and high binding efficiency to soil organic matter (SOM). These characteristics aid in the accumulation of the HMs in the soil for a longer period (Francová et al., 2020). Large specific surface areas, the presence of different surface functional groups and mineral matrix structure (goethite, humate and cerussite) are some of the governing factors that influence the binding efficiency of HMs to SOM (Shan et al., 2019). Furthermore, the plant's rhizospheres alter the surface of SOM, increasing its affinity for HMs (Shi et al., 2018).

In general, some HMs are essential, but when they reach a certain threshold, they become contaminant for the surrounding environment. Metals can also be classified into two categories, viz., essential and non-essential depending on the needs of the plant. Due to the concentration gradients and selective uptake of these metals, plants take essential HMs such as like iron (Fe), zinc (Zn), copper (Cu), and manganese (Mn) from the soil (Peralta-Videa et al., 2009). While the essential metals are necessary for various plant metabolic functions, non-essential metals are potentially toxic and carcinogenic, with no known functions. As a result, it is critical to assess the level of HM contamination in the soil and to identify their relationship with soil biotic communities, which will serve as a reference for future bioremediation strategies. Appropriate diagnostic tools are required to predict and evaluate the dynamics of the soil. To predict the changes in soil quality researchers have used a variety of

* Corresponding author.
E-mail addresses: sudipmitra@iitg.ac.in, sudipmitra@yahoo.com (S. Mitra).
[1] Equal contribution.
[2] ORCID: 0000-0002-1838-8264

https://doi.org/10.1016/j.jhazmat.2021.125869
Received 16 October 2020; Received in revised form 3 April 2021; Accepted 8 April 2021
Available online 20 April 2021